The Role of Stromal Cells in the Mouse Model of Respiratory Syncytial Virus Infection

A thesis submitted to Imperial College London for the degree of Doctor of Philosophy

Fahima Kausar

Respiratory Infections Section
National Heart and Lung Institute
Faculty of Medicine
Imperial College London
London W2 1PG

2016

Abstract

Respiratory Syncytial Virus (RSV) is the single most important cause of acute lower respiratory tract infections in infants. Most children are infected with RSV by the age of two, and the majority of them suffer only a simple cold. However, 1-3% develop severe bronchiolitis that requires hospitalisation and these children have a greater risk of developing recurrent wheeze and asthma-like symptoms in later childhood. There is currently no treatment or vaccine against RSV.

Despite its prevalence, the characteristics of RSV infection and spread in the host lung are not well characterised. Stromal cells are the functionally connective tissue of the lung and include alveolar type I and II (ATI/ATII) epithelial cells, endothelial cells and fibroblasts. These cells are slowly being recognised as important players in the response to respiratory infections through their expression of proinflammatory mediators and tissue repair proteins. However, the role of stromal cells in RSV infection *in vivo* has not been elucidated. We have been able to identify several important chemokines, cytokines and growth factors that are expressed by stromal cells in response to RSV *in vivo* using fluorescent activated cell sorting and gene expression analysis. Interestingly, our data show that ATII epithelial cells are a major source of growth factors while the non-epithelial, non-endothelial stromal cells are a major source of chemokines. In addition, when infecting lung fibroblasts *ex vivo* with RSV, many chemokines known to be important during RSV infection are produced. We further demonstrate that expression of several of these mediators *in vivo* is dependent on IFNAR signalling, illustrating the cellular crosstalk between stromal cells and alveolar macrophages in the lung during RSV infection, which is needed for effective viral clearance. Finally, we highlight the potential protective role of ATII epithelial cell-derived GM-CSF expression in the lung during RSV infection *in vivo*. Data from these experiments reveal novel and previously unknown roles of stromal cells in the response to RSV infection *in vivo* and highlight new targets, which could be modulated for potential therapeutic benefits.

Statement of Contribution

I hereby certify that all of the work in this thesis is my own.

Fahima Kausar 2016.

Copyright Declaration

The copyright of this thesis rests with the author and is made available under a Creative Commons Attribution Non-Commercial No Derivatives licence. Researchers are free to copy, distribute or transmit the thesis on the condition that they attribute it, that they do not use it for commercial purposes and that they do not alter, transform and build upon it. For any reuse or redistribution, researchers must make clear to others the licence terms of the work.

Acknowledgments

First and foremost, I would like to give my biggest thanks to my supervisor Cecilia Johansson. Without her non-stop enthusiasm and never-ending support, I would have not have achieved all the things I have in the past three years. I thank her for helping me become a better scientist and for showing me that women in Science can achieve great success. She has been an inspiration and I hope to emulate her brilliance as a supervisor and scientist one day.

Thanks to all of the Johansson group members past and present for all their help and support throughout my PhD. I learnt a great deal from you all, both scientifically and otherwise! I wish the last remaining survivor, Spiros Makris, all the best with his PhD and look forward to enjoying a cup of coffee together when it's all over! Also, a special thanks to my MSc student, Avneet Manghera for all her hard work and for being an absolute delight to work with. The distinction she received was well deserved.

Thanks to my second supervisor Fiona Culley for her project advice and critical analysis of my thesis, and thanks to Peter Openshaw and the rest of Respiratory Infections for their invaluable help and discussions throughout my three years. It has been a pleasure to work with such brilliant scientists.

This acknowledgement would not be complete without a special mention to two invaluable colleagues and great friends who made my three years so much more enjoyable and fun. Sasha Ashbourne-Lewis and Aleks Guvenel, thank you for always making me laugh and keeping me sane in the lab every day. Our ridiculous conversations, long lunches and silly moments made it so much easier to come in every day. I don't think I would have enjoyed my PhD as much without you both. We all started together, and I am glad we became such great friends. I will miss you both.

Last but not least, I would like to thank my friends and family for putting up with me during these three hard years. Thanks in particular to Hamdi, and my two

other ethnics, Jay and Sakine for being understanding and supportive during the difficult moments and for always cheering me up with the never-ending supply of quality food and banter!

To my wonderful boyfriend Afanasie, thank you so much for putting up with my complaining, antisocial hours and constant exhaustion. You helped me through the tough moments and told me I could always do it. You never stopped believing in me and I couldn't have done it without you. I am very lucky to have you in my life.

And finally, to my lovely family and especially my incredible mum, your wish of a doctor in the family is almost here. I hope I have made you proud.

Fahima Kausar

Table of Contents

Abstract **2**

Statement of Contribution **3**

Copyright Declaration **3**

Acknowledgments **4**

Table of Contents **6**

Abbreviations **9**

Figure Index **13**

Table Index **15**

1 Introduction **16**

1.1 Respiratory syncytial virus **16**

1.1.1 Clinical manifestation and epidemiology 16

1.1.2 Treatment 17

1.1.3 Genome and structure 18

1.2 Immune response to RSV **20**

1.2.1 Detection of virus 20

1.2.2 Induction of the immune response 22

1.2.3 Cellular responses 26

1.2.3.1 Epithelial cells 26

1.2.3.2 Alveolar macrophages 26

1.2.3.3 Neutrophils 28

1.2.3.4 Monocytes 28

1.2.3.5 Dendritic cells 29

1.2.3.6 Natural killer cells 30

1.2.3.7 T cells 31

1.2.3.8 B cells and humoural response 33

1.2.4 Soluble mediators 34

1.2.4.1 Cytokines 34

1.2.4.2 Interferons 36

1.2.4.3 Chemokines 38

1.2.4.4 Growth factors 42

1.3 Stromal cells **44**

1.3.1 Epithelial cells 46

1.3.2 Endothelial cells 47

1.3.3 Fibroblasts 47

1.3.4 Smooth muscle cells 48

1.3.5 Perciytes 48

1.4 Stromal cells in infection **49**

1.4.1 Epithelial cells in infection 49

1.4.2 Endothelial cells in infection 51

1.4.3 Fibroblasts in infection 52

1.4.4 Smooth muscle cells in infection 53

1.4.5 Perciytes in infection 53

2 Hypothesis and Aims **55**

2.1 Hypothesis **55**

2.2 Aims **55**

3 Materials 56
3.1 Consumables 56
3.2 Reagents and chemicals 56
3.3 Kits 57
3.4 Anaesthetics 57
3.5 Instruments 57
3.6 Software 58
3.7 Antibodies 59
3.8 Solutions, buffers and media 61
4 Methods 62
4.1 Animals 62
4.2 Bone marrow chimeras 62
4.3 Cell lines 62
4.4 Primary murine lung fibroblasts 63
4.5 Virus growth 63
4.6 Immunoplaque assay 64
4.7 Dosing of mice 64
4.7.1 Virus infection 64
4.7.2 Neutralising antibodies 65
4.8 Collection of cells and tissue 65
4.8.1 Bronchoalveolar lavage fluid (BALF) 65
4.8.2 Lung tissue for quantitative polymerase chain reaction (qPCR) 65
4.8.3 Lung tissue for flow cytometry 65
4.8.3.1 Dispase 65
4.8.3.2 Collagenase 66
4.9 Total and differential leukocyte cell count 66
4.10 Flow cytometry 67
4.11 Cell sorting 69
4.11.1 Fluorescence activated cells sorting (FACS) 69
4.11.2 Magnetic activated cell sorting (MACS) 70
4.11.2.1 Automated MACS 70
4.11.2.2 Manual MACS 70
4.12 RNA extraction 71
4.12.1 Lung lobes 71
4.12.2 Sorted cells 71
4.13 RNA quantification 72
4.13.1 NanoDrop 72
4.13.2 Bioanalyser 72
4.14 RNA to complimentary DNA (cDNA) conversion 72
4.15 RNA amplification and cDNA conversion 72
4.16 qPCR 72
4.17 qPCR array 75
4.18 Bradford assay 76
4.19 Enzyme linked immunoabsorbant assay (ELISA) 76
4.20 Luminex 77
4.21 Statistical analysis 77
5 Results 78
5.1 Stromal cells isolated using dispase digestion and fluorescent activated cell sorting 78
5.1.1 Dispase digestion of lungs yields higher numbers of ATII epithelial cells compared to collagenase digestion 79
5.1.2 Dispase digested total lung has less virus than total lung homogenate 84

5.1.3 Fluorescence-activated cell sorting yields pure populations of different stromal cell subsets compared to magnetic-activated cell sorting 89
5.1.3.1 Magnetic-activated cell sorting 89
5.1.3.2 Fluorescence-activated cell sorting 92
5.1.4 Summary 95
5.2 Expression of soluble mediators from stromal cells during RSV infection *in vivo* 97
5.2.1 CD45$^-$ stromal cells are a major source of cytokines, chemokines and growth factors, whilst CD45$^+$ leukocytes are a major source of type I IFNs 97
5.2.2 ATII epithelial cells are a major source of growth factors whilst other stromal cells are a major source of chemokines and cytokines 102
5.2.3 Gene expression of CXCL10 and type I IFNs is dependent on live RSV, whilst expression of CXCL1, CCL2, growth factors and cytokines is partially dependent on live RSV at 4hrs post infection 106
5.2.4 Other stromal cells induce expression of an array of chemokines during RSV infection *in vivo* 109
5.2.5 Protein expression of chemokines, cytokines and growth factors can be detected in stromal cells 116
5.2.6 Summary 119
5.3 The other stromal cell population contains fibroblasts and primary murine fibroblasts produce chemokines in response to RSV 129
5.3.1 Other stromal cells contain CD90$^+$ fibroblasts 129
5.3.2 Primary mouse lung fibroblasts secrete chemokines in response to RSV 132
5.3.3 Summary 134
5.4 Expression of mediators from stromal cells is partially dependent on IFNAR1 signalling 136
5.4.1 Generation of IFNAR1$^{-/-}$ bone marrow chimeras 137
5.4.2 Characterisation of IFNAR1$^{-/-}$ BM chimeras 140
5.4.3 Increased viral load in IFNAR1$^{-/-}$ KO BM chimeras compared to WT-WT BM chimeras 143
5.4.4 Decreased production of soluble mediators in BALF of IFNAR1 KO BM chimeras 145
5.4.5 Expression of ATII epithelial cell-derived mediators in not IFNAR1 dependent 149
5.4.6 Expression of CXCL10 is dependent on IFNAR1 on other stromal cells, whilst expression of CCL2 is partially dependent 153
5.4.7 Expression of type I IFNs from AMs is IFNAR1 dependent 157
5.4.8 Summary 159
5.5 GM-CSF antibody treatment can lead to increased weight loss and viral load during RSV infection *in vivo* 166
5.5.1 Intranasal administration of GM-CSF antibody alters disease severity and viral load during RSV infection 167
5.5.2 Combined intraperitoneal and intranasal administration of GM-CSF antibody leads to significant weight loss and increased viral load during RSV infection 174
5.5.3 Summary 177
6 Conclusions 181
7 Future directions 192
8 Bibliography 196

Abbreviations

A

ACK	ammonium chloride potassium
ADV	adenovirus
AIM2	absent in melanoma 2
ALR	AIM2-like receptor
AM	alveolar macrophage
APC	antigen presenting cell
APC	allophycocyanin
Areg	amphiregulin
ATI/II	alveolar type I/II
ATP	adenosine triphosphate

B

BALF	bronchoalveolar lavage fluid
BM	bone marrow
BSA	bovine serum albumin

C

cDC	conventional dendritic cell
cDMEM	complete DMEM
cDNA	complimentary DNA
cGAS	cyclic GMP-AMP synthase
CLR	C-type lectin receptor
Ct	cycle threshold

D

DAMP	damage associated molecular pattern
DC	dendritic cell
DC-SIGN	dendritic cell-specific intercellular adhesion molecule-3-grabbing non-integrin
DENV	Dengue virus
DMEM	Dulbecco's Modified Eagle Medium
DNA	deoxyribonucleic acid
DNase	deoxyribonuclease
dsRNA	double stranded RNA

E

EBV	Epstein–Barr virus
ECM	extracellular matrix
EDTA	ethylenediaminetetraacetic acid
EGF	epidermal growth factor
ELISA	enzyme-linked immunosorbent assay
EMCV	Encephalomyocarditis virus
EpCAM	epithelial cell adhesion molecule

F

FACS	fluorescence-activated cell sorting
FCS	fetal calf serum
FFU	focus forming unit
FGF(b)	fibroblast growth factor (basic)
FI-RSV	formalin-inactivated RSV
FITC	fluorescein isothiocyanate
FSC-A/W/H	forward scatter-area/width/height

G

GAG	glycosaminoglycan
GAPDH	glyceraldehyde 3-phosphate dehydrogenase
G-CSF	granulocyte-colony stimulating factor
GM-CSF	granulocyte-macrophage colony-stimulating factor

H

HASM	human airway smooth muscle
HBSMC	human bronchial smooth muscle cell
HBVP	human brain vascular pericytes
HCV	hepatitis C virus
HEp-2	human epithelial type 2
HIV-1	human immunodeficiency virus
HMVEC	human microvascular endothelial cell
hrs	hours
HSV-1/2	herpes simplex virus 1/2

I

IAV	influenza A virus
IFN	interferon
IFNAR	interferon-α/β receptor
IFNGR	interferon-gamma receptor
IFNLR1	interferon-lambda receptor 1
IL	interleukin
ILC2	type 2 cytokine–producing innate lymphoid cell
i.n.	intranasally
i.p.	intraperitoneally
IRF	interferon regulatory factor
ISG	interferon stimulated gene
ISGF3	interferon-stimulated gene factor 3
ISRE	interferon-sensitive response element
i.v.	intravenously

J

JAK	janus kinase
JEV	Japanese encephalitis virus

K

KO	knockout

L

LPS	lipopolysaccharide
LRTI	lower respiratory tract infection

M

MACS	magnetic activated cell sorting
MAVS	mitochondrial antiviral-signaling protein
MCMV	mouse cytomegalovirus
MDA5	melanoma differentiation-associated protein 5
MHC I/II	major histocompatibility complex I/II
mins	minutes
MMTV	mouse mammary tumor virus
MOI	multiplicity of infection
mRNA	messenger RNA
MYD88	myeloid differentiation primary response gene 88

N

NET	neutrophil extracellular trap
NFκB	nuclear factor kappa-light-chain-enhancer of activated B cells
NK	natural killer
NLR	NOD-like receptor
NLRP3	NLR family, pyrin domain containing 3
NOD	nucleotide oligomerisation domain
NS1/2	non-structural protein 1/2

P

PAMP	pathogen-associated molecular pattern
PBS	phosphate buffered saline
PCR	polymerase chain reaction
pDC	plasmacytoid dendritic cell
PE	phycoerythrin
PerCP	peridinin chlorophyll
PIV	parainfluenza virus
PRR	pattern recognition receptor
pro-SpC	pro-surfactant protein C
PVM	pneumonia virus of mice

Q

qPCR	quantitative PCR

R

RIG-I	retinoic acid-inducible gene 1
RLR	RIG-I-like receptor
RNA	ribonucleic acid
rpm	revolutions per minute
RSV	respiratory syncytial virus
RT	room temperature
RV	rhinovirus

S

secs	seconds
Sftpc	pro-surfactant protein C
SH	small hydrophobic
SMC	smooth muscle cell
SN	supernatant
SP	surfactant protein
SSC-A/W/H	side scatter-area/width/height
ssRNA	single stranded RNA
STAT1/2	signal transducers and activators of transcription 1/2

T

TGF	transforming growth factor
Th	T helper
TIR	Toll/interleukin-1 receptor
TLR	Toll-like receptor
TMB	3,3′,5,5′-tetramethylbenzidine
TNF	tumour necrosis factor
Treg	regulatory T cell
TRIF	TIR-domain-containing adapter-inducing interferon-β

U

UV	ultraviolet
UV-RSV	UV-inactivated RSV

V

VACV	vaccinia virus
VEGF	vascular endothelial growth factor
VSV	vesicular stomatitis Indiana virus

W

WMV	Wad Medani virus
WNV	West Nile virus
WT	wildtype

Figure Index

Figure 1.1: Main structural components of RSV
Figure 1.2: Sensing of viral nucleic acids by intraceullar PRRs
Figure 1.3: Type I IFN signaling
Figure 1.4: Stromal cells in the lower airway
Figure 4.1: Gating strategy for flow cytometry
Figure 5.1: Dispase-digestion of mouse lung liberates more $CD45^{-}EpCAM^{+}CD31^{-}$ ATII epithelial cells than collagenase-digestion
Figure 5.2: $CD45^{+}EpCAM^{+}CD31^{-}$ and $CD45^{+}EpCAM^{+}CD31^{+}$ cells express pro-SpC and do not express T1α
Figure 5.3: Dispase-digested lung contains less virus than lung homogenate
Figure 5.4. MACS of ATII epithelial cells and other stromal cells from lung
Figure 5.5. FACS of ATII epithelial cells, endothelial cells and other stromal cells from lung
Figure 5.6: $CD45^{-}$ stromal cells are a major source of growth factors, chemokines and cytokines, whilst $CD45^{+}$ leukocytes are a major source of type I IFNs during RSV infection
Figure 5.7: Differential expression of type I IFNs, cytokines, chemokines and growth factors from stromal cell populations and AMs during RSV infection
Figure 5.8: Expression of type I IFNs, cytokines, chemokines and growth factors from stromal cell populations and AMs during UV-inactivated and live RSV infection
Figure 5.9: Expression of additional chemokines, cytokines, IFNs, growth factors and surfactant proteins by stromal cells and AMs during RSV infection
Figure 5.10: Production of cytokines, chemokines and growth factors from stromal cell populations 18hrs post RSV infection
Figure 5.11: CD90 staining of other stromal cells from mouse lung
Figure 5.12: Primary fibroblasts express chemokines in response to RSV
Figure 5.13: Generation of BM chimeras
Figure 5.14: Gene expression of IFNAR1 from sorted stromal cells and AMs from BM chimeras

Figure 5.15: Lung viral load and total and differential cell counts of BALF from IFNAR1$^{-/-}$ BM chimeras 18hrs post RSV infection
Figure 5.16: Protein analysis of BALF from BM chimeras 18hrs post RSV infection
Figure 5.17: Gene expression of amphiregulin, GM-CSF and IL-33 from sorted stromal cells and AMs from BM chimeras 18hrs post RSV infection
Figure 5.18: Gene expression of CCL2, CXCL1, CXCL10 and IL-6 from sorted stromal cells and AMs from BM chimeric mice 18hrs post RSV infection
Figure 5.19: Gene expression of IFN-α5 and IFN-β from sorted stromal cells and AMs from BM chimeric mice 18hrs post RSV infection
Figure 5.20: Intranasal GM-CSF antibody treatment during RSV infection
Figure 5.21: Intranasal administration of GM-CSF antibody does not significantly alter viral load or cell infiltration at 18 and 96hrs post RSV infection
Figure 5.22: Protein analysis of BALF at 18 and 96hrs post RSV infection after intranasal GM-CSF antibody administration
Figure 5.23: Combined intraperitoneal and intranasal GM-CSF antibody treatment during RSV infection results in increased weight loss and viral load
Figure 6.1: Early responses and crosstalk in the lower airway during RSV infection in vivo.

Table Index

Table 1.1: PRRs involved in virus recognition

Table 1.2: Human and mouse chemokines

Table 1.3: G protein-coupled chemokine receptors

Table 3.1: Antibodies for flow cytometry

Table 3.2: Antibodies for MACS

Table 3.3: Antibodies for in vivo neutralisation

Table 3.4: Antibodies for immunoplaque assay

Table 3.5: Antibodies and standard for IL-6 ELISA

Table 3.6: Antibodies and standard for IFN-α ELISA

Table 3.7: Composition of solutions, buffers and media

Table 4.1: Cell populations sorted by FACS

Table 4.2: Cell populations sorted by MACS

Table 4.3: Primer and probe sequences for qPCR

Table 4.4: Reaction composition for relative quantification of Areg, Cxcl1, Cxcl5, Cxcl10, Cxcl12, Ccl2, Ccl7, Csf2, Il1a, Il1b, Il6, Il33, Ifnar1, Ifna5, Ifng, Sftpc, Tgfb, Vegf

Table 4.5: Reaction composition for absolute quantification of L-gene

Table 4.6: Reaction composition for absolute quantification of Ifnb and Tnfa

Table 4.7: Thermal profile for qPCR

Table 5.1: Mediators expressed by other stromal cells 12hrs post-RSV infection

Table 5.2: Mediators expressed by ATII epithelial cells 4hrs post-RSV infection

Table 5.3: Expected IFNAR1 expression and type I IFN production in BM chimeras

Table 5.4: Main contaminants for MACS sorted ATII epithelial cells and other stromal cells

1 Introduction

1.1 Respiratory syncytial virus

1.1.1 Clinical manifestation and epidemiology

Respiratory syncytial virus (RSV) is the most common cause of acute lower respiratory tract infections (LRTIs) in infants with more than 30 million cases of acute LRTIs and 66,000 deaths worldwide in children under the age of 5 (Nair et al., 2010). There are two subtypes of RSV - A and B, which differ mainly on variations of their cell surface glycoprotein (G protein) (Sullender et al., 1998). Both strains circulate simultaneously, although one usually predominates during seasonal outbreaks (Mufson et al., 1987). However the general consensus is that there is no major difference in virulence between the two. RSV infects nearly all children by the age of two, with two to six month olds at highest risk of infection (Glezen et al., 1986).

Primary RSV infection usually manifests as a self-limiting mild upper respiratory tract infection with symptoms of a cold (sore throat, rhinorrhoea) four to six days after initial exposure, normally through contact with other infected individuals. However 1-3% of children develop more serious LRTIs such as bronchiolitis; an inflammation of the bronchioles, or viral pneumonia which requires hospitalisation (Glezen et al., 1986; Henderson et al., 1979; Kim et al., 1973). Symptoms of LRTI occur due to the strong influx of inflammatory cells into the lung, increased mucus production and the cytopathic effects of the virus on airway epithelial cells that lead to lung damage and airway obstruction (Johnson et al., 2007; Habibi & Openshaw, 2012). Risk factors for acute RSV infection include preterm birth, chronic lung disease and congenital or acquired immunodeficiencies (Borchers et al., 2013). In addition, genetic polymorphisms in several innate immune genes have also been associated with severe RSV disease (Awomoyi et al., 2007; Janssen et al., 2007; Miyairi & DeVincenzo, 2008). Children who suffer from severe LRTI have an increased risk of developing

recurrent wheeze and asthma-like symptoms in later life (Blanken et al., 2013). Mortality is rare in previously healthy children from industrialised countries, but significantly higher in those from developing countries and those with pre-existing chronic lung disease (Nair et al., 2010; Hall et al., 2001). Reinfections are common throughout life, with symptoms either absent or mild and restricted to the upper respiratory tract.

In addition, RSV can also cause severe lower respiratory tract disease in the elderly and immunocompromised, and constitutes a significant cause of mortality and morbidity in these groups (Falsey et al., 2005; Walsh & Falsey, 2012; Hall et al., 2001).

1.1.2 Treatment

Treatment for acute RSV infection is largely supportive care, consisting of nasal suction, bronchodilators and intravenous fluids to alleviate symptoms. The broad-spectrum antiviral ribavirin which works to disrupt viral RNA replication, is approved for use in its nebulised form for severe RSV-induced bronchiolitis in children, however its effectiveness is controversial (Borchers et al., 2013). There is also a prophylactic drug Palivizumab (MedImmune), a monoclonal antibody against the surface fusion (F) protein, approved for use in high-risk infants for prevention of LRTI (IMpact-RSV, 1998; Feltes et al., 2003). Currently there is no vaccine for RSV, and one of the key contributors for the slow development of candidates is due to the unsuccessful formalin-inactivated vaccine (FI-RSV) from the 1960s which not only failed to provide protection in the clinical trials, but enhanced disease upon natural infection, resulting in two deaths and a further 80% of the vaccinated children requiring hospitalisation (Kim et al., 1969). Later studies showed that mice immunised with the vaccine induced $CD4^+$ T cells with a type 2 cytokine expression profile, suggesting that the vaccine generated an imbalanced response in favour of allergic type 2 responses, rather than antiviral type 1 response that could effectively clear the virus (Graham et al., 1993).

1.1.3 Genome and structure

RSV is a non-segmented negative-sense single-stranded RNA (ssRNA) virus belonging to the *Paramyxoviridae* family. The genome consists of 10 genes that encode for 11 proteins: non-structural proteins 1 and 2 (NS1 and NS2), nucleoprotein (N), phosphoprotein (P), matrix proteins M, M2.1 and M2.2, small hydrophobic protein (SH), attachment glycoprotein (G), fusion protein (F) and RNA-dependent RNA polymerase (L) (Fields et al., 2013; Lay et al., 2013) (Fig. 1.1).

The viral envelope contains the SH, G and F proteins, with G involved in attachment to the cell and F responsible for fusion of the viral and cellular membrane (Collins & Melero, 2011; McLellan et al., 2011). The SH protein has been suggested to be a viroporin which when oligomerised, forms ion channels and enhances membrane permeability in the host cell, increasing RSV infectivity (Gan et al., 2012). The current proposed model of RSV binding and entry into the first cell of contact - epithelial cells, suggests that the G protein binds to host cell surface glycosaminoglycans (GAGs) heparin and chondroitin sulphate (Lambert, 1988). This primary binding allows the F protein to bind to the recently discovered RSV receptor nucleolin (Tayyari et al., 2011) on host cells. This allows fusion of the virus and host cell membrane, and delivery of the RSV virion into the cell (Lay et al., 2013).

The M protein forms the inner layer of the viral envelope and is important for viral assembly. The ssRNA is associated with the N, P, M2.1 and L proteins, which are all required for transcription of the viral genome. The M2.2 protein is also involved in regulation of viral RNA transcription and replication (Cheng et al., 2005) however whether it is packaged in the virion is not known. The NS1/2 proteins have immunosuppressive roles, impeding the host type I interferon (IFN) response to the virus by inhibiting the induction and signaling of IFNs (Borchers et al., 2013; Spann et al., 2004).

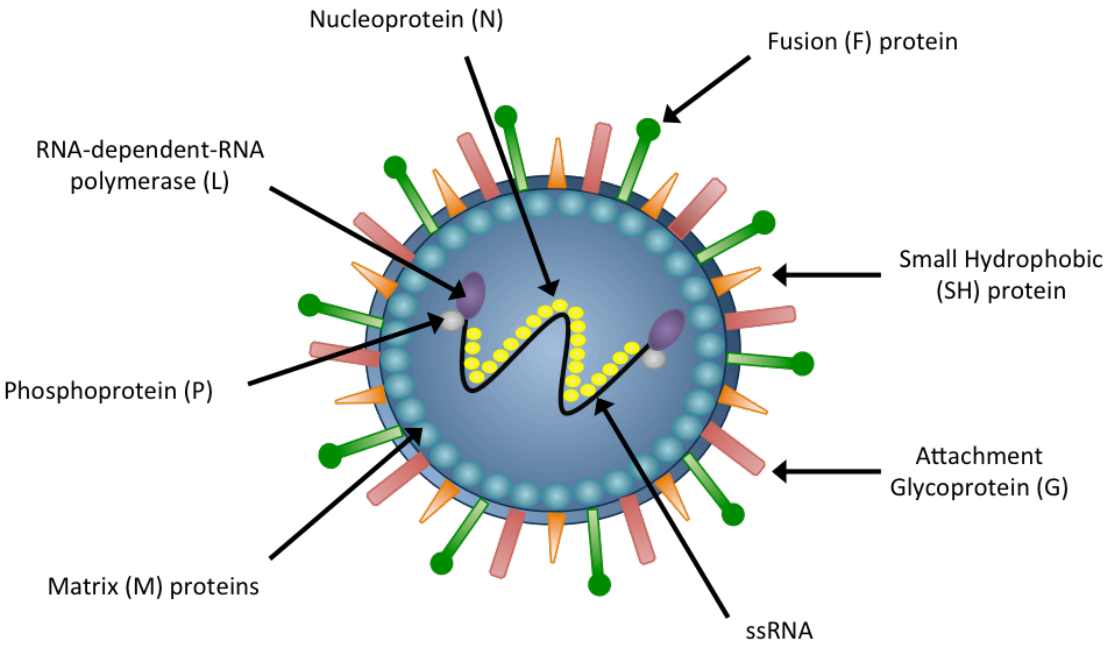


Figure 1.1: Main structural components of RSV. Simplified diagram depicting the main structural components of the RSV virion. The viral envelope contains three surface proteins: attachment glycoprotein G, fusion protein F and small hydrophobic protein SH. The matrix protein M forms the inner face of the envelope. The ssRNA is shown associated with nucleoprotein N, phosphoprotein P and large polymerase subunit L. Adapted from http://www.vtherm.com/rsv-bronchiolitis/.

1.2 Immune response to RSV

The primary immune response to RSV can be divided into 3 phases:

i. An early innate immune response during the first few hours after initial infection whereby cells such as airway epithelial cells, alveolar macrophages and dendritic cells detect virus and release proinflammatory cytokines and chemokines that attract other cells of the innate and adaptive immune response to the lung.
ii. An innate immune response characterised by an influx of inflammatory cells such as neutrophils, natural killer cells and monocytes into the airways.
iii. An adaptive immune response with antigen-specific effector T and B cells initiated by activated dendritic cells presenting viral antigens. T helper cells enhance the activity of immune cells, cytotoxic T cell cells kill virus-infected cells and B cells produce antibodies against the virus.

1.2.1 Detection of virus

RSV is initially detected by the host via pattern recognition receptors (PRRs); germ-line encoded innate immune receptors that recognise pathogen-associated molecular patterns (PAMPs). PRRs can be divided into several types, including Toll-like receptors (TLRs), retinoic acid-inducible gene 1 (RIG-I)-like receptors (RLRs), C-type lectin receptors (CLRs), nucleotide-binding oligomerisation domain (NOD)-like receptors (NLRs) and absent in melanoma 2 (AIM2)-like receptors (ALRs) which can recognise various virus molecules (Kawai & Akira, 2011; Hoving et al., 2014; Gürtler & Bowie, 2013; Jacobs & Damania, 2012; Pandey et al., 2015) (Table 1.1). PRRs that have been implicated to have a role during RSV infection include TLR2, 3, 4 and 7/8 (Segovia et al., 2012; Murawski et al., 2009; Rudd et al., 2005; Kurt-Jones et al., 2000; Haeberle et al., 2002; Lukacs et al., 2010), RLRs RIG-I and melanoma differentiation-associated protein 5 (MDA5) (Liu et al., 2007; Grandvaux et al., 2014; Bhoj et al., 2008; Demoor et al., 2012; Goritzka, Makris, et al., 2015a) and NLRs NOD2 (Sabbah et al., 2009) and NLRP3 (Segovia et al., 2012).

PRR	Type	Location	Viral ligand	Virus
TLR2	TLR	Cell surface	Unknown	RSV, HSV-1, VACV
TLR3	TLR	Endosome	dsRNA	RSV, HSV-1, WNV
TLR4	TLR	Cell surface	RSV F protein, MMTV envelope protein	RSV, MMTV
TLR7/8	TLR	Endosome	ssRNA	RSV, IAV, VSV, HIV-1
TLR9	TLR	Endosome	Unmethylated CpG DNA	MCMV, HSV1/2, ADV
RIG-I	RLR	Cytoplasm	5'ppp ssRNA, dsRNA	RSV, EBV, EMCV
MDA5	RLR	Cytoplasm	dsRNA	RSV, VACV, WMV, DENV
DC-SIGN	CLR	Cell surface	Carbohydrates	HIV-1, HCV
NLRP3	NLR	Cytoplasm	RSV SH protein, HCV RNA, EMCV 2B protein	RSV, HCV, EMCV
NOD2	NLR	Cytoplasm	ssRNA	RSV, IAV, VSV
cGAS	ALR	Cytoplasm	dsDNA	HSV-1, VACV
AIM2	ALR	Cytoplasm	dsDNA	VACV

Table 1.1: PRRs involved in virus recognition. dsDNA/RNA – double-stranded DNA/RNA; HSV1/2 - herpes simplex virus 1/2; VACV – vaccinia virus; WNV – Wad Medani virus; MMTV – mouse mammary tumour virus; IAV – influenza A virus; VSV – vesicular stomatitis Indiana virus; HIV-1 – human immunodeficiency virus 1; MCMV – mouse cytomegalovirus; ADV – adenovirus; EBV – Epstein-Barr virus; EMCV – Encephalomyocarditis virus; DENV – Dengue virus; HCV – hepatitis C virus. Adapted from (Oliveira-Nascimento et al., 2012; Kawai & Akira, 2011; Hoving et al., 2014; Gürtler & Bowie, 2013; Jacobs & Damania, 2012; Boehme & Compton, 2004).

1.2.2 Induction of the immune response

Stimulation of TLRs by RSV leads to activation of downstream adaptor proteins Toll/interleukin-1 receptor (TIR)-domain-containing adapter-inducing interferon-β (TRIF) for TLR3 and myeloid differentiation factor-88 (MyD88) for TLRs 2 and 7 (Fig. 1.2). TLR4 can activate both pathways. TRIF then activates interferon regulatory factor 3 (IRF3) to induce expression of type I IFNs, as well as nuclear factor kappa-light-chain-enhancer of activated B cells (NF-κB) to induce expression of proinflammatory cytokines and chemokines, whilst MyD88 activates IRF7 to induce type I IFNs and NF-κB for cytokines and chemokines (Perry et al., 2005).

As well as activating cell surface and endosomal TLRs, RSV also stimulates cytoplasmic RLRs and NLRs due to its replication cycle occurring in the cytosol (Borchers et al., 2013). MDA5 and RIG-I recognise the dsRNA and 5'ppp-ssRNA intermediates produced by replicating RSV (Fig. 1.2), which induces activation of the downstream adaptor protein mitochondrial antiviral signaling protein (MAVS) leading to NF-κB, IRF3 and IRF7 activation and subsequent expression of type I IFNs and proinflammatory cytokines and chemokines (Liu et al., 2007; Grandvaux et al., 2014).

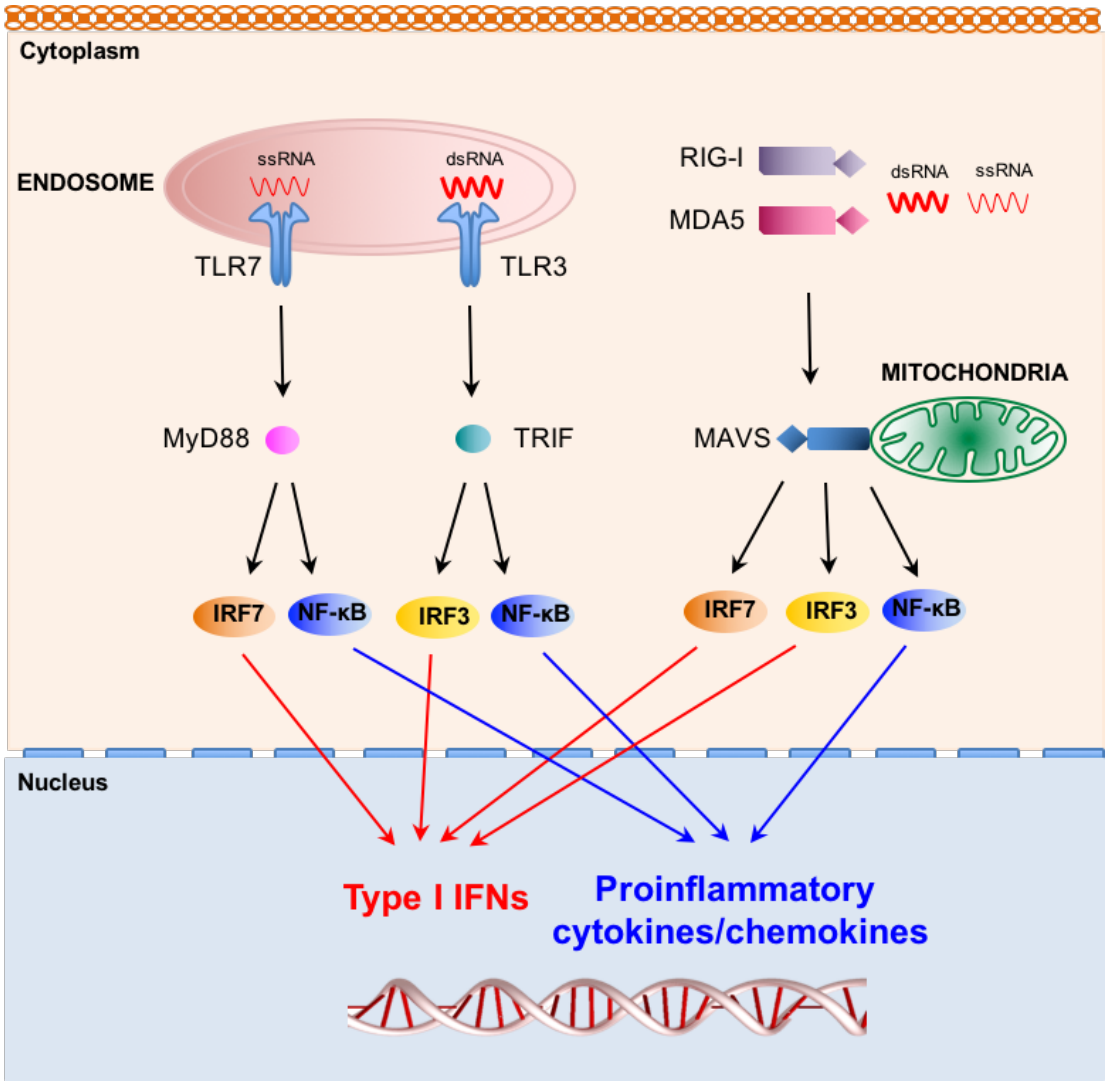


Figure 1.2: Sensing of viral nucleic acids by intracellular PRRs. Endosomal TLRs 3 and 7, and cytosolic PRRs RIG-I and MDA5 recognise viral nucleic acids such as ssRNA and dsRNA. TLR7 signals via the adaptor molecule MyD88 to activate IRF7 and NF-κB, whilst TLR3 signals via TRIF to activate IRF3 and NF-κB. RIG-I and MDA5 signal via the adaptor molecule MAVS to activate IRF3 and NF-κB. The IRFs translocate to the nucleus to enable transcription of type I IFNs, whilst NF-κB induces expression of proinflammatory cytokines and chemokines. Adapted from (Y. Sun et al., 2012).

The activation of IRF3 and IRF7 during initial detection of RSV is a critical component in the induction of the immune response to clear the virus. IRF3 is constitutively expressed in most cell types and induces expression of IFN-β and certain IFN-αs, whilst IRF7 is constitutively expressed in pDCs only and promotes expression of both IFN-αs and β (Au et al., 1995; Solis et al., 2006). Activation of these IRFs leads to the production of the early type I IFNs IFN-β and IFN-α1 (α4 in mice) from infected cells (Solis et al., 2006) and constitute the first limited wave of type I IFNs (Fig. 1.3). These secreted IFNs then bind to the IFN-α/β receptor (IFNAR) expressed on all nucleated cells, initiating the Janus kinase/signal transducer and activator of transcription (JAK/STAT) signaling pathway. STAT1 and STAT2 of this pathway then bind to IRF9 to form the multiprotein complex IFN-stimulated gene factor 3 (ISGF3). ISGF3 can then bind to specific DNA elements called ISRE (IFN-stimulated response elements) to induce transcription of IRF7, and subsequent induction of other IFN-αs and further IFN-β, in a positive feedback loop that produces the second amplified wave of type I IFNs (Takaoka & Yanai, 2006). This second amplified wave of type I IFNs is critical as it also induces the expression of hundreds of IFN-stimulated genes (ISGs), which include a wide range of proinflammatory cytokines, chemokines and soluble mediators (for a more in-depth analysis go to 1.2.4) needed to recruit and activate inflammatory cells to the site of infection, as well ISGs with direct antiviral effects. These latter cell intrinsic ISGs include 2'-5'-oligoadenylate synthetase 1 (OAS1), IFN-induced transmembrane protein (IFITM), viperin and protein kinase RNA-activated (PKR) which interfere with virus replication and limit productive infection (Goubau et al., 2013).

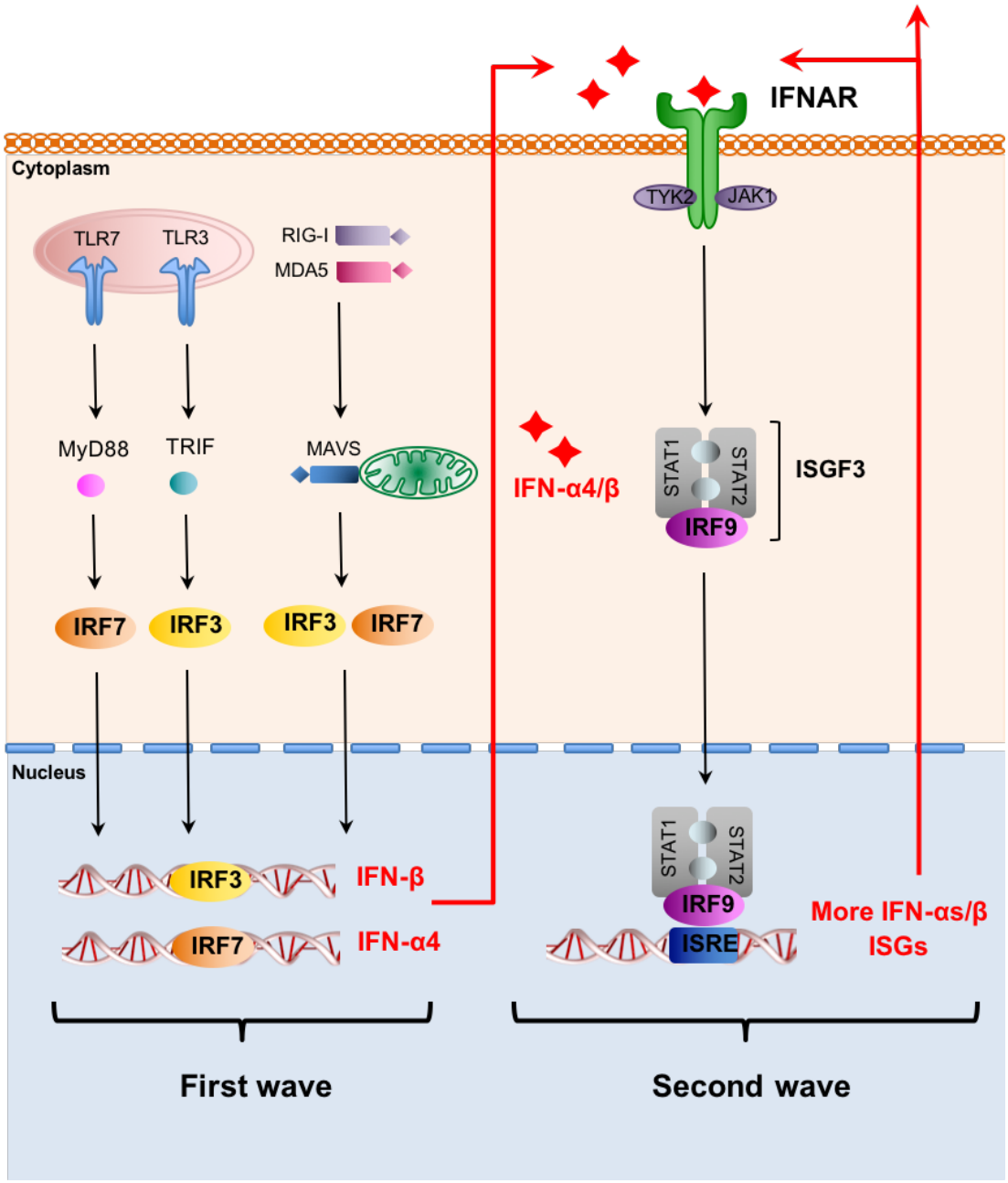


Figure 1.3: Type I IFN signaling. Viral activation of PRRs leads to activation of IRF3 and 7, which translocate to the nucleus to induce expression of IFN-β and IFN-α4 in mice (α1 in humans) generating the first limited wave of type I IFNs. These IFNs are secreted extracellulary and bind to IFNAR in an autocrine and paracrine manner and initiate the JAK/STAT signaling pathway. STAT1 and STAT2 bind to IRF9 to form ISGF3 which translocates to the nucleus to bind to specific IFN-stimulated response elements (ISRE), inducing transcription of ISGs and other IFN-αs and further IFN-β, in a positive feedback loop that generates the second amplified wave of type I IFNs. Adapted from (Y. Sun et al., 2012).

1.2.3 Cellular responses

Various cell types are involved in the response to RSV. These include resident lung cells such as epithelial cells and alveolar macrophages during the innate immune response, and recruited T and B cells during the adaptive response. This section will describe the major cellular responses as seen in human and mouse models of RSV infection, as well as from *in vitro* studies.

1.2.3.1 Epithelial cells

Epithelial cells line the airway and maintain a conduit for air to and from the alveoli. However, they are also one of the first cell types in the lung to come into contact with virus and as such, are one of the first lines of defence against RSV. This protection is provided via a physical barrier that includes tight junctions between the epithelial cells and is complimented by the mucociliary escalator (Vareille et al., 2011). Epithelial cells are also thought to secrete mediators that alert the immune system of infection and which recruit other immune cells to the site of infection, as well repair damaged and dead epithelial cells (Vareille et al., 2011). A more extensive description of epithelial cells, and their role during RSV is described in section 1.3.1 and 1.4.1 respectively.

1.2.3.2 Alveolar macrophages

Alveolar macrophages (AMs) are constitutively present in the lung and along with epithelial cells, are the first cells to encounter RSV when it enters the lower respiratory tract. These specialised tissue-resident cells reside in the lumen of the alveoli and are crucial in the maintenance and defense of the lung through their ability to remove dead cells and surfactant from the airways as well as their ability to phagocytose virus and virus-infected cells (Hussell & Bell, 2014). The growth factor granulocyte macrophage colony-stimulating factor (GM-CSF) is critical for AMs and is needed for development, proliferation, activation and survival of these cells (Shibata et al., 2001; Guilliams et al., 2013).

RSV antigen-positive AMs have been observed in lung tissue and bronchoalveolar lavage fluid (BALF) of mice and RSV-infected children (Jewell et al., 2010; Johnson et al., 2007; Midulla et al., 1993). In addition, mice depleted of AMs or with functional deficiencies in AMs show increased viral replication and virus-induced airway occlusion (Goritzka, Makris, et al., 2015a; Reed et al., 2008; Pribul et al., 2008; Benoit et al., 2006). In humans, AMs have been show to contain replicating virus that can infect other susceptible cells (Midulla et al., 1993) whist other studies have shown the opposite with viral shedding and replication limited in AMs *in vitro* (Kolli et al., 2014; Ravi et al., 2013; Stadnyk et al., 1997; Franke-Ullmann et al., 1995; Becker et al., 1991).

AMs are vital in the production of various proinflammatory mediators which are important for viral clearance. In mice, AMs have been shown to be a vital source of type I IFNs during RSV infection, and loss of this AM-derived type I IFNs leads to increased viral load and weight loss (Goritzka, Makris, et al., 2015a). In humans, AMs from BALF of RSV-infected children have been shown to express proinflammatory cytokines TNF-α and IL-1β (Midulla et al., 1993) and *in vitro* studies have shown them to further express cytokines and chemokines IL-6, IL-10, and CCL5 (Stadnyk et al., 1997; Panuska et al., 1995; Franke et al., 1994; Miller et al., 2004). Removal of AMs in mice leads to increased neutrophils and dendritic cells in the lung, but monocytes and natural killer cell recruitment and activation is reduced leading to ineffective viral clearance (Pribul et al., 2008; Kolli et al., 2014; Goritzka, Makris, et al., 2015a).

As previously stated, AMs also play a major role in the clearance of dead cells and debris, and during infection it is vital to remove dead and infected cells to prevent airway occlusion. Mice with defects in recognition and uptake of apoptotic cells were shown to have airway occlusion caused by the lack of removal of dead cells and debris post-RSV infection (Reed et al., 2008). This shows striking similarity to histopathological findings from children with fatal cases of RSV infection which also showed dead cells and occlusion in the lungs (Johnson et al., 2007; Welliver et al., 2007).

1.2.3.3 Neutrophils

Neutrophils are one of the first cells to migrate into the lung after RSV infection (Borchers et al., 2013). They are recruited from the blood to the site of infection by the release of potent neutrophil chemoattractants such as CXCL1 and CXCL8 (Kolaczkowska & Kubes, 2013). Neutrophils eliminate pathogens in several ways: phagocytosis, degranulation and by release of neutrophil extracellular traps (NETs) that immobilise the virus and prevent further spreading (Kolaczkowska & Kubes, 2013). The precise role of neutrophils in RSV pathogenesis is not clear. However, increased numbers of neutrophils have been observed in the airways of RSV-infected children and infants with RSV bronchiolitis (Everard et al., 1994; McNamara et al., 2004; Smith et al., 2001). Recruited neutrophils can cause epithelial damage through the release of free oxygen radicals and proteolytic enzymes which may exacerbate disease (Miyamoto et al., 2003) and cause epithelial damage and cell loss (Wang et al., 1998).

1.2.3.4 Monocytes

Monocytes are mononuclear phagocytes that arise from the bone marrow and circulate in the blood during steady state conditions. Under inflammatory conditions, monocytes traffic to the site of infection via CCR2 signaling which is dependent on the ligands CCL2 and CCL7 (Ginhoux & Jung, 2014) (for more in depth analysis on chemokine receptors/ligands and functions go to section 1.2.4.3). In the lung during RSV infection, monocyte recruitment has been shown to be a crucial mechanism of type I IFN-mediated antiviral activity in mice (Goritzka, Makris, et al., 2015a). *In vitro* studies have shown that monocytes can inhibit the spread of RSV to uninfected cells (Soukup & Becker, 2003) and express potent proinflammatory mediators such as IL-1β, IL-6, IL-15 and TNF-α (Takeuchi et al., 1998; Schijf et al., 2013; Ennaciri et al., 2007). In addition, RSV F protein has been shown to bind to TLR4 and the CD14 receptor on human monocytes, stimulating the release of IL-1β, IL-6, IL-8 and TNF-α (Kurt-Jones et al., 2000).

1.2.3.5 Dendritic cells

Dendritic cells (DCs) are the principle antigen-presenting cells (APCs) of the lung and are critical in the initiation of the adaptive immune response. Dendritic cells can be divided into plasmacytoid DCs (pDCs) and conventional DCs (cDCs). pDCs are a small subset of DCs that accrue mainly in the blood and lymphoid tissues. They express low levels of major histocompatibility complex class II (MHC-II) and co-stimulatory molecules in steady state as well as a narrow range of PRRs (Merad et al., 2013). cDCs populate most lymphoid and non-lymphoid tissues and have an enhanced ability to capture antigens, migrate and process and present antigens to naïve T cells, making them critical in initiating the adaptive immune response (Merad et al., 2013). In steady state, cDCs are immature and constantly survey the surrounding tissue environment for foreign antigens. Upon encountering foreign antigens or PAMPs that can activate PRRs, immature cDCs are triggered to mature. Lysosomes and antigen-processing machinery are activated to enhance peptide-MHC production, and CCR7 expression is upregulated to enable cDC migration to the lymph nodes (LNs). In addition co-stimulatory molecules CD80, CD86 and CD40 are also upregulated on the cell surface. Once cDCs have reached the LN, they present endogenous and exogenous antigens on MHC-I and MHC-II to $CD8^+$ and $CD4^+$ T cells respectively, and depending on the cytokine milieu secreted by cDCs during this interaction, different T cell lineages are induced (see section 1.2.3.7) (Mellman, 2013). cDCs in non-lymphoid tissues can be further divided into two major subsets: $CD103^+$ and $CD11b^+$ cDCs. $CD103^+$ cDCs are the main migratory subset during infection and are located within the epithelial layer of the airway (Hammad & Lambrecht, 2008). $CD103^+$ cDCs also have the ability to present exogenous non-cytosolic derived antigens via MHC-I in a process termed cross-presentation, making them potent activators of $CD8^+$ T cells during viral infection (Moltedo et al., 2011; Helft et al., 2012). $CD11b^+$ cDCs are the most abundant subset in the lung located in the lamina propria below the basement membrane (Plantinga et al., 2013) and are suggested to be the main producers of chemokines and cytokines in inflammation (Beaty et al., 2007; Plantinga et al., 2013).

In the nasal mucosa of children hospitalised with RSV, DC numbers correlate with viral load and persist for several weeks post infection (Gill et al., 2005). Mouse studies have shown there is a clear early influx of both pDCs and cDCs in the lungs and LNs in RSV infected mice (Beyer et al., 2004; Smit et al., 2006; Wang et al., 2006). However the kinetics remain controversial. There is general agreement that pDCs have a protective role during RSV infection and mouse models have shown that depletion of pDCs results in increased viral load, pulmonary inflammation and airway hyper-responsiveness (Wang et al., 2006; Smit et al., 2006). In contrast, cDCs are thought to contribute to pulmonary inflammation and pro-allergic responses. Studies have shown them to have a sustained capacity to induce T cell activation and proliferation which may result in excess immunopathology and increased sensitisation to antigens including allergens, which could lead to the development of allergic asthma after bronchiolitis (Beyer et al., 2004; Schwarze, 2008). The balance of cDC and pDC in RSV infection is further supported by studies in which both cDCs and pDCs were expanded in mice by Flt3L treatment prior to RSV infection to enhance the innate immune response. Once pDCs were depleted later on, this enhanced antiviral response was completely lost even though cDC numbers were maintained (Smit et al., 2008) highlighting that the balance between cDCs and pDCs is crucial for the outcome of RSV infection.

1.2.3.6 Natural killer cells

Natural killer (NK) cells play an important role in defending against viral infections via direct cytotoxicity and by the release of IFN-γ early on during infection. Direct cytotoxicity is mediated by the release of cytolytic granules containing perforin and granzymes onto the infected cell which induces apoptosis (Topham & Hewitt, 2009). Infected cells are identified by their downregulation of MHC-I, a virally induced mechanism used to avoid $CD8^+$ T cell detection and killing, as well as by expression of activating ligands, such as stress-induced ligands MHC-I polypeptide-related sequence A and B (MICA and MICB) (Topham & Hewitt, 2009). IFN-γ is a potent antiviral mediator that promotes increased antigen processing and presentation, primes DC function,

induces T cell differentiation towards the antiviral type 1 response and promotes antibody class-switching of IgM to IgA (Jost & Altfeld, 2013). However, studies have shown conflicting results on whether NK cells promote protection or pathology. RSV-induced bronchiolitis in young infants and children was shown to be associated with poor infiltration of NK cells into the airway (Welliver et al., 2007; De Weerd et al., 1998) and NK cell-depleted mice were shown to have increased viral lung load (Harker et al., 2010; Kaiko et al., 2010). In addition, IFN-γ from NK cells was shown to strongly stimulate the type 1 $CD8^+$ T cell response, and avoid type 2-induced pathology, thus providing protection from inappropriate host responses (Hussell & Openshaw, 1998; Kaiko et al., 2010). More recently however, NK cells have been shown to contribute to lung damage during the early stages of RSV infection in mice, thus suggesting they may also contribute to disease severity (Li et al., 2012).

1.2.3.7 T cells

Once professional APCs acquire and process virus antigens, they migrate to the LNs to present peptides to naïve T cells. After encountering their specific antigen, T cells differentiate into various subtypes depending on the cytokine milieu secreted by APCs and the way in which the antigen is presented to them. Antigens from cytosol-derived viral peptides are presented on MHC-I molecules to cytotoxic $CD8^+$ T cells, and extracellularly-derived peptides are presented on MHC-II molecules to helper $CD4^+$ T cells. Exogenous non-cytosolic derived antigens can also be presented via MHC-I in the process of cross-presentation (Blum et al., 2013). $CD4^+$ T cells further sub-divide into T helper (Th) subsets Th1, Th2 and Th17 as well as regulatory T (Treg) cells depending on the surrounding stimulating cytokines (Kara et al., 2014; Luckheeram et al., 2012).

Both $CD4^+$ and $CD8^+$ T cells have been implicated in viral clearance and exacerbation of RSV disease. When $CD8^+$ and $CD4^+$ T cells were depleted in mice, RSV replication was markedly prolonged, yet no illness was evident suggesting that the host immune response rather than virus-induced cytopathology was the primary determinant of disease (Graham et al., 1991). However, when RSV-

specific $CD8^+$ T cells were transferred to immunodeficient mice, persistent RSV infection was cleared within 5 days and in immunocompetent mice, the rate of viral clearance was proportional to the number of transferred $CD8^+$ T cells (Cannon et al., 1988). In a another study, transfer of antigen-specific $CD4^+$, $CD8^+$ or both T cells subsets into mice led to weight loss and increased severity of lung pathology during infection, and $CD4^+$ T cell recipients also developed pulmonary eosinophilia (Alwan et al., 1992). Furthermore, fewer $CD4^+$ T cells were required to decrease lung viral titre compared to $CD8^+$ T cells, and $CD4^+$ T cells also secreted more cytokines than $CD8^+$ T cells, suggesting that cell-for-cell, $CD4^+$ T cells were more antiviral and immunopathogenic than $CD8^+$ T cells during infection (Alwan et al., 1992). Both the perforin/granzyme pathway and Fas-FasL interaction are thought to be the mechanism of $CD8^+$ T cell cytotoxicity, however deletion of either of these pathways alone only delays viral clearance, and does not prevent it (Aung et al., 2001; Rutigliano & Graham, 2004).

In human cases of fatal RSV infection, there are discrepancies in the involvement of T cells. Human lung samples have been shown to be completely devoid of $CD8^+$ T cells (Welliver, 2008) as well as show $CD8^+$ T cells to outnumber $CD4^+$ T cells (Johnson et al., 2007). In hospitalised children with RSV bronchiolitis, $CD8^+$ T cell levels in the blood were inversely correlated with disease severity (De Weerd et al., 1998). In a recent human experimental RSV infection challenge, pulmonary RSV-specific $CD8^+$ T cells accumulated to high frequencies through to convalescence without continued proliferation (Jozwik et al., 2015). These cells displayed a tissue-resident memory phenotype, a recently defined subset of non-circulating memory T cells (Park & Kupper, 2015). The abundance of these cells before infection correlated with reduced symptoms and viral load suggesting that they confer protection against severe RSV disease (Jozwik et al., 2015). The antigenic targets of RSV-specific $CD8^+$ T cells have not been systematically examined, however several epitopes have been identified. These include peptides from the F, SH, M, M2, N, NS1 and NS2 proteins of RSV, but not G (Cherrie et al., 1992; Goulder et al., 2000; Jozwik et al., 2015) and it has been suggested that the lack of $CD8^+$ T cell responses to the G protein is a significant factor in inefficient viral clearance (Srikiatkhachorn & Braciale, 1997).

Viral infections typically induce a $CD4^+$ Th1 response to clear infection, however studies from severe RSV-infected children show elevated levels of $CD4^+$ Th2-specific cytokines (Lee et al., 2007; Legg et al., 2003). This suggests, and is consistent with other studies, which propose that an excessive type 2 and/or deficient type 1 immune response is responsible for causing severe disease and bronchiolitis (Becker, 2006; Hassan et al., 2008). However some studies have observed the complete opposite, and shown type 1 responses to be more immunopathological (Garofalo et al., 2001; Mobbs et al., 2002). The conflicting data on whether the $CD4^+$ or $CD8^+$ and type 1 or type 2 T cell response is protective or detrimental, suggests that it may be a balance of them all that leads to clearing of the virus rather than a skewed response to either type.

Tregs are crucial for maintaining tolerance to self antigens as well as to suppress potentially deleterious activities of T cells during infection (Josefowicz et al., 2012). Following RSV infection, activated Tregs accumulate in the lung and reduce disease severity, suppressing $CD4^+$ and $CD8^+$ T cells in mice (Durant et al., 2013; Loebbermann, Thornton, et al., 2012b). Furthermore, following vaccine-enhanced disease after FI-RSV vaccination, increased recruitment of Tregs was shown to ameliorate disease (Loebbermann et al., 2013). These studies suggest that Tregs have a protective role during RSV infection.

1.2.3.8 B cells and humoural response

The cell surface SH, G and F proteins are the main targets for the host humoural response against RSV. However, despite the SH and F proteins being well conserved, antibody responses are short term and only partially protective, and reinfections with the same strain of RSV are common throughout life (Borchers et al., 2013). B cell responses are initiated following antigen recognition via activated DCs that have migrated to lymphoid tissues. With the help of $CD4^+$ T cells, B cells differentiate into antibody-secreting plasma cells and memory B cells, with plasma cells producing antibodies that can directly neutralise the virus, block viral entry of cells, fix complement, promote phagocytosis and allow antibody-dependent cellular cytotoxicity (Chiu & Openshaw, 2015). Plasma cells

also migrate to survival niches in the bone marrow and lung following antigen clearance and are responsible for maintaining subsequent antibody titres (Chiu & Openshaw, 2015). The main antibody subtypes detected in serum and secretions against RSV are IgA, IgG and IgM (Habibi et al., 2015; Welliver et al., 1980; McIntosh et al., 1978; Kaul et al., 1981). Whether these antibodies are effective in preventing or clearing RSV infection is debatable, as antibody responses in patients with severe LRTI and mild upper respiratory tract infections are similar in magnitude, suggesting that development of RSV-induced LRTI is not due to poor antibody responsiveness (Welliver et al., 1980; Kaul et al., 1981). However IgA, which is important for defense at mucosal surfaces, has recently been suggested to be a correlate for protection against recurrent infection as those with nasal RSV-specific IgA prior to experimental infection with RSV, were less likely to develop PCR-confirmed RSV infection after RSV challenge (Habibi et al., 2015).

1.2.4 Soluble mediators

During the immune response, cells release soluble mediators such as cytokines, chemokines and growth factors to clear the virus and maintain tissue integrity. Although human and murine studies of RSV infection have identified various soluble mediators to be expressed overall during infection, and *in vitro* studies using cell lines have shown that RSV stimulation can induce certain cell types to express these soluble mediators, the cellular source of these soluble mediators *in vivo* and their exact role remain unclear or unknown.

1.2.4.1 Cytokines

Cytokines are a broad category of small proteins involved in cell signalling. They can be divided into various functional classes including interleukins, tumour necrosis factors, IFNs and chemokines. Some classifications also include growth factors under the cytokine nomenclature. For the purposes of this thesis IFNs,

chemokines and growth factors will be classed and discussed separately to all other cytokines (interleukins and tumour necrosis factors), which will otherwise fall under this section.

A wide range of cytokines have been detected *in vitro* and *in vivo* in response to RSV (Borchers et al., 2013; Zeng et al., 2011; Tripp et al., 2005). This section will expand on a few cytokines, particularly those that have been highlighted both in mouse and human, and those in which modulation leads to profound effects on the outcome of infection. The most common cytokines detected in response to RSV stimulation of human and mouse epithelial cell lines (tracheal, bronchiolar and/or alveolar) are IL-1β, IL-6, and TNF-α, and some of these as early as four hours (hrs) post stimulation (Schijf et al., 2013; Yoon et al., 2007; Das et al., 2005; Noah & Becker, 1993). IL-1β, IL-6 and TNF-α are important mediators of the inflammatory response, involved in cell differentiation, survival and apoptosis as well as induction of other proinflammatory cytokines (Akdis et al., 2011). In nasal secretions from children early in the course of RSV infection, cytokines IL-6 and TNF-α have been identified (Noah et al., 1995; Sheeran et al., 1999) and high IL-6 concentrations correlate with increased severity of illness (Hornsleth et al., 1998). These cytokines have also been shown to be induced in mouse models of RSV infection (Bhoj et al., 2008; Goritzka et al., 2014; Goritzka, Makris, et al., 2015a).

IL-10 is a regulatory cytokine that is induced in RSV-infected mice (Loebbermann, Schnoeller, et al., 2012a; Weiss et al., 2011; Sun et al., 2011) and has also been detected in nasal secretions and serum from infants with severe RSV bronchiolitis (Legg et al., 2003; Murai et al., 2007). RSV infection of IL-10 knockout mice resulted in more severe disease with enhanced weight loss and greater cell infiltration, however with no effect on viral load. These mice also had heightened levels of proinflammatory cytokines and chemokines and the proportion of IFN-γ producing T cells was enhanced, suggesting that IL-10 inhibits disease and inflammation during RSV infection (Loebbermann, Schnoeller, et al., 2012a). Transgenic expression of IL-10 in the nasal mucosa of mice (IL-10 transgenic mice) resulted in decreased viral replication in the nasal

mucosa and lung in association with increased cytotoxicity of nasal $CD4^+$ T cells (Ruan et al., 2001).

More recently, IL-33 has been shown to be elevated in nasal aspirates from infants hospitalised with RSV (Saravia et al., 2015). IL-33 is a multifaceted soluble mediator, it can function as a type 2 cytokine that can induce the recently identified population of naturally resident lung cells, group 2 innate lymphoid cells (ILC2s) to produce IL-13 (Neill et al., 2010). It can also behave as a damage-associated molecule or alarmin, as extracellular ATP released from damaged cells induces translocation of newly synthesised IL-33 from the nucleus to the cytoplasm (Carta et al., 2013; Kouzaki et al., 2011). Mice infected with RSV, were shown to have detectable IL-33 in the lung (Zeng et al., 2015b; Saravia et al., 2015) and this was shown to come from cells such as ATII epithelial cells (Saravia et al., 2015) and AMs (Qi et al., 2015). In addition, intranasal administration of recombinant IL-33 into mice resulted in increased airway hyperresponsiveness and a more severe RSV disease phenotype, suggesting that excessive IL-33 can have immunopathological effects (Saravia et al., 2015). Studies in Pneumonia Virus of Mice (PVM) infection models, a natural rodent pathogen of mice in the same family as RSV, was also shown to induce expression and release of IL-33 in mice (Kaiko et al., 2013).

1.2.4.2 Interferons

Interferons (IFNs) belong to a family of soluble mediators that provide robust antiviral immunity by restricting viral growth and spread. There are three types of IFNs. Type I IFNs, which encompass all the IFN-α subtypes (13 in human, 14 in mice), IFN-β, IFN-ε, IFN-κ and IFN-ω. Type II IFNs with one sole member IFN-γ, and type III IFNs made up of several IFN-λs (Durbin et al., 2013). Type I IFNs signal via the ubiquitously expressed receptor IFNAR, type II via the IFN-γ receptor (IFNGR) present on most cells, and type III via the IFN-λ receptor 1 (IFNLR1) expressed mostly on epithelial cells (Durbin et al., 2013; Beatty & Paterson, 2001; Mordstein et al., 2010). Only type I and III IFNs are induced directly in response to virus infections, with type I IFNs providing the most

critical antiviral role as they initiate the positive feedback loop required for amplified type I IFN response and the induction of ISGs (Vareille et al., 2011).
Induction of type I IFNs have been observed both *in vitro* and *in vivo* in mice in response to RSV (Jewell et al., 2007; Demoor et al., 2012; Bhoj et al., 2008; Goritzka et al., 2014). The importance of type I IFNs in the immune response to RSV is demonstrated through IFNAR knockout mice which displayed increased lung viral load and weight loss, as well as significantly reduced levels of proinflammatory cytokines and chemokines such as IL-6, IL-1β, TNF-α and CXCL10 (Goritzka et al., 2014). Furthermore, pretreatment of mice with IFN-α intranasally reduced viral load, inflammation and disease severity (Guerrero-Plata et al., 2005). Interestingly, administration of IFN-α2α to infants with established RSV infections did not reduce severity of illness (Chipps et al., 1993). Although, this may have been due to the route of IFN delivery (intramuscular) which may not have allowed IFN-α2α to reach the lung, suboptimal dosage or the time of IFN administration during the course of infection. Weak IFN-α staining has been observed in cells lining the airways of mice infected with RSV (Jewell et al., 2007). However more recently, it was shown that AMs were the major source of type I IFNs in mice during RSV infection, and these IFNs were critical in the recruitment of inflammatory monocytes via CCL2 to clear infection (Goritzka, Makris, et al., 2015a).

The type I IFN response is highly antiviral and as such RSV has evolved ways of circumventing this response. The RSV genome includes two proteins - NS1 and NS2, that can interfere with the induction of type I IFNs (Borchers et al., 2013). NS1 has been shown to bind to MAVS, inhibiting the MAVS-RIG-I interaction required for type I IFN production (Boyapalle et al., 2012; Ling et al., 2009) and NS2 induces the degradation of STAT2, interrupting IFNAR signaling and thus inhibiting the autocrine responses in infected cells (Swedan et al., 2009; Ramaswamy et al., 2006). This is further confirmed when RSV lacking the NS1 and NS2 genes induce higher levels of type I IFNs in macrophages as well as epithelial cells, compared to wildtype virus (Spann et al., 2004). More recently the NS2 protein has been shown to also promote shedding of infected epithelial cells resulting both in accelerated viral clearance but also acute distal airway

obstruction due to accumulation of detached epithelial cells (Liesman et al. 2014).

1.2.4.3 Chemokines

Chemokines belong to a family of soluble mediators that are involved in the recruitment of cells via the process of chemotaxis. They can be subdivided into four functionally distinct groups based on the spacing of highly conserved NH2-terminal cysteine residues: C, CC, CXC and CX_3C chemokines (Table 1.2) and they bind to G protein-coupled chemokine receptors differentially expressed on all leukocytes (Table 1.3) (Griffith et al. 2014). They are critical mediators of the immune response to RSV due to their role in recruiting and directing leukocytes to the site of infection to clear the virus, with many of them also being ISGs.

In vitro, murine alveolar epithelial cells were shown to produce CCL2, CCL5, CXCL10 and CXCL1 in response to RSV stimulation (Miller et al. 2004). *In vivo,* RSV-infected mice up regulate CCL2, CCL3, CCL5, CXCL10 and CXCL1 and it was shown that viral replication was necessary for optimal chemokine production (Miller et al. 2004, Bhoj et al. 2008, Lindell et al. 2008, Goritzka et al. 2014). Human *in vitro* studies have shown similar observations to mice studies with CXCL8 expressed after RSV stimulation in both bronchial and alveolar cell lines (Yoon et al. 2007, Schijf et al. 2013).

Chemokines elevated in respiratory aspirates from infants with RSV bronchiolitis include CCL2, CCL3, CCL5, CXCL8 and CXCL10 (Sheeran et al. 1999, Garofalo et al. 2001, McNamara et al. 2005). These correlated with the number of leukocytes present in the samples suggesting that chemokines were recruiting these cells into the airway and/or leukocytes themselves were secreting these chemokines. Furthermore, mouse models have shown that CCL2 is a critical chemokine in the innate immune response to RSV through its ability to recruit inflammatory monocytes that significantly limit viral load and disease severity (Goritzka, Makris, et al. 2015). Similarly, CCL3 has also been shown to be

important. CCL3 knockout mice have more RSV-specific T cells recruited to the lung, which is accompanied by increased weight loss and illness after infection (Tregoning et al. 2010). However, other studies have found CCL3 knockout mice to have a significant reduction in lung inflammation, although no difference in peak viral lung load was observed (Haeberle et al. 2001). Furthermore, CXCL10 was shown to increase more than 100-fold in RSV infected human airway epithelial cells (Ioannidis et al. 2012), and in mice, antibody-mediated neutralisation of CXCL10 resulted in significant increase in disease pathogenesis and impaired viral clearance (Lindell et al. 2008).

Overall these studies reveal that the most common chemokines detected in children with RSV bronchiolitis are neutrophil, monocyte/macrophage and T cell chemoattractants and depletion of these chemokines in mouse models leads to mostly impaired viral clearance, although reduced host-induced cytopathology is also seen.

Chemokine	Receptor (mouse receptor)	Main functions
CCL1	CCR8	Treg and monocyte migration
CCL2	CCR2	Monocyte migration
CCL3	CCR1, CCR5	Macrophage and NK cell migration
CCL4	CCR5	Monocyte and NK cell migration, T cell-DC interactions
CCL5	CCR1, CCR3, CCR5	T cell, macrophage and basophil migration, T cell-DC interactions
CCL7	CCR2, CCR3	Monocyte mobilisation
CCL8	CCR1, CCR2, CCR3, CCR5 (CCR8)	Type 2 response
CCL11	CCR3	Eosinophil and basophil migration
CCL12 *	CCR2	Monocyte migration
CCL13 **	CCR2, CCR3, CCR5	Type 2 response
CCL17	CCR4	Type 2 response
CCL18 **	CCR8	Type 2 response
CCL19	CCR7	T cell and DC homing to LN
CCL20	CCR6	T and B cell migration, Th17 response
CCL21	CCR6, CCR7	T cell and DC homing to LN
CCL22	CCR4	Type 2 response, Treg migration
CCL24	CCR3	Eosinophil and basophil migration
CCL25	CCR9	Thymocyte migration
CCL26	CCR3, CX3CR1	Eosinophil and basophil migration
CCL27	CCR10	T cell homing to skin
CCL28	CCR3, CCR10	T cell and IgA plasma cell homing to mucosa
CXCL1	CXCR2	Neutrophil migration
CXCL2	CXCR2	Neutrophil migration
CXCL3	CXCR2	Monocyte migration
CXCL4	Unknown	Procoagulant
CXCL5	CXCR2	Neutrophil migration
CXCL6 **	CXCR1, CXCR2	Neutrophil migration
CXCL7	CXCR2	Neutrophil migration/activation
CXCL8 **	CXCR1, CXCR2	Neutrophil migration
CXCL9	CXCR3	Type 1 response, $CD8^+$ T cell and NK cell migration
CXCL10	CXCR3	Monocyte, macrophage, T cell migration
CXCL11	CXCR3	T cell migration
CXCL12	CXCR4	Bone marrow homing
CXCL13	CXCR5	B cell positioning in LN
CXCL14	Unknown	Macrophage skin homing
CXCL16	CXCR6	ILC migration
XCL1	XCR1	Cross-presentation, T cell migration
XCL2 **	XCR1	T cell migration
CX3CL1	CX3CR1	Monocyte, T and NK cell migration

Table 1.2: Human and mouse chemokines. List of human and mouse cytokines (column 1), binding receptors (column 2) and main functions (column 3). Chemokines with as yet unknown functions have been excluded. *mouse only, ** human only. Adapted from (Griffith et al. 2014).

Chemokine Receptor	Receptor Expression
CCR1	Monocytes, macrophages, DCs, neutrophils, basophils
CCR2	Monocytes, macrophages, NK cells, basophils
CCR3	Eosinophils, basophils, mast cells
CCR4	Monocytes, $CD8^+$ T cells, Tregs, B cells
CCR5	Monocytes, macrophages, DCs, neutrophils, NK cells, Tregs
CCR6	Th17 cells, NK cells, Tregs
CCR7	T cells, B cells
CCR8	Monocytes, macrophages, Tregs
CCR9	DCs, B cells, thymocytes
CCR10	T cells, IgA plasma cells
CXCR1	Monocytes, neutrophils, NK cells, mast cells, basophils, $CD8^+$ T cells
CXCR2	Monocytes, neutrophils, NK cells, mast cells, basophils, $CD8^+$ T cells
CXCR3	DCs, NK cells, B cells, Tregs, $CD8^+$ T cells
CXCR4	Almost all leukocytes
CXCR5	T cells, B cells
CXCR6	NK cells, T cells, plasma cells
XCR1	Cross-presenting DCs
CX3CR1	Monocytes, macrophages, DCs, NK cells, T cells

Table 1.3: G protein-coupled chemokine receptors. List of chemokine receptors and receptor expression on leukocytes. Adapted from (Griffith et al. 2014).

1.2.4.4 Growth factors

Growth factors regulate a variety of cellular functions that are critical not only for normal lung development and homeostasis, but also during infection and injury. Their main functions include stimulating cellular growth, proliferation, differentiation and survival of both leukocytes and stromal cells (Doherty and Broide 2007). Functionally, growth factors are a type of cytokine as they are involved in cell signalling, but their main function of stimulating cell growth makes them separate from other cytokines. Types of growth factors include epidermal growth factors (EGFs), fibroblast growth factors (FGFs), granulocyte (macrophage) colony-stimulating factors (GM-CSF and G-CSF), transforming growth factors (TGFs) and vascular endothelial growth factors (VEGFs) (Doherty and Broide 2007). Some interleukin cytokines such as IL-2 and IL-7 are also defined as growth factors as they stimulate T cell proliferation and differentiation (Mackall et al. 2011, Boyman and Sprent 2012). Similarly, GM-CSF a potent growth factor of both leukocytes and stromal cells is more commonly referred to as just cytokine. For the purposes of this thesis, we have categorised interleukins separately as cytokines, as many are not involved in cell growth and grouped growth factors based on nomenclature.

In vitro, human alveolar epithelial cells infected with RSV showed elevated levels of VEGF as little as two hours post infection (Lee et al. 2000), as well as fibroblastic growth factor basic (FGFb) and EGF (Dosanjh et al. 2003). TGF-β, GM-CSF, G-CSF and amphiregulin, a member of the EGF family, have also been detected from either human alveolar or bronchial epithelial cultures infected with RSV (Noah and Becker 1993, Soukup and Becker 2003, Monick et al. 2005, McCann and Imani 2007, Gibbs et al. 2009, Ishioka et al. 2011). Mice infected with recombinant RSV expressing GM-CSF, showed significantly reduced viral load compared to infection with wildtype virus and mice also had increased numbers of DCs and AMs with significantly increased expression of MHC-II on DCs, suggesting enhanced antigen presentation (Bukreyev et al. 2001). This suggests a protective role of GM-CSF in RSV infection, particularly in regards to the function of AM and DCs. Amphiregulin was shown to be important in

prolonging the survival of RSV-infected cells as well as inducing the release of CXCL8 from these cells, suggesting a role in both inflammation and repair during infection (Monick et al. 2005) and more recently was found to be elevated in mouse lungs up to 8 days post RSV infection (Goritzka, Pereira, et al. 2015).

Overall various cytokines, chemokines, IFNs and growth factors are detected during RSV infection *in vivo* in mouse and humans. However, the cellular sources for the majority of these mediators *in vivo* are not known. Nearly all *in vitro* data have come from various immortalised or primary epithelial cell lines that have been stimulated with RSV at multiplicity of infection (MOIs) that may not recapitulate what is happening in the lung. Whilst these epithelial cells have been shown to express various soluble mediators in response to RSV, they may not be the major cellular source *in vivo* and other types of stromal cells need to be investigated to determine their contribution.

1.3 Stromal cells

Stromal cells are the structural and connective tissue cells of an organ. In the lung these include epithelial cells, endothelial cells, fibroblasts, pericytes and smooth muscle cells (Perros et al. 2011) (Fig. 1.4). Their general function is to provide support, compartmentalisation and structural barriers in the lung, as well as allowing selective transport of molecules and cells across barriers to maintain lung function. As such they have a relatively high turnover rate that ensure the integrity of the lung remains stable (Perros et al. 2011).

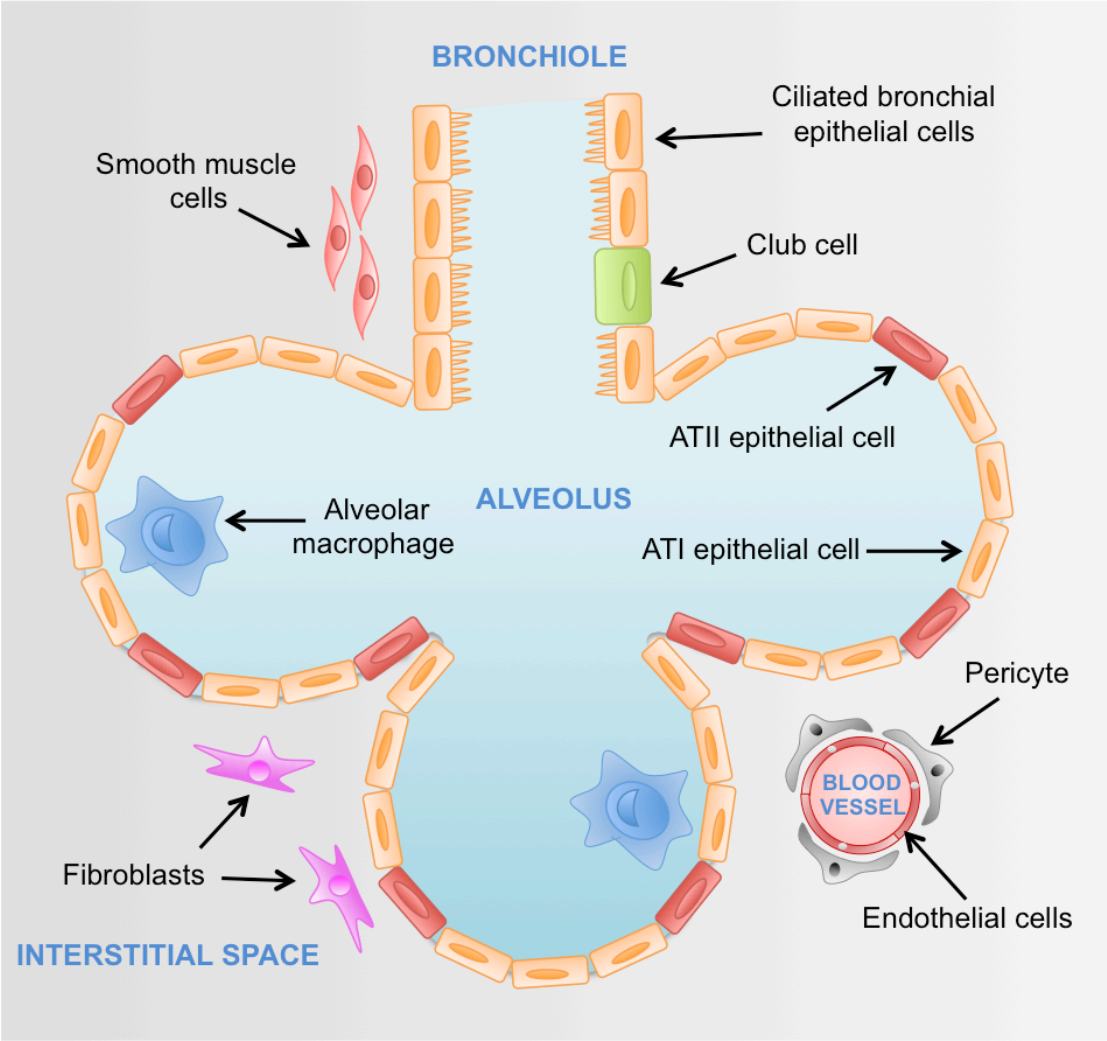


Figure 1.4: Stromal cells in the lower airway. The various types of stromal cells in the lower airway include those in the terminal bronchioles and alveoli. Bronchioles are lined with ciliated epithelial cells as well as club cells which secret proteins that protect the bronchioles. Alveolar type I and II (ATI/II) epithelial cells make up the lining of the alveoli, whilst smooth muscle cells and fibroblasts are found below the epithelium and in the interstitial space. Blood vessels line the respiratory tract and are made up of further stromal cells including vascular endothelial cells and pericytes. Adapted from (Hussell and Bell 2014).

1.3.1 Epithelial cells

The respiratory tract of the lung is lined with epithelial cells, which are an important primary contact for RSV when it enters the lung and are thought to be the primary cell type for viral propagation (Borchers et al. 2013). The respiratory epithelium is considered to provide a physical and functional barrier against virus infection that can promote early inflammatory responses that activate the immune system to eventually clear the virus (Vareille et al. 2011). The lung is divided into four main compartments: the trachea, bronchi, bronchioles and alveoli, and several types of epithelial cells characterise these different sections (Bantikassegn et al. 2015). Basal, goblet and ciliated cells compose the bronchi with the latter two crucial for maintaining the mucus membrane (Crystal et al. 2008), whilst club cells (formerly known as Clara cells) are primarily found in the bronchioles and produce club cell secretory protein (CCSP) that controls inflammation and oxidative stress in the lungs (Wang et al. 2012). Epithelial cells in the alveoli are characterised into alveolar type I (ATI) and alveolar type II (ATII) epithelial cells. ATI cells are the bigger of the subtypes, covering 95% of the surface area but only comprising 20% of the total epithelial cells in the alveoli and are involved in gas exchange (Fehrenbach 2001). ATII cells are smaller and comprise the remaining 5% surface area and 80% of total cells, and are crucial for the production of surfactants that regulate alveolar surface tension which is important for gas exchange (Fehrenbach 2001). ATII epithelial cells also produce antiviral surfactants, such as surfactant protein (SP) A and D that can act as opsonins (Vareille et al. 2011). ATII cells are considered the stem cells of the alveolar epithelium and continually replace both ATI and ATII cells at a cell turnover time (time taken to replace all cells of a given population) of 4-5 weeks, which can rapidly change to 3 days during injury (Fehrenbach 2001).

1.3.2 Endothelial cells

Endothelial cells form the inner lining of blood and lymphatic vessels. Both of these vessels serve distinct yet complementary functions, mainly in regulating tissue homeostasis as well as modulating immune responses, and as such their respective endothelial cells perform different functions (Podgrabinska et al. 2002). Lymphatic endothelium helps to regulate fluid and pressure equilibrium in tissues and also direct cells from tissues to the LNs (Podgrabinska et al. 2002). Blood and vascular endothelium play a major role in the extravasation of immune cells from the blood to the site of inflammation and are therefore thought to be more important in the immune response (Middleton et al. 2002). In the process of chemotaxis in blood vessels, chemokines from lung cells at the site of infection are transcytosed by vascular endothelial cells to their luminal surface and presented on GAGs to leukocytes migrating in the blood. Chemokines bound at the luminal endothelial cell surface build up in concentration, which leads to binding and activation of receptors on the leukocyte cell surface, and firm attachment of the leukocyte to the endothelial cell. Leukocytes then migrate transcellularly or through intercellular junctions across the blood vessel, and via the chemokine gradient, migrate to the site of infection (Gerhardt and Ley 2015). As well as presenting chemokines from other cells to attract blood leukocytes, vascular endothelial cells have been suggested to produce and present their own mediators such as CX3CL1 in response to proinflammatory cytokines such as TNF-α and IL-1α *in vitro* (Bazan et al. 1997, Middleton et al. 2002).

1.3.3 Fibroblasts

Fibroblasts are the most common cells of connective tissue in mammals, and synthesise extracellular matrix (ECM) and collagen that make up the structural framework of tissue (Kalluri and Zeisberg 2006). They exhibit several phenotypes including non-contractile fibroblasts, contractile myofibroblasts and protomyofibroblasts, however the markers that can fully differentiate them have yet to be conclusively identified (McAnulty 2007). As the primary source of ECM constituents – a single fibroblast can synthesis approximately 3.5 million

procollagen molecules a day (McAnulty et al. 1991), fibroblasts are considered the chief mediators of scar formation and tissue fibrosis in the lung and their role in airway remodeling after injury is well characterised (Descalzi et al. 2007, Bergeron et al. 2010, Westergren-Thorsson et al. 2010). Further roles of fibroblasts include regulation of epithelial differentiation, inflammation and wound healing, in which fibroblast interaction with both epithelial cells and immune cells has been highlighted (Tomasek et al. 2002, Parsonage et al. 2005, Kalluri and Zeisberg 2006).

1.3.4 Smooth muscle cells

Lung smooth muscle cells (SMCs) are cells that form a sheath around the respiratory tract and blood vessels (Kim and Vu 2006). SMCs lining blood vessels (termed vascular SMCs) are important for maintaining appropriate blood pressure by contracting and relaxing to change the luminal diameter of vessels (Rensen et al. 2007). Lung SMCs, similarly to fibroblasts, are also known for airway remodeling due to the fact that they can secret large amount of ECM components and exhibit increased proliferation and migration, particularly after inflammation (Owens et al. 2004). They are also heavily linked to development of asthma, and exacerbations of asthma are associated with viral respiratory tract infections. However little is known about their function in the immune response to infection.

1.3.5 Perciytes

Pericytes are cells that wrap around endothelial cells, forming the outer lining of blood vessels (Armulik et al. 2011). Their existence and role has for a long time been largely neglected, however they are now being shown to be essential components of blood vessels and important regulators of vascular formation, stabilisation, remodeling and function (Armulik et al. 2005, Bergers and Song 2005, Armulik et al. 2011). However, inconsistencies and a lack of a consensus pan-pericyte marker mean that studies on these cells *in vivo* during infection are restricted.

1.4 Stromal cells in infection

An emerging theme in respiratory infections is that stromal cells can produce cytokines, chemokines, IFNs and growth factors that can determine the quantity and quality of the immune response (Perros et al. 2011). However, literature is limited and a major reason for this is due to the lack of cell-specific markers for these cell types that can accurately distinguish them *in vivo*. Furthermore, unlike leukocytes and lymphocytes, the majority of stromal cells are connected to one another via tight junctions, which adds a further level of difficulty when isolating these cells (Perros et al. 2011). As such, the majority of studies on stromal cells and their production of mediators during infection have used cell lines, with very limited data from *in vivo* models. The following section will describe what is known to date about the role of epithelial cells, endothelial cells, fibroblasts and pericytes both *in vivo* and *in vitro* in RSV as well as in different infection models.

1.4.1 Epithelial cells in infection

RSV

There have been various *in vitro* studies looking at human and mouse airway epithelial cells in response to RSV. These studies have shown RSV to infect primary human nasal and bronchial epithelial cells, mainly ciliated, from the apical side and in small clumped patches (Wright et al. 1997, Zhang et al. 2002, Tayyari et al. 2011, Villenave et al. 2012, Guo-Parke et al. 2013). Mouse alveolar epithelial cell lines have been shown to produce type I IFNs (Jewell et al. 2007, Ioannidis et al. 2012) and that this could be in part dependent on the MAVS signaling pathway (Demoor et al. 2012). Furthermore, upon stimulation with RSV, alveolar epithelial cell lines from both mouse and human, as well primary and immortalised human bronchial epithelial cell cultures have been shown to produce a variety of chemokines and cytokines that could modulate the immune response. These include chemokines CCL2, CCL5, CXCL1, CXCL5, CXCL8, CXCL9 and CXCL10 (Tristram et al. 1998, Miller et al. 2004, Okabayashi et al. 2009,

Ioannidis et al. 2012, Levitz et al. 2012) and cytokines IL-6 and IL-33 (Tristram et al. 1998, Jewell et al. 2007, Ioannidis et al. 2012, Levitz et al. 2012, Ioannidis et al. 2013). In addition, growth factors such as TGF-β, G-CSF, VEGF and amphiregulin have also been detected from human alveolar or bronchial epithelial cultures infected with RSV (Noah and Becker 1993, Lee et al. 2000, Soukup and Becker 2003, Monick et al. 2005, McCann and Imani 2007, Gibbs et al. 2009, Ishioka et al. 2011) as well as GM-CSF from both murine and human alveolar epithelial cell lines (Monick et al. 2005, Ishioka et al. 2011, Albrecht et al. 2012).

In vivo studies on epithelial cells are far more limited, and only a handful of studies have been performed in mice, with human studies further limited to a few fatal cases of RSV. These studies mainly provide data on the location of the virus in the lung epithelium, with very few expanding on the mediators produced by these cells. These latter studies observed limited IFN-α staining in cells lining the airways (suggested to be epithelial cells) of RSV-infected mice (Jewell et al. 2007) and IL-33 expression from ATII epithelial cells from mice infected with RSV (Saravia et al. 2015). Immunohistochemical staining of bronchiolar and alveolar tissue from infants who had died of RSV infection showed viral antigen present in both the ciliated bronchiolar and non-ciliated alveolar epithelial cells (Johnson et al. 2007, Welliver et al. 2007). Similarly in mouse studies, viral infection was observed in the epithelium lining the bronchi and bronchioles (Bhoj et al. 2008) and alveolar spaces (Jewell et al. 2007) after RSV inoculation. When identifying nucleolin as a candidate receptor for RSV, Tayyari et al showed that RSV and nucleolin overlapped on the apical side of airway epithelial cells in mice (Tayyari et al. 2011).

Other infections

Human cytomegalovirus (HCMV) infection is mostly associated with the salivary glands however the lung is known to be heavily involved during the disease and may exemplify the situation in other organs. Lung tissue sections from patients suffering from acute HCMV infection showed that the majority of infected cells were alveolar epithelial cells (Sinzger et al. 1995). Studies from influenza A virus (IAV) infection have shown IL-33 production in alveolar epithelial cells in mice

(Le Goffic et al. 2011) and CCL5, CXCL10, IL-6 and IFN-β from primary human alveolar epithelial cells (Chan et al. 2005). Human lung explants subsequently infected with IAV showed virus to be exclusively detected in ATII epithelial cells with minor involvement of AMs (Weinheimer et al. 2012). Furthermore, in a rhinovirus (RV) infection model, human alveolar epithelial cell lines were shown to express chemokines CCL5 and CXCL8 in response to infection (Chun et al. 2013).

1.4.2 Endothelial cells in infection

RSV

Literature on the role of endothelial cells in RSV infection is extremely limited, and to our knowledge it has only been shown that RSV can readily infect human endothelial cell lines (Arnold and König 2005).

Other infections

Histological data from fatal cases of IAV infection have shown endothelial cells to express IL-6 (Nakajima et al. 2013) and IFN-β (Deng et al. 2008). *In vitro*, human pulmonary microvascular endothelial cells (HMVECs) infected with IAV showed expression of IL-1β, IL-6, IL-8, TNF-α, CCL5 and CXCL10 (Kim et al. 2015, Zeng, Belser, et al. 2015). Furthermore the virus replicated within endothelial cells and this lasted up to 48hrs post infection (Kim et al. 2015). In a rare study using sorted endothelial cells from IAV infected mouse lung, elevated expression of CCL2, CCL5 and CXCL10 were observed in these cells in response to infection (Teijaro et al. 2011). *Legionella pneumophila* a gram-negative bacterium that causes severe pneumonia was shown to infect and grow within cultured human endothelial cells suggesting a potential role in the systematic spread of the pathogen (Chiaraviglio et al. 2008). Similarly *Mycobacterium tuberculosis* was shown to infect human endothelial cell lines with replication detected 48hrs post infection (Mehta et al. 2006).

1.4.3 Fibroblasts in infection

RSV

Human foetal lung fibroblast cell lines produced an array of mediators including proinflammatory cytokines IL-6, chemokines CCL2, CCL3, CXCL8 and CXCL10 and growth factors G-CSF, GM-CSF and VEGF, 24hrs post stimulation with RSV (Seki et al. 2013). These cells have also been shown to produce IL-11, a chemokine belonging to the IL-6 family (Elias et al. 1994, Einarsson et al. 1996) and primary mouse lung fibroblasts have been shown to express IFN-β in response to RSV stimulation (Bhoj et al. 2008).

Other infections

Lung tissue sections from patients suffering from acute HCMV infection showed that fibroblasts were a major population of HMCV-infected cells (Sinzger et al. 1995) and infection of human lung fibroblasts with HCMV showed induced expression of CCL2 and IL-6, with the latter showing continuous upregulation up to 72hrs post infection (Wolf et al. 2012, Murayama et al. 2014). IL-1β, IL-6, TNF-α, CCL5, CXCL8 and CXCL10 have been detected from human foetal lung fibroblast cell lines infected with IAV (Kim et al. 2015) and parainfluenza virus (PIV) (Yoshizumi et al. 2010), with the latter also detecting increased expression of growth factors GM-CSF and G-CSF 24hrs post infection (Yoshizumi et al. 2010). VEGF has also been detected from primary and immortalised fibroblasts after RV infection (Ghildyal et al. 2005, De Silva et al. 2006). Primary human bronchial fibroblasts were highly susceptible to RV infection, with CXCL8 and IL-6 rapidly induced by both live and UV-inactivated virus, whilst CCL5 was only expressed with live virus, suggesting that viral replication is required for induction of certain mediators during infection (Bedke et al. 2009). Interestingly, IFN-β expression was not significantly altered (Bedke et al. 2009), however primary human bronchial fibroblasts stimulated with the synthetic dsRNA analogue Poly (I:C) have been shown to rapidly induced IFN-β mRNA (Campbell-Harding et al. 2013).

1.4.4 Smooth muscle cells in infection

RSV

SMCs cultured from human tracheas where shown to be permissive to infection by RSV (Elias et al. 1997, Moore et al. 2006) and were also shown to produce IL-11 in response to infection (Elias et al. 1997).

Other infections

In vivo, SMCs located in the wall of the small bronchi have been shown to be permissive to HMCV infection as seen from lung tissue samples from HMCV-infected individuals (Sinzger et al. 1995). Infection of human airway smooth muscle cells (HASM) from asthmatics and non-asthmatics with RV showed production of IL-6 and IL-8, with the latter only from asthmatic HASM (Oliver et al. 2006). *Chlamydophila pneumonia* is a major cause of bacterial pneumonia in humans and is associated with asthma development. Human bronchial smooth muscle cells (HBSMC) infected with *Chlamydophila pneumonia* showed increased production of IL-6 and FGFb (Rödel et al. 2000). Addition of IL-6 antibody to cultures diminished FGFb expression, suggesting FGFb production is dependent on IL-6, and that chlamydial infection of SMCs provokes a cytokine response that may contribute to structural remodeling of airways in chronic asthma (Rödel et al. 2000).

1.4.5 Perciytes in infection

To our knowledge, there is no literature to date on the role of pericytes in the immune response to RSV infection. Other infection models have shown that primary human brain vascular pericytes (HBVPs) infected with HCMV to produce CXCL8, CXCL11, CCL5, TNF-α, IL-1β and IL-6 (Alcendor et al. 2012) and brain pericytes from rats were susceptible to Japanese encephalitis virus (JEV) and could release IL-6 (Chen et al. 2014). Furthermore, increased levels of VEGF were detected in HBVPs after infection with the bacterium *Bartonella henselae*

suggesting a role for pericytes in promoting endothelial cell proliferation and the formation of new vessels (Varanat et al. 2013).

Overall it is becoming highly apparent that stromal cells, at least *in vitro*, are not bystanders in response to viral stimulation as these studies have shown them to produce a plethora of soluble mediators that have critical proinflammatory, antiviral and reparative roles. However, it is also strongly apparent that there is a major gap in knowledge of how these cells contribute to the response to virus infections *in vivo*, and none more so than in RSV. Various cytokines, chemokines, IFNs and growth factors are detected *in vivo* from human and mouse studies of RSV infection, however the cellular sources for the majority of these mediators are not known. Stromal cells could be a source of these mediators as they are a major component of the structure of the lung, and so have the potential to create a proinflammatory environment that can induce a robust and effective antiviral response to clear the virus, as well as resolve lung immunopathology. If and how they do this, would contribute immensely to the understanding of how the host responds to RSV infection and ultimately provide clues on how to prevent or at least, ameliorate disease.

2 Hypothesis and Aims

2.1 Hypothesis

Stromal cells are infected by RSV *in vivo* and express soluble mediators that can recruit cells and create an inflammatory environment in the lung. They can also express mediators important for maintaining barrier integrity during infection *in vivo*. These mediators are important for the antiviral response.

2.2 Aims

i. Determine whether stromal cells are infected with RSV *in vivo.*
ii. Identify mediators produced by stromal cells during RSV infection *in vivo.*
iii. Establish whether expression of mediators from stromal cells is dependent on type I IFN signalling *in vivo* using mixed IFNAR1$^{-/-}$ bone marrow chimeric mice.
iv. Evaluate if stromal cell-derived mediators are important for viral clearance and reduced severity of disease during RSV infection *in vivo.*

3 Materials

3.1 Consumables

ELISA MaxiSorp plates	Nunc, Roskilde, Denmark
Phase Lock Gel eppendorfs	VWR, Leicestershire, UK

3.2 Reagents and chemicals

Bovine serum albumin (BSA)	Sigma-Aldrich, Dorset, UK
Bradford Reagent	Sigma-Aldrich, Dorset, UK
CD31 MicroBeads	Miltenyi Biotec, Surrey, UK
CD45 MicroBeads	Miltenyi Biotec, Surrey, UK
Collagenase D	Roche, Welwyn Garden City, UK
3,3'-Diaminobenzidine (DAB)	Sigma-Aldrich, Dorset, UK
Dulbecco's Modified Eagle Medium (DMEM)	PAA, Pasching, Austria
Foetal calf serum (FCS)	Gibco, Paisley, UK
Dispase II	Roche, Welwyn Garden City, UK
DNase I	Sigma-Aldrich, Dorset, UK
EDTA	Sigma-Aldrich, Dorset, UK
Extravidin-peroxidase	Sigma-Aldrich, Dorset, UK
L-glutamine	Gibco, Paisley, UK
Low melting point agarose	Sigma-Aldrich, Dorset, UK
Lipopolysaccharide (LPS)	Invivogen, CA, USA
LIVE/DEAD® Fixable Aqua Dead Stain	Life Technologies, Paisley, UK
MACS buffer	Miltenyi Biotec, Surrey, UK
Phosphate buffered saline (PBS)	PAA, Pasching, Austria
Penicillin-Streptomycin	PAA, Pasching, Austria
Protease Inhibitor Cocktail Tablets	Roche, Welwyn Garden City, UK
QuantiTec Probe PCR Kit	Qiagen, Crawley, UK
Rat IgG2b anti-mouse CD16/CD32 (Fc block)	BD Bioscience, Oxford, UK
Streptavidin-HRP	Biosource, Paisley, UK

Streptavidin Microbeads	Miltenyi Biotec, Surrey, UK
Sytox Blue Dead Cell Stain	Life Technologies, Paisley, UK
TMB Single Solution	Invitrogen, Paisley, UK
Trizol Reagent	Invitrogen, Paisley, UK
Trypan Blue	Sigma-Aldrich, Dorset, UK
Trypsin:EDTA	Sigma-Aldrich, Dorset, UK
Tween20	Sigma-Aldrich, Dorset, UK

3.3 Kits

Albumin ELISA Quantitation Set	Bethyl Laboratories, TX, USA
Cytokine Mouse Magnetic 20-plex	Invitrogen, Paisley, UK
ELISA kits (CCL2, CXCL1, CXCL10, GM-CSF)	R&D Systems, MN, USA
High Capacity RNA-to-cDNA Kit	Applied Biosystems, Paisley, UK
ProcartaPlex Mouse IFN-alpha3/IFN-beta 2-plex	eBioscience, Hatfield, UK
RNA 6000 Nano Kit	Agilent Technologies, CA, USA
RNA 6000 Pico Kit	Agilent Technologies, CA, USA
RNeasy Mini Kit	Qiagen, Crawley, UK
RNeasy Micro Kit	Qiagen, Crawley, UK
RT^2 PreAMP cDNA Synthesis Kit	Qiagen, Crawley, UK
RT^2 Profiler PCR Arrays – PAMM-150Z	Qiagen, Crawley, UK
RT^2 Profiler PCR Arrays – PAMM-122Z	Qiagen, Crawley, UK
QuantiText Whole Transcriptome Kit	Qiagen, Crawley, UK
Quick-Diff Kit	Reagena, Toivala, Finland

3.4 Anaesthetics

Isofluorane	Centaur, Somerset, UK
Pentobarbitone	Centaur, Somerset, UK

3.5 Instruments

2100 Bioanalyzer	Agilent Technologies, CA, USA

7500 Fast Real-Time PCR system	Applied Biosystems, Paisley, UK
BD FortessaLSR	BD Bioscience, NJ, USA
BD FACSAria II	BD Bioscience, NJ, USA
BioPlex 200	Bio-Rad Laboratories, Hertfordshire, UK
Cytospin III Cytocentrifuge	Thermo Scientific, DE, USA
CX-2000 UV Crosslinker	UVP, CA, USA
Eppendorf centrifuge 5810R (Rotor A-4-81)	Eppendorf, Cambridge, UK
Gene Amp PCR System 9700	Applied Biosystems, Paisley, UK
gentleMACS dissociator	Miltenyi Biotec, Surrey, UK
Heraeus Megafuge 40R (Rotor 75003807)	Thermo Scientific, DE, USA
NanoDrop 1000 Spectrophotometer	Thermo Scientific, DE, USA
Sorvall Legend Micro 21	Thermo Scientific, DE, USA
SPECTRAMax Plus S384	Molecular Devices, Berkshire, UK
TissueLyser LT	Qiagen, Crawley, UK
Ultrasonic Water Bath- XUBA3	Asynt, Cambridge, UK

3.6 Software

7500 Fast System SDS v1.4	Applied Biosystems, Paisley, UK
BioPlex Manager software v6.1	Bio-Rad Laboratories, Hertfordshire, UK
FACSDiVa	BD Bioscience, Oxford, UK
FlowJo v9.7	Tree Star, OR, USA
GraphPad Prism v6.0	GraphPad Software, CA, USA
RT^2 Profiler PCR Arrays data analysis v3.5	Qiagen, Crawley, UK
SoftMax Pro v5.2	Molecular Devices, Berkshire, UK

3.7 Antibodies

Table 3.1: Antibodies for flow cytometry

Antigen	Clone	Fluorochrome	Isotype	Final Concentration	Supplier
CD11c	HL3	PE-CF594	Armenian Hamster IgG_1, λ2	1µg/ml	BD Bioscience, Oxford, UK
CD31	390	PE	Rat (Lew) $IgG_{2a, K}$	2µg/ml	Biolegend, Cambridge, UK
CD45	30-F11	APC-Cy7	Rat $IgG_{2a, K}$	0.5µg/ml	Biolegend, Cambridge, UK
CD90	778053	APC	Rat IgG_{2a}	1µg/ml	R&D Systems, MN, USA
EpCAM	G8.8	PerCP/Cy5.5	Rat $IgG_{2a, K}$	2µg/ml	Biolegend, Cambridge, UK

Table 3.2: Antibodies for MACS

Antigen	Clone	Conjugate	Isotype	Final Concentration	Supplier
EpCAM	G8.8	Biotin	Rat $IgG_{2a, K}$	0.75µg/ml	eBioscience, Hatfield, UK

Table 3.3: Antibodies for *in vivo* neutralisation

Antigen	Clone	Isotype	Supplier
mGM-CSF	MPI-22E9	Rat IgG_{2a}	Bio X Cell, NH, USA
Trinitrophenol (isotype control)	2A3	Rat IgG_{2a}	Bio X Cell, NH, USA

Table 3.4: Antibodies for immunoplaque assay

Antigen	Clone	Conjugate	Supplier
RSV	Polyclonal	Biotin	AbD Serotec, Oxford, UK

Table 3.5: Antibodies and standard for IL-6 ELISA

Antibody	Clone	Conjugate	Isotype	Final Concentration	Supplier
Capture	MP5-20F3	-	Rat IgG_1	4µg/ml	BD Bioscience, Oxford, UK
Detection	MP5-32C11	Biotin	Rat IgG_{2a}	1µg/ml	BD Bioscience, Oxford, UK
Standard	Recombinant IL-6	-	-		BD Bioscience, Oxford, UK

Table 3.6: Antibodies and standard for IFN-α ELISA

Antibody	Clone	Conjugate	Isotype	Final Concentration	Supplier
Capture	F18	-	Rat IgG_1	1µg/ml	Cambridge Bioscience, Cambridge, UK
1st Detection	Polyclonal rabbit anti-IFN-α	-	-	0.2µg/ml	PBL Biomedical Laboratories, PA, USA
2nd Detection	Polyclonal Mouse anti-rabbit	Biotin	Mouse IgG	1:1000	Jackson ImmunoResearch PA, USA
Standard	Recombinant IFN-α	-	-		Cambridge Bioscience, Cambridge, UK

3.8 Solutions, buffers and media

Table 3.7: Composition of solutions, buffers and media

	Composition	Final Concentration
Complete DMEM	DMEM Heat-inactivated FCS L-glutamine Penicillin-Streptomycin	1x 10% 2mM 100U/ml
Serum-free DMEM	DMEM L-glutamine Penicillin-Streptomycin	1x 2mM 100U/ml
ACK buffer	Distilled water NH_4Cl $KHCO_3$ Na_2EDTA	 0.15mM 1mM 0.1mM
Staining buffer	PBS BSA EDTA NaN_3	1x 1% 0.05mM 0.005%
Coating buffer	$NaHCO_3$ p.H 8.2	0.1M
Washing buffer	PBS Tween20	1x 0.05%
Blocking solution	PBS FCS NaN_3	1x 2.5% 0.02%
Stop solution	H_2SO_4	1M
Bronchoalveolar lavage media	PBS EDTA	1x 5mM

4 Methods

4.1 Animals

Wildtype (WT) C57BL/6 mice were purchased from Charles River or Harlan (UK) and type I interferon α/β receptor knockout mice (IFNAR1$^{-/-}$) were obtained from C Reis e Sousa (The Francis Crick Institute, UK) and screened to ensure the genotype was maintained. All mice were bred and maintained in pathogen-free conditions, and gender and age-matched mice 8-10 weeks old were used for each experiment. All animal studies were approved by the UK Home Office and performed in accordance with the ARRIVE guidelines.

4.2 Bone marrow chimeras

BM chimeras were generated using female, aged-matched C57BL/6 (WT) and IFNAR1$^{-/-}$ (KO) mice. The mice were kept on water supplemented with antibiotics (Baytril, 700μl in 500ml water) before and after irradiation. Recipient mice were irradiated with 900 rads. Donor BM cells were obtained from non-irradiated mice. Female mice were sacrificed and the tibia and femur removed and PBS used to flush BM out from the bones, which were then pooled for each mouse strain. Red blood cells (RBCs) were lysed and 6hrs post-radiation 4x10^6 BM cells were transferred intravenously (i.v.) to each irradiated recipient mouse via the tail vein to obtain the following BM chimeras (denoted as donor BM-recipient mouse): WT-WT, KO-WT, WT-KO and KO-KO. Mice were left for at least 8 weeks and maintained on antibiotic water until infection with RSV.

4.3 Cell lines

Human epithelial type 2 (HEp-2) cells (ATCC, UK) were cultured and passaged in complete DMEM (cDMEM) at 37°C, 5% CO_2.

4.4 Primary murine lung fibroblasts

Lung fibroblasts cultures were obtained according to the protocol published by Baglole et al (2005) with slight modifications. Briefly, cDMEM was used to grow single cell lung preparations on tissue culture petri dishes for at least 3 weeks. Then using 0.5% trypsin:EDTA solution (Sigma, UK) and cells scrapers, confluent fibroblasts were removed and collected. For experimentation, 45,000 fibroblasts were seeded per well in a 96-well flat-bottomed tissue culture plate and incubated for 48hrs before being stimulated with different multiplicity of infection (MOIs) of RSV and UV-inactivated RSV (UV-RSV), or LPS (1ng/ml, Invivogen, USA) for 18hrs. Supernatant (SN) was collected and cells resuspended in Trizol™ Reagent (Invitrogen, UK) for RNA extraction.

4.5 Virus growth

Human RSV A2 strain was grown in HEp-2 cells. $1x10^7$ HEp-2 cells were first seeded in a $175cm^2$ culture flask in 30ml of cDMEM, and left to grow to 80% confluency in a 37°C, 5% CO_2 incubator. Medium was then removed and the cell monolayer washed with 10ml of serum-free DMEM (sfDMEM). Cells were infected with an MOI 0.1 of RSV in 4ml sfDMEM. A control flask with 4ml of sfDMEM only was prepared in parallel. Flasks were incubated for 2hrs at 37°C, and rotated 90° every 15mins to ensure even coverage of the virus across the monolayer. 30ml of cDMEM was then added and flasks left to incubate for a further 24hrs at 37°C. FCS was then reduced to 2% by removing 25ml of medium from the flask, centrifuging and aspirating the SN before resuspending the pellet with 25ml sfDMEM and adding back to the flask. Flasks were left to incubate for a further 24-48hrs. When 80% of the cells had detached from the flask, cells were removed using a cell scraper and sonicated for 2mins. Cells were then spun at 300 *x g* for 5mins, 4°C. The SN containing virus was aliquoted and rapidly snap frozen in liquid nitrogen. The control flask was treated in the same way.

4.6 Immunoplaque assay

To assess virus stock concentration, immunoplaque assay was performed. $2x10^4$ HEp-2 cells were seeded per well in a 96-well flat-bottom plate in cDMEM and left to incubate at 37°C overnight until confluent. Cells were then washed with sfDMEM and virus in serial dilutions starting at 200x dilution in duplicate, were added to cells in 50µl volume and left to incubate for 2hrs at 37°C on a shaker. Wells were then topped up with 150µl of cDMEM and further incubated at 37°C overnight. Medium was expelled and cells washed with 100µl of PBS, before fixing with 100µl of 2% hydrogen peroxide in methanol for 20mins. Wells were then washed twice with PBS with 1% BSA (PBS/BSA), and 100µl of biotinylated anti-RSV antibody (AbD Serotec, UK; 1:500 in PBS/BSA) was added to each well and incubated for 2hrs at room temperature (RT). Cells were then washed twice with PBS/BSA. 100µl of extravidin peroxidase (Sigma, UK; 1:500 in PBS/BSA) was added followed by washing twice with PBS/BSA. 50µl of DAB (Sigma, UK) was added and plates kept in the dark at RT until plaques were visible. The reaction was stopped using PBS, and plaques counted using a light microscope. Focus-forming units (FFUs) per ml were calculated as: *number of plaques x dilution of virus x 20.*

4.7 Dosing of mice

4.7.1 Virus infection

Mice were lightly anaesthetised with inhaled Isoflourane (Centaur, UK) and oxygen at 2 litres per minute and infected intranasally (i.n.) with 100µl of 1.5–$2.0x10^6$ FFUs of RSV. As control, RSV was exposed to UV light for 2mins in a CX-2000 UV crosslinker (UVP, USA) before i.n. administration.

4.7.2 Neutralising antibodies

Mice were lightly anaesthetised with Isoflourane (Centaur, UK) and oxygen at 2 litres per minute and challenged with various doses of GM-CSF antibody or isotype antibody (Bio X Cell, USA) at various timepoints i.n. and/or intraperitoneally (i.p.).

4.8 Collection of cells and tissue

Mice were sacrificed by i.p. injection of 100µl of Pentobarbital (Centaur, UK).

4.8.1 Bronchoalveolar lavage fluid (BALF)

BALF was obtained by injecting 1ml BALF media into the lung via the trachea using a cannulated syringe. The lungs were flushed three times, and the recovered BALF then spun down at 3500 *x g* for 5mins and the SN stored at -80°C. The cell pellet was resuspended in 200µl ACK buffer for 5mins and the reaction stopped using 800µl cDMEM. Cells were spun at 3500 *x g* for 5mins, the SN expelled and cells resuspended in 500µl cDMEM. Cells were analysed for total and differential leukocyte cell count (see section 4.9).

4.8.2 Lung tissue for quantitative polymerase chain reaction (qPCR)

Lungs were first perfused with PBS via the heart, and then dissected out and snap frozen in liquid nitrogen before storage in -80°C.

4.8.3 Lung tissue for flow cytometry

4.8.3.1 Dispase

Lungs were perfused with PBS via the heart and single cell suspension obtained from an adapted protocol by Messier et al (2012). Firstly, 3ml of dispase II

(5mg/ml; Roche, UK) at 37°C was injected into the lung via the trachea using a cannulated syringe followed by 0.5ml of low-melting point agarose at 45°C. The chest cavity was then iced for 2mins to set the agarose before lungs were dissected out and further incubated in 2ml dispase for 30mins at RT. Lungs were then put in 5ml cDMEM supplemented with DNase I (30µg/ml; Sigma-Aldrich, UK) and dissociated using the gentleMACS™ dissociator (Miltenyi Biotec, UK) according to manufacturer's instructions. Lung cells were filtered using a 100µm filter before spinning at 200 *x g* for 10mins, the cell pellet resuspended in ACK buffer for 5mins. The reaction was stopped using cDMEM and cells spun again at 200 *x g* for 10mins. Cells were resuspended in media and plated at $1x10^6$ cells/well for cell surface antigen staining.

4.8.3.2 Collagenase

Lungs were perfused with PBS via the heart, dissected out into 2.5ml cDMEM containing 2.5ml of Collagenase D (1mg/ml; Roche, UK) and DNase I (30µg/ml; Sigma-Aldrich, UK). Lungs were dissociated on the gentleMACS™ dissociator (Miltenyi Biotec, UK) according to manufacturer's instructions and then left to incubate for 1hr on a shaker at 37°C. Lungs were further dissociated using a gentleMACS™ dissociator, before adding 5ml PBS and spun at 300 *x g* for 5mins. The cell pellet was resuspended in 5ml ACK buffer for 5mins, before adding 5ml cDMEM and spun again at 300 *x g* for 5mins. The cell pellet was then resuspended in cDMEM, filtered using a 100µm filter and plated at $1x10^6$ cells/well for cell surface antigen staining.

4.9 Total and differential leukocyte cell count

For total cell count, an aliquot of cell suspension from processed BALF or single cell lung suspension was counted using Trypan Blue for dead cell exclusion. For differential leukocyte cell count, 100µl of cell suspension from processed BALF was placed in a cytofunnel attached to a glass slide and run on a Cytospin III Cytocentrifuge (Thermo Scientific, USA) at 400rpm for 5mins. Slides were left to dry, then fixed and stained using Quick-Diff staining kit (Reagena, Finland). 300

cells per slide were counted using a light microscope, characterising macrophage, lymphocyte and granulocyte populations.

4.10 Flow cytometry

$1x10^6$ cells/well were plated in a 96-well round-bottomed polypropylene plate and washed with PBS. Cells were incubated with 100µl LIVE/DEAD® Fixable Aqua Dead Stain (1:500 in PBS; Life Technologies, UK) for 30mins at 4°C in the dark. Cells were washed and then incubated with 50µl purified rat IgG2b anti-mouse CD16/CD32 receptor antibody Fc Block (1:200 in staining buffer; BD Biosciences, UK) for 20mins at 4°C. Cells were washed with staining buffer and then incubated with fluorochrome-conjugated antibodies against cell surface markers for 30mins at 4°C in the dark (see table 3.1). Cells were washed twice and resuspended in staining buffer, before acquisition on BD LSRFortessa using FACSDiVa software (BD Bioscience, USA) and following the gating strategy shown in Fig. 4.1.

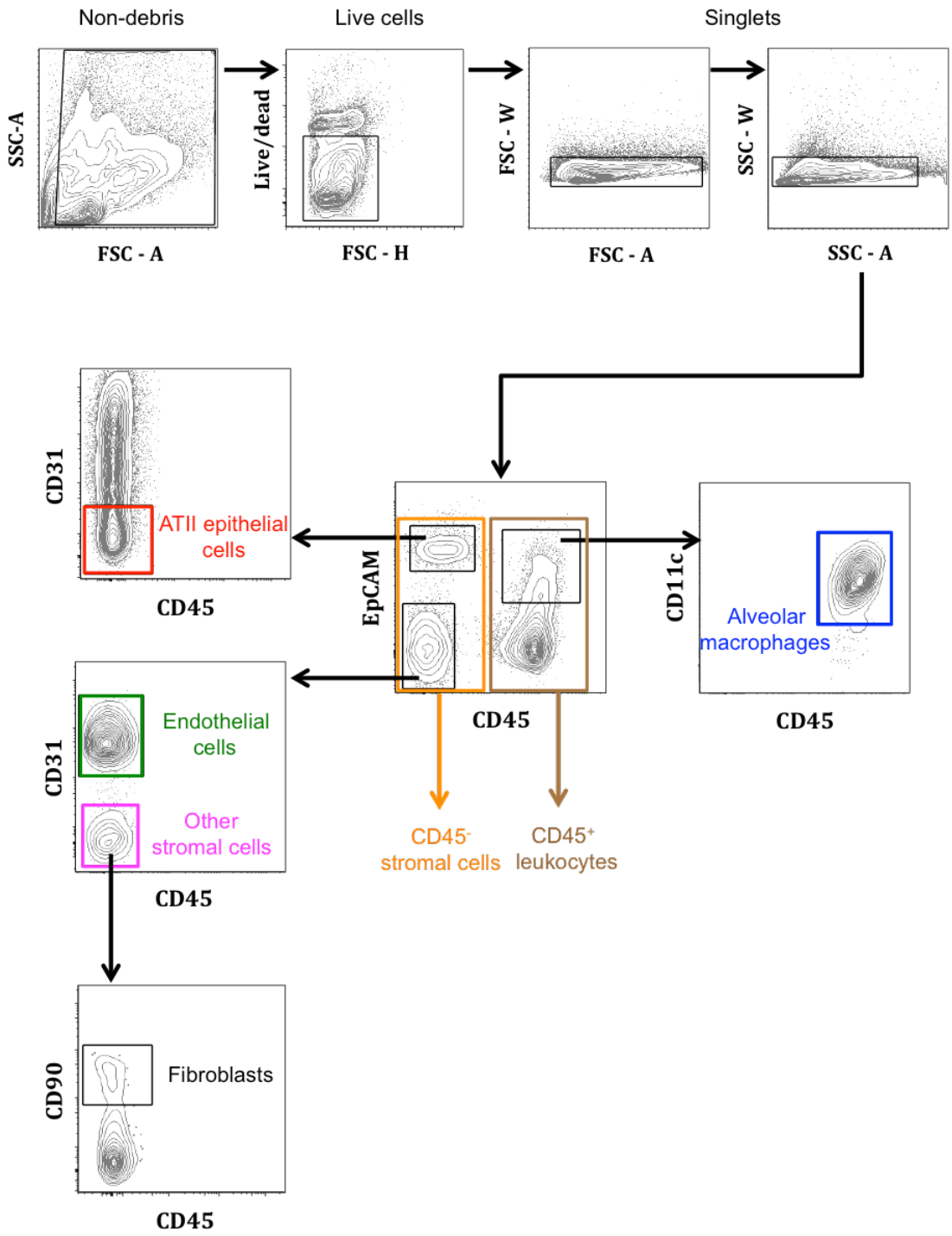


Figure 4.1: Gating strategy for flow cytometry. Lung cells were first gated to remove debris, dead cells and doublets using forward/side scatter - area/height/width (FSC/SSC - A/H/W) and a viability dye. CD45 and EpCAM discrimination was then used to separate all stromal cells and all leukocytes, which then allowed alveolar macrophages (AMs), ATII epithelial cells, endothelial cells, other stromal cells and fibroblasts to be further identified using markers CD31, CD11c and CD90.

4.11 Cell sorting

4.11.1 Fluorescence activated cells sorting (FACS)

Single-cell lung suspensions were incubated with Fc Block (1:200; BD Biosciences, UK) for 20mins at 4°C. Cells were washed with staining buffer and then incubated with fluorochrome-conjugated antibodies against cell surface markers for 30mins at 4°C in the dark as before (see Table 3.1). Cells were washed twice and resuspended in cell staining buffer. Sytox Blue Dead Cell Stain (1:8000; Life Technologies, UK) was added to cells before running on a BD FACSAria III using FACSDiVa software (BD Bioscience) to sort for several populations (see Fig. 4.1 for gating strategy and Table 4.1 for populations). Sorted cells were reanalysed to confirm purity and spun down and resuspended in 1ml Trizol™ Reagent (Invitrogen, UK) and stored at -80°C. Purity was always >95%.

Table 4.1: Cell populations sorted by FACS

Population	Cell surface antigens
All $CD45^+$ cells	$CD45^+$
All $CD45^-$ cells	$CD45^-$
Alveolar macrophages	$CD45^+CD11c^+EpCAM^+$
ATII epithelial cells	$CD45^-CD31^-EpCAM^+$
Endothelial cells	$CD45^-CD31^+EpCAM^-$
Other stromal cells	$CD45^-CD31^-EpCAM^-$

4.11.2 Magnetic activated cell sorting (MACS)

4.11.2.1 Automated MACS

Cell populations sorted via MACS are shown in Table 4.2. After cells were obtained in single-cell suspension using dispase (see section 4.8.3.1) cells were spun down and resuspended in MACS buffer (Miltenyi Biotec, UK) and 100µl of anti-CD45 MicroBeads and 100µl of anti-CD31 MicroBeads (Miltenyi Biotec, UK) was added per $1x10^9$ cells and incubated for 15mins at 4°C on a nunator. Cells were washed with MACS buffer at 200 *x g* for 10mins and then resuspended to $1x10^9$ cells/ml before filtering with a 100µm filter. Cells were then sorted with an autoMACS Pro Seperator (Miltenyi Biotec, UK) using the program **deplete_s** to obtain $CD45^-CD31^-$ cells. These cells were then incubated with Fc Block (1:200) for 20 mins at 4°C, before washing and resuspending in MACS buffer to $1x10^9$ cells/ml. Cells were then incubated with EpCAM-biotin antibody (0.75µg/ml; eBioscience, UK) 30mins at 4°C on a nunator. Cells were washed and resuspended in MACS buffer before Streptavidin Microbeads (100µl per $1x10^9$ cells) (Miltenyi Biotec, UK) was added to cells for 15mins at 4°C on a nunator. Cells were then washed, resuspended in MACS buffer and filtered using a 100µm filter. Cells were sorted using program **possel** to obtain $CD45^-CD31^-EpCAM^+$ and $CD45^-CD31^-EpCAM^-$ cells. Purity was confirmed at each sorting step using flow cytometry (always >95%). Sorted cells were spun down and resuspended in 1ml Trizol™ Regeant (Invitrogen, UK) and stored at -80°C.

4.11.2.2 Manual MACS

Cells were prepared and stained as described for automated MACS, but instead of running cells through the autoMACS Pro Seperator, LD columns (Miltenyi Biotec, UK) were used as per manufacturers instructions to obtain sorted cells (Table 4.3). Purity was confirmed at each sorting step using flow cytometry (always >95%).

Table 4.2: Cell populations sorted by MACS

Population	Cell surface antigens
ATII epithelial cells	$CD45^{-}CD31^{-}EpCAM^{+}$
Other stromal cells	$CD45^{-}CD31^{-}EpCAM^{-}$

4.12 RNA extraction

4.12.1 Lung lobes

Frozen lung lobes were brought to RT and homogenised in 1ml Trizol™ Reagent (Invitrogen, UK) using a tissue lyser (TissueLyser LT, Qiagen, UK). 200µl chloroform was added and samples shaken vigorously for 15 seconds (secs), before leaving for 10mins at RT. Homogenised lungs were then spun at 12,000 *x g* for 15mins at 4°C. The upper aqueous phase containing RNA was removed and processed from step 5 of the RNeasy Mini Kit (Qiagen, UK) according to manufacturers instructions.

4.12.2 Sorted cells

Frozen cells in Trizol™ Reagent (Invitrogen, UK) were brought to RT and transferred to Phase Lock Gel eppendorfs (VWR, UK). 200µl chloroform was added and samples shaken vigorously for 15secs, before leaving for 10mins at RT. Samples were then spun at 12,000 *x g* for 10mins at 4°C, and the upper aqueous layer processed from step 5 of the RNeasy Mini Kit (>500,000 sorted cells) or the RNeasy Micro Kit (<500,000 sorted cells).

4.13 RNA quantification

4.13.1 NanoDrop

RNA yields from whole lung were determined using a NanoDrop 1000 Spectrophotometer (Thermo Scientific, USA).

4.13.2 Bioanalyser

RNA yields from sorted cells were determined using a 2100 Bioanalyser using the RNA 6000 Nano and Pico kits (Agilent Technologies, USA).

4.14 RNA to complimentary DNA (cDNA) conversion

1µg of RNA from lung lobes or 9µl of RNA from sorted cells (µl as low levels of RNA and therefore unable to precisely quantify) or primary fibroblasts was reverse-transcribed using a High Capacity RNA-to-cDNA kit according to manufacturer's instructions (Applied Biosystems, UK).

4.15 RNA amplification and cDNA conversion

RNA from sorted cells was amplified and reverse-transcribed using the QuantiTect Whole Transcriptome Kit according to manufacturer's instructions (Qiagen, UK).

4.16 qPCR

To quantify mRNA levels in lung tissue, sorted lung cells and primary fibroblasts, qPCR reactions were performed using primers and probes listed in Table 4.3 together with QuantiTec Probe PCR Kit (Qiagen, UK) and target cDNA, for either relative (Table 4.4) or absolute (Table 4.5/6) quantification. To exclude

variances in starting material and enzymatic efficiency, results were normalised to the housekeeping gene *Gapdh* (18S for amplified RNA). For absolute quantification of RSV L-gene and *Ifnb, Tnfa and Ifnl*, the exact number of copies of the target gene was calculated using a plasmid DNA standard curve for each gene. For relative quantification of *Areg, Cxcl1, Cxcl5, Cxcl10, Cxcl12, Ccl2, Ccl7, Csf2, Il1a, Il1b, Il6, Il10, Il33, Ifnar1, Ifna5, Ifna6, Ifng, Sftpc, Tgfb and Vegf* the expression of the target gene was expressed relatively to *Gapdh* (18S for amplified RNA). First, the ΔCt (Δ Cycle threshold) between the target gene and *Gapdh* for each sample was calculated, followed by calculation of $2^{-\Delta Ct}$. Reactions were run using the thermal profile in Table 4.7 on a 7500 Fast Real-Time PCR system and analysis was performed using 7500 Fast System SDS Software (Applied Biosystems, UK).

Table 4.3: Primer and probe sequences for qPCR

Primer/Probe	Sequence (5'-3')	Supplier
L-gene forward	gaactcagtgtaggtagaatgtttgca	Invitrogen, UK
L-gene reverse	ttcagctatcattttctctgccaat	Invitrogen, UK
L-gene probe	tttgaacctgtctgaacattcccggtt	Eurofins, Germany
***Ifnb* forward**	ccatcatgaacaacaggtggat	Invitrogen, UK
***Ifnb* reverse**	gagagggctgtggtggagaa	Invitrogen, UK
***Ifnb* probe**	ctccacgctgcgttcctgctgtg	Eurofins, Germany
***Tnfa* forward**	catcttctcaaaattcgagtgacaa	Invitrogen, UK
***Tnfa* reverse**	tgggagtagacaaggtacaaccc	Invitrogen, UK
***Tnfa* probe**	cacgtcgtagcaaac	Eurofins, Germany
Areg, Cxcl1, Cxcl5, Cxcl10, Cxcl12, Ccl2, Ccl7, Csf2, Il1a, Il1b, Il6, Il33, Ifnar1, Ifna5, Ifng, Sftpc, Tgfb, Vegf	Not revealed by supplier	Applied Biosystems, UK

Table 4.4: Reaction composition for relative quantification of *Areg, Cxcl1, Cxcl5, Cxcl10, Cxcl12, Ccl2, Ccl7, Csf2, Il1a, Il1b, Il6, Il33, Ifnar1, Ifna5, Ifng, Sftpc, Tgfb, Vegf*

Reagent	Volume (ul/reaction)
Master Mix	6.25
Target primer/probe	0.63
Nuclease-free water	4.62
TOTAL	11.50
cDNA	1.00

Table 4.5: Reaction composition for absolute quantification of L-gene

Reagent	Volume (µl/reaction)
Master Mix	6.25
Forward primer (5µM)	2.25
Reverse primer (5µM)	0.75
Probe (5µM)	0.44
Nuclease-free water	1.81
TOTAL	11.50
cDNA	1.00

Table 4.6: Reaction composition for absolute quantification of *Ifnb and Tnfa*

Reagent	Volume (µl/reaction)
Master Mix	6.25
Forward primer (5µM)	2.25
Reverse primer (5µM)	2.25
Probe (5µM)	0.44

Nuclease-free water	0.31
TOTAL	11.50
cDNA	1.00

Table 4.7: Thermal profile for qPCR

Temperature	Time	Cycles
50°C	2mins	1
90°C	10mins	1
95°C **60°C**	15secs 1min	45

4.17 qPCR array

All arrays and kits were purchased from Qiagen (UK). Arrays on sorted cells were performed using RT^2 Profiler PCR Arrays, with pre-amplification of cDNA using the RT^2 PreAMP cDNA Sythesis Kit and primer mixes specific to each array, according to the manufacturer's instructions. Arrays used were Mouse Chemokines & Cytokines (PAMM-150Z) and Mouse Antiviral Response (PAMM-122Z), in 89-gene format. Arrays were run using sorted cells from two separate experiments, and compared to the same sorted population from a naïve counterpart. Analysis was performed using manufacturers software (RT^2 Profiler PCR Arrays data analysis v3.5 (Qiagen, UK) using housekeeping genes *Gapdh* and 18S to give a fold increase or decrease value for each gene by comparing infected population to naïve control.

4.18 Bradford assay

Total BALF protein levels were determined via Bradford assay. First, protein standards ranging from 0.1-1.4mg/ml were made using BSA. 5µl of protein standard or sample was then added to separate wells in a 96 well plate followed by 250µl of Bradford Reagent and left on a shaker for 30secs. Plates were left to incubate at RT for a further 5mins before measuring absorbance levels on a SpectraMax Plus plate reader at 595 nm and analysed using SoftMax Pro software (Molecular Devices, USA).

4.19 Enzyme linked immunoabsorbant assay (ELISA)

Cytokine and chemokine protein levels were measured using 96-well ELISA MaxiSorp™ plates (Nunc, Denmark) and ELISA kits (CXCL1, CXCL10, CCL2 and GM-CSF) from R&D Systems (UK) according to manufacturer's instructions. For IL-6 and IFN-α measurement, plates were coated with capture antibody in coating buffer overnight at 4°C (Table 3.5 and 3.6). Plates were washed 3 times with washing buffer and blocked for 2hrs at RT with blocking solution. Plates were washed again and 50µl of sample and standard were added and incubated for 2hrs at RT. For IL-6, plates were then washed before adding biotinylated detection antibody. For IFN-α, plates were then washed and primary detection antibody added for 2hrs at RT and then washed again before addition of biotinylated secondary detection antibody for 1hr. Plates for both were then washed and incubated with extravidin-peroxidase (Sigma-Aldrich, UK) for 30mins, RT before addition of TMB substrate (Life Technologies, UK). Once desired colourisation was reached, the reaction was stopped using stop solution. Optical density measurements were acquired on a SpectraMax Plus plate reader at 450 nm and analysed using SoftMax Pro software (Molecular Devices, USA).

4.20 Luminex

Protein levels were measured using Cytokine Mouse Magnetic 20-plex (Invitrogen, UK) and ProcartaPlex Mouse IFN-alpha3/IFN-beta 2-plex (eBioscience, UK) according to manufacturer's instructions and analysed using a BioPlex 200 and BioPlex Manager software v6.1 (Bio-Rad Laboratories, UK).

4.21 Statistical analysis

Statistical analysis was performed using GraphPad Prism 6 (GraphPad Software Inc.). Two-group comparisons were performed using unpaired, two-tailed Student's *t*-test. One-way ANOVA with Tukey's post hoc test was used to compare multiple groups and two-way ANOVA with Bonferri's post hoc test was used to compare weight loss and gene expression between several groups over time. For all tests, a value of $p<0.05$ was considered significant. *$p\leq0.05$, **$p\leq0.01$, ***$p\leq0.001$, ****$p\leq0.0001$, ND: not detectable.

5 Results

5.1 Stromal cells isolated using dispase digestion and fluorescent activated cell sorting

The study of stromal cells *in vivo* is limited both by lack of highly specific markers that can conclusively discriminate between different subsets, and the difficulty in isolating them from mouse lung. The latter is particularly true for alveolar epithelial cells, which are considered more fragile and easily injured compared to other cell types (Gonzalez and Dobbs 2013). Tracheal epithelial cells are also problematic to isolate due to the small size of the murine trachea meaning a considerable number of mice are required to obtain enough cells for downstream analysis, with most studies opting to culture cells to expand numbers (Lam et al. 2011, You and Brody 2013). In addition, purifying bronchiolar epithelial cells such as club cells from murine lungs has been met with limited success (Wang et al. 2012). To our knowledge, pericytes have not been isolated and purified from mouse lung, and few studies have attempted isolation of endothelial cells and fibroblasts (Teijaro et al. 2011, Akamatsu et al. 2013).

The isolation and purification of viable stromal cells from the lung requires dedicated proteolytic enzymes for each cell type, meaning that not all stromal cell subsets, in particular epithelial cells subsets, can be isolated at the same time. ATII epithelial cells are regarded to be more immunologically active than ATI cells (Chuquimia et al. 2013) and thus more literature is available on isolating this subset (Corti et al. 1996, Messier et al. 2012). In addition, the vast majority of studies on lung epithelial cells in both humans and mouse use ATII epithelial cell lines, and these studies have shown them to express a wide range of mediators in response to RSV infection (see section 1.4.1) suggesting they could have a potentially important role *in vivo*.

Therefore with these considerations in mind, an isolation method was optimised to liberate and purify different stromal cell populations from mouse lung, with the aim in particular to obtain the best combination of ATII epithelial cell purity, viability and yield for further downstream analysis.

5.1.1 Dispase digestion of lungs yields higher numbers of ATII epithelial cells compared to collagenase digestion

Proteolytic enzymes are used to digest tissues to give rise to single-cell suspensions of organs for further identification and analyses of the different cell subsets within. Mammalian organs such as the lung are comprised of cells and the ECM, the latter of which is further divided into the interstitial matrix and basement membrane, which provides structural and biochemical support to the cells (Suki et al. 2005). The ECM constituents include collagen, elastin, fibronectin and various proteoglycans, with the most abundant and vital component for structural integrity being collagen (Suki et al. 2005). Thus it is these ECM components, in particular collagen, that need to be digested to liberate cells.

Collagenases are metalloproteinases that cleave bonds within collagen, and are a widely used tissue-digestion enzyme to prepare single-cell preparations from the lung (Lancelin and Guerrero-Plata 2011). Bacterially-derived collagenases such as ones from *Clostridium histolyticum,* exhibit wider substrate specificity than vertebrate collagenases (Hu et al. 2002) and are the most commonly used in lung-cell preparations. Stromal cells such as endothelial cells and fibroblasts have been liberated from mouse lung using collagenase (Teijaro et al. 2011, Akamatsu et al. 2013).

Dispase, another type of metalloproteinase isolated from *Bacillus polymyxa,* also cleaves collagen but with a high specificity for collagen IV, a type of collagen found specifically in the basement membrane of the ECM, just below the epithelium layer (Stenn et al. 1989). With this characteristic it has been

suggested as a preferred tissue-digestion enzyme when isolating ATII epithelial cells from the lung (Corti et al. 1996, Messier et al. 2012).

To first determine which enzyme would enable viable isolation of different lung stromal cell populations, published isolation protocols for each enzyme were followed to obtain single-cell suspensions from the lung and then stained with antibodies against cell surface antigens to identify stromal cell populations using flow cytometry. Stromal cell populations were determined using the markers CD45, a common leukocyte antigen that separates all leukocytes from all stromal cells, EpCAM an epithelial cell adhesion molecule, and CD31, an endothelial cell marker. These were use to identify ATII epithelial cells ($CD45^{-}EpCAM^{+}CD31^{-}$), endothelial cells ($CD45^{-}EpCAM^{-}CD31^{+}$) and a mixed population of non-endothelial non-epithelial cells termed other stromal cells ($CD45^{-}EpCAM^{-}CD31^{-}$) which we postulated to contain a large proportion of fibroblasts as well as possibly pericytes and SMCs (see Fig. 4.1 for gating strategy). These specific markers combinations were based on previously published data that have been used to identify these cells (Corti et al. 1996, Messier et al. 2012, Unkel et al. 2012). Fibroblasts were not further distinguished from other stromal cells at this stage.

The results revealed that dispase-digestion of lungs yielded a population of $CD45^{-}$ stromal cells that had clear distinction of $EpCAM^{+}$ and $EpCAM^{-}$ subsets (Fig. 5.1a), which allowed identification of ATII epithelial cells following CD31 discrimination (Fig. 5.1b). Endothelial and other stromal cells were also very easily distinguishable, with no overlap with ATII epithelial cells (Fig. 5.1c). Collagenase digestion however, gave a population of $CD45^{-}$ cells with no clear EpCAM positive and negative separation (Fig. 5.1d). Thus a clear ATII epithelial cell population could not be discerned (Fig. 5.1e). Collagenase did give distinct separation of endothelial cells and other stromal cells based on CD31 expression (Fig. 5.1f), however the lack of clear EpCAM separation of $CD45^{-}$ cells meant that the identification and purity of these subsets from ATII cells was difficult to ascertain from collagenase digestion. As a result, the frequency and numbers of ATII epithelial cells obtained was significantly lower from collagenase-digested

lungs (Fig. 5.1g/h). As ATII epithelial cells were not clearly separated from endothelial cells and other stromal cells using collagenase digestion, dispase will henceforth be used to liberate stromal cell subsets from the lung.

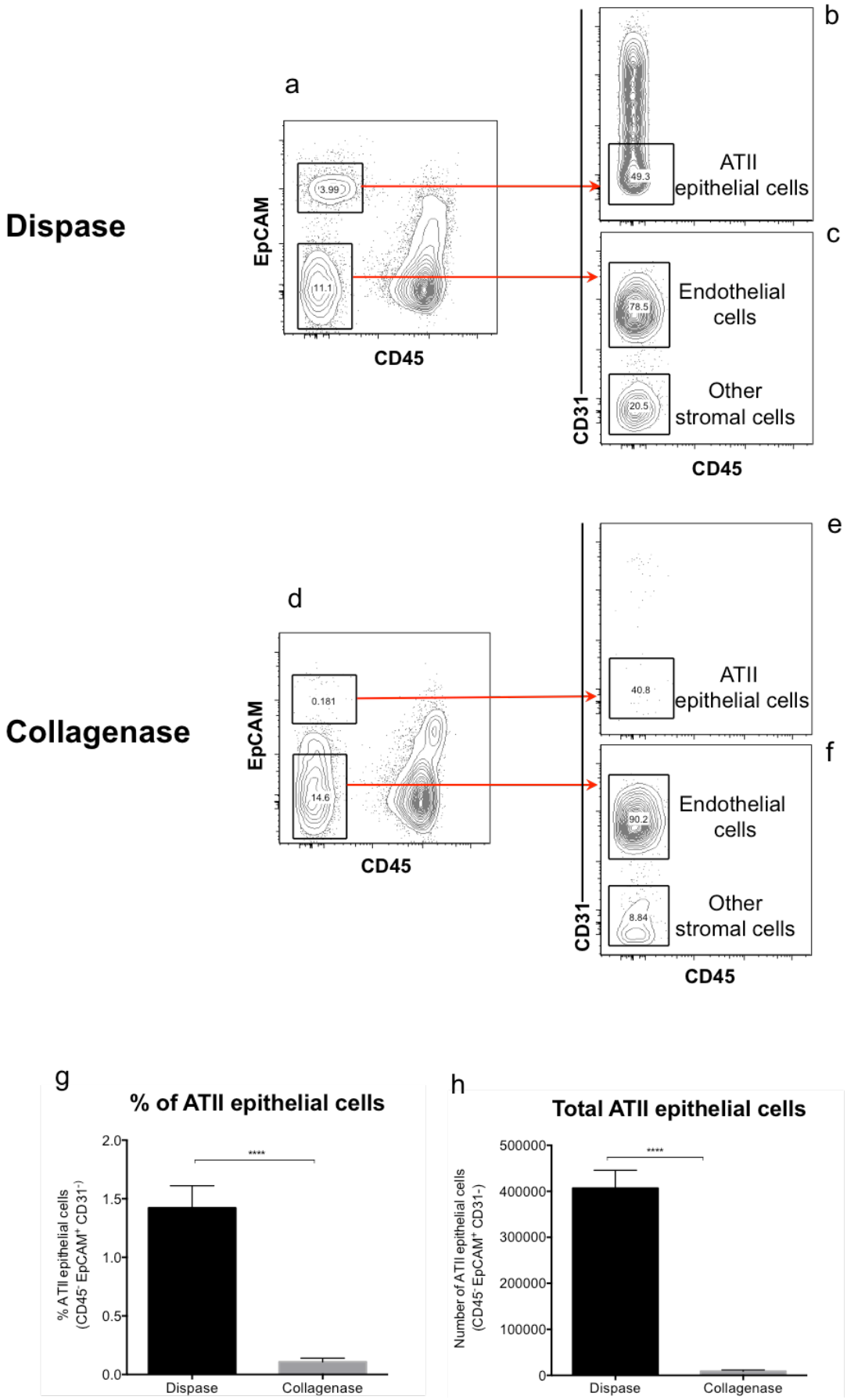

Dispase
a
b
c
EpCAM
CD45
3.99
11.1
49.3
78.5
20.5
ATII epithelial cells
Endothelial cells
Other stromal cells
CD31
CD45
Collagenase
d
e
f
0.181
14.6
40.8
90.2
8.84
ATII epithelial cells
Endothelial cells
Other stromal cells
CD31
CD45
g
% of ATII epithelial cells
% ATII epithelial cells (CD45- EpCAM+ CD31-)
2.0
1.5
1.0
0.5
0.0
****
Dispase
Collagenase
h
Total ATII epithelial cells
Number of ATII epithelial cells (CD45- EpCAM+ CD31-)
500000
400000
300000
200000
100000
0
****
Dispase
Collagenase

Figure 5.1: Dispase-digestion of mouse lung liberates more CD45$^-$EpCAM$^+$CD31$^-$ ATII epithelial cells than collagenase-digestion. C57BL/6 mice lungs were digested with either collagenase or dispase into single-cell suspension and then stained with antibodies against cell-surface antigens CD45, CD31 and EpCAM before analysis on a flow cytometer. Live singlets were gated on CD45 and EpCAM expression (a/d) followed by CD31 expression to identify ATII epithelial cells (b/e) and endothelial cells and other stromal cells (c/f). Frequency (g) and number (h) of ATII epithelial cells from dispase and collagenase digestion of mouse lung. Data representative (a-f) and pooled (g/h) of 4 separate experiments with 2-4 mice per group. Pooled data shown as mean ± SEM with statistical significance determined using two-tailed, unpaired Student's *t*-test. **** $p \leq 0.0001$.

5.1.2 Dispase digested total lung has less virus than total lung homogenate

Dispase digestion leads to better dissociation of ATII epithelial cells from the lung for further downstream analysis. Digestion with dispase however, leads to the loss of ATI epithelial cells in the subsequent single-cell lung suspension (Messier et al. 2012). This may be due to cleavage of cell surface markers that can identify ATI epithelial cells, which dispase digestion has been suggested to do for various other surface markers (Autengruber et al. 2012), or more likely that due to the fragile nature of ATI epithelial cells, dispase digestion may lead to cell death and loss of ATIs. ATI epithelial cells are thought to be the main cellular target for RSV (Borchers et al. 2013) and thus may contain a high proportion of virus in the lung. Therefore, to confirm both loss of ATI epithelial cells and purity of ATII epithelial cells from dispase digestion, and to determine the potential contribution of ATI epithelial cells to viral load in the lungs, the following experiments were performed.

To confirm purity of ATII epithelial cells and the lack of ATI cells from dispase-digestion, cells were analysed for expression of either the intracellular ATII epithelial cell marker pro-surfactant protein C (pro-SpC) or a suggested cell surface ATI epithelial cell marker T1α, by flow cytometry. An intracellular marker for ATI epithelial cells was unavailable, meaning the lack of T1α expression could suggest either a lack of ATI epithelial cells or cleavage of T1α by dispase. However, the use of intracellular pro-SpC staining would at least confirm definite ATII epithelial cell identification. Analysis revealed that ATII epithelial cells – classified as $CD45^{-}EpCAM^{+}CD31^{-}$, were almost all positive for pro-SpC expression (Fig. 5.2a) and completely negative for T1α expression (Fig. 5.2c) confirming that these cells are nearly all ATII epithelial cells and not ATI.

Dispase-digestion of the lung also liberates a population of stromal cells that are $CD45^{-}EpCAM^{+}CD31^{+}$ (Fig. 5.1b). These cells express EpCAM suggesting they are epithelial cells, but also express the endothelial cell marker CD31, meaning that they are not the classically defined population of ATII epithelial cells. To confirm whether these cells are another subset of ATII epithelial cells or possibly ATI

cells, these cells were also analysed for pro-SpC and T1α expression. The data revealed that $CD45^{-}EpCAM^{+}CD31^{+}$ cells were again almost all positive for pro-SpC (Fig. 5.2b) but negative for T1α (Fig. 5.2d), suggesting that these cells are not ATI cells, but a subset of ATII epithelial cells that express CD31. Despite the positive staining for pro-SpC, these "non-classical" ATII epithelial cells will not be analysed further. No other lung cells were positive for pro-SpC or T1α (data not shown).

Thus, dispase digestion yields a highly pure population of ATII epithelial cells, but no ATI epithelial cells.

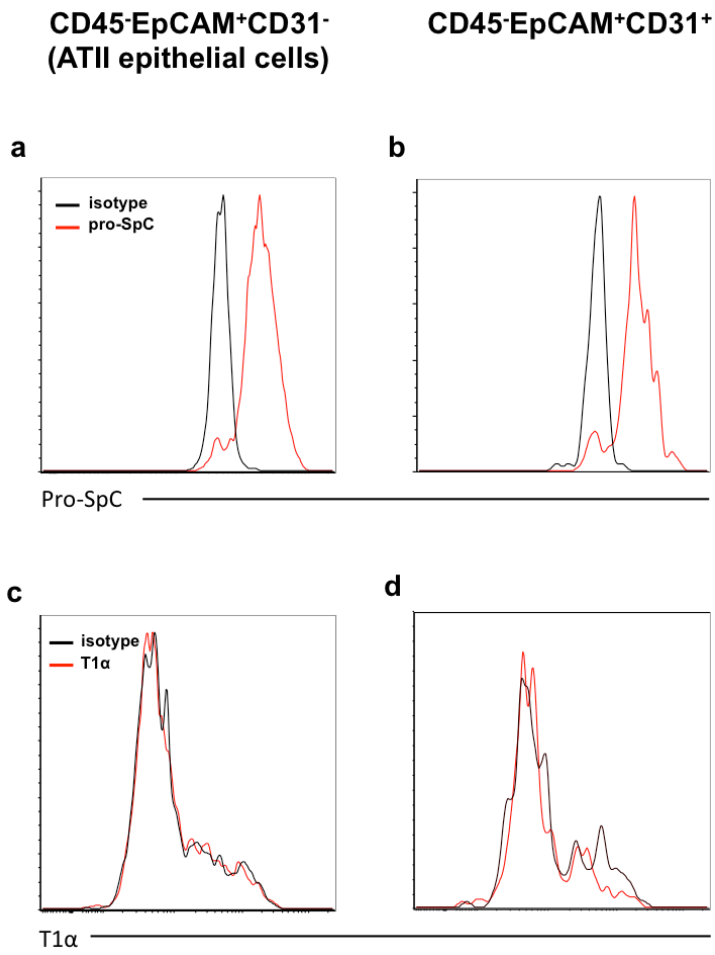


Figure 5.2: CD45⁺EpCAM⁺CD31⁻ and CD45⁺EpCAM⁺CD31⁺ cells express pro-SpC and do not express T1α. C57BL/6 mice lungs were digested with dispase into single-cell suspension and then stained with antibodies against CD45, CD31, EpCAM, T1α and pro-SpC before analysis on a flow cytometer. Histogram plots show live, singlet CD45⁺EpCAM⁺CD31⁻ (ATII epithelial cells) (left plots) and CD45⁺EpCAM⁺CD31⁺ cells ("non-classical" ATII epithelial cells) (right plots) expression of pro-SpC (a/b) and T1α (c/d). Black histograms depict the isotype control and the red histograms depict full staining. Data show one experiment with 3 pooled mice.

As dispase-digestion does not yield a detectable population of ATI epithelial cells (Fig. 5.2), the potential loss of viral lung load was determined to assess the potential contribution of ATI epithelial cells to viral load in the lungs. Mice were infected with RSV and lungs taken at 12 and 48hrs post infection, and either enzymatically digested with dispase into a single cell suspension, or mechanically dissociated into a lung homogenate. The lung homogenate contains material from all cells of the lung that may otherwise be lost by dispase digestion. RNA was extracted and viral load quantified via gene expression for RSV L gene. The data revealed that dispase-digested lungs contained significantly less virus than lung homogenate at 12 and 48hrs post RSV infection (Fig. 5.3). Between 10-100 fold less L gene copies were detected in dispase-digested lungs compared to lung homogenate. This strongly suggests that dispase digestion leads to the loss of cells, most likely ATI cells, that contain a large proportion of RSV and that the stromal cells being examined in this study (ATII epithelial cells, endothelial cells and other stromal cells), may not be the main cellular target for RSV.

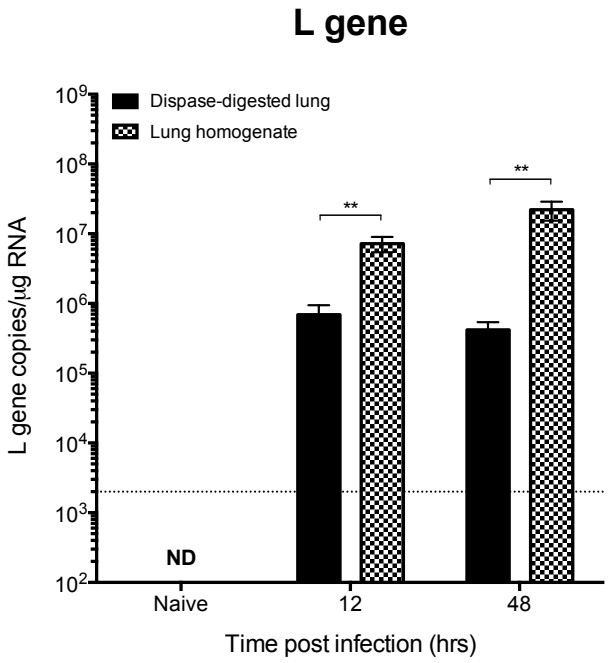


Figure 5.3: Dispase-digested lung contains less virus than lung homogenate. C57BL/6 mice were infected with $1.5x10^6$ FFU of RSV intranasally and lungs taken at 12 and 48hrs post infection. Lungs from naïve mice were taken without inoculation. Lungs were then removed and either digested with dispase into single-cell suspension (black bars) or mechanically dissociated into a homogenate (checked bars) for each time point. RNA was then extracted, converted to cDNA and then analysed for RSV L gene via qPCR. L gene copies were determined using a plasmid standard with the dashed line representing the lower detection limit. Results show pooled data from 2 separate experiments with 4-5 mice per time point. Data shown as mean ± SEM. Statistical significance was determined using two-tailed, unpaired Student's *t*-test. ** *p≤0.01.* ND: not detectable.

5.1.3 Fluorescence-activated cell sorting yields pure populations of different stromal cell subsets compared to magnetic-activated cell sorting

Dispase digestion of lungs liberates distinct populations of stromal cells from mouse lung (Fig. 5.1). To collect purified populations of different stromal cell subsets for downstream analysis, cell-sorting methods were compared to evaluate which delivered the highest yield and purity of cells.

5.1.3.1 Magnetic-activated cell sorting

Magnetic-activated cell sorting (MACS) uses magnetic beads conjugated to antibodies against cell-surface antigens to bind to cells and separate them based on positive or negative expression of the antigen. Cells that are positive for the antigen bind to the bead, and using magnetic force are separated from cells that do not express the antigen and do not bind the beads. The technique is limited in the number and combination of populations that can be sorted and although the final yield of sorted cells is high, the method does not allow the removal of debris, dead cells and doublets from sorted populations (Messier et al. 2012, Tomlinson et al. 2013). Dead cells have disrupted cell membranes making them sticky and able to bind non-specifically to antibodies, thus compromising purity of the final sorted population (Diamond and DeMaggio 2012). This is especially a problem in the lung where there is a lot of cell death during sample processing.

To sort stromal cells using MACS, mouse lungs were digested with dispase into single-cell suspension and stained with anti-CD45-conjugated and anti-CD31-conjugated Microbeads simultaneously. Cells were then run through the autoMACS separator to deplete all $CD45^+$ and $CD31^+$ cells. These $CD45^-CD31^-$ cells were then stained with EpCAM-biotin followed by Streptavidin-conjugated Microbeads, and run through the autoMACS again to obtain both $CD45^-CD31^-EpCAM^+$ (ATII epithelial cells – positive fraction) and $CD45^-CD31^-EpCAM^-$ (other

stromal cells – negative fraction). Endothelial cells ($CD45^{-}CD31^{+}EpCAM^{-}$) were not sorted using this protocol.

Using MACS, ATII epithelial cell frequency (including both live and dead cells) went from 3-7% of total cells before sorting (Fig. 5.4a/b) to 40-50% post-sort (Fig. 5.4c/d) and other stromal cell frequency from 45-50% (Fig. 5.4e/f) to 96-98% (Fig. 5.4g/h). However, sorted ATII epithelial cells contained a high proportion of dead cells, which constituted 70-85% of the total sample, with the rest being $CD45^{+}$ and $EpCAM^{-}$ cells (Fig. 5.4c/d). The other stromal cell population contained only 1-5% dead cells and moderate contamination from other cell types (Fig. 5.4g/h). Therefore, with exclusion of dead cell and undesired cell contamination, an actual final sorting purity of approximately 15-30% and 92-97% was obtained for ATII epithelial cells and other stromal cells respectively (Fig. 5.4i). The final yield of sorted cells was between 1.0–3.6x10^{6} for ATII epithelial cells and 4.3–21.0x10^{6} for other stromal cells (Fig. 5.4j).

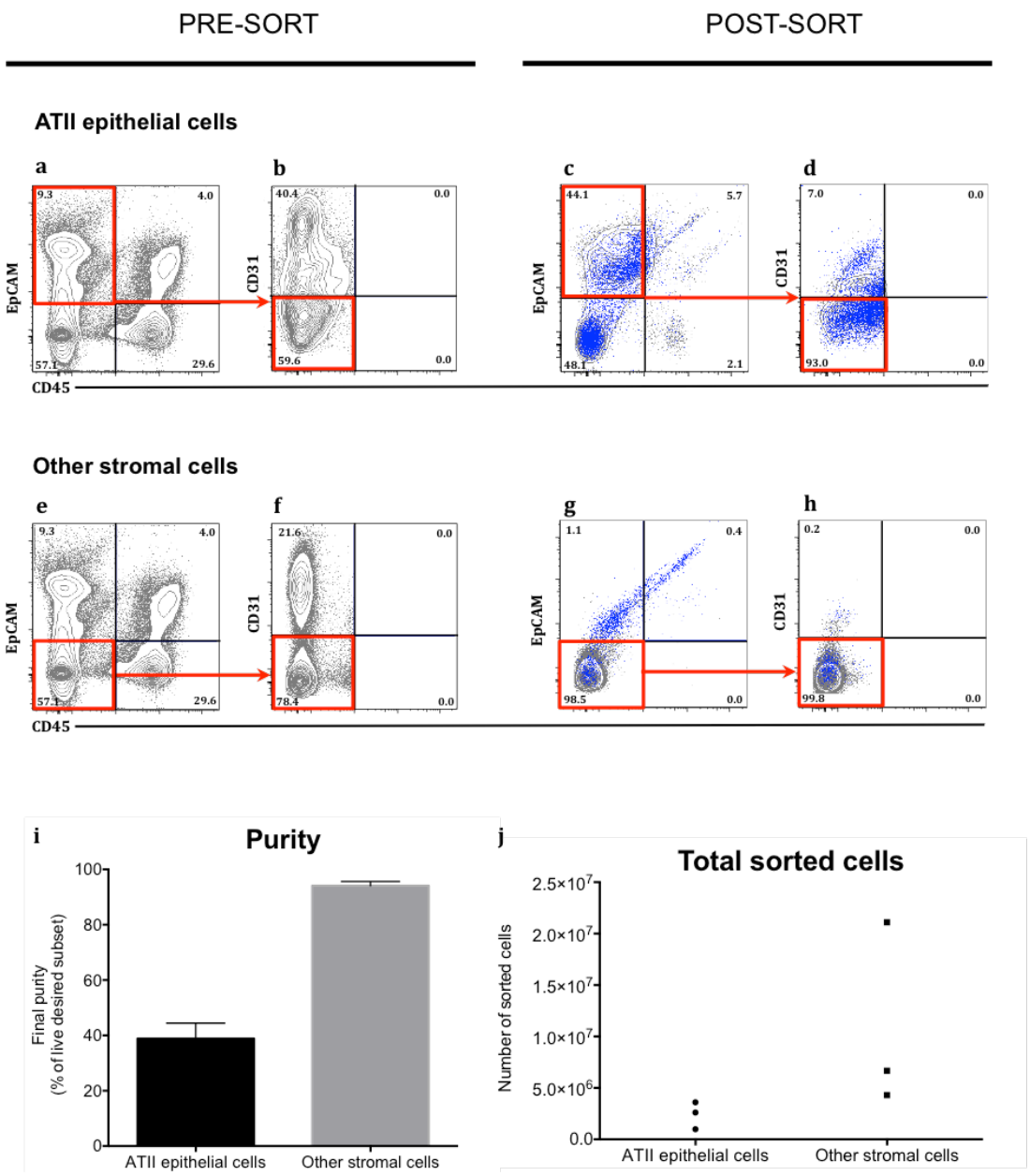


Figure 5.4. MACS of ATII epithelial cells and other stromal cells from lung. C57BL/6 mice lungs were digested with dispase into single-cell suspension and then stained with anti-CD45-conjugated and anti-CD31-conjugated Microbeads and run on an autoMACS Pro Separator using program **depletes.** The $CD45^{-}CD31^{-}$ fraction was collected and then stained with EpCAM-biotin and Streptavidin Microbeads and run on program **possel_s** to collect both $CD45^{-}CD31^{-}EpCAM^{+}$ (ATII epithelial cells) and $CD45^{-}CD31^{-}EpCAM^{-}$ (other stromal cells). Purity was checked by analysing an aliquot of pre and post sorted samples by flow cytometry. Flow cytometric plots show ATII epithelial cells (a-d) and other stromal cells (e-h) with no previous debris, dead cell or singlet gating (grey contour with gate frequencies) to illustrate the complete composition of the samples pre and post-sort. Dead cells are highlighted in blue for post-sort samples (c/d and g/h). The final purity (percentage of live sorted cells) (i) and total sorted cells (j) obtained. Data representative (a-h) and pooled (i/j) of 3 separate experiments with 5 pooled mice each. Pooled data shown as mean ± SEM.

5.1.3.2 Fluorescence-activated cell sorting

To further develop a sorting protocol to obtain a higher purity and range of stromal cells in order to be able to perform gene expression analysis, fluorescent-activated cell sorting (FACS) was performed. FACS, like MACS, sorts cells based on cell-surface antigen expression, however it utilises antibodies conjugated to fluorochromes that can be excited by lasers in a flow cytometer to collect cells based on positive or negative expression. Each cell is individually characterised and in this way, a much wider and specific range of cell subsets can be sorted and debris, dead cells and doublets can be excluded increasing final purity. However, the process is significantly more time consuming than MACS and yields of sorted cells are far smaller (Tomlinson et al. 2013).

To sort stromal cells using FACS, mouse lungs were digested with dispase into single-cell suspension and stained with antibodies against CD45, CD31 and EpCAM as well as a viability dye (see Fig. 4.1 for gating strategy). Three populations of stromal cells were sorted using a FACSAria cell sorter: ATII epithelial cells, endothelial cells and other stromal cells.
Using FACS, ATII epithelial cell frequency (including both live and dead cells) went from 5-8% before sorting (Fig. 5.5a/b) to 92-96% post-sort (Fig. 5.5c/d), endothelial cells from 12-18% (Fig. 5.5e/f) to 96-98% (Fig. 5.5g/h) and other stromal cell frequency from 40-50% (Fig. 5.5i/j) to 90-99% (Fig. 5.5k/l). For all three sorted subsets dead cell contamination was always less than 5% with little to no contamination from other cell types. Therefore, with exclusion of dead cell and undesired cell contamination, an actual final sorting purity of 90-96%, 95-97% and 90-98% was obtained for ATII epithelial cells, endothelial cells and other stromal cells respectively (Fig. 5.5m). The final yield of sorted cells was between 0.8–2x10^5 for ATII epithelial cells, 1.0–1.7x10^6 for endothelial cells and 0.4–0.5x10^6 for other stromal cells (Fig. 5.5n).
Overall, these results show that although MACS yields higher numbers of sorted cells, FACS provides higher purity of sorted cells and the ability to sort three different stromal cell populations. Therefore, FACS sorting will be carried forward to purify stromal cell subsets from mouse lung.

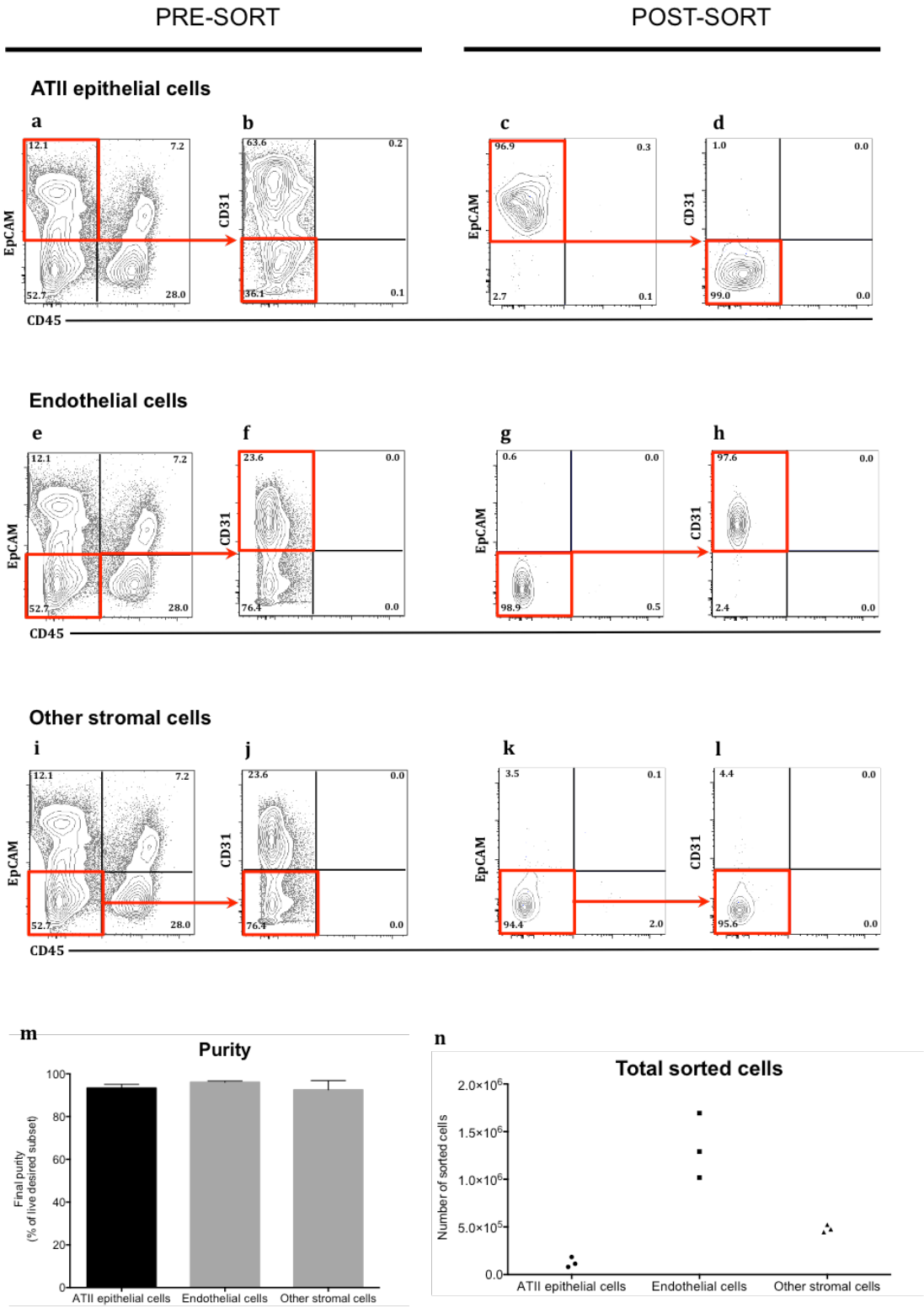

PRE-SORT
POST-SORT
ATII epithelial cells
a
b
c
d
EpCAM
CD31
CD45
12.1
7.2
52.7
28.0
63.6
0.2
36.1
0.1
96.9
0.3
2.7
0.1
1.0
0.0
99.0
0.0
Endothelial cells
e
f
g
h
12.1
7.2
52.7
28.0
23.6
0.0
76.4
0.0
0.6
0.0
98.9
0.5
97.6
0.0
2.4
0.0
Other stromal cells
i
j
k
l
12.1
7.2
52.7
28.0
23.6
0.0
76.4
0.0
3.5
0.1
94.4
2.0
4.4
0.0
95.6
0.0
m
Purity
Final purity
(% of live desired subset)
100
80
60
40
20
0
ATII epithelial cells
Endothelial cells
Other stromal cells
n
Total sorted cells
Number of sorted cells
2.0×10^6
1.5×10^6
1.0×10^6
5.0×10^5
0.0
ATII epithelial cells
Endothelial cells
Other stromal cells

Figure 5.5. FACS of ATII epithelial cells, endothelial cells and other stromal cells from lung. C57BL/6 mice lungs were digested with dispase into single-cell suspension and stained with antibodies against CD45, CD31 and EpCAM. Cells were then sorted on a FACSAria cell sorter, first gating out debris, dead cells and doublets before sorting for the following populations $CD45^{-}CD31^{-}EpCAM^{+}$ (ATII epithelial cells), $CD45^{-}CD31^{-}EpCAM^{-}$ (other stromal cells) and $CD45^{-}CD31^{+}EpCAM^{-}$ (endothelial cells). Purity was checked by analysing an aliquot of pre and post sorted samples by flow cytometry. Flow cytometric plots show ATII epithelial cells (a-d), endothelial cells (e-h) and other stromal cells (i-l) with no previous gating on debris, dead cell or singlets (grey contour with gate frequencies) to illustrate the complete composition of the samples pre and post-sort. Dead cells are highlighted in blue for post-sort samples (c/d, g/h, k/l). The final purity (percentage of live sorted cells) (m) and total sorted cells (n) obtained. Data representative (a-l) and pooled (m/n) of 3 separate experiments with 5 pooled mice each. Pooled data shown as mean ± SEM.

5.1.4 Summary

The investigation of stromal cells *in vivo* is limited due to the difficulties in isolating these cells from the lung. In this study, an isolation and purification protocol was developed to obtain high viable yields of purified stromal cell subsets from mouse lung. Using the proteolytic enzyme dispase, clear populations of ATII epithelial cells, endothelial cells, and the mixed population other stromal cells predicted to contain fibroblast, pericytes and SMCs was achieved (Fig. 5.1). The use of dispase, a protease specifically suggested for ATII epithelial cell isolation (Corti et al. 1996, Messier et al. 2012), leads to the loss of ATI epithelial cells (Fig. 5.2) which are considered to be one of the main targets for RSV infection the lung (Borchers et al. 2013). This can potentially be seen through the significant decrease in total lung viral load titre when comparing total lung homogenate to cell suspension obtained through dispase-digestion (Fig. 5.3). It is possible that dispase may be cleaving T1α, the cell surface ATI marker used to identify these cells in this study. However, nearly all EpCAM positive cells stained positively for the intracellular ATII epithelial cell marker pro-SpC, suggesting this may not be the case, and that ATI epithelial cells are lost via cell death during dispase processing. Therefore, the role of ATI epithelial cells cannot be examined in this study, but needs to be kept in consideration as a major target for virus infection.

A sorting protocol was then developed to collect pure viable populations of stromal cell subsets for further downstream analysis. MACS allowed sorting of two different populations; ATII epithelial cells and other stromal cells and provided a considerably high yield of each cell type. However, purity was considerably low with dead cells in particular, making up most of the sample (Fig. 5.4). Endothelial cells could not be sorted with MACS due to the significantly increased cell loss and death of all subsets with the additional staining and washing steps needed to isolate these cells. FACS allowed sorting of three stromal cell populations, ATII epithelial cells, endothelial cells and other stromal cells. The yield from FACS was much lower than MACS, however purity was much higher with at least 90% purity of each sorted cell type (Fig. 5.5). Thus,

although the yield from FACS is lower than MACS, the ability to sort three different stromal cell populations and the capability to exclude dead cells allows the study of a wider range of stromal cell subsets at high purity for further sensitive downstream analysis, that will be less likely to be confounded by other cell subsets. Thus, dispase digestion and FACS will be taken forward to isolate stromal cells from the lung for experimentation in this study.

5.2 Expression of soluble mediators from stromal cells during RSV infection *in vivo*

5.2.1 CD45$^-$ stromal cells are a major source of cytokines, chemokines and growth factors, whilst CD45$^+$ leukocytes are a major source of type I IFNs

Human cases of RSV infection have shown various proinflammatory and antiviral mediators to be expressed during infection. In particular, cytokines IL-6 and IL-33 and chemokines CCL2, CXCL8 and CXCL10 have been detected in the airway and secretions of RSV-infected children (Noah et al. 1995, Hornsleth et al. 1998, Sheeran et al. 1999, Garofalo et al. 2001, McNamara et al. 2005, Saravia et al. 2015). These mediators have also been detected *in vivo* in mice during RSV infection, along with type I IFNs and growth factors GM-CSF and amphiregulin, and further experimentation have shown many of them to be critical in viral clearance (Bukreyev et al. 2001, Guerrero-Plata et al. 2005, Monick et al. 2005, Jewell et al. 2007, Bhoj et al. 2008, Lindell et al. 2008, Goritzka, Makris, et al. 2015, Goritzka, Pereira, et al. 2015). The cell types responsible for the production of these mediators during RSV infection *in vivo* have not been fully identified.

To initially determine the contribution of all stromal cells in the induction of the above mediators during RSV, a time course of infection was performed in mice with lung cells FACS sorted based on CD45 expression at 4, 12 and 18hrs post-infection. These time points allowed observation of mediators induced very early during infection as well as during the first replication cycle of RSV. CD45 is common leukocyte antigen and expressed on hematopoietic cells (such as lymphocytes and leukocytes), but not on non-hematopoietic cells (such as stromal cells) (McKinney-Freeman et al. 2009). This allowed broad isolation of CD45$^+$ leukocytes and CD45$^-$ stromal cells from the lung. Cells were also sorted from uninfected (naïve) mice to give baseline gene expression before infection. Sorted cells were then analysed for gene expression via RT-qPCR of growth

factors amphiregulin and GM-CSF, chemokines CXCL1, CXCL10 and CCL2, cytokines IL-33 and IL-6 and type I IFNs IFN-α5 and IFN-β. RSV L gene was also quantified to determine lung viral load. Gene expression in sorted cells was compared to total lung expression, a sample of the dispase-digested single-cell suspension of the lung before cell-surface staining and FACS. This allowed us to determine if a certain sorted population was enriched for a particular gene, and thus a potential major source of the mediator. This would be identified by higher expression in the sorted cell compared to total lung. Gene expression comparisons were also performed between different sorted cell populations, to determine which had a larger relative contribution.

The data revealed that RSV was present in both $CD45^-$ stromal cells and $CD45^+$ leukocytes across the whole time course of infection (Fig. 5.6a). $CD45^+$ leukocytes had significantly more virus than $CD45^-$ stromal cells at 4hrs; with approximately 10 fold more L gene copies, and a trend towards more virus at 12 and 18hrs post RSV infection compared to $CD45^-$ stromal cells. However, neither population of sorted cells had higher virus load compared to total lung cells suggesting that neither were particularly enriched for the virus (Fig. 5.6a). Viral load decreased in $CD45^+$ leukocytes after 4hrs, plateauing at 12 and 18hrs whilst $CD45^-$ stromal cell viral load remained relatively unchanged across the time course (Fig. 5.6a).

Gene expression analysis of soluble mediators revealed that $CD45^-$ stromal cells were the dominating population expressing all chemokines, cytokines and growth factors tested (Fig. 5.6b-d), whilst $CD45^+$ leukocytes dominated in the expression of the type I IFNs IFN-α5 and IFN-β (Fig. 5.6e). Gene expression peaked between 4 and 12hrs for IL-33 and growth factors (Fig. 5.6c/d), whilst IL-6, chemokines and type I IFNs peaked between 12 and 18hrs post infection (Fig. 5.6b/c/e). CXCL1, CXCL10, CCL2, IL-6 and IL-33 were all expressed in $CD45^-$ stromal cells at levels higher than in $CD45^+$ leukocytes and more significantly, higher than total lung across the time course of infection, signifying enrichment of these genes in the stromal cell population (Fig. 5.6b/c). There was significantly higher expression of CXCL10 at 12hrs and IL-33 at 4hrs in $CD45^-$ stromal cells versus total lung (Fig. 5.6b/c). CXCL10, CCL2 and IL-6 were also

induced in $CD45^+$ leukocytes, however levels were never above total lung expression, suggesting minor contribution *in vivo* (Fig. 5.6b/c). The growth factors amphiregulin and GM-CSF were most dominantly induced in in $CD45^-$ stromal cells, with little to no expression in $CD45^+$ leukocytes suggesting that stromal cells are a major cellular source of these mediators during RSV infection in *vivo* (Fig. 5.6d). Interestingly, amphiregulin, GM-CSF and IL-33 were detected in total lung and $CD45^-$ stromal cells in naïve mice, demonstrating basal expression of these mediators *in vivo* (Fig. 5.6d). Lastly, expression of type I IFNs, IFN-α5 and IFN-β peaked at 12hrs post infection and was confined solely to $CD45^+$ leukocytes with minimal to no expression from $CD45^-$ stromal cells (data also shown in (Goritzka, Makris, et al. 2015)). However, type I IFN expression levels in $CD45^+$ leukocyte levels did not significantly exceed total lung gene expression (Fig. 5.6e).

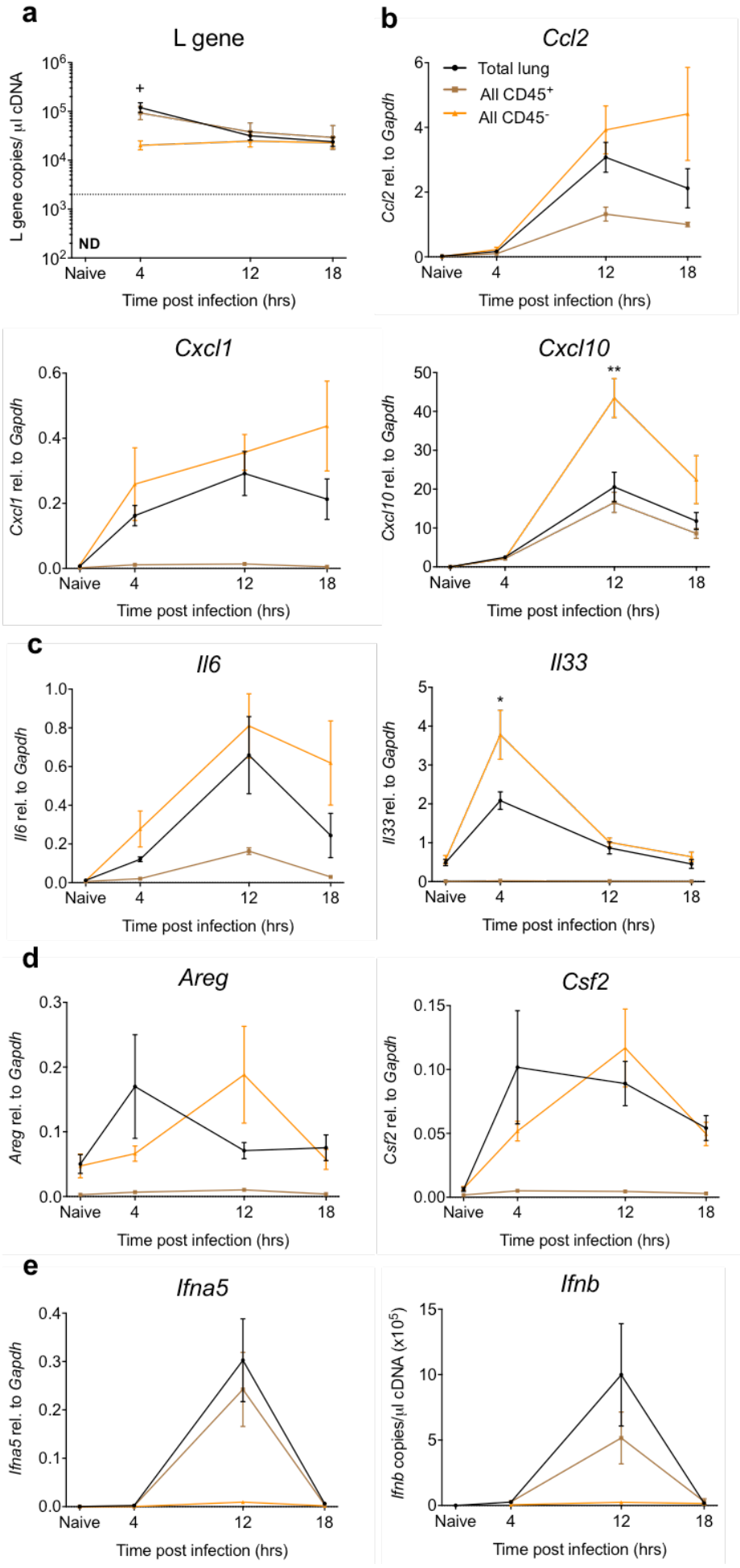

a
L gene
L gene copies/ µl cDNA
ND
Naive
4
12
18
Time post infection (hrs)
b
Ccl2
Total lung
All CD45+
All CD45-
Ccl2 rel. to Gapdh
Cxcl1
Cxcl1 rel. to Gapdh
Cxcl10
Cxcl10 rel. to Gapdh
c
Il6
Il6 rel. to Gapdh
Il33
Il33 rel. to Gapdh
d
Areg
Areg rel. to Gapdh
Csf2
Csf2 rel. to Gapdh
e
Ifna5
Ifna5 rel. to Gapdh
Ifnb
Ifnb copies/µl cDNA (x10⁵)

Figure 5.6: CD45$^-$ stromal cells are a major source of growth factors, chemokines and cytokines, whilst CD45$^+$ leukocytes are a major source of type I IFNs during RSV infection *in vivo*. C57BL/6 mice were infected with 1.5x10^6 FFU of RSV intranasally and lungs taken at 4, 12 and 18hrs post infection. Lungs from naïve mice were taken without inoculation. Lungs were digested with dispase and the single-cell suspension stained with anti-CD45 antibody. Cells were FACS sorted for live singlet CD45$^+$ leukocytes and CD45$^-$ stromal cells. A sample of the single-cell suspension before sorting was also taken to represent the total lung. RNA was extracted from cells, converted to cDNA and analysed for gene expression of RSV L gene for viral load (a), chemokines CCL2, CXCL1 and CXCL10 (b), cytokines IL-6 and IL-33 (c), growth factors amphiregulin (*Areg*) and GM-CSF (*Csf2*) (d), and type I IFNs IFN-α5 and IFN-β (e) via qPCR. Copy numbers for L gene and IFN-β were determined using a plasmid standard with the dashed line representing the lower detection limit. For all other genes, expression is shown relative to the housekeeping gene *Gapdh*. ND: not detectable. Statistically significant differences between CD45$^-$ and total lung is represented by '*' and between CD45$^-$ and CD45$^+$ sorted cells '+'. Results show 6-9 sorts per time point, with 3-5 mice pooled per sort and data presented as mean ± SEM. Statistical significance was determined using two-way ANOVA with Bonferonni's post hoc test. * $p \leq 0.05$, ** $p \leq 0.01$.

5.2.2 ATII epithelial cells are a major source of growth factors whilst other stromal cells are a major source of chemokines and cytokines

To next determine which particular types of stromal cells were contributing to the growth factors, chemokines and cytokines detected in the $CD45^-$ stromal cell population during RSV infection shown in Fig. 5.6, three different stromal cell subsets were sorted from the $CD45^-$ stromal cell population (see Fig. 4.2 for gating strategy): ATII epithelial cells, endothelial cells and other stromal cells. AMs were also sorted to represent a cell subset from the $CD45^+$ leukocyte population and acted as a non-stromal cell comparison, and a cell type our group have analysed in detail (Goritzka, Makris, et al. 2015). A longer time course of infection was performed which included 4, 12, 18, 48 and 96hrs post infection to capture the full innate immune response, and cells were sorted at each time point as well as before infection (naïve). Sorted cells were then analysed for gene expression of the mediators as described above.

The data revealed that virus was present in all the different stromal cell subsets as well as in AMs, at all time points studied (Fig. 5.7a). Peak viral load differed between the different cell populations with total lung and AMs peaking at 4hrs, ATII epithelial cells peaking at 18hrs and endothelial cells and other stromal cells peaking at 96hrs post infection (Fig. 5.7a). All stromal cell subsets had a trend towards increased viral load between 48 and 96hrs post infection, whilst AMs were the only population that decreased in the number of L gene copies detected (Fig. 5.7a). However, at no time point during infection was viral load significantly higher in any of the stromal cell populations or AMs compared to total lung, suggesting (as in 5.1.2) that the main cellular target of RSV infection *in vivo* may not be one of these four populations. However, there was significantly more virus in AMs at 4hrs compared to ATII epithelial cells and endothelial cells (Fig. 5.7a). This is most likely uptake of the input virus, as viral replication is unlikely to occur so early after infection.

Analysis of soluble mediator gene expression, showed that ATII cells were a major source of the growth factors amphiregulin and GM-CSF as well as the

cytokine IL-33, with expression at all time points above total lung (Fig. 5.7b). Notably, there was minimal to no expression in endothelial cells, other stromal cells or AMs. Levels of amphiregulin were significantly increased compared to total lung expression at all time points but highest between 48 and 96hrs, suggesting ATII epithelial cells are a major cellular source throughout infection *in vivo* (Fig.5.7b). GM-CSF levels were significantly enriched in ATII epithelial cells between 4 and 18hrs and IL-33 at 4hrs, compared to total lung (Fig. 5.7b). Interestingly, all three genes were detected at baseline in naive mice in ATII epithelial cells and total lung, with expression increasing after infection and returning to baseline at 18hrs and 48hrs for IL-33 and GM-CSF, respectively. Whilst for amphiregulin, gene expression levels were still maintained above baseline levels even at 96hrs post infection (Fig. 5.7b).

The other stromal cells were revealed to be a major source of the chemokines CXCL1, CXCL10 and CCL2 with gene expression levels significantly above total lung at the peak time points (12-18hrs), which decreased back to naïve levels between 48-96hrs (Fig. 5.7c). CXCL1 was also detected in ATII epithelial cells between 4 and 12hrs and CXCL10 in endothelial cells at 12hrs with levels above, albeit not significantly different, from total lung or other stromal cells suggesting a smaller relative contribution *in vivo* (Fig. 5.7c). The other stromal cells were also a major source of the cytokine IL-6, with significantly higher gene expression than total lung at 12-18hrs post infection (Fig. 5.7c). Interestingly, IL-6 was also detected at baseline, before infection in other stromal cells, but by 96hrs post infection levels were undetectable.

Detectable levels of IFN-β were seen in all stromal cell subtypes (<30,000 copies) albeit below total lung expression and peaking between 12 and 18hrs post infection (Fig. 5.7d). However, of the four sorted populations, the major cellular source of IFN-β was shown to be AMs, which showed significantly increased levels of gene expression compared to total lung at 12hrs (approximately 300,000 copies versus 150,000) (Fig. 5.7d). Similarly, IFN-α5 gene expression was detected mainly from AMs at 12hrs post infection, with levels significantly above total lung at 12 and 18hrs, with minimal expression from stromal cell subsets (Fig. 5.7d).

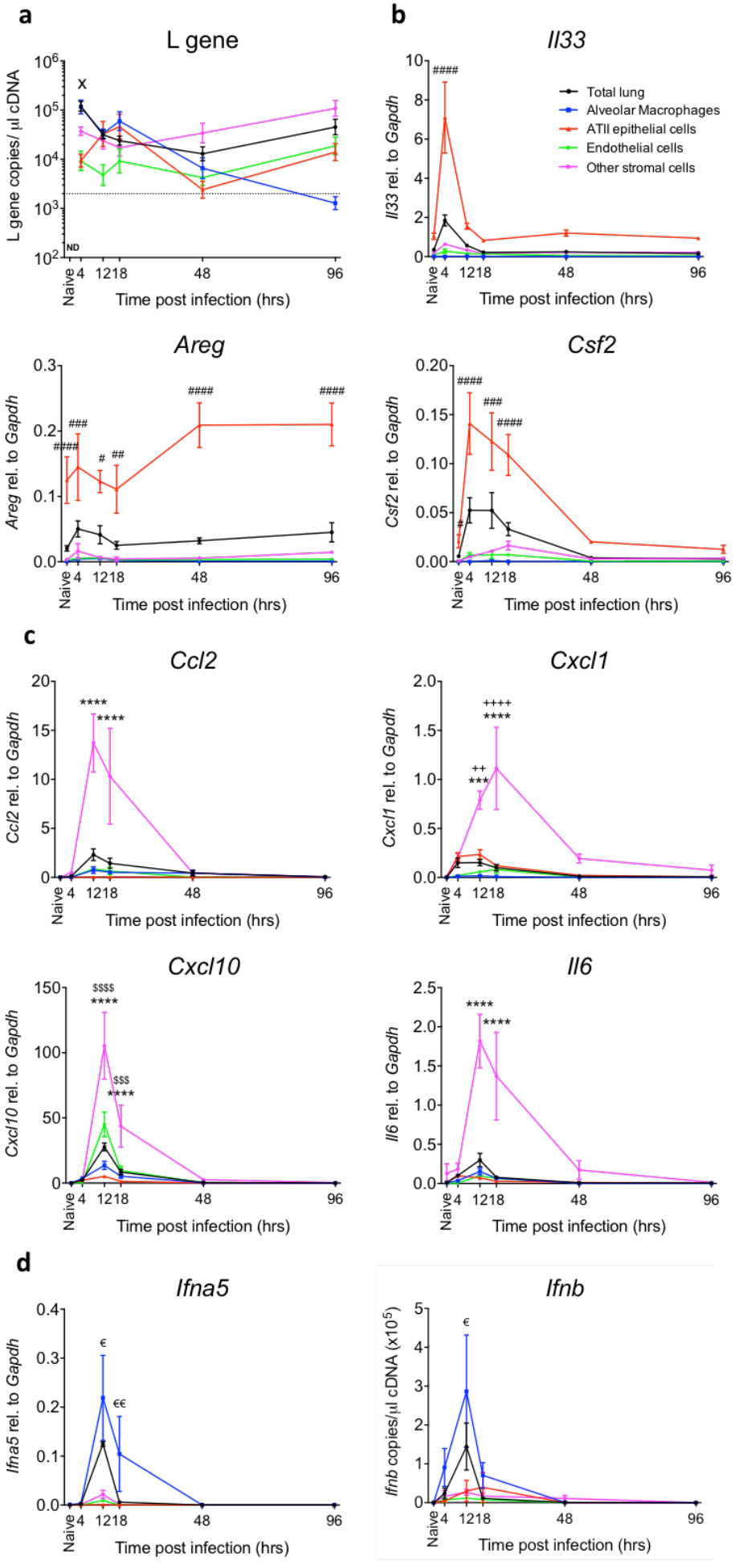

a
L gene
L gene copies/ µl cDNA
ND
Naive
Time post infection (hrs)
b
Il33
Il33 rel. to Gapdh
Total lung
Alveolar Macrophages
ATII epithelial cells
Endothelial cells
Other stromal cells
Areg
Areg rel. to Gapdh
Csf2
Csf2 rel. to Gapdh
c
Ccl2
Ccl2 rel. to Gapdh
Cxcl1
Cxcl1 rel. to Gapdh
Cxcl10
Cxcl10 rel. to Gapdh
Il6
Il6 rel. to Gapdh
d
Ifna5
Ifna5 rel. to Gapdh
Ifnb
Ifnb copies/µl cDNA (x10^5)

Figure 5.7: Differential expression of type I IFNs, cytokines, chemokines and growth factors from stromal cell populations and AMs during RSV infection. C57BL/6 mice were infected with $1.5x10^6$ FFU of RSV intranasally and lungs taken at 4, 12, 18, 48 and 96hrs post infection. Naïve mice were taken without inoculation. Lungs were digested with dispase and stained with antibodies against CD45, CD31, CD11c and EpCAM. Cells were FACS sorted for three different live singlet stromal cell populations ($CD45^-EpCAM^+CD31^-$ ATII epithelial cells, $CD45^-EpCAM^-CD31^+$ endothelial cells and $CD45^-EpCAM^-CD31^-$ other stromal cells) as well as alveolar macrophages (AMs; $CD45^+EpCAM^+CD11c^+$). Purity was always >95% for all sorted populations. A sample of the single-cell suspension before sorting was also taken to represent the total lung. RNA was extracted from cells, converted to cDNA and analysed for gene expression of RSV L gene for viral load (a), amphiregulin (*Areg*), GM-CSF (*Csf2*) and IL-33 (b), CCL2, CXCL1, CXCL10 and IL-6 (c) and IFN-β and IFN-α5 (e) via qPCR. Copy numbers for L gene and IFN-β were determined using a plasmid standard with the dashed line representing the lower detection limit. For all other genes, expression is shown relative to the housekeeping gene *Gapdh*. ND: not detectable. Statistically significant differences between ATII epithelial cells and total lung is represented by '#', between other stromal cells and total lung '*', between AMs and total lung '€', between other stromal cells and ATII epithelial cells '+', between stromal cells and endothelial cells '$' and between AMs and ATII epithelial cells or endothelial cells 'x'. Results show 3-4 sorts per time point, with 5 mice pooled per sort and data presented as mean ± SEM. Statistical significance was determined using two-way ANOVA with Bonferonni's post hoc test. ** p≤0.05, ** p≤0.01*, **** p≤0.001, **** p≤0.0001.*

5.2.3 Gene expression of CXCL10 and type I IFNs is dependent on live RSV, whilst expression of CXCL1, CCL2, growth factors and cytokines is partially dependent on live RSV at 4hrs post infection

To determine whether gene expression of the early soluble mediators detected in stromal cells was dependent on live virus, mice were inoculated with UV-inactivated RSV and stromal cell subsets and AMs sorted at 4hrs post infection. 4hrs was chosen as most mediators were detected at this time point (Fig. 5.7). Cells were also sorted from live RSV-infected and naïve mice for comparison.

The results showed that L gene was only detected in mice inoculated with live RSV, confirming that UV-inactivated RSV contains no live virus (Fig, 5.8a). Live virus was required for gene expression of CXCL10, IFN-α5 and IFN-β as minimal to no expression was detected from UV-inactivated virus (Fig. 5.8b). Gene expression of GM-CSF, amphireguin and IL-33 was detected in total lung and ATII epithelial cells as shown previously (Fig. 5.7b and Fig. 5.8c). Amphiregulin was detected in naïve ATII epithelial cells and there was no considerable increase after exposure to UV-inactivated or live RSV (Fig. 5.8c). For GM-CSF and IL-33, live virus stimulated increased levels of gene expression compared to naïve and UV-inactivated RSV exposed ATII epithelial cells (Fig. 5.8c) suggesting that although dead virus can illicit some response from stromal cells, live virus is required to induce a robust response. Similarly, expression of IL-6, CXCL1 and CCL2 was slightly induced with UV-inactivated virus, but live virus incited much higher levels, signifying the requirement of live virus for a more potent response (Fig. 5.8c).

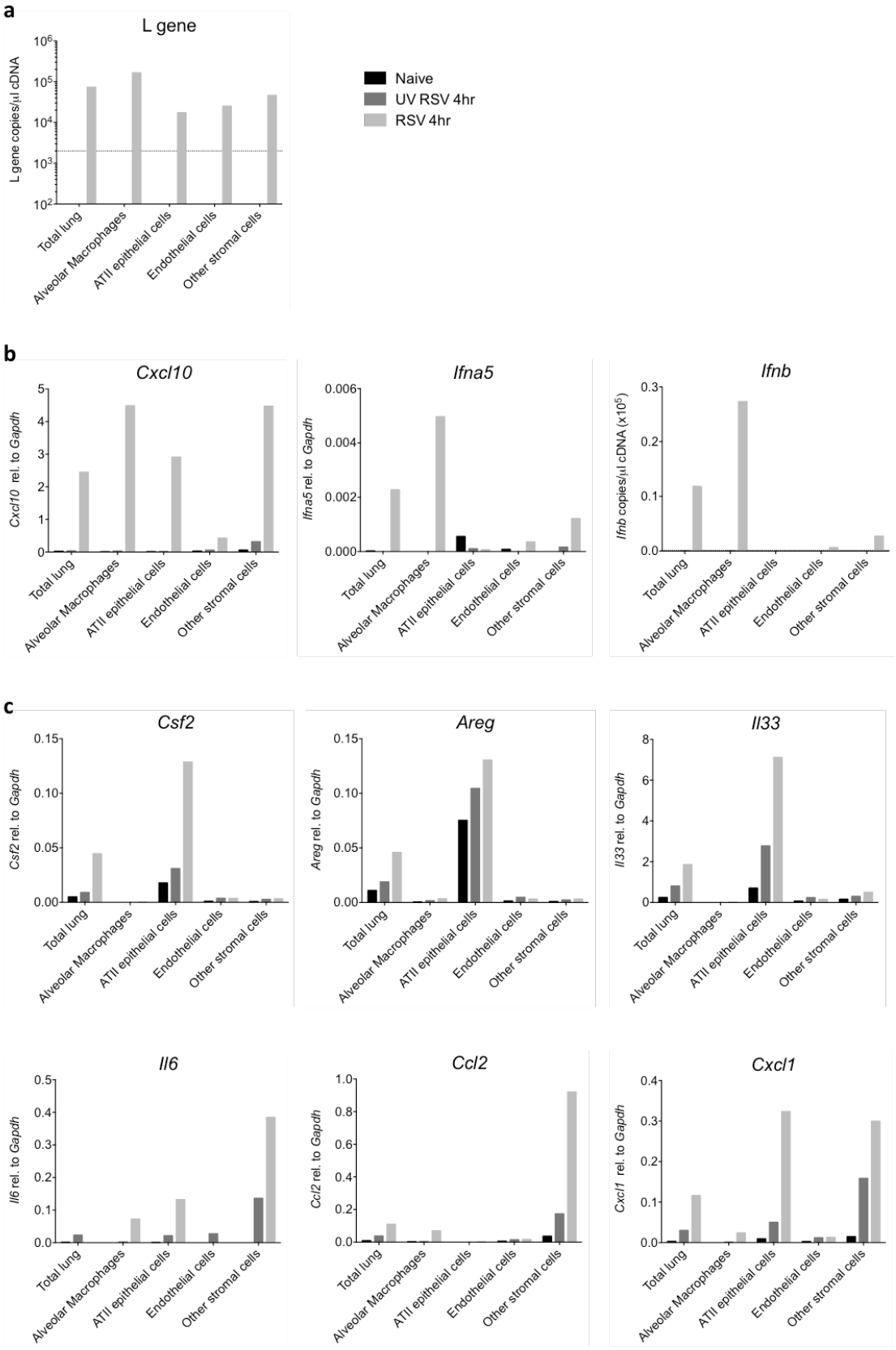

a
L gene
L gene copies/µl cDNA
Naive
UV RSV 4hr
RSV 4hr
b
Cxcl10
Cxcl10 rel. to Gapdh
Ifna5
Ifna5 rel. to Gapdh
Ifnb
Ifnb copies/µl cDNA (x10^5)
c
Csf2
Csf2 rel. to Gapdh
Areg
Areg rel. to Gapdh
Il33
Il33 rel. to Gapdh
Il6
Il6 rel. to Gapdh
Ccl2
Ccl2 rel. to Gapdh
Cxcl1
Cxcl1 rel. to Gapdh
Total lung
Alveolar Macrophages
ATII epithelial cells
Endothelial cells
Other stromal cells

Figure 5.8: Viral load and gene expression of type I IFNs, cytokines, chemokines and growth factors from stromal cell populations and AMs during UV-inactivated and live RSV infection. C57BL/6 mice were innoculated with $1.5x10^6$ FFU of UV-inactivated or live RSV intranasally and lungs were taken at 4hrs post infection. Naïve mice were taken without inoculation. Lungs were digested with dispase and stained with antibodies against CD45, CD31, CD11c and EpCAM. Cells were then FACS sorted for live singlet ATII epithelial cells, endothelial cells, other stromal cell and AMs. Purity was always >95% for all sorted populations. A sample of the single-cell suspension before sorting was also taken to represent the total lung. RNA was extracted from cells, converted to cDNA and analysed for gene expression of RSV L gene for viral load (a), CXCL10, IFN-α5 and IFN-β (b) and GM-CSF (*Csf2*), amphiregulin (*Areg*), IL-33, IL-6, CCL2 and CXCL1 (c) via qPCR. Copy numbers of L gene and IFN-β were determined using a plasmid standard with the dashed line representing the lower detection limit. For all other genes, expression is shown relative to the housekeeping gene *Gapdh*. Results show one sort per time point with 5 mice pooled per sort and the mean of duplicate qPCR reactions.

5.2.4 Other stromal cells induce expression of an array of chemokines during RSV infection *in vivo*

The data so far have revealed that during RSV infection, of the three stromal cells subsets investigated, other stromal cells are a major source of the chemokines CXCL1, CXCL10 and CCL2, as well as the cytokine IL-6, whilst ATII epithelial cells are a major source of growth factors GM-CSF and amphiregulin and the cytokine IL-33. To establish if this trend of chemokine production from other stromal cells and growth factor production from ATII cells occurs for more than the mediators initially tested, and to determine a broader view of the chemokines and cytokines induced by these stromal cell subsets during RSV infection, deeper gene expression analysis was performed. The amount of RNA extracted from sorted cells is limited as the number of cells obtained from sorting via FACS is low (Fig. 5.5n). Therefore, in the following experiments mice were infected with RSV, stromal cells FACS sorted and the extracted RNA amplified. This allowed more extensive gene expression analysis via qPCR for additional genes of interest as well as via gene expression arrays covering a broader range of IFNs, cytokines, chemokines and growth factors.

First, stromal cell subsets and AMs were sorted at 4, 18 and 96hrs post RSV infection. Cells from naïve mice were also sorted. RNA was extracted and amplified before gene expression analysis via qPCR of additional mediators observed from previous *in vitro* and *in vivo* studies of RSV (see section 5.1.3) such as chemokines CCL7, CXCL5 and CXCL12, cytokines TNF-α, IL-1α and IL-1β, IFN-γ, and growth factors TGF-β and VEGF.

The data revealed that of the additional chemokines investigated, CCL7 a monocyte chemoattractant, and CXCL5 a neutrophil chemoattractant were also expressed by other stromal cells after RSV infection *in vivo* (Fig. 5.9a). CXCL12, bone marrow homing chemokine, showed minimal to no expression in all of the stromal cells subsets and AMs, but was detected in total lung suggesting that another lung cell population is the source of this chemokine *in vivo*. Analysis of cytokines revealed that proinflammatory cytokines TNF-α and IL-1α were

enriched in AMs minimal expression from other stromal cells and no expression from ATII epithelial cells and endothelial cells (Fig. 5.9b). IL-1β was detected in other stromal cells and AMs, but at levels lower than total lung suggesting that they are not the prominent source of this cytokine *in vivo* (Fig. 5.9b).

The type I IFNs IFN-α5 and IFN-β were observed to come mainly from AMs (Fig. 5.7d). Expression of the type II IFN, IFN-γ had little to no expression from either AMs or stromal cells, but was detected in total lung, suggesting another cellular source in the lung, most probably NK cells (Fig. 5.9c).

Analysis of transforming growth factor β (TGF-β) whose roles include cell growth arrest, differentiation and apoptosis, revealed that AMs were a major source of this mediator whilst other stromal cells were a minor source during RSV infection *in vivo* (Fig. 5.9d). VEGF was highly expressed by endothelial cells with minor expression from ATII epithelial cells and other stromal cells (Fig, 5.9d). Interestingly, whilst VEGF gene expression levels dramatically decreased at 18hrs post infection after an initial rapid increase, levels from endothelial cells did not return back down to baseline and continued to increase to 96hrs post infection (Fig. 5.9d).

Pro-surfactant protein C is a marker of ATII epithelial cells and expression was observed via flow cytometry in these cells in naïve mice (Fig, 5.2a). To further confirm these findings and to see if expression was altered during RSV infection, gene expression of pro-surfactant protein C (*Sftpc*) was also analysed across the time course of infection. *Sftpc* was only expressed in ATII epithelial cells and no other sorted population. This confirms the identity and purity of this sorted cell population. Additionally, *Sftpc* expression dramatically decreased post infection all the way to the end of the time course suggesting that infection considerably impacts expression (Fig. 5.9e).

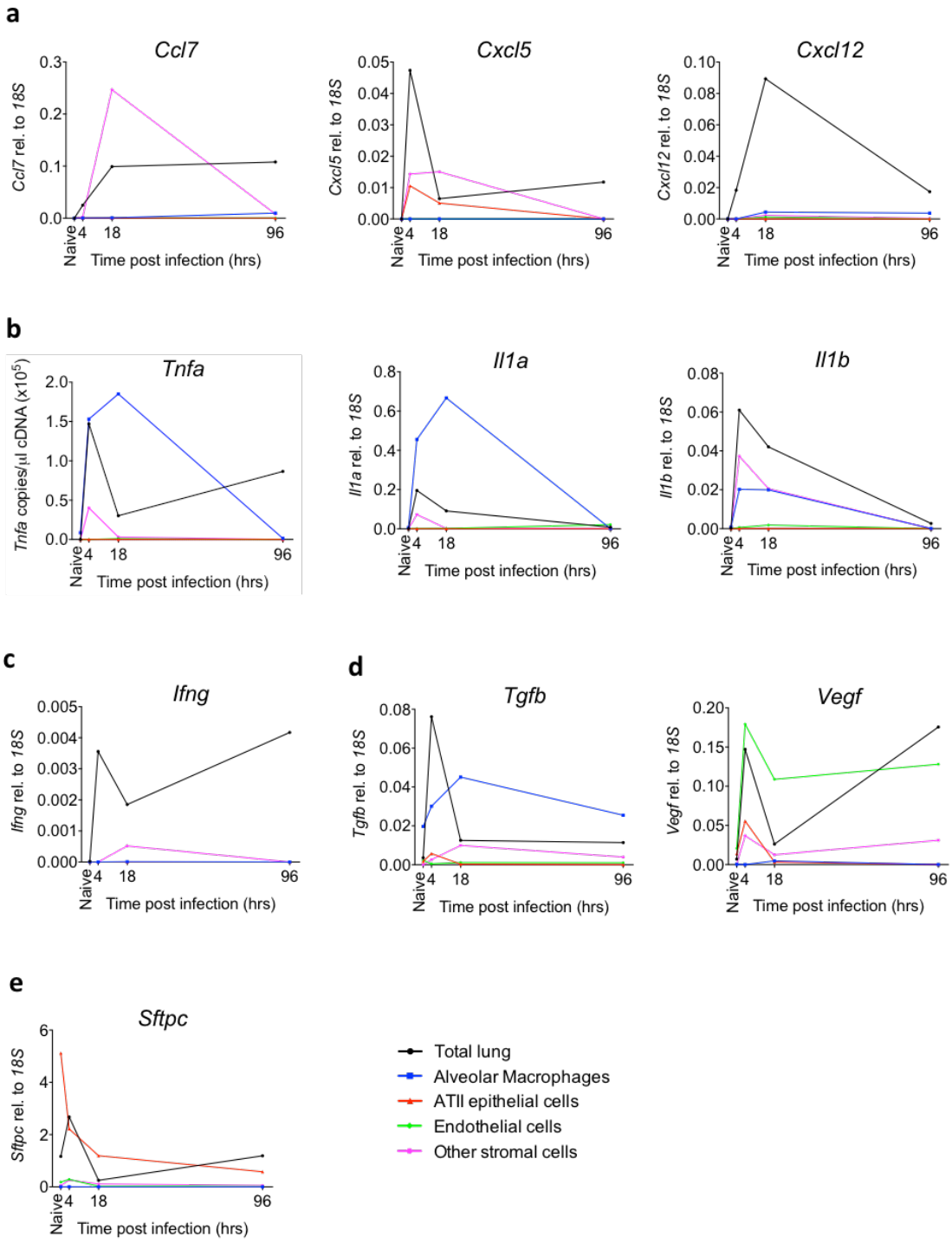

a
Ccl7
Ccl7 rel. to 18S
0.3
0.2
0.1
0.0
Naive
4
18
96
Time post infection (hrs)
Cxcl5
Cxcl5 rel. to 18S
0.05
0.04
0.03
0.02
0.01
0.00
Naive
4
18
96
Time post infection (hrs)
Cxcl12
Cxcl12 rel. to 18S
0.10
0.08
0.06
0.04
0.02
0.00
Naive
4
18
96
Time post infection (hrs)
b
Tnfa
Tnfa copies/µl cDNA (x10^5)
2.0
1.5
1.0
0.5
0.0
Naive
4
18
96
Time post infection (hrs)
Il1a
Il1a rel. to 18S
0.8
0.6
0.4
0.2
0.0
Naive
4
18
96
Time post infection (hrs)
Il1b
Il1b rel. to 18S
0.08
0.06
0.04
0.02
0.00
Naive
4
18
96
Time post infection (hrs)
c
Ifng
Ifng rel. to 18S
0.005
0.004
0.003
0.002
0.001
0.000
Naive
4
18
96
Time post infection (hrs)
d
Tgfb
Tgfb rel. to 18S
0.08
0.06
0.04
0.02
0.00
Naive
4
18
96
Time post infection (hrs)
Vegf
Vegf rel. to 18S
0.20
0.15
0.10
0.05
0.00
Naive
4
18
96
Time post infection (hrs)
e
Sftpc
Sftpc rel. to 18S
6
4
2
0
Naive
4
18
96
Time post infection (hrs)
Total lung
Alveolar Macrophages
ATII epithelial cells
Endothelial cells
Other stromal cells

Figure 5.9: Expression of additional chemokines, cytokines, IFNs, growth factors and surfactant proteins by stromal cells and AMs during RSV infection. C57BL/6 mice were infected with $1.5x10^6$ FFUs of RSV intranasally and lungs taken at 4, 18 and 96hrs post infection. Naïve mice were taken without inoculation. Lungs were digested with dispase and stained with antibodies against CD45, CD31 and EpCAM. Cells were FACS sorted for live singlet ATII epithelial cells, endothelial cells, other stromal cells and alveolar macrophages. Purity was always >95% for all sorted populations. A sample of the single-cell suspension before sorting was also taken to represent the total lung. RNA was extracted from cells, and converted to cDNA and amplified using the QuantiTect Whole Transcriptome Kit. Gene expression was then performed via qPCR for chemokines CCL7, CXCL5 and CXCL12 (a), cytokines, IL-1α and IL-1β (b), type II IFN IFN-γ (c), growth factors TGF-β and VEGF (d) and pro-surfactant protein C (*Sftpc*) (e). Copy numbers for TNF-α was determined using a plasmid standard with the dashed line representing the lower detection limit ($0.002x10^5$). For all other genes, expression is shown relative to the housekeeping gene 18S ribosomal RNA (*Gapdh* not used due to sensitivity to pre-amplification process). Results show one sort per time point, with 5 mice pooled per sort

These results so far have demonstrated that of the three stromal cells populations studied, other stromal cells and ATII epithelial cells are the more active subsets in terms of the numbers and types of soluble mediators induced during RSV infection *in vivo*. Therefore, to obtain a more comprehensive and broader view of the mediators expressed by these two populations at the peak of their activity, mice were infected with RSV, and ATII epithelial cells sorted at 4hrs post infection and other stromal cells at 12hrs, to represent the peak gene expression activity of both cells *in vivo* (Fig, 5.7). Cells were also sorted from naïve mice for comparison. RNA from sorted cells was amplified and run on Qiagen RT^2 Profiler PCR Array for Cytokine and Chemokines (PAMM-150Z) and Antiviral Response (PAMM-122Z), and covering a broad range of IFNs, cytokines, chemokines and growth factors.

Gene expression array analysis of other stromal cells showed that many mediators were induced by these cells 12hrs post infection *in vivo*, and strikingly, more than half of these were chemokines (15/27) (Table 5.1). Of the total 23 chemokines analysed, 15 were expressed >5 fold – the minimum threshold set for induced expression - in other stromal cells from RSV infected mice compared to naïve mice. Interestingly, of these, CCL4, CCL12 and CCL20 were increased more than 50 fold. CCL2, CCL7, CXCL3, CXCL5 and CXCL9 more than 500 fold and CXCL10 more than 1000 fold compared to naïve (Table 5.1). Out of the non-chemokine mediators expressed above the threshold by other stromal cells, only IL-6 was induced more than 50 fold in RSV infected mice compared to naïve mice (Table 5.1). IFN-α2, IFN-β1 and IFN-γ were detected, as well as the growth factors GM-CSF, G-CSF and M-CSF in other stromal cells from RSV infected mice compared to naïve mice. Additional mediators induced during infection in other stromal cells were cytokines IL-1α, IL-1β, TNF, OSM (oncostatin M) and TNFSF10 (Table 5.1).

	Gene (Protein)	Function
Interferons	***Ifna2***	Anti-viral
	Ifnb1	Anti-viral
	Ifng	Anti-viral
Cytokines	***Il1a***	Proinflammatory
	Il1b	Proinflammatory
	Il6 *	Proinflammatory
	Osm	Proinflammatory
	Tnf	Pro-apoptotic
	Tnfsf10 **(TRAIL)**	Pro-apoptotic
Chemokines	***Ccl2 *****	Monocyte chemoattractant
	Ccl3	Macrophage chemoattractant
	Ccl4 *	Macrophage chemoattractant
	Ccl5	T-cell chemoattractant
	Ccl7 **	Monocyte chemoattractant
	Ccl12 *	Monocyte chemoattractant
	Ccl20 *	T-cell chemoattractant
	Cxcl1	Neutrophil chemoattractant
	Cxcl3 **	Monocyte chemoattractant
	Cxcl5 **	Neutrophil chemoattractant
	Cxcl9 **	T-cell chemoattractant
	Cxcl10 ***	Leukocyte chemoattractant
	Cxcl11	T-cell chemoattractant
	Cxcl13	B-cell chemoattractant
	Xcl1	T-cell chemoattractant
Growth factors	***Csf1*** **(M-CSF)**	Growth factor
	Csf2 **(GM-CSF)**	Growth factor
	Csf3 **(G-CSF)**	Growth factor

Table 5.1: Mediators expressed by other stromal cells 12hrs post-RSV infection. C57BL/6 mice were infected with $1.5x10^6$ FFU of RSV intranasally and lungs taken 12hrs post infection. Naïve mice were taken without inoculation. Lungs were digested with dispase and stained with antibodies against CD45, CD31 and EpCAM. Cells were FACS sorted for live singlet other stromal cells ($CD45^-EpCAM^-CD31^-$). Purity was always >95% for all sorted populations. RNA was extracted from the sorted cells, and using the Qiagen RT^2 PreAMP cDNA synthesis kit converted to cDNA and amplified before running on Qiagen RT^2 Profiler PCR Array Cytokine and Chemokines (PAMM-150Z) and Antiviral Response (PAMM-122Z). The table shows IFNs, cytokines, chemokines and growth factors induced >5 fold in sorted other stromal cells post-RSV infection compared to naïve, in 2 separate arrays. * >50 fold increase, ** >500 fold increase, *** >1000 fold increase. OSM: oncostatin M; TRAIL: TNF-related apoptosis-inducing ligand, M-CSF: macrophage colony-stimulating factor. Results are pooled from 2 replicates of each array with separate naïve and 12hr sorts for each replicate, with 5 mice pooled per sort.

In contrast, gene expression array analysis of ATII epithelial cells showed them to express considerably fewer mediators at their peak time point of 4hrs post infection *in vivo* (Table 5.2). Of the 91 genes analysed, ATII epithelial cells from RSV infected mice induced only 10 genes >5 fold compared to ATII epithelial cells from naïve mice. Of these only five were chemokines, and only one was induced more than 50 fold (CXCL10). IL-6 was the only cytokine that was induced >50 fold. Mediators detected in ATII epithelial cells in Fig. 5.7 were all detected using the array, with IL-21, TNFSF10, CCL20, CXCL3, CXCL5 and M-CSF gene expression also observed in ATII epithelial cells from RSV infected mice compared to naïve mice (Table 5.2).

	Gene (Protein)	Function
Cytokines	***Il6* ***	Proinflammatory
	Il21	Proinflammatory
	***Tnfsf10* (TRAIL)**	Pro-apoptotic
Chemokines	***Ccl20***	T-cell chemoattractant
	Cxcl1	Neutrophil chemoattractant
	Cxcl3	Monocyte chemoattractant
	Cxcl5	Neutrophil chemoattractant
	***Cxcl10* ***	Leukocyte chemoattractant
Growth factors	***Csf1* (M-CSF)**	Growth factor
	***Csf2* (GM-CSF)**	Growth factor

Table 5.2: Mediators expressed by ATII epithelial cells 4hrs post-RSV infection. C57BL/6 mice were infected with $1.5x10^6$ PFU of RSV intranasally and lungs taken 4hrs post infection. Naïve mice were taken without inoculation. Lungs were digested with dispase and stained with antibodies against CD45, CD31 and EpCAM. Cells were FACS sorted for live singlet ATII epithelial cells ($CD45^-EpCAM^+CD31^-$). Purity was always >95% for all sorted populations. RNA was extracted from sorted cells, and using the Qiagen RT2 PreAMP cDNA synthesis kit converted to cDNA and amplified before running on a Qiagen RT^2 Profiler PCR Array Cytokine and Chemokines (PAMM-150Z). Table shows cytokines, chemokines and growth factors induced >5 fold in sorted ATII epithelial cells post-RSV infection compared to naïve, in one array. * >50 fold increase. TRAIL: TNF-related apoptosis-inducing ligand, M-CSF: macrophage colony-stimulating factor. Results are from a one array containing separate naïve and 4hr sorts, with 5 mice pooled per sort.

Overall, the deeper gene expression analysis using amplified cDNA has further demonstrated the notion that other stromal cells are, compared to the ATII epithelial cells and endothelial cells as well as AMs, a more dominant source of chemokines during RSV infection *in vivo*, and thus a potent recruiter of inflammatory cells during the immune response.

5.2.5 Protein expression of chemokines, cytokines and growth factors can be detected in stromal cells

So far, analysis of soluble mediators induced in stromal cells during RSV infection has concentrated on gene expression. We next sought to investigate soluble mediator induction from stromal cells by analysing protein production. Sorted stromal cell subsets were analysed using a 20-plex Luminex assay. Intracellular cytokine staining for CCL2, IL-6 and GM-CSF using flow cytometry was also tested however this was not sensitive enough to detect protein expression in stromal cell subsets and was not continued. For Luminex detection of chemokines and cytokines, total lung cells and sorted stromal cell subsets from naïve mice and mice 18hrs post RSV infection, were homogenised in the presence of proteinase inhibitor and the supernatant added to the Luminex. The time point 18hrs was chosen as gene expression of the chemokines and cytokines analysed in stromal cell subsets peaked between 12 and 18hrs. However, as gene expression for mediators detected in ATII epithelial cells was mainly at 4hrs (Fig. 5.7), it is likely protein expression of these mediators would be missed. Levels of cytokines and chemokines detected in the stromal cells were then normalised to a per cell basis, based on the number of sorted cells obtained for each subtype.

Of the 19 proteins analysed, nine were not detected/under detection limit in both total lung and sorted stromal subsets in naïve mice and 18hrs post RSV infection (GM-CSF, TNF-α, IL-4, IL-5, IL-10, IL-12p40, IL-13, IL-17 and IFN-γ – data not shown). Five mediators were only detected in total lung with expression in stromal cell subsets either not detected or under the detection limit (VEGF,

CCL3, IL-1α, IL-1β and IL-6 – data not shown). However, five were detected above the threshold in total lung and stromal cell subsets (Fig. 5.10). The chemokines CCL2, CXCL10 and CXCL9 were all only detected after RSV infection, with no expression in naïve mice (Fig. 5.10a-c). CCL2 was detected in other stromal cells and endothelial cells post RSV infection, but induced most strongly in other stromal cells (Fig, 5.10a). However, CCL2 levels in other stromal cells were not considerably higher than total lung levels. CXCL9 and CXCL10 were also detected in other stromal cells and endothelial cells 18hrs post infection, however other stromal cell levels were considerably higher with approximately 4 and 8 fold more, respectively (Fig. 5.10b/c). Unlike CCL2 however, levels of CXCL9 and CXCL10 in other stromal cells were much higher than total lung levels, with 3 and 4-fold increase in CXCL9 and CXCL10 respectively, thus suggesting that other stromal cells are a major cellular source of these chemokines *in vivo*.

Fibroblast growth factor (FGF) was detected in both naïve and RSV infected mice from other stromal cells, with little to no production in endothelial cells and ATII epithelial cells (Fig. 5.10d) suggesting that other stromal cells are a dominant cellular source of FGF *in vivo*.

IL-2 protein was also detected in naïve and RSV infected mice, and interestingly, was mainly from ATII epithelial cell with little to no production from endothelial cells and other stromal cells, and was considerably higher than whole lung production (Fig. 5.10e).

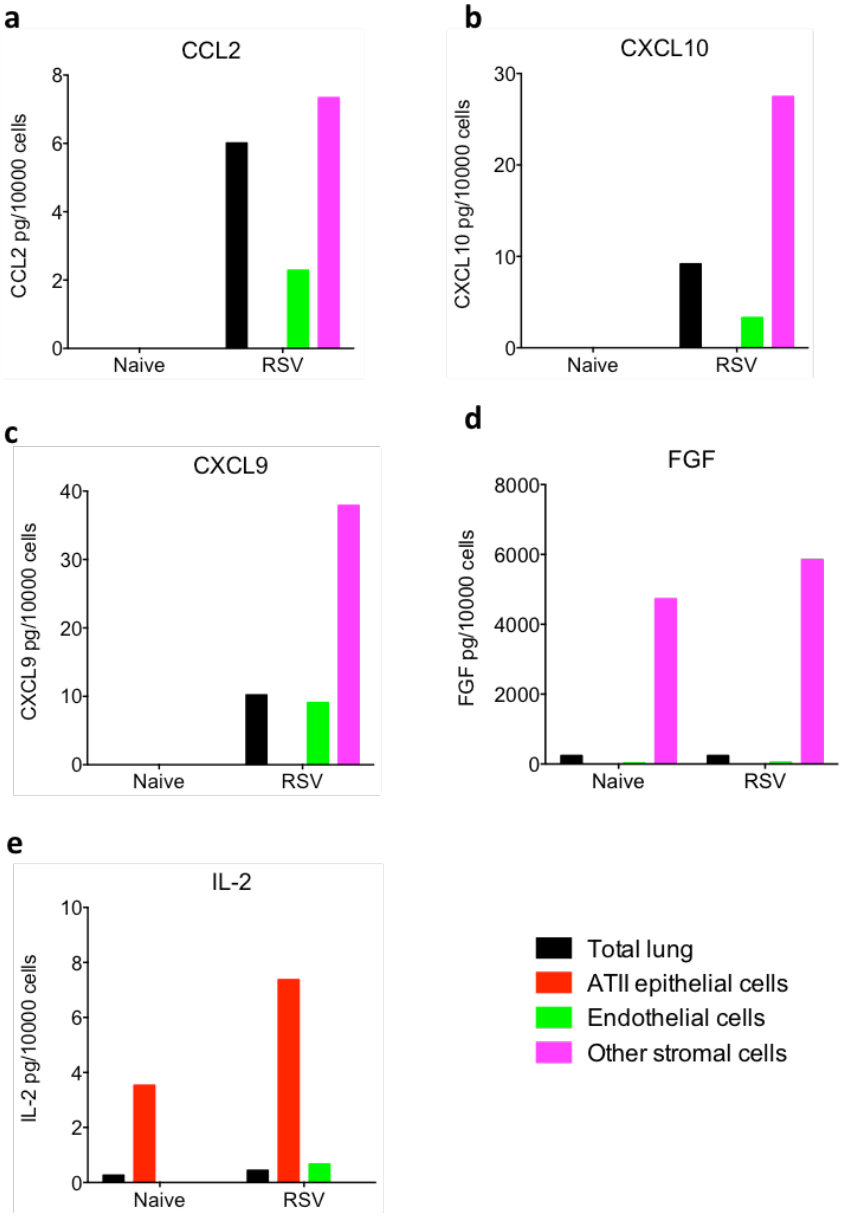


Figure 5.10: Protein production of cytokines, chemokines and growth factors from stromal cell populations 18hrs post RSV infection. C57BL/6 mice were infected with 1.5x10^6 FFU of RSV intranasally and lungs taken at 18hrs post infection. Naïve mice were taken without inoculation. Lungs were digested with dispase and stained with antibodies against CD45, CD31, and EpCAM. Cells were then FACS sorted for live singlet ATII epithelial cells, endothelial cells and other stromal cells. Purity was always >95% for all sorted populations. A sample of the single-cell suspension before sorting was also taken to represent the total lung. Cells were then homogenised in proteinase inhibitor and resultant supernatant applied to a Mouse Cytokine Magnetic 20-Plex Panel and processed according to manufacturer's instructions to determine protein levels. Protein levels were then back-calculated to a per cell basis based on the number of sorted cells obtained via FACS for each stromal subtype and displayed as pg per 10,000 cells on graphs (a-e). Only data above the detection limit before back-calculation is plotted (CCL2: 26pg, CXCL10: 57pg, CXCL9: 76pg, FGF: 352pg, IL-2: 8pg). FGF: fibroblast growth factor. Results shown are from one Luminex panel with one sort per time point and 5 pooled mice per sort.

5.2.6 Summary

Cytokines such as IL-6 and IL-33, and chemokines CCL2, CXCL8 and CXCL10 have been detected in the airway and secretions of RSV-infected children (Noah et al. 1995, Hornsleth et al. 1998, Sheeran et al. 1999, Garofalo et al. 2001, McNamara et al. 2005, Saravia et al. 2015). These mediators have also been detected in mice infected with RSV, along with type I IFNs and growth factors such as GM-CSF and amphiregulin, and many of these have been shown to be critical for viral clearance (Bukreyev et al. 2001, Guerrero-Plata et al. 2005, Monick et al. 2005, Jewell et al. 2007, Bhoj et al. 2008, Lindell et al. 2008, Goritzka, Makris, et al. 2015, Goritzka, Pereira, et al. 2015). The cellular sources and their relative contributions to the expression of these mediators *in vivo* are not clear. In addition, the involvement of stromal cells in the response to RSV infection *in vivo* is particularly understudied, and whether they contribute to the expression of the mediators observed during infection or any others, is unknown. Furthermore, whether stromal cell subsets are infected by RSV *in vivo,* has yet to be fully demonstrated.

To begin to answer these questions, the lung was initially separated into a broad population of $CD45^-$ stromal cells and $CD45^+$ leukocytes, and gene expression of several critical type I IFNs, chemokines, cytokines and growth factors were analysed over a time course of RSV infection. The results strikingly revealed that $CD45^-$ stromal cells expressed all chemokines, cytokines and growth factors tested, and at levels above $CD45^+$ leukocytes and total lung. This introduced the notion that stromal cells are a major cellular source of these mediators during RSV infection *in vivo* (Fig. 5.6). Type I IFNs, on the other hand were induced much more strongly from $CD45^+$ leukocytes, with minor to no contribution from stromal cells (Fig. 5.6). Peak expression of these mediators, as well as the return to baseline levels before infection, differed depending on the target gene, suggesting they have temporal regulation and/or originate from different subpopulations of stromal cells.

To uncover this further, different subsets of stromal cells were sorted from the $CD45^-$ population: ATII epithelial cells, endothelial cells and other stromal cells. Other stromal cells are a mixed population of cells postulated to contain (mainly) fibroblasts, pericytes and smooth muscle cells. Analysis of these three sorted subsets over a time course of RSV infection revealed a striking division of gene expression of mediators (Fig. 5.7). ATII epithelial cells were a major cellular source of the growth factors amphiregulin and GM-CSF as well as the cytokine IL-33 with little to no expression from endothelial cells or other stromal cells, and peak gene expression of the latter two was very early on at 4hrs post infection (Fig. 5.7b). This supports *in vitro* data that has shown amphiregulin and GM-CSF expression in epithelial cell cultures infected with RSV (Monick et al. 2005, Ishioka et al. 2011, Albrecht et al. 2012), and further confirms a recent study showing IL-33 expression from murine ATII epithelial cells during RSV infection *in vivo* (Saravia et al. 2015). These results suggest that ATII epithelial cells are most active during the first few hours of infection *in vivo*, which is logical as they are one of the first cells of contact for the virus in the lung. The expression of the IL-33 very early on by these cells suggests that ATII epithelial cells may be important for alerting the immune system of infection as IL-33 can act as an alarmin (Neill et al. 2010). IL-33 also functions as a type 2 cytokine, and its receptor ST2 is expressed on ILC2s and Th2 cells (Neill et al. 2010), and studies have demonstrated that administration of recombinant IL-33 can induce a more severe RSV disease state in mice due to a more type 2 allergic response (Saravia et al. 2015). This suggests that regulation of IL-33 expression from ATII epithelial cells may be critical target to prevent severe RSV infection, as children hospitalised with RSV also have elevated levels of IL-33 in their lungs (Saravia et al. 2015). The expression of growth factors GM-CSF and amphiregulin from ATII epithelial cells very early on during infection (the latter continuing to be expressed until at least 96hrs post infection), may also be important for effective management and clearance of the virus as well as for maintaining barrier integrity. *In vitro*, amphiregulin has been shown to prolong the survival of RSV-infected cells and induce the expression of the potent neutrophil chemoattractant CXCL8 from these cells (Monick et al. 2005). Neutrophils are one of the first cells to be recruited during viral lung infections to control virus

spread (Borchers et al. 2013, Kolaczkowska and Kubes 2013) and thus the expression of amphiregulin from ATII epithelial cells very early during infection may act to enhance neutrophil recruitment. However, amphiregulin is primarily known for maintaining and restoring epithelial barrier integrity following damage from virus infection (Zaiss et al. 2015). Specifically IAV studies have demonstrated that amphiregulin promotes the regeneration of the bronchial epithelium and the subsequently survival of mice from infection (Monticelli et al. 2011). Thus in RSV, amphiregulin expression from ATII epithelial cells during the first few hours of infection as shown in this study, to at least day 8 post infection (Goritzka, Pereira, et al. 2015) may be critical for continually restoring surrounding damaged ATI and ATII epithelial cells and controlling infection. GM-CSF is a potent stimulator of AMs needed for development, proliferation, activation and survival (Shibata et al. 2001, Guilliams et al. 2013). Expression of GM-CSF from ATII epithelial cells during the early stages of RSV infection *in vivo* may be critical for the enhancing of AM activity for efficient phagocytosis of virus and virus particles at the start of infection. Indeed, mice infected with recombinant RSV expressing GM-CSF have increased numbers of AM and DCs with increased antigen presentation in the latter and significantly reduced viral load (Bukreyev et al. 2001). The enhanced number and activity of APCs may be critical for the robust and efficient induction of the adaptive response to clear the virus. GM-CSF is also important for maintaining the alveolar epithelial barrier during injury (Christensen et al. 2000, Beck et al. 2009) with survival from adult respiratory distress syndrome correlating with increased levels of BALF GM-CSF (Matute-Bello et al. 2000). Thus, like amphiregulin, expression of GM-CSF from ATII epithelial cells during RSV infection *in vivo* may also be vital for restoring dead and damaged epithelial cells and maintaining an effective lung epithelial barrier to prevent further spread of the virus and a functional airway.

Other stromal cells were a major source of the chemokines CCL2, CXCL1 and CXCL10 and cytokine IL-6 during RSV infection *in vivo* with gene expression peaking between 12 and 18hrs post infection (Fig. 5.7c). CCL2 and CXCL10 protein was also detected from other stromal cells, confirming expression to functional protein (Fig. 5.10a/b). Endothelial cells also expressed CXCL10, the

only mediator enriched from this stromal cell subset and IAV studies have shown human microvascular endothelial cells to express CXCL10 *in vitro* (Teijaro et al. 2011). However during RSV infection, gene expression from endothelial cells was significantly lower than other stromal cells, suggesting the latter is a potentially more dominant cellular source of CXCL10 (Fig. 5.7c). Human foetal fibroblast cultures infected with RSV have been shown to express CCL2, CXCL10, CXCL8 (a neutrophil chemokine similar to CXCL1) and IL-6 (Seki et al. 2013). Brain pericytes have been shown to induce CXCL8 and IL-6 in response to HMCV infection *in vitro* and similarly SMCs have also been shown to express CXCL8 and IL-6 in response to RV infection (Oliver et al. 2006). These studies support the hypothesis that other stromal cells contain one or a mix of these cell types, and highlight a potentially unknown role of these cells during RSV infection *in vivo*. The potent expression of CXCL1, CXCL10 and CCL2 from other stromal cells suggests that they are vital for the recruitment of critical immune cells such as neutrophils, T cells and monocytes during RSV infection *in vivo*, in particular during the release of the first viral progeny 12hrs post infection (Graham and Anderson 2013). Indeed, the critical role of CCL2 for the recruitment of inflammatory monocytes for effective viral clearance during RSV infection *in vivo* has been demonstrated by our group previously (Goritzka, Makris, et al. 2015). However, the cellular source in this study was not identified. The data from this present study reveals that other stromal cells could be this cellular source of CCL2, and is supported from other infection models which have also demonstrated that stromal cells in the cornea are a source of CCL2 needed for monocyte recruitment during HSV-1 infection (Conrady et al. 2013). However, which cell type specifically expresses CCL2 in the mixed population of other stromal cells during RSV infection needs to be further identified. CXCL1 is a potent recruiter of neutrophils, which are required during the early stages of viral infection to contain the virus. However, they are also the most abundant cell type detected in the BALF of children hospitalised with RSV-bronchiolitis (Everard et al. 1994, Smith et al. 2001, McNamara et al. 2004). The identification of significant CXCL1 expression from other stromal cells demonstrates that resident non-epithelium non-endothelium structural cells may be vital for the recruitment of early phagocytic cells to rapidly contain the virus to prevent

initial spread of the virus. The critical role of CXCL10 and its receptor CXCR3 in the recruitment of T cells during RSV infection *in vivo* has also been demonstrated from studies where neutralisation of either CXCL10 and CXCR3 increased disease pathogenesis and impaired viral clearance, and this was associated with a significant decrease in RSV-specific $CD8^+$ T cells (Lindell et al. 2008). Again the source of CXCL10 was not identified. Data from this study potentially reveals other stromal cells to be the cellular source. Overall, the clear dominant expression of critical chemokines from other stromal cells during RSV infection *in vivo* compared to ATII epithelial cells, endothelial cells and AMs demonstrates that other stromal cells could be potential targets for modulation to both increase proinflammatory responses to RSV infection in the case of a weak immune response to the virus, as well as cellular targets to reduce disease severity caused by the over-exuberant influx of inflammatory cells that promote immunopathology.

Initial gene expression analysis on sorted stromal cell subsets was limited due to the low yield of RNA obtained, and thus only a few selective genes were analysed. To examine further mediators and to obtain a broader and more comprehensive view of the genes induced by stromal cells subsets during RSV infection in *vivo*, cDNA from sorted cells was amplified, and gene expression further examined over a time course of RSV infection. Furthermore, in another set of experiments, ATII epithelial cells and other stromal cells were sorted at their peak time points of activity during infection *in vivo*, cDNA from these sorted cells amplified and then analysed via gene expression arrays. In addition, we looked beyond gene expression and also analysed protein production of mediators from sorted stromal cell subsets via Luminex assays to expand the analysis.

Deeper gene and protein investigation further highlighted the robust chemokine expression from other stromal cells and the limited overall response from ATII epithelial cells and endothelial cells (Table 5.1 and 5.2, Fig. 5.9). Gene expression of 12 additional chemokines relating to monocyte, neutrophil and T cell recruitment were detected from amplified cDNA from other stromal cells from

RSV infected mice including CCL7, CCL12, CXCL5 and CXCL11 (Table 5.1 and Fig. 5.9). CCL7 and CXCL5 were enriched in other stromal cells, and gene expression of CXCL9 increased by >500 fold in RSV infected other stromal cells compared to naïve, and protein was also detected via Luminex suggesting highly induced expression (Fig. 5.10c). Many of these additional chemokines are related to those that have been found in secretions from children hospitalised with RSV-bronchiolitis suggesting that other stromal cells induce robust infiltration of inflammatory cells by secreting multiple mediators with similar chemoattractant functions during RSV infection *in vivo*. CCL7 and CCL12 are both monocyte attracting chemokines like CCL2, and all three signal via the same chemokine receptor CCR2 (Shi and Pamer 2011). Similarly, CXCL9 and CXCL11 recruit T cells like CXCL10, and use the common receptor CXCR3 (Lindell et al. 2008, Van Raemdonck et al. 2015).

Cytokines IL-1α, IL-1β and TNF were additionally detected in other stromal cells but determined to be a minor cellular source with AM instead being a major source *in vivo*. In addition, Luminex assay was unable to detect these cytokines in sorted stromal cell lysates suggesting either low protein expression, or high turnover of the proteins by the lung. Oncostatin M, a cytokine related to IL-6 (Richards 2013) and TNFSFS10, a cytokine related to TNF (Brenner et al. 2015) were also detected in the other stromal cells. Low fold induction of additional growth factors including G-CSF were observed from amplified cDNA from other stromal cells from RSV infected mice compared from naïve mice. Other stromal cells were also a minor source of TGF-β and VEGF, whilst FGF was detected at high concentrations in both naïve and RSV infected other stromal cells, with production increasing with infection (Fig. 5.10). IL-1β, TNF-α, G-CSF, VEGF and FGF have been detected from culture supernatants from RSV infected foetal fibroblast cell lines (Seki et al. 2013). Similarly, after infection with IAV and PIV IL-1β and TNF-α production has been observed from the same cell line (Yoshizumi et al. 2010, Kim et al. 2015) again proposing that fibroblasts may constitute a major population of the other stromal cells. Additionally, human brain pericytes also express CXCL11, IL-1β and TNF-α in response to HCMV infection, hinting that their lung counterparts may also be a subset of cells within the other stromal cell population (Alcendor et al. 2012). Interestingly, VEGF was

the only additional cytokine enriched in endothelial cells with expression still elevated at 96hrs post infection. VEGF has multiples roles including angiogenesis and also acts as a permeability factor (Barratt et al. 2014). In an ovine model of RSV infection, pre-treatment of animals with recombinant VEGF before RSV infection lead to decreased viral load and pulmonary inflammation (Meyerholz et al. 2007, Olivier et al. 2011). Overall, the relatively less potent expression of cytokines and growth factors expression compared to chemokines in other stromal cells, suggests that although these cells have the ability to express mediators that increase inflammation and stimulate other cells, other stromal cells are most actively involved in the recruitment of cells during RSV infection.

Conversely, ATII epithelial cells induced far less mediators with growth factor M-CSF, cytokines IL-21 and TNFS10, and chemokines CCL20, CXCL3 and CXCL5 the only genes induced in the amplified cDNA, as well as IL-2 protein from sorted cell cell lysate (Fig. 5.9 and Table 5.2). Again, several of these additional mediators (M-CSF, CXCL5 and IL-2) are related to those attributed to have minor and or major expression (GM-CSF and CXCL1) from ATII epithelial cells in this study (Fig. 5.7). M-CSF stimulates proliferation and activation of macrophages and monocytes like GM-CSF, whilst CXCL5 is a neutrophil chemoattractant like CXCL1. Interestingly, IL-2 is most commonly associated with activated $CD4^+$ T cells (Boyman and Sprent 2012) and its expression from ATII epithelial cells in this study is quite surprising. In keeping with this, literature on epithelial expression of IL-2 is scarce and has only shown human airway epithelial cells to constitutively express IL-2 and increase expression after addition of histamine (Aoki et al. 1997). It is hard to speculate if the IL-2 expression from ATII epithelial cells during RSV infection is significant, as $CD4^+$ T cells were not examined in this study, therefore the relative contribution of IL-2 from ATII epithelial cells cannot be established. Although, IL-2 is a potent T cell growth factor and thus follows the prominent expression of other growth factors GM-CSF and amphiregulin from ATII epithelial cells. Nonetheless, IL-2 has been demonstrated to be important during RSV infection, as mice infected with recombinant RSV expressing IL-2 had significantly lower viral load compared to mice infected with wildtype virus (Bukreyev et al. 2000).

Type I IFNs are critical antiviral mediators during RSV (Guerrero-Plata et al. 2005, Goritzka et al. 2014), and $CD45^+$ leukocytes, in particular AMs, were shown to be a major source of these IFNs during infection *in vivo* (Fig. 5.6 and 5.7). This is supported by studies which have shown similar results and further gone on to show that loss of AM-derived type I IFNs lead to increased viral lung load and weight loss (Goritzka, Makris, et al. 2015). *In vitro* studies have also suggested that both upper tracheal/bronchial and lower alveolar epithelial cells, are robust source of type I IFNs during RSV (Jewell et al. 2007, Demoor et al. 2012, Ioannidis et al. 2012) and weak IFN-α staining has been observed in cells lining the airways of RSV infected mice (Jewell et al. 2007). We detected no IFN-α5 gene induction in ATII epithelial cells during RSV infection, but low levels of IFN-β were detected from ATII epithelial cells (and other stromal cells) (Fig. 5.7). However, this was significantly less than what we found in AMs, implying that ATII epithelial cells (and other stromal cells) are not a major source of type I IFNs *in vivo* (Fig. 5.7d). The lack of robust type I IFN production from ATII epithelial cells *in vivo* could be due to the antagonistic effects of the RSV NS proteins on the IFN signalling pathway (Swedan et al. 2009, Boyapalle et al. 2012), as RSV lacking the NS proteins induce higher levels of type I IFNs in epithelial cells than wildtype virus (Spann et al. 2004). It is possible that the inhibitory effects of the NS proteins is not as potent in AMs maybe due to abortive replication of RSV in AMs and possibly abrogated NS expression (Ravi et al. 2013). It is also possible that other types of epithelial cells such as tracheal, bronchial or ATI epithelial cells are different in their expression of type I IFNs, and comparative analysis would reveal this. Finally, the type II IFN, IFN-γ was detected in total lung, with minimal expression from other stromal cells with expression still increasing at 96hrs post RSV infection, suggesting another cells type – most likely NK cells (Kaiko et al. 2010) to be the major cellular source.

Virus was detected in all stromal cell subsets as well as AMs during RSV infection, although the main reservoir for the virus was not one of these populations. As speculated, the main cellular target for RSV in the lower airway is most likely ATI epithelial cells, as there was a significant decrease in viral load

in lung digested with dispase, which contains no T1a$^+$ ATI epithelial cells, compared to total lung homogenate (Fig. 5.3). This could be confirmed by isolation of ATI and ATII epithelial cells from separate RSV infected mice. Nevertheless, this study demonstrates for the first time that ATII epithelial cells, endothelial cells and the mixed population of other stromal cells, are infected by RSV *in vivo*. The initial peak of viral load at 4hrs is due to the input virus from inoculation of the mice, which goes down by 12hrs, whilst the peak at 18hrs suggests potential viral replication. Alveolar epithelial cells have been shown to contain virus both from fatal cases of RSV and *in vivo* in mice (Jewell et al. 2007, Johnson et al. 2007, Welliver et al. 2007). However, whether the virus was live and replicating in the stromal cell populations was not determined. Between 18 and 96hrs post infection there was a trend towards more virus in all stromal subsets and a decrease in AMs, again suggestive of viral replication in stromal cells but clearance in AMs. This is supported by studies showing that viral replication is limited in AMs *in vitro* (Becker et al. 1991, Franke-Ullmann et al. 1995, Stadnyk et al. 1997, Ravi et al. 2013, Kolli et al. 2014). Live virus was required for the expression of CXCL10, IFN-α5 and IFN-β (Fig. 5.8b). GM-CSF, amphiregulin, IL-33, IL-6, CCL2 and CXCL1 were induced with live RSV, with little to no induction (compared to naïve) with UV-inactivated virus (Fig. 5.8c). This suggests that live virus is important for type I IFN production and ISGs such as CXCL10, and is also needed for robust expression of CCL2, CXCL1, IL-6, IL-33, GM-CSF and amphiregulin. It should also be considered that expression of mediators might not require infection of the cell itself, but is in response to mediators released by other infected cells, viral PAMPs released from other infected cells, or to damage-associated molecular patterns (DAMPs).

Taken all together, this project demonstrates for the first time the relative contributions of three different stromal cell populations and AMs in the expression of mediators important for inducing an inflammatory environment and maintaining barrier integrity in the lung during RSV infection *in vivo.* Strikingly, the data have revealed that other stromal cells express and are a major source of chemokines and several cytokines during RSV, whilst ATII epithelial cells are a major source of several growth factors. Endothelial cells

contribute very little to expression of critical mediators during RSV infection and type I IFNs are mainly from $CD45^+$ leukocytes, in particular AMs. The striking extensive expression of chemokines from other stromal cells suggests that they are heavily involved in the recruitment of immune cells to the site of infection, whilst the limited expression of many mediators including chemokines, and enriched expression of GM-CSF and amphiregulin suggests ATII epithelial cells may be more critical for barrier repair and/or proliferation of cells. The temporal differences in the expression of mediators from ATII epithelial cells and other stromal cells suggest that ATII epithelial cells have a key role during the first few hours of RSV infection *in vivo*, whilst other stromal cells are more important during the later, albeit still early stages. ATII epithelial cells line the alveoli and are thus one of the first cells to come into contact with the virus, which supports their expression of mediators very early on during infection. Fibroblasts, smooth muscle cells and pericytes are found below the epithelial layer and thus may encounter virus after the epithelial barrier has been damaged, and therefore express mediators several hours after ATII epithelial cells. They could also respond, as described previously, to mediators expressed by epithelial cells, viral PAMPs or to DAMPs, and not necessarily to infection themselves. The location of these potential other stromal cells in close proximity to the site of infection and to blood vessels means that they are highly suited to induce the recruitment of inflammatory cells from the blood to the lung to clear the infection. These results point out the important cellular crosstalk that happens within the tissue during infection and the clear division of chemokine, cytokine, IFN and growth factor production that orchestrate the recruitment of cells and antiviral immunity.

5.3 The other stromal cell population contains fibroblasts and primary murine fibroblasts produce chemokines in response to RSV

This study has demonstrated the other stromal cell population as an important source of chemokines during RSV infection *in vivo*. As mentioned, this subset is a mixed population of non-epithelial non-endothelial cells, which is hypothesised to contain mainly fibroblasts, pericytes and SMCs. All three cell types have been shown to express chemokines and other soluble mediators in response to various virus stimulations *in vitro*, including RSV (see section 1.4). However, the lack of absolute cell-specific markers and difficulty in isolating these cells from the lung has limited extensive studies *in vivo*. Fibroblasts in particular, are slowly being recognised as a potential vital source of proinflammatory mediators during infection (Phipps et al. 1990, Smith et al. 1997, Perros et al. 2011). *In vitro* studies have shown human foetal fibroblasts cell lines infected with RSV to express chemokines CCL2, CCL3, CXCL8 and CXCL10 and cytokines IL-6 and IL-11 (Elias et al. 1994, Einarsson et al. 1996, Seki et al. 2013). These *in vitro* data support the hypothesis that other stromal cells contain a population of fibroblasts, which may be the cellular source of chemokines detected *in vivo*.

5.3.1 Other stromal cells contain CD90$^+$ fibroblasts

Fibroblasts are a heterogeneous population of stromal cells, differing not only between organs, but also within an anatomical site. They exhibit several phenotypes including non-contractile fibroblasts, contractile myofibroblasts and protomyofibroblasts, (McAnulty 2007). Various fibroblast markers exist, however none of them are exclusive to fibroblasts and are present in all phenotypes. These include fibroblast-specific protein 1 (FSP1) which despite its name, can also be detected on macrophages (Österreicher et al. 2011), α-smooth-muscle-actin (α-SMA) which is also found on SMCs and pericytes (Skalli et al. 1989) and vimentin, found on all mesenchymal cells (Satelli and Li 2011). All three are also intracellular markers, which means they cannot be used for cell

sorting as permeabilisation induces damage to the cell membrane which would compromise cell viability. Thus surface antigen markers are required, of which there are far less well-characterised possibilities. CD90 or Thy1.1 is a 25-kD cell surface glycoprotein that was originally described as a marker of thymocyte differentiation in mice (Lee et al. 1998). However, it has been found on fibroblasts of all species studied to date (Haeryfar and Hoskin 2004). As well as $CD90^+$ fibroblasts, $CD90^-$ fibroblasts also exist, and both have been identified as the two major subsets of fibroblasts in mouse lung (Phipps et al. 1989). Culturing of these subsets reveals that $CD90^-$ fibroblasts spread more and contain more extensive microfilament and microtubule network than $CD90^+$, which are more spindly and often lipid-containing (Phipps et al. 1989).

To determine the contribution of fibroblasts to the other stromal cell population, dispase-digested mouse lung cells were stained for CD90 and $CD90^{+/-}$ cells were identified within the other stromal cell population. Flow cytometric analysis revealed that approximately 7% of the other stromal cells stained positively CD90, whilst the remaining 93% were $CD90^-$ (Fig. 5.11). The $CD90^-$ population as well as containing $CD90^-$ fibroblasts, may also contain other types of cells that are $CD90^-$, and as such the precise percentage cannot be ascertained from this experiment. This could be investigated using additional morphological analysis and further dissection of combination of markers.

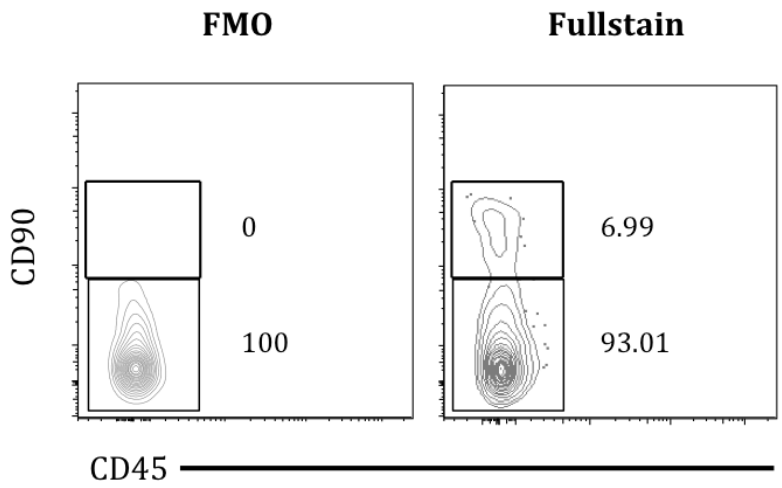


Figure 5.11: CD90 staining of other stromal cells from mouse lung. Lungs from C57BL/6 were dispase-digested into single cell suspension and stained with antibodies against CD45, CD31, EpCAM and CD90. As a control, fluorescence minus one (FMO) for CD90 was performed to obtain the $CD90^{+}$ and $^{-}$ gate. Cells were then analysed by flow cytometry. Cells were first gated on live, singlet other stromal cells (as shown in Fig. 4.1) and then on CD90. Results show one experiment from one mouse.

5.3.2 Primary mouse lung fibroblasts secrete chemokines in response to RSV

To further determine if fibroblasts could be the source of the chemokines detected from other stromal cells during RSV infection *in vivo*, primary fibroblasts were cultured from mouse lung (Fig. 5.12a) and exposed to RSV. Lipopolysaccharide (LPS) was used as a positive control. Levels of CXCL1, CXCL10 and CCL2, which were detected *in vivo* (Fig. 5.7), were quantified from the culture supernatant after 18hrs.

The data revealed that primary fibroblasts expressed all three chemokines in response to RSV, with CCL2 most highly expressed (Fig. 5.12b), followed by CXCL10 (Fig. 5.12c) and finally CXCL1 (Fig. 5.12d). UV-inactivated RSV at MOI 2 did elicit CCL2 production from fibroblasts, however this was lower than live RSV, suggesting live virus is needed for robust production as demonstrated by gene expression analysis from our *in vivo* studies (Fig. 5.8b). RSV at MOI 1 induced the highest levels of CCL2 averaging 1.8ng/ml (Fig. 5.12b). CXCL10 was only induced with live virus and was not expressed in the media control or with UV-inactivated virus (Fig. 5.12c) suggesting that it is strongly (live) virus-dependent. CXCL1 production from primary fibroblasts was noticeable lower than CCL2 and CXCL10 production across different RSV concentrations (Fig. 5.12d). Production was similar across different MOIs, ranging between 0.25 and 0.4ng/ml, including UV-inactivated virus (Fig. 5.12d). Media alone induced CXCL1 production albeit at lower levels than with virus, altogether suggesting that CXCL1 production from primary fibroblasts is not completely dependent on live virus.

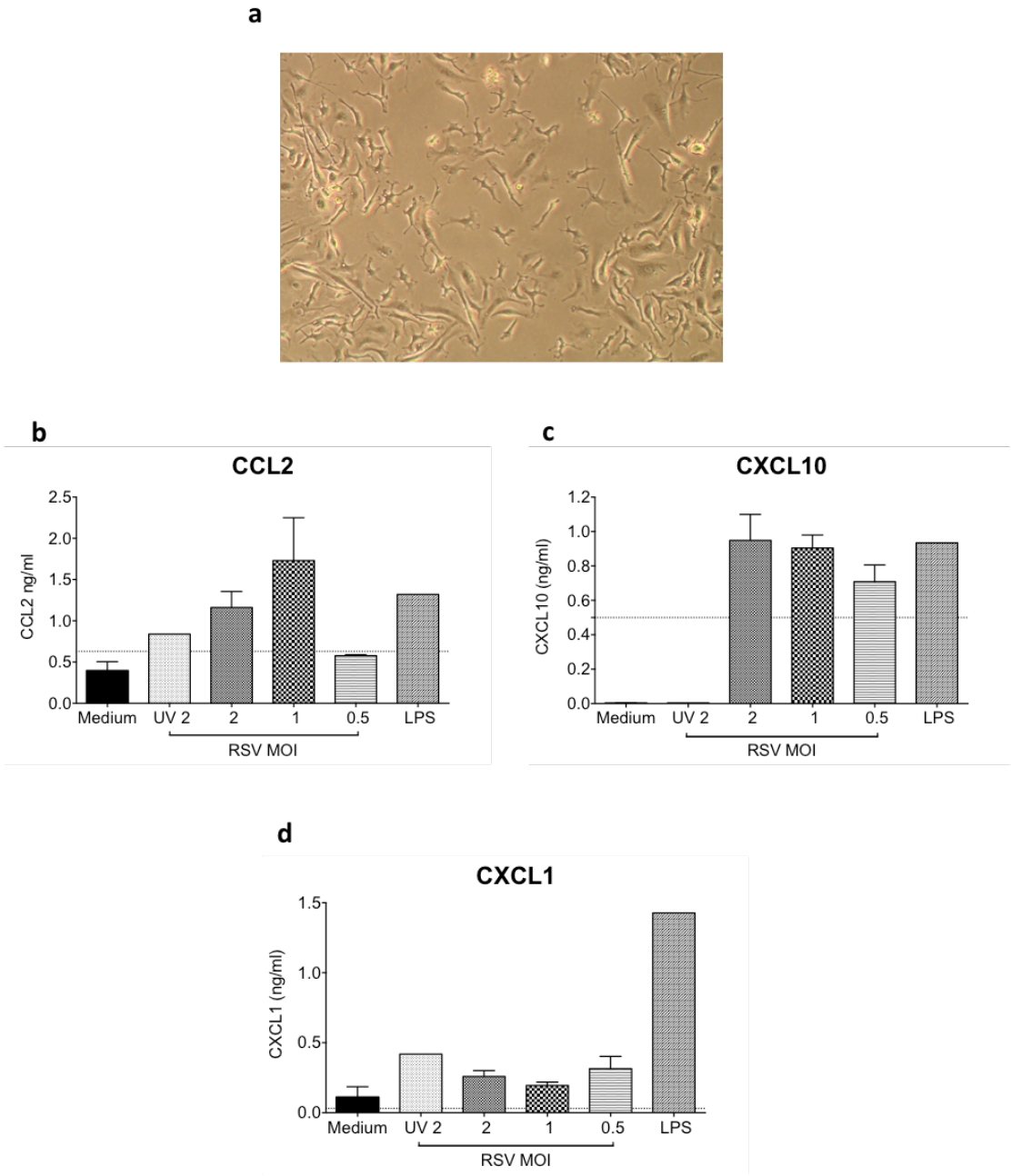


Figure 5.12: Primary fibroblasts express chemokines in response to RSV. Primary fibroblasts were cultured from C57BL/6 mouse lungs. Briefly, lungs were dissected into small pieces and cultured for 3 weeks in petri dishes containing cDMEM at 37°C. Resultant fibroblasts (a, 20x magnification) were then detached and seeded in 96 well plates at 45,000 cells/well before stimulation with medium, UV-inactivated RSV and RSV at different MOIs. LPS stimulation (1ng/ml) was used as positive control (b-d). 18hrs post-stimulation S/N was removed and levels of CCL2, CXCL10 and CXCL1 determined via ELISA. Dashed lines represents lower detection limits. Results show one experiment with 1-2 individual cultures per condition, from cultures containing pooled lungs of 5 mice. Data presented as mean + range where possible.

5.3.3 Summary

Fibroblasts are a heterogeneous population of stromal cells that are slowly being recognised as active contributors to the immune response during infection. Their role in cancer and the autoimmune disease rheumatoid arthritis, have been studied more extensively and have demonstrated that they are key for inflammatory mediator production (Pap et al. 2000, Silzle et al. 2004, Huber et al. 2006, Kalluri and Zeisberg 2006). The other stromal cell subset sorted from mouse lung is a potent source of chemokines and is made up of a mixed population of cells, of which one of them is hypothesised to be fibroblasts. CD90 is a suggested cell surface fibroblast marker that can be used to separate $CD90^+$ and $CD90^-$ fibroblasts after elimination of endothelial cells, epithelial cells and leukocytes that can also express CD90. Using flow cytometry, a population of $CD90^+$ fibroblasts can be identified from the other stromal cell subset (Fig. 5.11). The majority of the other stromal cells are $CD90^-$ and it cannot be conclusively stated that these cells are all $CD90^-$ fibroblasts as this negative fraction could also contain $CD90^-$ non-fibroblast cells such as pericytes and SMCs. $CD90^+$ and $CD90^-$ fibroblasts are the two major populations of fibroblasts identified in the lung (Phipps et al. 1989), however the relative percentages of each is not clear. It is possible that the $CD90^-$ fibroblasts make up the main subset in the lung, but as pericytes and SMCs cannot be distinguished out from the $CD90^-$ population, it is not possible as yet to confirm the exact cellular composition of the other stromal cells. Neural/glial antigen 2 (NG2) is a suggested marker for pericytes and could be added to eliminate these cells from the $CD90^-$ population, however there is no specific marker available to remove SMCs that is not also present on fibroblasts.

To further observe the role of fibroblasts in response to RSV, primary fibroblasts were cultured from mouse lung and infected with RSV to determine whether they mimicked the response of the other stromal cells as seen *in vivo* (Fig. 5.12) Cultures of primary fibroblasts were obtained from mice using a well-established protocol that yielded both $CD90^+$ and $CD90^-$ fibroblasts (Baglole et al. 2005). We were unable to confirm the percentage of $CD90^+$ and $CD90^-$ fibroblasts due to limited number of cells. After stimulation with RSV, these cultures expressed

chemokines CCL2, CXCL10 and CXCL1 confirming what we detected from the other stromal cells *in vivo* (Fig. 5.12). CCL2 was induced the highest, whilst CXCL10 was the only chemokine only induced by live virus. The production of these mediators from fibroblasts supports data from a recent study that demonstrated similar chemokine production from a foetal lung fibroblast cell line in response to RSV (Seki et al. 2013) and strongly suggests that fibroblasts could be a major cell population within the other stromal cell subset. The importance of CCL2 expression from fibroblasts was highlighted in a study by Kitamura et al, who demonstrated that in an ovalbumin model of asthma, DC trafficking to the mesenteric lymph node was dependent on CCL2 expression by fibroblasts, and that mice that lacked fibroblast-derived CCL2 had abrogated adaptive immunity (Kitamura et al. 2011). In RSV, the importance of CCL2 is demonstrated through its recruitment of inflammatory monocytes, which are crucial for viral clearance, and resolution of disease (Goritzka, Makris, et al. 2015). Thus altogether, the observation of $CD90^+$ fibroblasts in the other stromal cell population, along with primary cultures of fibroblasts expressing CCL2, CXCL10 and CXCL1 supports the hypothesis that the expression of chemokines that is observed from the other stromal cells in response to RSV infection *in vivo*, could be from fibroblasts and that this fibroblast-derived CCL2 is vital for viral clearance.

5.4 Expression of mediators from stromal cells is partially dependent on IFNAR1 signalling

This study has revealed that stromal cells can express various mediators in response to RSV infection *in vivo*. To further understand the mechanisms of this induction from stromal cells, we next evaluated whether expression of these mediators was dependent on type I IFN signalling (Aim 3), as it was recently shown that IFNAR1 was important for driving overall proinflammatory responses during RSV infection *in vivo* (Goritzka et al. 2014).

Type I IFNs are potent mediators in the immune response to viruses. Not only do they induce an antiviral state in infected and neighbouring cells, they also stimulate innate immune cells and enhance adaptive immune responses. Type I IFNs signal through the type I IFN receptor IFNAR, which is made up of two subunits IFNAR1 and IFNAR2, with IFNAR1 crucial for signalling (Jaks et al. 2007, de Weerd et al. 2013). Activation of IFNAR ultimately leads to robust induction of various type I IFNs as well as hundreds of ISGs, some which include chemokines such as CCL2 and CXCL10 (Trinchieri 2010). Initiation of this signalling pathway first consists of an initial limited wave of IFN expression induced by viral detection via PRRs, and is mediated by a restricted group of IFNs, IFN-β and IFN-α1 (α4 in mice) (Solis et al. 2006). These IFNs then act in an autocrine and/or paracrine manner via IFNAR to induce more type I IFNs, which then via a positive feedback loop, generate the amplified and robust second wave of IFNs consisting of more type I IFNs and hundreds of ISGs (Takaoka and Yanai 2006).

IFNAR1-deficient mice have greater viral burden and decreased survival compared to wildtype animals in West Nile Virus and mouse coronavirus infection (Cervantes-Barragán et al. 2009, Pinto et al. 2014). In the former study, conditional deletion of IFNAR1 on bone-marrow derived cells such as DCs and AMs had almost identical responses to complete IFNAR1 deletion, revealing that IFNAR signalling on bone-marrow derived cells is crucial for viral clearance (Pinto et al. 2014). Only recently has the importance of type I IFN signalling in

RSV been demonstrated conclusively *in vivo*. Goritzka et al showed IFNAR signalling to be important for viral clearance and reducing disease severity. This study further revealed that in addition to its recognised role in antiviral resistance, IFNAR signalling acts as a central driver of early proinflammatory responses through amplification of chemokine, cytokine and growth factor expression (Goritzka et al. 2014). Further investigation went on to reveal AMs were the major source of type I IFNs, suggesting that IFN expression from AMs is critical for IFNAR-dependent induction of robust and effective chemokine, cytokine and growth factor responses during RSV infection *in vivo* (Goritzka, Makris, et al. 2015).

As these studies have highlighted, IFNAR signalling has profound effects on the overall expression of soluble mediators induced during RSV infection in mouse lung. To expand on these results and determine whether IFNAR signalling on stromal cells is crucial for induction of cytokines, chemokines and growth factors observed from these cells, bone-marrow chimeras were generated using IFNAR1 knockout mice to create mice that had deficient IFNAR signalling on stromal cells (non-haematopoietic cells) and/or bone-marrow derived cells (haematopoietic cells). These mice were subsequently infected with RSV and gene expression of soluble mediators from stromal cells subsets from different combination of chimeras was compared to determine the relative contribution of IFNAR signalling on induction of these mediators. Total viral lung load, cell infiltration and levels of soluble mediators in BALF were also evaluated.

5.4.1 Generation of IFNAR1$^{-/-}$ bone marrow chimeras

Bone-marrow (BM) chimeras were generated using C57BL/6 (WT) and IFNAR1$^{-/-}$ (KO) mice. IFNAR1$^{-/-}$ mice lack all signalling in response to IFN-α/β (Muller et al. 1994). Briefly mice were irradiated with an absorbed radiation dose (rad) of 900 to kill all BM cells (i.e. hematopoietic cells/leukocytes). There is the possibility of radioresistant hematopoietic cells such as γδ T cells that could survive in irradiated mice, however they are not thought to contribute to the

early response during RSV infection. Next, 4x10^6 BM cells/mouse were transferred intravenously (i.v) 6hrs post irradiation. The following BM chimeras were generated as a result (Fig. 5.13) and the anticipated IFNAR1 expression and type I IFN production for each is outlined in Table 5.3.

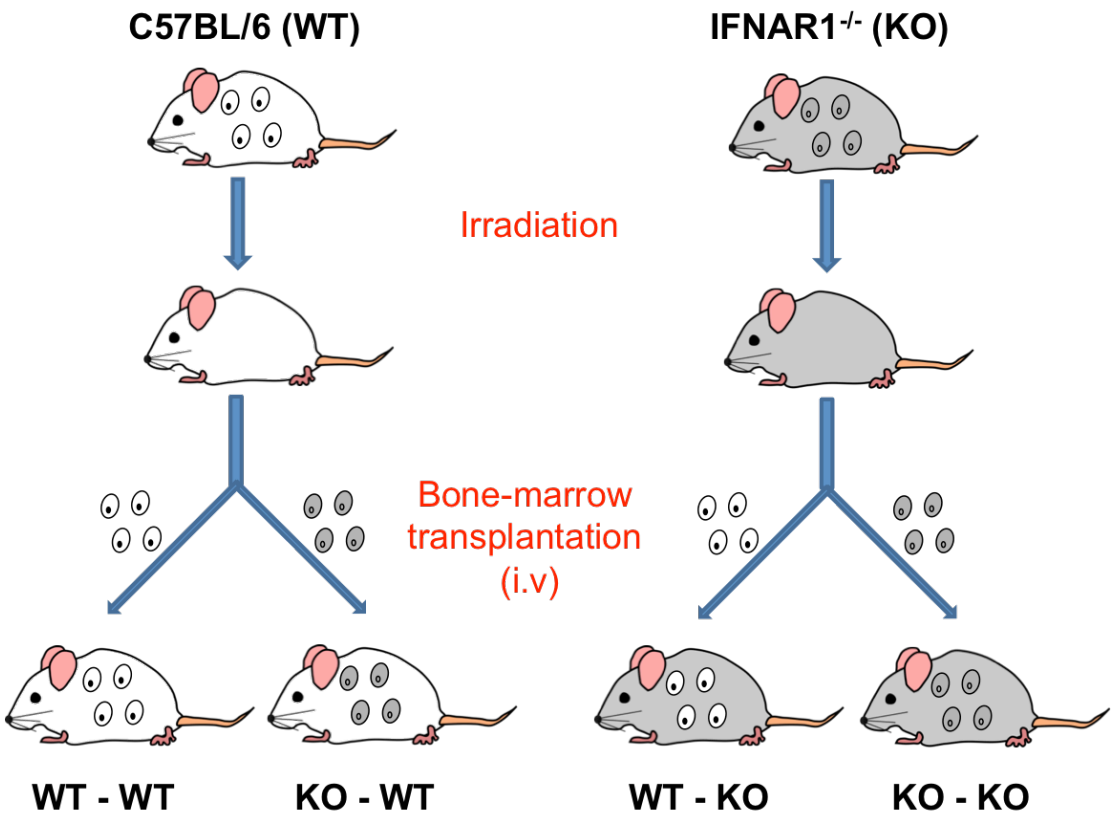


Figure 5.13: Generation of BM chimeras. To establish recipient mice, female, age-matched C57BL/6 (WT) and IFNAR1$^{-/-}$ (KO) were irradiated with 900 rads to kill all BM cells. Donor BM cells were obtained from non-irradiated female, aged-matched C57BL/6 and IFNAR1$^{-/-}$ mice. Briefly mice were sacrificed and the tibia and femur bones removed. PBS was used to flush BM out from the bones, which were then pooled for each mouse strain. RBCs were lysed and 6hrs post-irradiation 4x10^6 BM cells were transferred intravenously (i.v.) to each irradiated recipient mouse via the tail vein to obtain the following BM chimeras (denoted as donor BM transferred into recipient mouse): WT-WT, KO-WT, WT-KO and KO-KO. Mice were left for at least 8 weeks and maintained on antibiotic water until infection with RSV. Note: colours of mice are for illustrative purposes only and do not depict strain background.

BM chimera (BM – recipient)	IFNAR1 expression	Type I IFN First limited wave (IFNAR1 non-dep)	Type I IFN Second amplified wave (IFNAR1 dep)
WT - WT	BM and SC	BM and SC	BM and SC
KO - KO	None	BM and SC	None
WT - KO	BM only	BM and SC	BM only
KO - WT	SC only	BM and SC	SC only

Table 5.3: Expected IFNAR1 expression and type I IFN production in BM chimeras. List of generated BM chimeras (column 1), the expression of IFNAR1 on BM-derived cells (BM) and stromal cells (SC) (column 2) and predicted production of type I IFNs from BM and SCs (column 3 and 4) for each BM chimeric mouse model. Expression of the first limited wave of IFNs is IFNAR1 non-dependent (non-dep) and expression of the second amplified wave is IFNAR1 dependent (IFNAR1-dep).

To summarise, all BM chimeras are predicted to be able to generate the first limited wave of type I IFNs, which is induced by viral recognition via PRRs and independent of IFNAR1 signalling. WT-WT mice express IFNAR1 on both BM-derived and stromal cells, and can also induce the second amplified wave of type I IFNs through the signalling via IFNAR. These mice should respond as normal non-chimeric WT mice to RSV infection. KO-KO chimeric mice have no IFNAR1 expression on either BM-derived or stromal cells. These mice cannot induce the second amplified wave of type IFNs. WT-KO chimeric mice express IFNAR1 on BM-derived cells only and therefore the second type I IFN wave can only be generated from BM-derived cells. KO-WT chimeric mice express IFNAR1 on stromal cells only and therefore can only generate the second amplified wave from stromal cells. As AMs which are BM-derived cells have been shown to be the main producers of type I IFNs during RSV infection *in vivo* (Goritzka, Makris, et al. 2015) and thus responsible for the robust positive feedback loop of type I

IFN production, KO-WT mice may not actually be able to induce a strong IFNAR1-dependent second wave of type I IFNs (from stromal cells), which may make them more vulnerable than predicted, to RSV infection. Thus although the second wave will be from stromal cells (Table 5.3), the production will be limited in these cells from these mice.

Chimeric mice were infected with RSV at least 8 weeks post irradiation and lungs and BALF taken 18hrs post infection. One lung lobe from each lung was taken to determine viral load (Fig, 5.15) and the rest of the lobes were pooled for each group and FACS sorted for stromal cell subsets and AMs to determine gene expression of soluble mediators (Fig. 5.17-19). Differential counts and cytokine and chemokine production was performed on BALF (Fig. 5.15/16). Chimeras for three independent experiments were generated, however due to logistical constraints one set did not have a WT-WT group, and another set could only be sorted via MACS. Thus, statistical analysis could not be performed for gene expression on sorted cells. Mice in experiment one were infected 8 weeks post bone marrow transfer, and mice in experiments two and three were infected 12 or 13 weeks post bone marrow transfer respectively.

5.4.2 Characterisation of IFNAR1$^{-/-}$ BM chimeras

To confirm chimerism and proper reconstitution of the transferred BM in the chimeric mice, gene expression of IFNAR1 was performed on sorted stromal cell subsets and AMs. A total lung sample before sorting was also analysed.

The results showed that for chimeras generated for experiment one and two and FACS sorted, each had the correct expression of IFNAR1 on the desired cell population, confirming the predicted generation of the different chimeric mice (Fig. 5.14a). No cells expressed IFNAR1 in KO-KO chimeric mice, and all cells expressed IFNAR1 in WT-WT chimeric mice. In the mixed chimeras, IFNAR1 gene expression was as expected, with only AMs expressing IFNAR1 in WT-KO and only the stromal cells in the KO-WT group (Fig. 5.14a). The results from

MACS sorted cells for experiment three were more inconclusive (Fig. 5.14b). Only ATII epithelial cells and other stromal cells could be sorted via MACS, and purity was significantly lower with an average purity of 56% and 33% respectively, compared to 98% and 99% from FACS sorted cells (data not shown). The main contaminant to purity for MACS sorted cells was dead cells making up almost 50% of total cells. This may explain why IFNAR1 expression was not detected as expected on other stromal cells as the majority of cells were dead and IFNAR1 transcripts may have been degraded.

Nonetheless, the results from FACS sorted stromal cell subsets confirm chimerism of the mice generated.

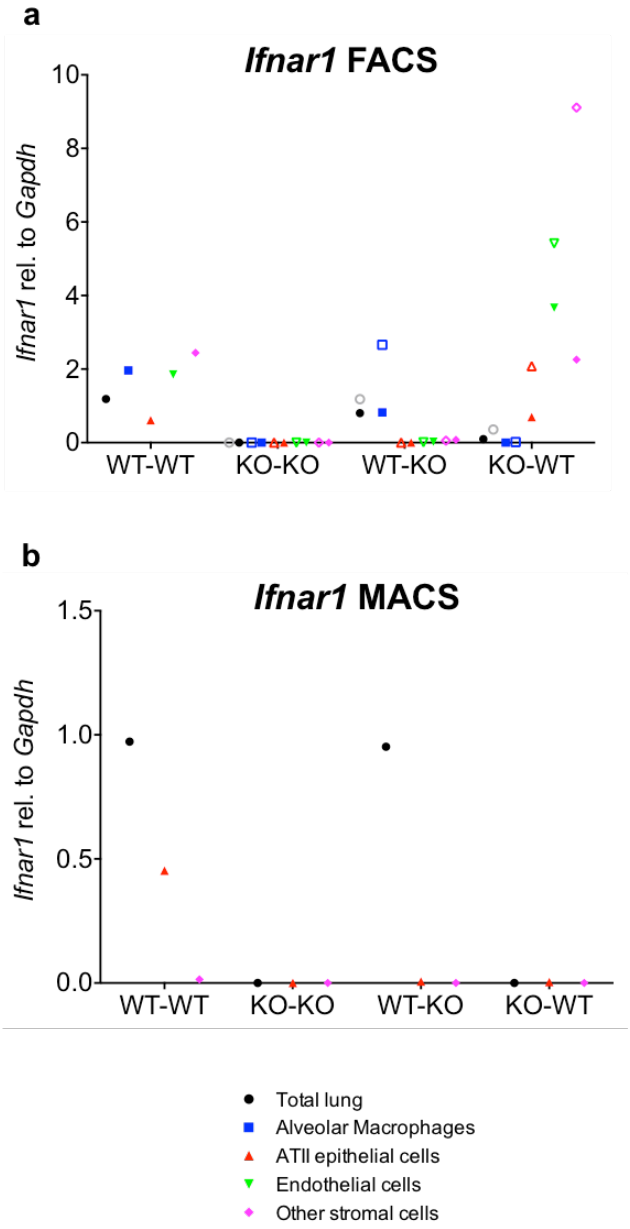


Figure 5.14: Gene expression of IFNAR1 from sorted stromal cells and AMs from BM chimeras. Lungs from BM chimeric mice were digested with dispase and stained with antibodies against CD45, CD31, CD11c and EpCAM and a live/dead dye before sorting via FACS (a) on live singlet AMs, ATII epithelial cells, endothelial cells and other stromal cells. For MACS (b), cells were incubated with anti-CD45 and anti-CD31 Microbeads and sorted via manual MACS using LS columns to obtain ATII epithelial cells and other stromal cells. Sorted cells as well as an aliquot of single cell suspension of total lung for both methods were then analysed for gene expression of IFNAR1 via RT-qPCR. Expression of the target gene is shown as relative expression to the housekeeping gene *Gapdh*. Results for FACS (a) show 1-2 sorts with 3-5 mice pooled per group per sort and for MACS (b) show 1 sort with 5-7 mice pooled per group. In (a) open symbols represent experiment one and filled symbols, experiment two of chimeric mice. Data presented individual results from each sort.

5.4.3 Increased viral load in IFNAR1$^{-/-}$ KO BM chimeras compared to WT-WT BM chimeras

RSV infection of the chimeric mice showed that WT-WT mice had the least amount of virus in the lungs compared to all other groups, whilst KO-KO mice had the most 18hrs post infection (Fig. 5.15a). KO-KO mice also had significantly more virus than WT-KO and similar levels to KO-WT mice (Fig. 5.15a). These data suggest that even with IFNAR1 expression on stromal cells in KO-WT, this does not provide significantly more protection from early viral replication.

The number of cells in the BALF was not significantly different between the different groups, however there was more spread in KO-KO and WT-KO mice (Fig 5.15b). Macrophage and neutrophil percentages were similar in BALF between WT-WT, KO-KO and KO-WT mice averaging 45% and 55% total cells respectively, however there was a noticeable decrease in macrophage numbers (30%) and an increase in neutrophils (70%) in WT-KO compared to all groups, which was show to be statistically significantly compared to KO-WT (Fig. 5.15c). This significant difference did not seem to have a correlation to lung viral load, as WT-KO and KO-WT had relatively similar L gene copies in the lung suggesting that there was no significant impact on viral clearance.

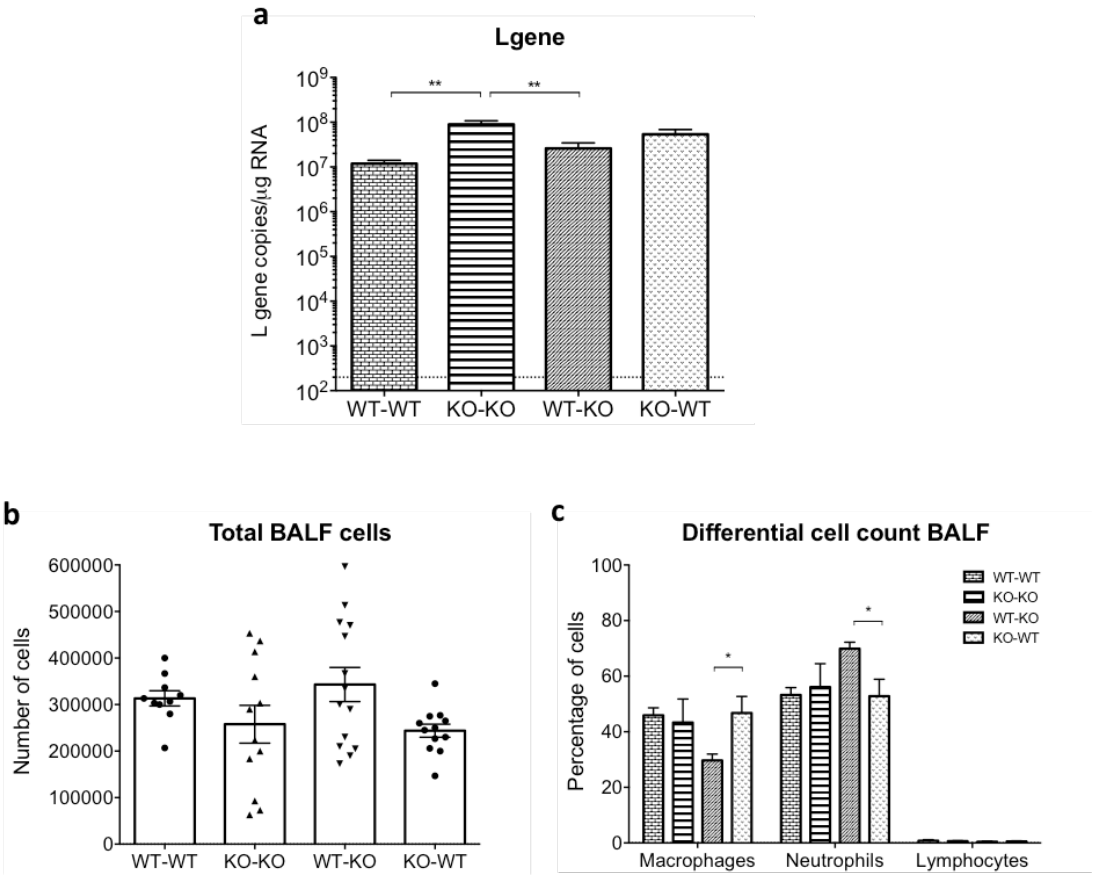


Figure 5.15: Lung viral load and total and differential cell counts of BALF from IFNAR1$^{-/-}$ BM chimeras 18hrs post RSV infection. BM chimeras were infected with 1.5x10^6 FFU of RSV intranasally at least 8 weeks post irradiation. Mice were euthanised 18hrs post RSV infection and lung and BALF taken. Viral load was determined via quantification of RSV L gene in lungs using qPCR using a plasmid standard with lower detection limit represented as a dashed line and levels shown as per µg RNA as it is from whole lung (a). Total cell number (b) and the percentages of macrophages, lymphocytes and neutrophils (c) in BALF were determined. Differential cells count in BALF of naive uninfected mice was always >98% macrophages (data not shown). Results show pooled data from three separate experiments with 3-7 mice per group except for the WT-WT group, which is from two separate experiments with 5 mice per group. Results are presented as mean ± SEM. Statistical significance was determined using one-way ANOVA with Tukey's post hoc test. ** p≤0.05, ** p≤0.01*.

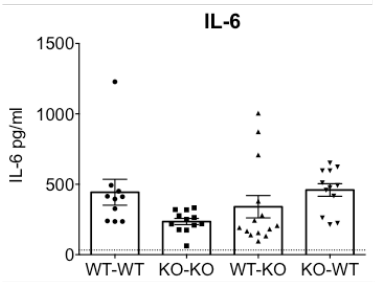
5.4.4 Decreased production of soluble mediators in BALF of IFNAR1 KO BM chimeras

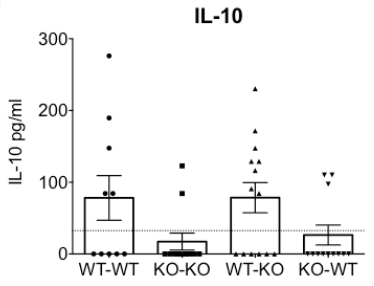
Analysis of BALF for soluble mediator protein expression using Luminex and ELISAs revealed that overall, KO-KO mice had no or significantly less production of the measured soluble mediators compared to all other groups, in particular to WT-WT mice (Fig. 5.16). WT-WT mice produced IL-6, IL-10, IL-12p40, CCL2, CXCL1, CXCL9, CXCL10, IL-1β, TNF-α, IFN-α and IFN-γ (as has been previously reported (Goritzka et al. 2014)). KO-KO mice produced significantly lower levels of CXCL1, CXCL9, TNF-α and IFN-α and a trend towards lower IL-10 and IL-6 compared to WT-WT mice. CCL2, CXCL10, IL-1β and IFN-γ were not expressed at all in KO-KO mice but detected in other groups. Interestingly, the only mediator expressed in higher levels in KO-KO compared to all other groups was VEGF, and was completely absent in WT-WT chimeric mice (Fig. 5.16). VEGF gene expression was detected in amplified cDNA from wildtype mice during RSV infection (Fig. 5.9). However, gene expression is a more sensitive method of detection, and protein levels in the BALF of WT-WT chimeric mice may have a high turnover rate or be too low to detect.

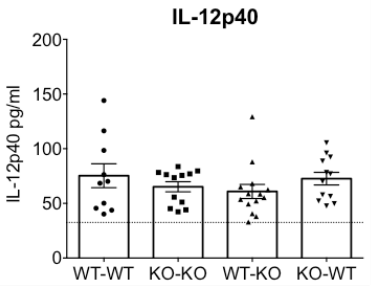
In regards to the soluble mediator production, WT-KO mice behaved more similarly to WT-WT mice, and KO-WT behaved more similarly to KO-KO mice (Fig. 5.16). For IL-6, IL-10 and IL12-p40 there were no major differences in the production between the groups of chimeric mice suggesting that it is not dependent on IFNAR1 signalling. However, WT-KO mice produced CCL2, CXCL1, CXCL9 and CXCL10 suggesting that IFNAR1 expression on BM-derived cells induces the expression of these mediators. However, the levels of these chemokines were still lower than WT-WT levels suggesting that IFNAR1 expression on stromal cells is required for a complete robust response. Levels of IL-1β and TNF-α were the same in WT-KO mice as WT-WT mice, suggesting that expression of IFNAR1 on BM-derived cells alone, is enough to reach WT-WT levels and is not dependent on IFNAR1 signalling on stromal cells. Indeed, AMs were shown to be the major source of IL-1β using amplified RNA (Fig. 5.9).

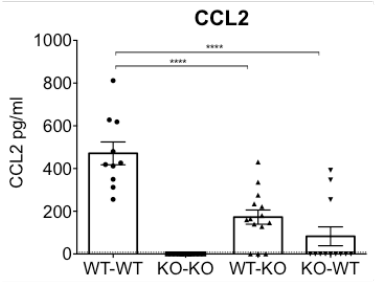
Levels of soluble mediators in KO-WT showed a very similar trend to those in KO-KO. However, it is difficult to ascertain whether this is due to the expression of these mediators not being dependent on IFNAR1 signalling on stromal cells, or whether the lack of the robust second wave of type I IFNs due to inability of IFNAR1 KO AM to provide this. Indeed, IFN-α and IFN-β levels in the BALF of KO-WT were almost identical to KO-KO averaging 2000 U/ml and 150pg/ml respectively in both groups, which is significantly less than both WT-WT and WT-KO mice. The similar levels of IFN-α and IFN-β in WT-WT and WT-KO further supports this notion that type I IFN production is mainly from BM-derived cells and even with IFNAR1 on stromal cells, the robust amplification of type I IFNs is dependent on BM-derived cells. Thus if the expression of other soluble mediators is dependent on IFNAR1 on stromal cells, it is hard to ascertain from this BM chimera experiments. This could be resolved by rIFN-α/β administration into KO-WT mice, which would allow stromal cell IFNAR1 dependent induction of mediators to occur.

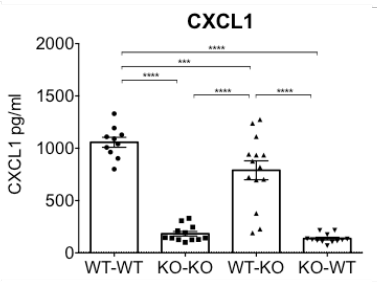
Mediators not detected in any groups were FGF, GM-CSF, IL-1α, IL-2, IL-4, IL-5, IL-13, IL-17 and CCL3.

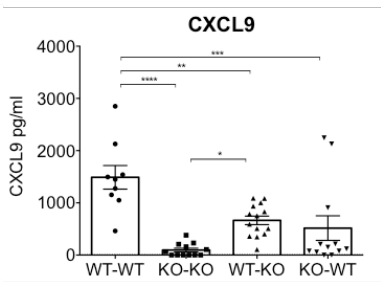

IL-6
IL-6 pg/ml
1500
1000
500
0
WT-WT
KO-KO
WT-KO
KO-WT

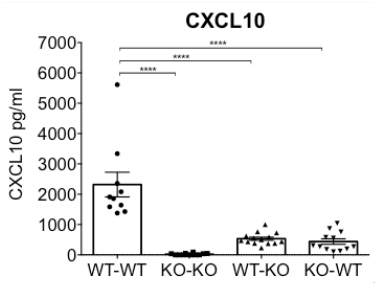

IL-10
IL-10 pg/ml
300
200
100
0
WT-WT
KO-KO
WT-KO
KO-WT

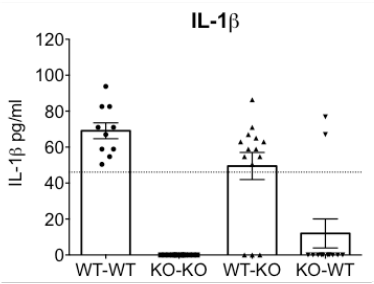

IL-12p40
IL-12p40 pg/ml
200
150
100
50
0
WT-WT
KO-KO
WT-KO
KO-WT

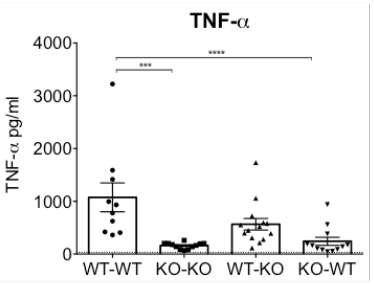

CCL2
CCL2 pg/ml
1000
800
600
400
200
0
WT-WT
KO-KO
WT-KO
KO-WT

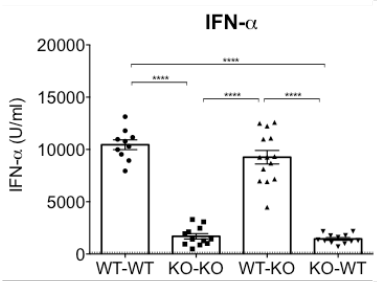

CXCL1
CXCL1 pg/ml
2000
1500
1000
500
0
WT-WT
KO-KO
WT-KO
KO-WT

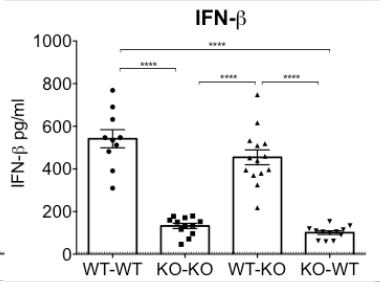

CXCL9
CXCL9 pg/ml
4000
3000
2000
1000
0
WT-WT
KO-KO
WT-KO
KO-WT

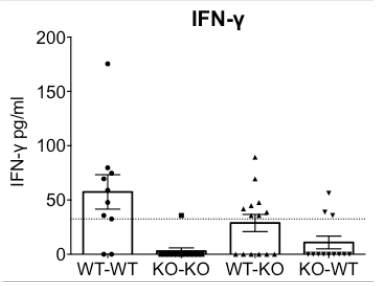

CXCL10
CXCL10 pg/ml
7000
6000
5000
4000
3000
2000
1000
0
WT-WT
KO-KO
WT-KO
KO-WT


IL-1β
IL-1β pg/ml
120
100
80
60
40
20
0
WT-WT
KO-KO
WT-KO
KO-WT


TNF-α
TNF-α pg/ml
4000
3000
2000
1000
0
WT-WT
KO-KO
WT-KO
KO-WT


IFN-α
IFN-α (U/ml)
20000
15000
10000
5000
0
WT-WT
KO-KO
WT-KO
KO-WT


IFN-β
IFN-β pg/ml
1000
800
600
400
200
0
WT-WT
KO-KO
WT-KO
KO-WT


IFN-γ
IFN-γ pg/ml
200
150
100
50
0
WT-WT
KO-KO
WT-KO
KO-WT

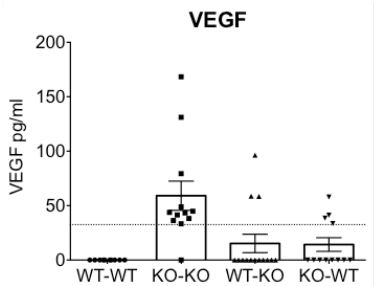

VEGF
VEGF pg/ml
200
150
100
50
0
WT-WT
KO-KO
WT-KO
KO-WT

Figure 5.16: Protein analysis of BALF from BM chimeras 18hrs post RSV infection. BALF was applied to Mouse Cytokine Magnetic 20-Plex Panel (Luminex) and processed according to the manufacturer's instructions to determine protein levels. CXCL1 and IFN-α levels were determined via ELISA. Lower detection limit represented as a dashed line. Mediators not detected in any groups: FGF, GM-CSF, IL-1α, IL-2, IL-4, IL-5, IL-13, IL-17 and CCL3. Each dot represents an individual mouse. Results show pooled data from three separate experiments with 3-7 mice per group except in the WT-WT group, which is from two separate experiments with 5 mice per group. Results are presented as mean ± SEM. Statistical significance was determined using one-way ANOVA with Tukey's post hoc test. ** p≤0.05, ** p≤0.01*, **** p≤0.001, **** p≤0.0001.*

5.4.5 Expression of ATII epithelial cell-derived mediators in not IFNAR1 dependent

Next, stromal cell populations were sorted from lungs of the different chimeras and gene expression analysis performed for genes described in 5.2 to reveal the cell specific dependencies of IFNAR1 signalling for expression of mediators. As mentioned previously due to logistical constraints, sorting was done via FACS for two experiments and via MACS for one experiment. As such MACS provided only ATII epithelial cells and other stromal cells for gene expression analysis and at a lower purity to FACS, therefore will be displayed separately to cells sorted by FACS.

Overall the data revealed that mediators mostly expressed by ATII epithelial cells in 5.2 were not dependent on IFNAR1 signalling 18hrs post RSV infection (Fig. 5.17). Then again, these mediators showed peak expression at 4hrs post infection (5.2) and therefore 18hrs may be too late to investigate whether ATII epithelial cell-derived mediators are dependent on IFNAR1 signalling. However, it was not possible to do several time points. Gene expression of amphiregulin, GM-CSF or IL-33 from FACS sorted ATII epithelial cells (Fig. 5.17a) from KO-KO, WT-KO and KO-WT was enriched and did not differ considerably between the groups. ATII epithelial cells from WT-WT mice for which only one FACS sort was performed did not seem to express GM-CSF or IL-33, however this was most probably due to a technical issue rather than a true result as MACS sorted WT-WT ATII epithelial cells (Fig. 5.17b) showed expression of these mediators as expected. In MACS sorted cells expression between ATII epithelial cells from different chimeras did not differ, although there was a trend towards less GM-CSF from KO-WT. As mentioned previously, MACS sorted cells had considerably lower purity, compared to FACS sorted cells (Table 5.4). In particular other stromal cells were contaminated with up to 20% ATII epithelial cells. This may explain the high level of GM-CSF and IL-33 expression detected in the other stromal cells, which was not seen in FACS sorted cells, or from previous experiments (Fig. 5.17).

Table 5.4: Main contaminants for MACS sorted ATII epithelial cells and other stromal cells.

ATII epithelial cells	Other stromal cells
~45% dead cells	~50% dead cells
~5% other stromal cells	~20% ATII epithelial cells

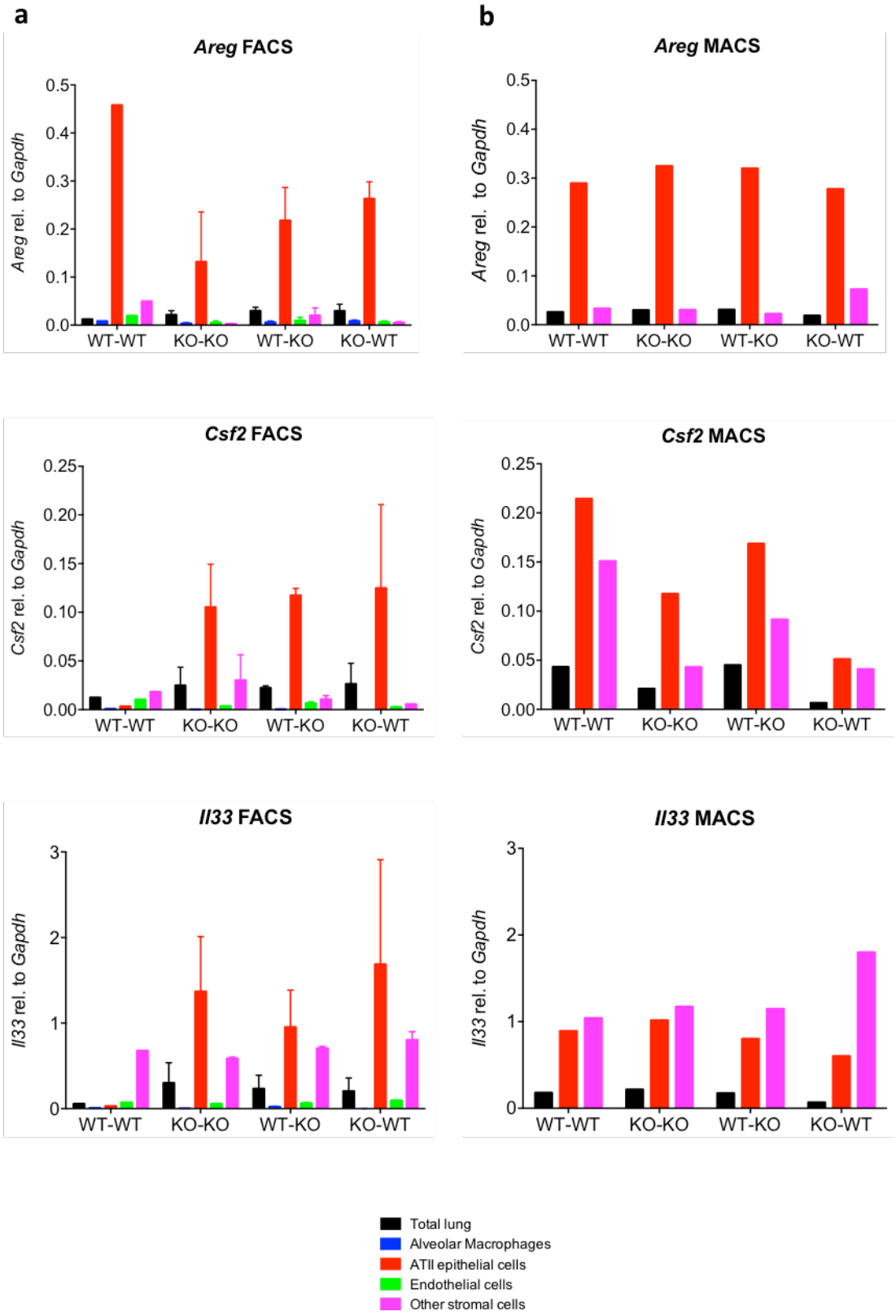

a
Areg FACS
Areg rel. to Gapdh
0.5
0.4
0.3
0.2
0.1
0.0
WT-WT
KO-KO
WT-KO
KO-WT
b
Areg MACS
Areg rel. to Gapdh
0.5
0.4
0.3
0.2
0.1
0.0
WT-WT
KO-KO
WT-KO
KO-WT
Csf2 FACS
Csf2 rel. to Gapdh
0.25
0.20
0.15
0.10
0.05
0.00
WT-WT
KO-KO
WT-KO
KO-WT
Csf2 MACS
Csf2 rel. to Gapdh
0.25
0.20
0.15
0.10
0.05
0.00
WT-WT
KO-KO
WT-KO
KO-WT
Il33 FACS
Il33 rel. to Gapdh
3
2
1
0
WT-WT
KO-KO
WT-KO
KO-WT
Il33 MACS
Il33 rel. to Gapdh
3
2
1
0
WT-WT
KO-KO
WT-KO
KO-WT
Total lung
Alveolar Macrophages
ATII epithelial cells
Endothelial cells
Other stromal cells

Figure 5.17: Gene expression of amphiregulin, GM-CSF and IL-33 from sorted stromal cells and AMs from BM chimeras 18hrs post RSV infection. Stromal cell populations and AMs were sorted from BM chimeras 18hrs post RSV infection. Lungs were digested with dispase and (a) stained with antibodies against CD45, CD31, CD11c and EpCAM and a live/dead dye before sorting via FACS for live singlet AMs, ATII epithelial cells, endothelial cells and other stromal cells. (b) For MACS, cells were incubated with anti-CD45 and anti-CD31 Microbeads and sorted via manual MACS using LS columns to obtain ATII epithelial cells and other stromal cells. Sorted cells as well as an aliquot of single cell suspension of total lung for both methods were then analysed for gene expression of amphiregulin (*Areg*), GM-CSF (*Csf2*) and *Il33* via RT-qPCR. Expression of the target gene is shown as relative expression to the housekeeping gene *Gapdh*. Results for FACS (a) show 1-2 sorts with 3-5 mice pooled per group per sort and for MACS (b) show 1 sort with 5-7 mice pooled per group. Data displayed as mean + range where possible.

5.4.6 Expression of CXCL10 is dependent on IFNAR1 on other stromal cells, whilst expression of CCL2 is partially dependent

Analysis of genes strongly upregulated by other stromal cells such as CCL2, CXCL10, CXCL1 and IL-6 (as shown previously Fig. 5.7) showed that similar upregulation patterns from these cellular sources were detected in chimeric mice (Fig. 5.18). The results revealed that CXCL10 and CCL2 were the only mediators that showed full or partial dependence on IFNAR1 signalling. In particular, expression of IFNAR1 on other stromal cells (KO-WT) was critical for robust CXCL10 and CCL2 expression from these cells (Fig. 5.18). CCL2 expression from other stromal cells was present in KO-KO mice both in FACS and MACS sorted cells, but at a lower level than WT-WT, demonstrating that CCL2 can be expressed without IFNAR1 signalling but not to its full capacity. CCL2 was not detected in BALF via Luminex in KO-KO mice (Fig. 5.16), however this may have been due to threshold of detection not being sensitive enough compared to RT-qPCR. Levels of CCL2 expression were detected in WT-KO in MACS and FACS, but the other stromal cells from KO-WT showed almost similar levels to WT-WT levels (Fig, 5.18). This trend was not as clear in MACS sorted other stromal cells from KO-WT (Fig, 5.18b). However, this experiment was only performed once and MACS sorted cells had less purity than FACS, which may have diluted out the CCL2 expression from other stromal cells due to contamination of ATII epithelial cells. Similarly, and more strikingly, CXCL10 gene expression seemed to be almost completely dependent on IFNAR1 signalling and again only fully restored with IFNAR1 expression on other stromal cells (Fig. 5.18). CXCL10 gene expression was absent in other stromal cells in KO-KO mice, partially restored in WT-KO mice but still noticeably lower than WT-WT. Only in KO-WT other stromal cells was CXCL10 expression levels comparable to WT-WT levels, both in MACS and FACS sorted cells, suggesting IFNAR1 expression on other stromal cells is crucial for strong induction. Levels of CXCL1 from other stromal cells from all groups were similar suggesting that it is not IFNAR1 dependent, and similarly IL-6 expression was comparable between all groups, except KO-WT other stromal cells had a trend towards higher expression.

Thus overall, expression of CCL2 and CXCL10 from other stromal cells during RSV infection *in vivo* seemed to partially or fully dependent on IFNAR1 signalling, on other stromal cells, whilst expression of CXCL1 and IL-6 did not.

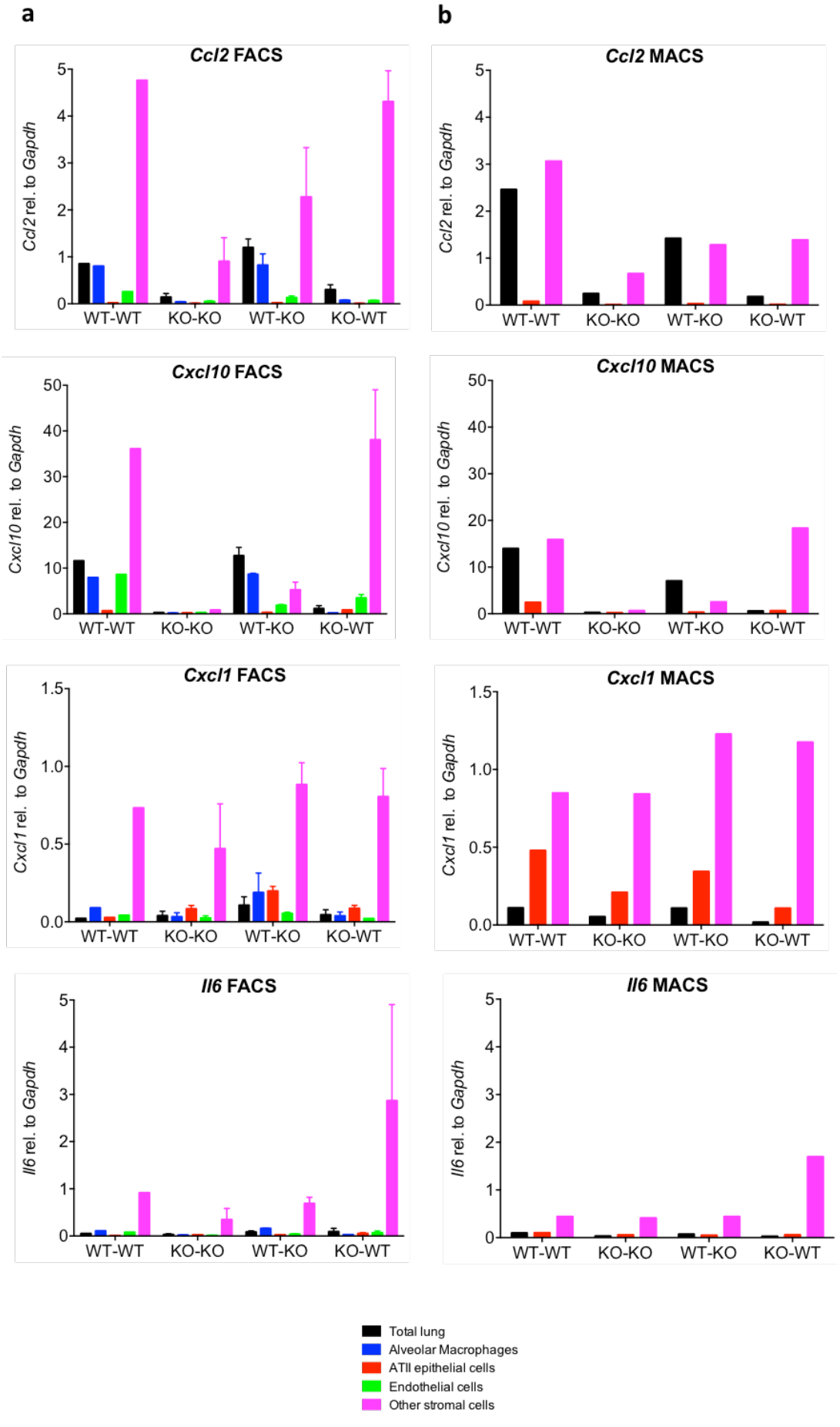

a
b
Ccl2 FACS
Ccl2 MACS
Cxcl10 FACS
Cxcl10 MACS
Cxcl1 FACS
Cxcl1 MACS
Il6 FACS
Il6 MACS
Ccl2 rel. to Gapdh
Cxcl10 rel. to Gapdh
Cxcl1 rel. to Gapdh
Il6 rel. to Gapdh
WT-WT
KO-KO
WT-KO
KO-WT
Total lung
Alveolar Macrophages
ATII epithelial cells
Endothelial cells
Other stromal cells

Figure 5.18: Gene expression of CCL2, CXCL1, CXCL10 and IL-6 from sorted stromal cells and AMs from BM chimeric mice 18hrs post RSV infection. Stromal cell populations and AMs were sorted from BM chimeras 18hrs post RSV infection. Lungs were digested with dispase and (a) stained with antibodies against CD45, CD31, CD11c and EpCAM as well as a live/dead dye before sorting via FACS for live singlet AMs, ATII epithelial cells, endothelial cells and other stromal cells. (b) For MACS cells were incubated with anti-CD45 and anti-CD31 Microbeads and sorted via manual MACS using LS columns of ATII epithelial cells and other stromal cells. A sample of the single-cell suspension before sorting was also taken to represent the total lung. RNA was extracted from cells, converted to cDNA and analysed for gene expression of CCL2, CXCL1, CXCL10 and IL-6 via RT-qPCR. Expression of the target gene is shown as relative expression to the housekeeping gene *Gapdh*. Results for FACS (a) show 1-2 sorts with 3-5 mice pooled per group per sort and for MACS (b) show 1 sort with 5-7 mice pooled per group. Data displayed as a mean + range where possible.

5.4.7 Expression of type I IFNs from AMs is IFNAR1 dependent

Analysis of type I IFN expression which was shown to be mainly from AMs in 5.2, revealed unsurprisingly that gene expression of IFN-α5 and IFN-β from AMs were dependent on IFNAR1 signalling, with noticeably lower expression in KO-KO mice (Fig. 5.19). Furthermore, only AMs from WT-KO mice had higher levels of IFN-α5 and IFN-β than WT-WT, whilst KO-WT had levels similar to KO-KO. This demonstrates that IFNAR1 expression in AMs alone is enough to induce robust type I IFN gene expression. Of note, there were low levels of IFN-β detected in all groups including KO-KO mice suggesting that IFN-β is still expressed independent of IFNAR1 signalling, but the data suggests that IFNAR1 on AMs is important for the expression of type I IFNs (here shown by IFN-α5) via the positive feedback loop.

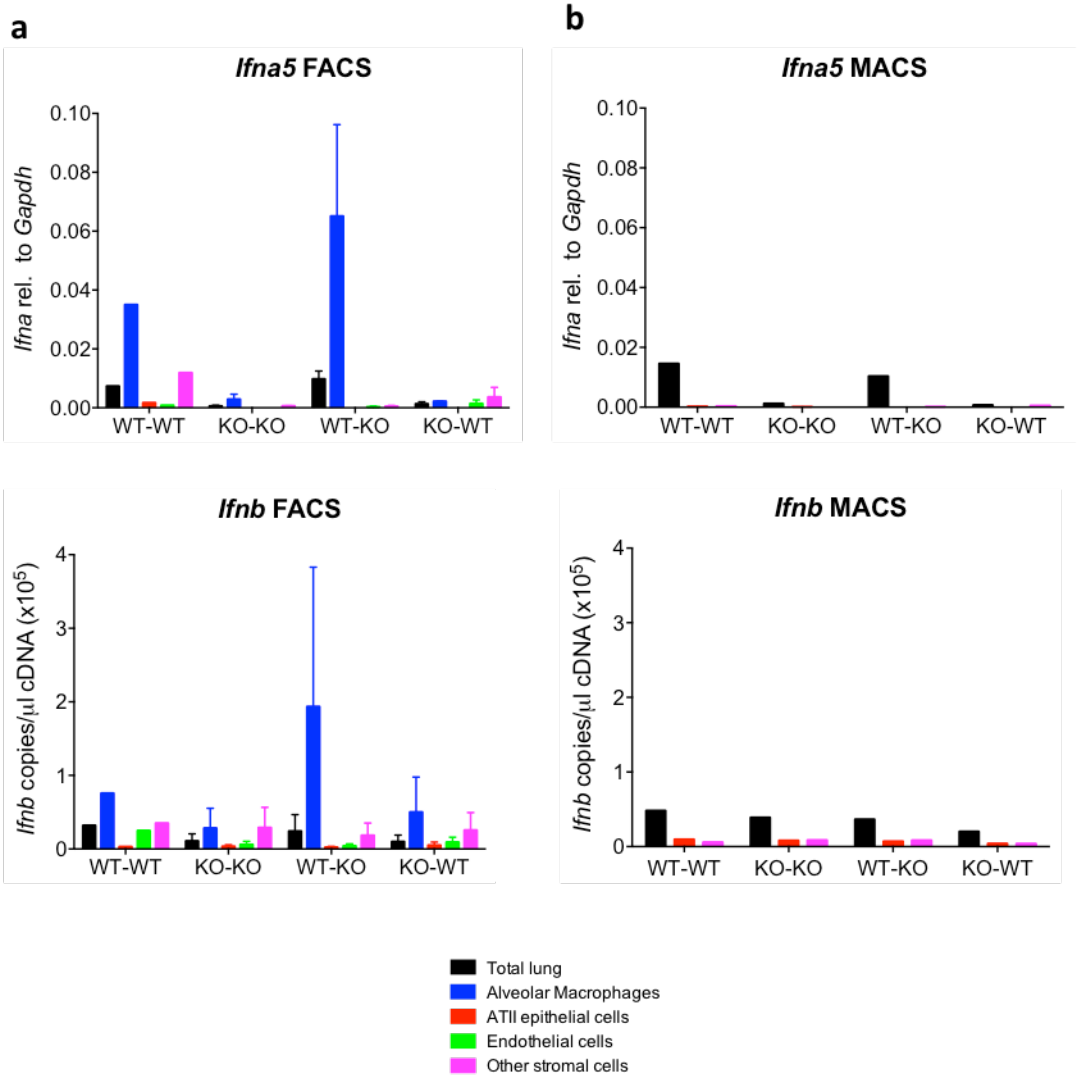


Figure 5.19: Gene expression of IFN-α5 and IFN-β from sorted stromal cells and AMs from BM chimeric mice 18hrs post RSV infection. Stromal cell populations and AMs were sorted from BM chimeras 18hrs post RSV infection. Lungs were digested with dispase and (a) stained with antibodies against CD45, CD31, CD11c and EpCAM as well as a live/dead dye before sorting via FACS for live singlet AMs, ATII epithelial cells, endothelial cells and other stromal cells. (b) For MACS cells were incubated with anti-CD45 and anti-CD31 Microbeads and sorted via manual MACS using LS columns of ATII epithelial cells and other stromal cells. A sample of the single-cell suspension before sorting was also taken to represent the total lung. RNA was extracted from cells, converted to cDNA and analysed for gene expression of IFN-α5 and IFN-β via RT-qPCR. Expression of IFN-α5 is shown as relative expression to the housekeeping gene *Gapdh*. Copy numbers IFN-β were determined using a plasmid standard. Results for FACS (a) show 1-2 sorts with 3-5 mice pooled per group per sort and for MACS (b) show 1 sort with 5-7 mice pooled per group. Data presented as mean + range.

5.4.8 Summary

Type I IFNs are potent mediators in the immune response to viruses, inducing both an antiviral state in infected and neighbouring cells, as well as stimulating innate immune cells and enhancing adaptive immune responses. Recently, IFNAR signalling has been shown to be a central driver of early proinflammatory responses through amplification of chemokine, cytokine and growth factor expression during RSV infection *in vivo* (Goritzka et al. 2014). AMs were shown to be the source of the type I IFNs needed for driving this proinflammatory induction (Goritzka, Makris, et al. 2015). These studies however, did not reveal the cell-specific dependence of IFNAR signalling for expression of these mediators *in vivo*. In this study the critical role of IFNAR signalling on other stromal cells for the autonomous expression of CCL2 and CXCL10 is revealed, whilst the IFNAR-independence of ATII epithelial cells on expression of growth factors and other ATII epithelial cell-derived mediators is also demonstrated.

BM-chimeras generated using IFNAR1 knockout mice, which did not express IFNAR1 either on stromal cells, BM-derived cells or both, had increased viral burden in the lungs compared to wildtype mice (Fig. 5.15). This supports and builds on data from Goritzka et al who demonstrated that IFNAR1$^{-/-}$ mice had significantly higher viral load up to 14 days post RSV infection compared to wildtype mice (Goritzka et al. 2014), and mirrors findings from studies with other viruses which showed increased viral burden in IFNAR1$^{-/-}$ mice (Cervantes-Barragán et al. 2009, Trinchieri 2010, Pinto et al. 2014). Chimeric IFNAR1$^{-/-}$ (KO-KO) mice had the highest viral load followed by KO-WT and then WT-KO. This demonstrates that IFNAR1 expression on stromal cells alone, is enough to reduce viral load, but is not as efficient as IFNAR1 on BM-derived cells. However, KO-WT mice have an extra limitation; although IFNAR is present on stromal cells, BM-derived cells (such as AMs) do not produce type I IFNs that can signal via IFNAR on stromal cells. AMs have been shown to be the major source of type I IFNs during RSV infection *in vivo* (Goritzka, Makris, et al. 2015) and data from this project have shown stromal cells to induce little type I IFNs during infection (Fig. 5.6/7). Indeed, IFN-α and IFN-β in BALF in KO-WT is almost

identical to KO-KO mice with completely diminished levels, whilst amounts in WT-KO are similar to WT-WT (Fig. 5.16) again proving that a BM cell is the source of type I IFNs during RSV infection. Thus, from the data so far, it is not possible to conclusively state whether IFNAR signalling on stromal cells is more/less protective than IFNAR signalling on BM-derived cells. Administration of rIFN-α/β to KO-WT mice, which would allow any potential IFNAR-dependent signalling to occur on stromal cells would answer this question. However despite this limitation, our data supports the findings of previous studies, that lack of type I IFN expression from BM-derived cells due to loss of IFNAR signalling, is vital for controlling viral lung load, and also highlights IFNAR signalling on stromal cells to have a role in controlling viral burden.

Cellular infiltration into the lung was similar between all chimeric groups except WT-KO, which had more neutrophils. However, this did not seem to have a correlation to lung viral load, suggesting that it does not have an effect on viral clearance (Fig. 5.15). Indeed viral load in IFNAR1$^{-/-}$ and wildtype lungs consistently increases regardless of a decrease or increase in neutrophils in the BALF during the first 48hrs of infection (Goritzka et al. 2014). Interestingly, levels of CXCL1, a potent neutrophil chemoattractant, is higher in BALF in WT-KO mice compared to KO-KO and KO-WT, albeit still lower than WT-WT suggesting that CXCL1 levels in the lung is strongly dependent on IFNAR1 on BM-derived cells with minor dependence on stromal cells (Fig. 5.16). This observation does not have a mirrored effect on neutrophil infiltration, as despite almost completely diminished CXCL1 protein levels, KO-KO and KO-WT have the same neutrophil percentages as WT-WT. To note, both the chemokine production and the neutrophil infiltration in BALF were only determined at one time point and it is possible that a more detailed time course would reveal changes later on. In addition, other neutrophil chemoattractants such as CXCL5 could be compensating for the lack of CXCL1 expression and recruiting neutrophils in KO-KO and KO-WT mice. CXCL5 was detected on the gene array analysis of sorted other stromal cells and ATII epithelial cells (Fig. 5.9, Table 5.1/2) supporting this notion, and further analysis of CXCL5 in BALF of the BM chimeras would demonstrate its role. Thus overall, IFNAR signalling does not

seem to have a great influence influx of neutrophils during the first 18hrs of infection.

Similar to CXCL1, levels of other soluble mediators in the BALF of KO BM chimeras were again, overall lower than WT-WT mice (Fig. 5.16). KO-KO mice had the most striking loss of expression of nearly all chemokines and cytokines analysed and recapitulates the findings from Goritzka et al that IFNAR signalling is critical for robust cytokine and chemokine induction during RSV infection (Goritzka et al. 2014). KO-WT mice that express IFNAR1 on stromal cells only, behaved similarly to KO-KO mice, with decreased soluble mediators in BALF compared to mice that had IFNAR1 on BM-derived cells, which behaved more similarly to WT-WT mice although never fully reached WT-WT levels. As stated above, the limitation with the KO-WT mice not having amplified type I IFNs for stromal cells to signal with using IFNAR does not enable a conclusion to be made as to whether loss of mediators in these mice is due to expression not being dependent on IFNAR signalling on stromal cells and lack of IFNAR1 on BM-derived cells, or whether lack of available type I IFNs is preventing IFNAR signalling on stromal cells to occur to induce expression of the mediators. The latter hypothesis is further supported with the findings particularly of chemokine production in BALF, which show that WT-KO mice do not reach WT-WT mice levels of expression of CCL2, CXCL10, CXCL9 and CXCL1 (Fig. 5.16). This demonstrates that IFNAR signalling on BM-derived cells is not enough to completely restore wildtype level expression, and therefore must also be induced by IFNAR signalling on stromal cells. This is most striking with CCL2 and CXCL10 gene expression in which WT-KO production is at almost identical KO-WT levels.

Due to lack of potent type I IFN responses in BALF and from sorted cells in KO-KO BM chimeras, it could be hypothesised that type II or type III IFNs may compensate for the loss of these antiviral mediators to protect the host from severe disease as all three groups of IFNs signal via different receptors. This has been demonstrated in studies of IAV infection (Jewell et al. 2010, Crotta et al. 2013). However, IFN-γ in BALF was either undetected or considerably lower

than WT-WT for all KO BM chimeras suggesting this is not the case. Levels of IFN-λ were not analysed but other studies suggest IFN-λ is not highly induced during RSV infection and that its production is dependent on the IFNAR signalling (Goritzka et al. 2014). Levels of IL-12p40 did not differ between the groups of BM-chimeras, demonstrating IFNAR-independent production. However these results go against the findings of Goritzka et al who observed diminished IL-12p40 levels in the lungs of IFNAR1$^{-/-}$ mice compared to wildtype (Goritzka et al. 2014). It is not clear why there is a discrepancy between this study and our findings, however it is possible that KO-KO BM chimeras differ in their expression of IL-12p40 compared to their non-irradiated IFNAR1$^{-/-}$ counterparts due to a process during their generation during irradiation. In addition the BM chimeric mice were older and only one time point was studied. Interestingly, VEGF was the only mediator detected in BALF in KO-KO mice 18hrs post RSV infection, with minimal expression in WT-KO and KO-WT, and no expression in WT-WT. This is supported by gene expression data from amplified cDNA from wildtype total lung, which showed VEGF expression to be downregulated at 18hrs post RSV infection (Fig. 5.9). However, VEGF gene expression was also induced before and after 18hrs in wildtype mice. Therefore it is not clear whether VEGF expression is IFNAR dependent from analysis of chimeric mice at this time point as we are missing the peak time point of expression. However, as previous studies have demonstrated the protective role of VEGF in reducing viral load (Olivier et al. 2011) KO-KO mice may be expressing more VEGF at times when WT-WT are not, in attempt to reduce viral spread as these mice have significantly higher viral burden.

Overall, analysis of viral load and production of soluble mediators in the lung of BM chimeras hint at the importance of IFNAR signalling on stromal cells during RSV infection. Viral load is higher in mice that have IFNAR either on stromal cells or BM-derived cells only and the production of potent proinflammatory chemokines and cytokines is lost in KO-KO mice and only partially restored in both mice where IFNAR is only present on BM-derived cells, suggesting IFNAR on stromal cells is required for full robust production.

We then went on to evaluate cell specific dependencies and whether IFNAR expression is directly required on ATII epithelial cells, endothelial cells and other stromal cells for expression of mediators that have been observed being induced by these cells during RSV infection. Analysis of mediators from sorted ATII epithelial cells from different BM chimeras did not reveal any strikingly clear dependency on IFNAR signalling for the expression GM-CSF, amphiregulin or IL-33 (Fig. 5.17). Certainly, the lack of replicates and unavoidable use of MACS which yields considerably lower purity of sorted cells hinders the clear determination of this and further experimental repeats with FACS need to be performed to confirm this. However, data from Goritzka et al demonstrated that GM-CSF was completely absent in BALF of IFNAR1-deficient mice (non-chimeric) (Goritzka et al. 2014), a finding also observed in this study (KO-KO chimeras) but surprisingly also in WT-WT chimeric mice (data not shown) which may have been due to levels being below the threshold of detection. This suggests that the total GM-CSF production in the lung is dependent on IFNAR signalling, however gene expression from sorted ATII epithelial cells, which we have shown to be a major source of GM-CSF during infection, does not fully support these data and needs to be further investigated. IL-33 dependency on IFNAR signalling has been investigated more recently and revealed IL-33 protein levels in IFNAR1$^{-/-}$ mice infected with IAV were comparable to those in wildtype mice, demonstrating that IFNAR signalling does not regulate IL-33 expression (Duerr et al. 2016). To our knowledge, the role of IFNAR signalling on amphiregulin expression has not been characterised. However, mice that lack the PRR adaptor molecules MyD88, TRIF and MAVS and subsequently have no induction of IFN-αs during RSV infection, show no difference in the level of expression of amphiregulin in the lung suggesting that, at least, amphiregulin is not dependent on signalling via IFN-αs (Goritzka, Pereira, et al. 2015). Thus overall, our data does not suggest IFNAR-dependent expression of mediators from ATII epithelial cells during RSV infection *in vivo*, but further analysis needs to be performed to confirm these findings.

Gene expression analysis of other stromal cells revealed a more convincing picture of IFNAR-dependent expression of meditators. CXCL10 gene expression

was completely lost from other stromal cells from KO-KO mice, which was slightly increased in WT-KO mice. Surprisingly, the CXCL10 levels were back to WT-WT levels in KO-WT mice (Fig. 5.18). This was evident in both FACS and MACS sorted cells, providing more strength to this observation. The expression of CXCL10 from other stromal cells in KO-WT mice might further suggest that low levels of IFN-β (in the absence of IFN-αs) may result in CXCL10 gene expression. AMs are also a minor source of CXCL10, and also followed the same trend in which WT-WT expression levels was restored with IFNAR1 expression on these cells (Fig. 5.18). Interestingly, CXCL10 protein levels in BALF for KO-WT mice was significantly lower than WT-WT and was at levels more similar to KO-KO and WT-KO. Indeed, gene expression analysis is far more sensitive than protein assays, which may explain the differences in CXCL10 protein detection. However, other cell types not examined in this study could be contributing to the total CXCL10 production, and the turnover rate and binding for CXCL10 is not known. In addition, soluble mediators were measured from BALF; an alternative would be to measure protein levels from lung homogenate to evaluate what is being produced by cells in the tissue. CCL2 gene expression showed a partial dependence of IFNAR signalling on other stromal cells after FACS sorting cells, but was less clear after MACS sorting. CCL2 gene expression was induced in other stromal cells from KO-KO mice, suggesting an IFNAR-independent mechanism of production such as via NF-κB but was only restored to WT-WT levels of expression in KO-WT mice. CXCL10 and CCL2 are ISGs (Trinchieri 2010) and as such, it is not surprising that the transcription of these genes from other stromal cells is dependent on IFNAR expression on these cells. Gene expression of IL-6 and CXCL1 from other stromal cells did not demonstrate an obvious IFNAR signalling requirement and they are therefore most likely induced in an NF-κB-dependent mechanism. Interestingly, whilst this IFNAR1-independent expression of CXCL1 agrees with findings in complete IFNAR1 KO mice during RSV infection by Goritzka et al, IL-6 expression was shown to be IFNAR1-dependent in this study (Goritzka et al. 2014). It is not clear why there is a difference between this study and our findings, however it could be due to the reasons as mentioned above previously. Nevertheless, overall the findings demonstrate that IFNAR expression on other stromal cells is required for

transcription of soluble mediators such as CXCL10 and CCL2 during RSV infection. Conversely, mediators such as IL-6 and CXCL1 can rely on IFNAR-independent mechanisms for expression from other stromal cells, and may be alternative pathway for induction of inflammation in the absence of IFN induction.

Lastly, gene expression of type I IFNs from sorted cells was shown, as expected, to be dependent on IFNAR1 expression on the cellular source, AMs (Fig. 5.19), which results from this study have confirmed (section 5.2). Expression of IFN-α5 from AMs was almost completely lost in KO-KO and KO-WT mice, but restored in WT-KO mice in which IFNAR signalling is available on BM-derived cells. Other stromal cells showed minor expression of IFN-α5 in WT-WT mice, and showed no expression in KO-KO and WT-KO mice, but regained minimal expression in KO-WT mice in which IFNAR signalling is on stromal cells. IFN-β was constitutively expressed in all BM-chimeras AMs and to a lesser extent in other stromal cells, but showed robust induction with IFNAR presence on BM-derived cells confirming both the IFNAR-dependent amplification of type I IFNs and that AMs a the main driver of type I IFN production during RSV infection *in vivo* (Trinchieri 2010, Goritzka, Makris, et al. 2015).

Polymorphisms in innate immune genes, particularly those that control the IFN system have been associated with variation in disease severity (Awomoyi et al. 2007, Janssen et al. 2007). In this study by Janssen et al, polymorphisms in the IFN-α5 gene showed one of the strongest associations with RSV bronchiolitis in a cohort of hospitalised children. It is possible that deficiencies in efficient type I IFN signalling may result in an inadequate induction of potent chemoattractants such as CXCL10 and CCL2, which we have shown to have partial or full dependence of IFNAR signalling on the secreting cell. These chemokines have been shown to be critical for efficient viral clearance and reducing disease severity in mice, with CCL2 in particular highlighted as being vital for the recruitment of inflammatory monocytes which play a major role in restricting virus production and dampening disease severity (Lindell et al. 2008, Goritzka, Makris, et al. 2015).

5.5 GM-CSF antibody treatment can lead to increased weight loss and viral load during RSV infection *in vivo*

This study has highlighted various soluble mediators highly expressed by stromal cells in the lung in response to RSV infection *in vivo*. To further understand the roles of these stromal cell-derived mediators during infection and what effect they have in the response and thus answering aim 4 of this study, one of these mediators, GM-CSF, was investigated further. GM-CSF is a growth factor originally identified for its effects on the survival, maturation and differentiation of leukocytes. However, it also a potent growth factor for alveolar epithelial cells and has a critical role in maintaining the lung barrier integrity (Trapnell and Whitsett 2002, Sever-Chroneos et al. 2011). In a recent study, allergen-sensitised mice infected with RSV showed bronchial hyperreactivity and increased infiltration of inflammatory cells compared to non-sensitised mice and this was accounted for by immature AMs overproducing IL-6 and TNF-α (Naessens et al. 2015). However, administration of GM-CSF into the lungs induced complete AM maturation in allergen-sensitised mice and protected from increased RSV-induced hyperreactivity and inflammation (Naessens et al. 2015). In another study, mice infected with RSV expressing GM-CSF (RSV-GMCSF), had significantly reduced viral load compared to infection with wildtype virus and the RSV-GMCSF infected mice also had increased numbers of AMs and DCs with increased expression of MHC-II on the latter (Bukreyev et al. 2001). These studies propose that GM-CSF has a highly protective role during RSV infection *in vivo*. However, these studies have limitations – the former used allergic mice and the latter utilised overexpression of GM-CSF, and thus these findings do not fully elucidate the role of the physiological levels of GM-CSF induced in the lung during RSV infection. Therefore, to test if the GM-CSF we have shown to be expressed by ATII epithelial cells during RSV infection *in vivo* has a protective role, GM-CSF was neutralised using GM-CSF antibodies before and after infection to determine whether the expression of GM-CSF in the lung is important for viral clearance and maintaining barrier integrity.

5.5.1 Intranasal administration of GM-CSF antibody alters disease severity and viral load during RSV infection

Mice were given GM-CSF antibody (αGM-CSF) intranasally (as previously described by (Yamashita et al. 2002)) one day before RSV infection, and then again at 6 and 24hrs post infection. This was to allow neutralisation of GM-CSF detected in the naïve lungs (Fig. 5.7b), as well as the induction of GM-CSF seen post infection (Fig. 5.7b). One group of mice were also intranasally dosed with an isotype antibody as a control, and both were compared to a group of mice receiving RSV only. Mice were weighed daily for 9 days to determine weight loss, as a quantitative measure of RSV induced illness, and lungs and BALF taken at day 10 post infection to measure viral lung load and cell infiltration.

The results revealed that mice receiving GM-CSF antibody had less weight loss compared to the RSV only group with 92% and 85% original weight respectively at day 6, the day of peak weight loss (Fig. 5.20a). However, mice receiving the isotype control were not significantly different to αGM-CSF treated mice at day 6, also having less weight loss than RSV only mice (Fig. 5.20a). Thus whether GM-CSF neutralisation or the addition of antibody into the lung itself caused this decreased weight loss is not clear. All groups recovered back to their original weight by day 9 (Fig. 5.20a). αGM-CSF treated mice had a non-significant trend towards less virus in the lung than RSV only mice at day 10 post infection (Fig. 5.20b). The number of BALF cells in the lung was significantly less in RSV only mice at day 10, however again, there was no significant difference between αGM-CSF and isotype treated mice (Fig. 5.20c). Thus, whether this difference is due to GM-CSF neutralisation is not clear. Differential leukocyte counts revealed only macrophages and lymphocytes present in the BAL at day 10 post infection in all groups with approximately 80% macrophages and 20% lymphocytes for all three (Fig. 5.20d).

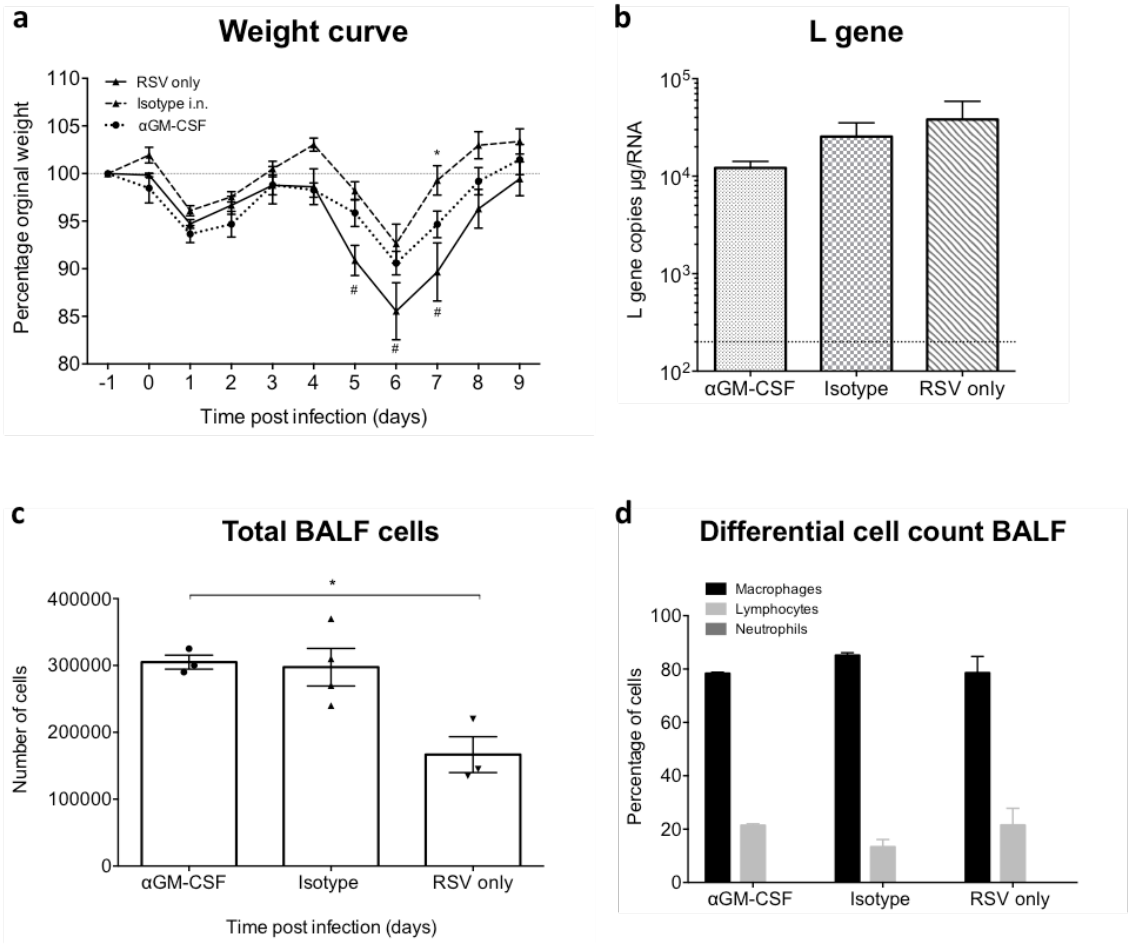
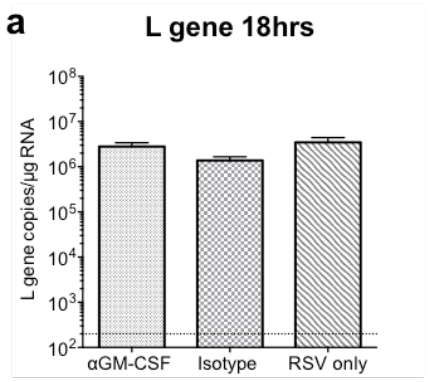


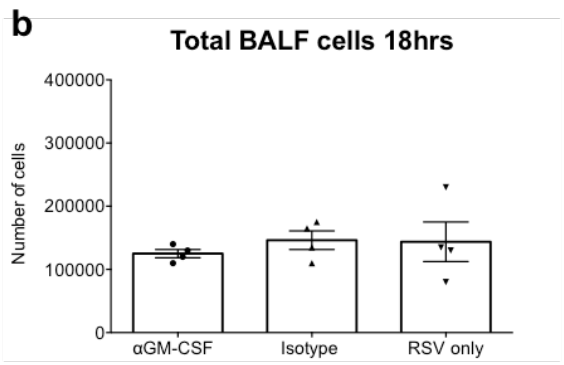
Figure 5.20: Intranasal GM-CSF antibody treatment during RSV infection. C57BL/6 mice were given either 25µg of GM-CSF antibody (αGM-CSF: clone MP1-22E9) or isotype antibody (IgG2a, clone 2A3) intranasally one day before RSV infection (day -1) and again at 6 and 24hrs post infection. An RSV only group that received only RSV was also included. Mice were infected with $1.5x10^6$ FFUs of RSV intranasally at day 0. Weight was monitored daily and plotted as percentage of original weight, with dashed line representing original weight at day -1 (a). Mice were euthanized at day 10 post RSV infection. Viral load was determined via quantification of RSV L gene in lungs via RT-qPCR using a plasmid standard with the lower detection limit represented as a dashed line (b). Total cell number (c) and the percentages of macrophages, lymphocytes and neutrophils (d) in BALF were also determined. Data show one experiment with 3-4 mice per group. Results are presented as mean ± SEM. Statistical significance was determined using two-way ANOVA with Bonferonni's post hoc test with significance between αGM-CSF and RSV represented as "#" and between αGM-CSF and isotype as "*" (a); and one-way ANOVA with Tukey's post hoc test (b-d). ** $p \leq 0.05$.*

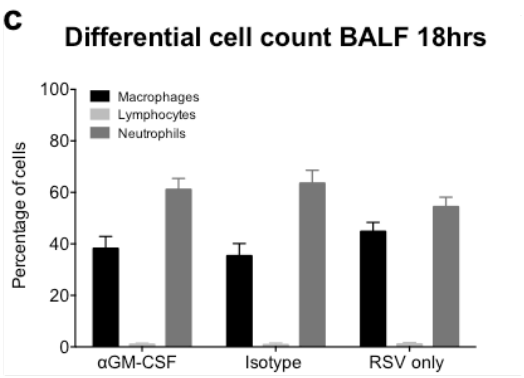
As there was no difference between αGM-CSF and isotype treated mice, and because GM-CSF gene expression is detected in ATII epithelial cells extremely early on post infection and declines rapidly straight after, the early effects of more frequent and concentrated GM-CSF antibody treatment was determined. Mice were given 100μg of GM-CSF antibody intranasally (as previously described by (Vlahos et al. 2010)) one day before RSV infection, and 25μg intranasally at 6, 24, 48 and 72hrs post infection. Isotype and RSV only groups were again included and mice were sacrificed at 18 and 96hrs post infection.

At 18hrs post infection, viral load was similar between all three groups with more than 10^6 L gene copies detected (Fig. 5.21a). The number of BALF cells was not significantly different between the three groups, averaging at 110,000 total cells (Fig. 5.21b). Similarly, leukocyte percentages were not different with approximately 40% macrophages and 60% neutrophils in all three groups (Fig. 5.21c). At 96hrs post infection, viral load was slightly increased compared to 18hrs and was again very similar in all groups, reaching 10^6-10^7 L gene copies (Fig. 5.21d). Total BALF cells increased in all groups at 96hrs compared to 18hrs but was not significantly different between groups, averaging 250,000 cells (Fig. 5.21e). The number of neutrophils dramatically decreased at 96hrs post infection compared to 18hrs, averaging 10% in all groups and macrophages percentages increased at 96hrs to 60-80%. Lymphocytes were observed in the BALF at 96hrs, averaging between 20-30% across the three groups, however none of these observations were significantly different between the groups (Fig. 5.21f).

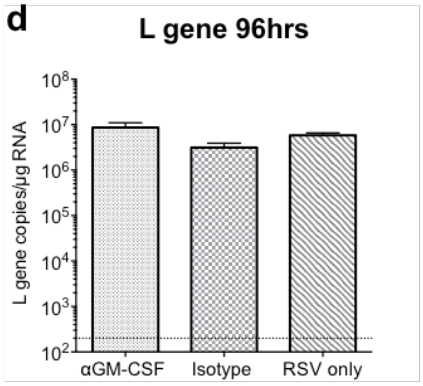
18hrs

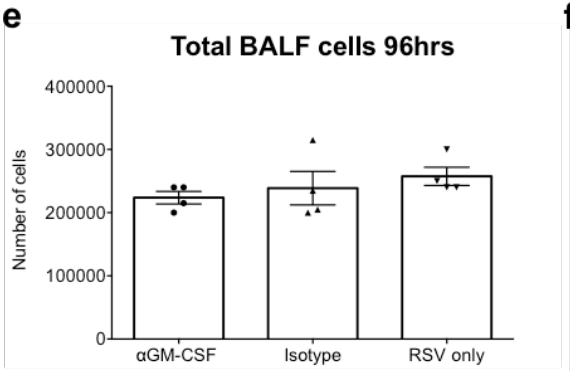

a
L gene 18hrs
L gene copies/µg RNA
10^8
10^7
10^6
10^5
10^4
10^3
10^2
αGM-CSF
Isotype
RSV only


b
Total BALF cells 18hrs
Number of cells
400000
300000
200000
100000
0
αGM-CSF
Isotype
RSV only


c
Differential cell count BALF 18hrs
Percentage of cells
100
80
60
40
20
0
Macrophages
Lymphocytes
Neutrophils
αGM-CSF
Isotype
RSV only

96hrs


d
L gene 96hrs
L gene copies/µg RNA
10^8
10^7
10^6
10^5
10^4
10^3
10^2
αGM-CSF
Isotype
RSV only


e
Total BALF cells 96hrs
Number of cells
400000
300000
200000
100000
0
αGM-CSF
Isotype
RSV only

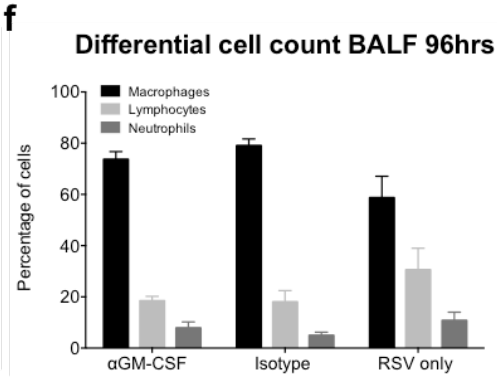

f
Differential cell count BALF 96hrs
Percentage of cells
100
80
60
40
20
0
Macrophages
Lymphocytes
Neutrophils
αGM-CSF
Isotype
RSV only

Figure 5.21: Intranasal administration of GM-CSF antibody does not significantly alter viral load or cell infiltration at 18 and 96hrs post RSV infection. C57BL/6 mice were given either 100µg of GM-CSF antibody (αGM-CSF: clone MP1-22E9) or isotype antibody (IgG2a, clone 2A3) intranasally one day before RSV infection (day -1) and 25µg intranasally at 6, 24, 48 and 72hrs post RSV infection. An RSV only group that received only RSV was also included. Mice were infected with $1.5x10^6$ FFUs of RSV intranasally. Mice were euthanized at 18hrs (a-c) and 96hrs (d-f) post RSV infection. Viral load was determined via quantification of RSV L gene in lungs via RT-qPCR using a plasmid standard, with lower detection limit represented as a dashed line (a/d). Total cell number (b/e) and the percentages of macrophages, lymphocytes and neutrophils (c/f) in BALF were also determined. Data show one experiment with 4-5 mice per group, per time point. Results are presented as mean ± SEM. Statistical significance was determined using and one-way ANOVA with Tukey's post hoc test.

As no significant differences in viral load and cell infiltration were detected between the αGM-CSF treated and RSV only mice at either time point during infection (Fig. 2), the levels of different soluble mediators in the lung between the groups were investigated. BALF from all three groups at both 18 and 96hrs post infection were analysed using ELISA for CCL2, CXCL1, CXCL10 and IL-6. Albumin levels were also measured to observe any changes to epithelial barrier integrity. To ensure neutralisation of GM-CSF in the lung by the GM-CSF antibody, GM-CSF levels in the BALF were also measured.

The results revealed that although there was a trend toward less GM-CSF detected in the BALF of GM-CSF antibody treated mice, this was not significantly different to RSV only or isotype control treated mice (Fig. 5.22). This suggested that there was not complete neutralisation of GM-CSF in the lungs of GM-CSF antibody treated mice. Further BALF analysis revealed that there were higher levels of CCL2, CXCL1, CXCL10 and IL-6 at 18hrs compared to 96hrs in all three groups, with minimal to no production at 96hrs. However, levels of these proteins were not significantly different between groups at 18hrs (Fig. 5.22). Albumin was detected at high concentrations at 18hrs with similar levels between the groups at approximately 10mg/ml and this decreased to 3-5mg/ml at 96hrs, with a trend towards less in the αGM-CSF treated mice (Fig. 5.22).

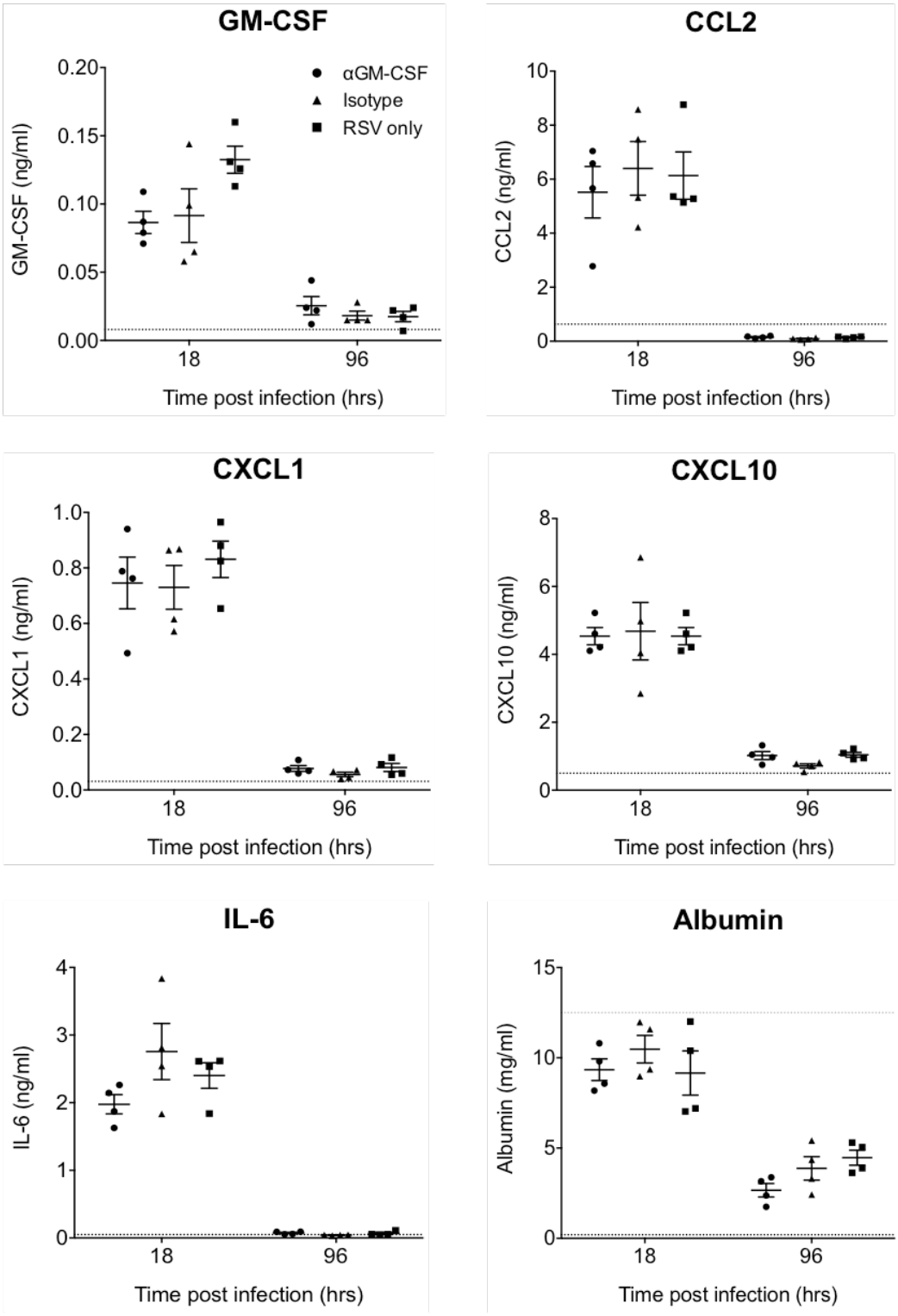


Figure 5.22: Protein analysis of BALF at 18 and 96hrs post RSV infection after intranasal GM-CSF antibody administration. GM-CSF, CCL2, CXCL1, CXCL10, IL-6 and albumin protein levels were determined in BALF via ELISA in αGM-CSF treated, isotype treated and RSV only groups at 18 and 96hrs post RSV infection. Black and grey dashed lines represent lower and upper detection limits respectively. Results are presented as mean ± SEM. Statistical significance was determined using and one-way ANOVA with Tukey's post hoc test.

5.5.2 Combined intraperitoneal and intranasal administration of GM-CSF antibody leads to significant weight loss and increased viral load during RSV infection

The data so far has shown that administration of GM-CSF antibody intranasally does not fully neutralise all the GM-CSF in the lung, therefore the dosing regime was modified. We decided to give a higher initial dose of GM-CSF antibody intraperitoneally at day -1 (as previously described by (Deepe et al. 1999, Lenzo et al. 2012)). This increased initial dose was expected to better neutralise GM-CSF, and was given intraperitoneally to avoid introducing too much protein into the lung, which may effect the establishment of RSV infection itself. Mice were given 400μg of GM-CSF antibody intraperitoneally one day before RSV infection, followed by two 25μg intranasal doses at 6 and 24hrs post infection. Mice were weighed daily for 9 days to determine weight loss and lungs and BALF taken at day 10 post infection to measure viral lung load and cell infiltration.

The data revealed that strikingly, mice receiving the combined αGM-CSF dosing had significantly more weight loss than isotype treated and RSV only mice, reaching 85% of their original weight compared to 93% in isotype treated and RSV only mice, at day 6, the day of peak weight loss (Fig. 5.23a). Interestingly, there was also significantly more weight loss in the αGM-CSF treated mice compared to RSV only group already at day 1 post RSV infection and again at day 4 which continued on to day 6 (Fig. 5.23a). Furthermore, αGM-CSF treated mice still had not returned to their original weight at day 9, whilst both the isotype treated and RSV only group did. Isotype treated mice remained at similar weight to RSV only mice throughout the time course, supporting the notion that GM-CSF antibody treatment was the cause of the weight loss (Fig. 5.23a). Viral load was also significantly higher in αGM-CSF treated mice with twice as many RSV L gene copies compared to isotype treated and RSV only mice which had almost identical levels at day 10 post infection (Fig. 5.23b). Cell infiltration into the lung was not different between the three groups with total BALF cells averaging around 250,000 cells (Fig. 5.23c) and leukocyte populations similar with 80-90% macrophages and 10-20% lymphocytes at day 10 (Fig. 5.23d). Total protein

analysis on BALF revealed there was significantly more protein in the airways of αGM-CSF treated mice compared to isotype control treated and RSV only mice, suggestive of more permeable lung tissue (Fig. 5.23e).

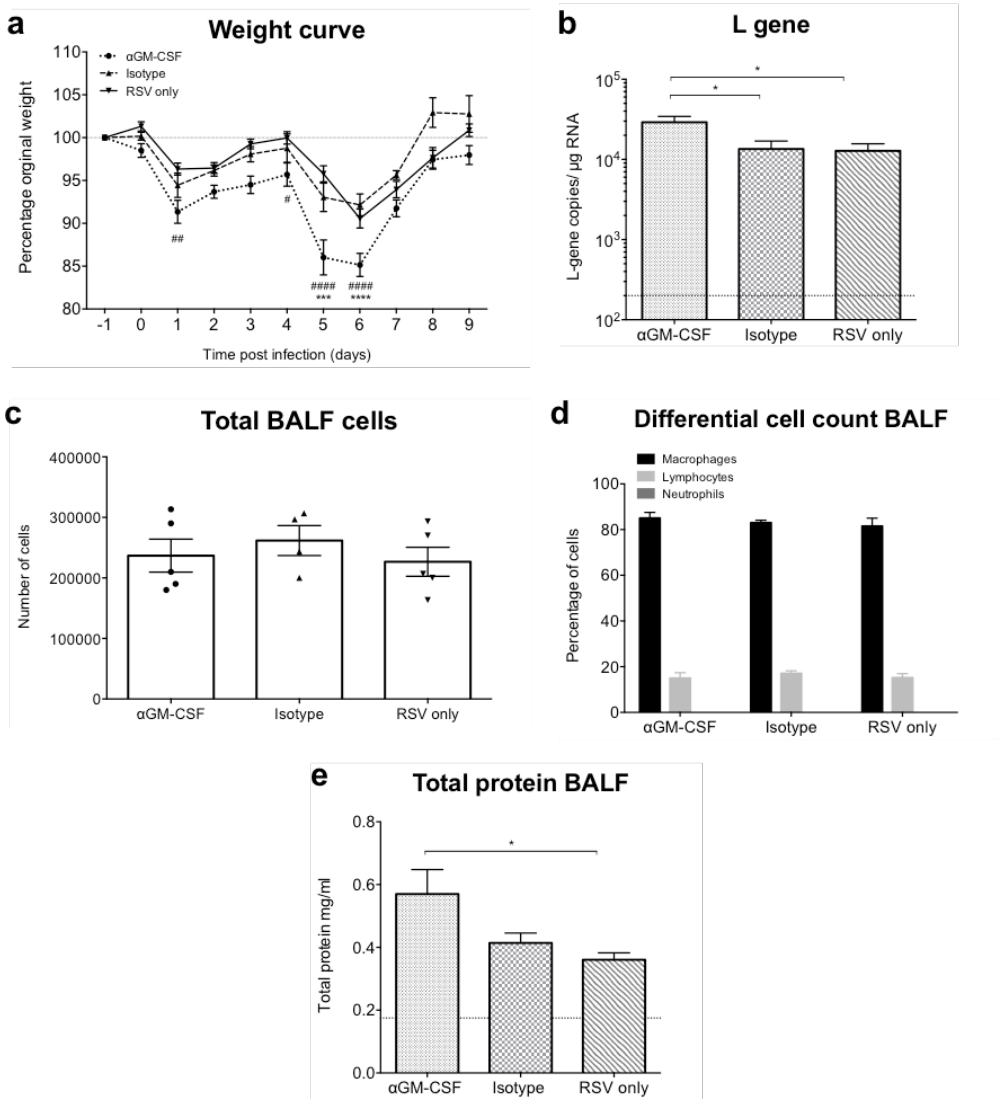


Figure 5.23: Combined intraperitoneal and intranasal GM-CSF antibody treatment during RSV infection results in increased weight loss and viral load. C57BL/6 mice were given either 400µg of GM-CSF antibody (αGM-CSF: clone MP1-22E9) or isotype antibody (IgG2a, clone 2A3) intraperitoneally one day before RSV infection (day -1) and 25µg intranasally at 6 and 24hrs post infection. An RSV only group that received only RSV was also included. Mice were infected with $1.5x10^6$ FFUs of RSV intranasally. Weight was monitored daily and plotted as percentage of original weight with dashed line representing original weight at day -1 (a). Mice were euthanised at day 10 post RSV infection. Viral load was determined via quantification of RSV L gene in lungs via RT-qPCR using a plasmid standard with lower detection limit represented as a dashed line (b). Total cell number (c) and the percentages of macrophages, lymphocytes and neutrophils (d) in BALF were also determined. Total BALF protein levels were determined was calculated via Bradford assay (e). Data shows one experiment with 4-5 mice per group. Results are presented as mean ± SEM. Statistical significance was determined using two-way ANOVA with Bonferonni's post hoc test (a) with significance between αGM-CSF and RSV represented as "#" and between αGM-CSF and isotype as "*"; and one-way ANOVA with Tukey's post hoc test (b-d). . ** p≤0.05, ** p≤0.01, *** p≤0.001, **** p≤0.0001.*

5.5.3 Summary

GM-CSF is a growth factor originally discovered to simulate the proliferation of granulocytes and macrophages from BM precursor cells (Burgess et al. 1977). Since its discovery it is now recognised to have numerous roles on AMs and DCs, including enhancing cytokine production, phagocytosis and antigen presentation (Morrissey et al. 1987, Berclaz et al. 2002, Gomez-Cambronero et al. 2003, Fleetwood et al. 2007). As such, GM-CSF deficient mice have increased susceptibility to lung infections (Seymour et al. 1997, LeVine et al. 1999) and abnormalities in the turnover of pulmonary surfactant, a role performed by AMs, that leads to accumulation of surfactant into the alveoli and to pathology similar to alveolar proteinosis (Dranoff et al. 1994). Indeed, studies have shown that when treated with recombinant GM-CSF, mice can survive lethal bacterial infection (Steinwede et al. 2011), IAV infection (Huang et al. 2010, 2011) and reverse alveolar proteinosis-like disease in GM-CSF deficient mice (Shibata et al. 2001). GM-CSF is also important for maintaining the alveolar epithelial barrier during injury (Christensen et al. 2000, Paine et al. 2003, Beck et al. 2009, Cakarova et al. 2009, Unkel et al. 2012) with survival from adult respiratory distress syndrome correlating with increased levels of BALF GM-CSF (Matute-Bello et al. 2000). Furthermore, mice infected with RSV expressing GM-CSF have reduced viral load and increased numbers of AMs and DCs (Bukreyev et al. 2001). However, the role of physiological GM-CSF produced in the lung during RSV infection has not been investigated.

In this study, combined intraperitoneal and intranasal administration of GM-CSF antibody results in increased weight loss and viral load in mice during RSV infection, suggesting GM-CSF has important effects on disease severity and viral clearance (Fig. 5.23). This supports the findings which showed mice infected with RSV-GMCSF had significantly reduced viral load compared to wildtype virus infection (Bukreyev et al. 2001). The level of GM-CSF neutralisation in the lung using the combined dosing regime was not ascertained in our study and would be important to determine in order to confirm complete neutralisation.

However, as isotype control treated mice behaved similarly to RSV only mice, this strongly suggests that the increased weight loss and viral load was due to the effect of the neutralising GM-CSF antibodies. Administration of GM-CSF antibodies intranasally alone has unclear effects as it behaves very similar to isotype antibody suggesting that pre-instillation of lungs with antibody/protein may have an effect on the development of infection (Fig. 5.20-22).

One of the major deficiencies from the lack of GM-CSF is the impaired function of AMs and DCs, which include reduced phagocytosis, activation, antigen presentation and TLR expression (Paine et al. 2001, Shibata et al. 2001, Unkel et al. 2012). Functional studies on AMs and DCs were not carried out in this study, however it could be speculated that the increased disease severity and viral load observed in αGM-CSF treated mice could be a result of subpar AMs and DCs that cannot efficiently phagocytose virus and present viral antigens to T cells. Indeed mice infected with RSV-GMCSF had increased numbers of AMs and DCs with increased MHC-II on the latter suggesting enhanced activation, and mice also have increased numbers of IFN-γ $CD4^+$ T cells (Bukreyev et al. 2001). Furthermore in IAV studies, ATII epithelial cell-derived GM-CSF mediates recovery from IAV infection by inducing the recruitment and sufficient activation of DCs and for their migration to lymph nodes (Unkel et al. 2012). Thus, the significant weight loss seen in our study from αGM-CSF treated mice and the significantly increased viral load, even at day 10, suggests that there could be inefficient T cell activation and recruitment needed to completely clear the virus, and this is in turn due to lack of activation and maturation of AMs and DCs from neutralisation of GM-CSF. Analysis of AM and DC activation as well as T cell recruitment into the lungs of αGM-CSF treated mice would confirm these speculations.

Another facet of why there is increased severity of illness seen in GM-CSF antibody treated mice is that in addition to activating DCs and AMs. GM-CSF can also induce AMs to secrete further mediators that induce alveolar epithelial cell activity during infection. Co-culture studies have shown that the expression of GM-CSF from ATII epithelial cells is dependent on AM-derived TNF-α, and this

elicited proliferation of epithelial cells in an autocrine manner (Cakarova et al. 2009). Furthermore, GM-CSF deficient ATII epithelial cells did not proliferate in response to TNF-α. Neutralisation of TNF-α in the lung led to impaired alveolar epithelial cell proliferation in LPS-injured mice and GM-CSF deficient mice showed decreased alveolar epithelial cell proliferation and continued alveolar barrier dysfunction after LPS treatment (Cakarova et al. 2009). Thus, as well as activating AMs to be more phagocytic, GM-CSF is needed to induce AM production of proinflammatory cytokines that are needed for more robust response from ATII epithelial cells to limit viral spread and immunopathology through loss of barrier integrity.

GM-CSF also exerts beneficial effects on the lung epithelium. Alveolar-derived GM-CSF has been shown to be vital in mediating epithelial cell proliferation in inflammatory and hyperoxic lung injury, and crucial for repair and restoration of lung barrier function (Paine et al. 2003, Cakarova et al. 2009, Unkel et al. 2012) Although albumin levels were not quantified, mice treated with GM-CSF antibody via the combined dosing route have increased total protein in the airways compared to isotype treated and RSV only mice, suggesting a more permeable epithelial barrier and increased alveolar injury. Increased albumin leakage and alveolar apoptosis is seen in GM-CSF deficient mice and less leakage and apoptosis in ATII epithelial cells is seen in mice overexpressing GM-CSF in ATII epithelial cells during IAV infection compared to wildtype mice (Unkel et al. 2012). This demonstrates that GM-CSF is critical for repair and restoration of epithelial cells and maintaining a tight epithelial barrier. Similarly, mice overexpressing GM-CSF in ATII epithelial cells are also protected from hyperoxic lung injury, having less alveolar wall apoptosis and decreased albumin in the BALF compared to wildtype mice (Paine et al. 2003). Thus, it could be speculated that the increase in disease severity and viral load in the αGM-CSF treated mice in our study could also be due to loss of epithelial barrier integrity provided by GM-CSF. Measuring albumin leakage in to the airways and markers of apoptosis such as annexin V on ATII epithelial cells would reveal this.

Altogether the preliminary findings from this study suggest that the ATII epithelial derived-GM-CSF is a vital mediator for limiting severity of illness and viral clearance during RSV infection. Evidence from previous studies support this notion, and further suggest it is in particular, the GM-CSF dependent cross-talk between alveolar epithelial cells, AMs and DCs may be a crucial mechanism for this increased protection. Thus based on these beneficial effects, therapeutic administration of GM-CSF might be considered to increase the phagocyte-mediated innate immune response and accelerate epithelial barrier repair processes during infection.

6 Conclusions

Respiratory syncytial virus (RSV) is major cause of upper respiratory tract infections, also known as a cold, as well as the most frequent cause of lower respiratory tract infections (LRTI) in infants. It is also a significant cause of morbidity and mortality in the elderly and immunocompromised. LRTI is most commonly manifested as bronchiolitis or viral pneumonia and risk factors such as preterm birth, chronic lung disease and congenital or acquired immunodeficiencies have been linked to RSV-induced LRTI (Borchers et al. 2013). In addition, genetic polymorphisms in innate immune genes have also been associated with severe RSV disease (Awomoyi et al. 2007, Janssen et al. 2007, Miyairi and DeVincenzo 2008). There are currently no vaccines or effective immunotherapies for RSV-induced LRTI, and treatment is limited to palliative care (Borchers et al. 2013).

During the early stages of virus infection in the lung, cells release soluble mediators such as type I IFNs, cytokines, chemokines and growth factors to clear the virus and repair tissue damage caused during infection. The most common mediators detected in the airways of RSV-infected children include monocyte, neutrophil and T cell chemokines CCL2, CCL5, CXCL8 and CXCL10 (Sheeran et al. 1999, Garofalo et al. 2001, McNamara et al. 2005) and proinflammatory cytokines and IFNs such as TNF-α, IL-1β, IL-6, IL-33 and IFN-α (Hornsleth et al. 1998, Sheeran et al. 1999, Garofalo et al. 2001, McNamara et al. 2005, Tabarani et al. 2013, Saravia et al. 2015). These mediators have also been detected *in vivo* in mice, along with additional type I IFNs and the growth factors GM-CSF and amphiregulin, and further experimentation has shown many of them to be critical in viral clearance and reducing disease severity (Bukreyev et al. 2001, Guerrero-Plata et al. 2005, Monick et al. 2005, Bhoj et al. 2008, Lindell et al. 2008, Goritzka, Makris, et al. 2015, Goritzka, Pereira, et al. 2015). These mediators initiate many important functions during viral infection of the lung including recruitment, activation and proliferation of immune cells such as monocytes, macrophages, neutrophils and T cells, induction of an antiviral state in cells and the surrounding environment, and the repair and restoration of the

lung epithelial barrier. Only recently were AMs shown to be the major source of type I IFNs during RSV infection in mice (Goritzka, Makris, et al. 2015), and IL-33 detected from ATII epithelial cells, AMs and DCs (Qi et al. 2015, Saravia et al. 2015). However, the cellular source of these other mediators during RSV infection *in vivo* has not been identified and would be important to determine in order to characterise the key players in response to RSV infection and how they could be modulated for potential therapeutics.

Stromal cells are the structural and connective tissue cells of an organ, and in the lung include epithelial cells, endothelial cells, fibroblasts, pericytes and smooth muscle cells (SMCs). It is slowly emerging that these cells can produce soluble mediators that can determine the quantity and quality of the immune response during infection (Perros et al. 2011). Lung stromal cells are notoriously difficult to study *in vivo* and therefore most studies have investigated their function using cell lines. However, these studies suffer disadvantages in not taking into account the complete lung environment and the contribution of other resident and recruited cells to the immune response and control of infection. Furthermore, they make the assumption that these cell types come into direct contact with the virus, or in the high concentrations of virus that are used in studies. This is in comparison to the situation in the lung where these cells might not meet the virus directly or in very low concentrations. The limited *in vivo* data on stromal cells have centred mainly on RSV antigen staining of lung tissue from humans and mice showing virus present in airway cells (Jewell et al. 2007, Johnson et al. 2007, Welliver et al. 2007, Bhoj et al. 2008). In addition, weak IFN-α staining in cells lining the airways of infected mice has been observed (Jewell et al. 2007) and ATII epithelial cells were more recently shown to be a source of IL-33 in mice (Saravia et al. 2015). The role of fibroblasts, endothelial cells, pericytes and SMCs in the response to RSV *in vivo* has not been demonstrated, and the relative contributions of these and other stromal cells is not known.

In this project, the role of lung stromal cells: ATII epithelial cells, endothelial cells and a mixed population termed other stromal cells, were investigated to address the question of whether stromal cells are a source of mediators that can recruit

cells and induce an antiviral and proinflammatory environment in the lung as well as express mediators that are important for maintaining barrier integrity during infection RSV *in vivo*. The data revealed that many of the soluble mediators identified in both human and mice as highly induced and/or critical to viral clearance, to be expressed by these cell types, demonstrating previously unknown potential cellular sources of these meditators. We for the first time, demonstrate their relative expression from lung cells during RSV infection, and reveal the striking division of responses between different cells of the lung. In addition, we demonstrate that expression of several of these mediators is dependent on IFNAR signalling, illustrating the cellular crosstalk between stromal cells and AMs in the lung during RSV infection, which is needed for effective viral clearance. Finally, we highlight the potential protective role of ATII epithelial cell-derived GM-CSF expression in the lung during RSV infection *in vivo*, demonstrating its capacity as a prospective target for therapeutics.

In this study we utilised dispase and fluorescence activated cell sorting (FACS) to obtain purified populations of three stromal cells subsets from mouse lung to investigate the role of stromal cells during RSV infection *in vivo*. This method was chosen as it allowed the examination of ATII epithelial cells; a stromal cell subset suggested to be highly active during respiratory infection from *in vitro* studies, as well as endothelial cells and other stromal cells at high purity. However, the drawback of this method was the loss of ATI epithelial cells, which are considered to be a major cellular target for RSV. Indeed, whilst we were able to demonstrate for the first time that the three stromal cell populations studied in this project were infected with RSV *in vivo* (Aim 1), none of the three populations (or AMs) showed significant enrichment of virus suggesting that another cell type is the main target for infection. Comparison of lung cells after dispase digestion to total lung (unprocessed) revealed significantly less virus in the former where ATI epithelial cells are known to be lost. This led us to speculate that ATI epithelial cells are the main target cells for virus infection. Both ATI and ATII epithelial cells have been shown to contain virus in children with RSV bronchiolitis (Johnson et al. 2007). However, the relative viral load in these cells has not been determined. It would be interesting to compare ATI epithelial cell

viral load to ATII epithelial cells, endothelial cells and other stromal cells as well as their contribution to expression of soluble mediators during RSV infection *in vivo*. However, difficulties in isolating ATI epithelial cells mean that comparisons could only be done using separate digestion methods in different mice. This leads to the obvious drawback of not being able to truly compare the relative contributions of the different cell types. As an alternative, lung tissue sections could be analysed via immunohistochemistry. However, separate stainings would need to be done for different mediators and lung architecture may be hard to distinguish without the additional use of markers to identify different stromal cells, which themselves have not yet been fully identified. Nevertheless, the findings from this study demonstrate RSV infection of ATII epithelial cells, endothelial cells and other stromal cells *in vivo*, indicating that virus can indeed pass beyond the alveolar epithelial barrier and infect endothelium and surrounding stromal cells, a notion which is slowly coming to light (Holgate et al. 2004, Perros et al. 2011). Whether the virus detected in stromal cells was infectious replicating virus, was not determined in this study and would be valuable to know to understand how RSV spreads in the lung, and whether stromal cells are complicit in this. However, the presence of virus in these cells demonstrates that drugs such as ribavirin, which work to limit viral replication, may be more effective if they can penetrate beyond the alveolar epithelial barrier and to the underlying stromal cells where virus is also present which may better control disease severity.

Various soluble mediators have been detected in airways of children with RSV bronchiolitis and several of these have been demonstrated to be critical for effective viral clearance and recovery from infection. However, the cellular sources of all but type I IFNs (Goritzka, Makris, et al. 2015), and until recently IL-33 (Saravia et al. 2015), have not been identified *in vivo*. In this project, initial investigation revealed that when comparing all leukocytes and all stromal cells in the lung, both leukocytes ($CD45^+$ cells) and stromal cells ($CD45^-$ cells) contribute to the expression of various mediators during the innate immune response to the virus. However surprisingly, stromal cells are the more dominant source of all the cytokines, chemokines and growths factors tested,

whilst leukocytes are the major source of type I IFNs during the early stages of infection. Deeper investigation revealed that of the three stromal cell subsets further isolated, ATII epithelial cells had a relatively small role in the expression of soluble mediators but were the major source of growth factors GM-CSF and amphiregulin, and this was during the first few hours after infection. In contrast, other stromal cells, a population shown to contain a subset of fibroblasts, expressed a vast array of chemokines as well as several proinflammatory cytokines. For example, they were the dominant source of chemokines CCL2, CXCL1 and CXCL10 during the first 18hrs of infection. Endothelial cells were much more limited in their expression of mediators, and thus had a relatively less dominant role than ATII epithelial cells and other stromal cells during RSV infection.

These findings demonstrate for the first time the relative contributions of these particular stromal cells to the inflammatory environment during RSV infection *in vivo* (Aim 2) and strongly suggest that in particular, other stromal cells can generate a very active response in the wake of infection, and are not idle cells providing only structural support. The striking division of mediators expressed by the different subsets of stromal cells also highlights the differential roles of these cell types during infection. Other stromal cells are heavily involved in the recruitment of inflammatory cells and inducing a proinflammatory state at the site of infection, whilst ATII epithelial cells are more critical for barrier repair and activation of APCs.

The other stromal cell subset was shown to contain a population of fibroblasts and *in vitro* data has demonstrated that fibroblast and ATII epithelial cell cultures can express many different mediators in response to RSV (Miller et al. 2004, Monick et al. 2005, Okabayashi et al. 2009, Ishioka et al. 2011, Seki et al. 2013). However, this has not been comprehensively shown *in vivo.* Despite the identification of fibroblasts in the mixed other stromal cell population, these cells were not separately sorted and analysed for gene expression and thus we cannot as yet, specifically allocate expression to these cells *in vivo*. However, cultures of primary RSV-exposed fibroblasts expressed all chemokines observed to be highly enriched in the other stromal cells during infection and is supported by

data from previous studies (Seki et al. 2013). This leads us to speculate that fibroblasts could be a major source of chemokines in particular, *in vivo*. Fibroblasts constitute a major cellular component of the ECM below the epithelial layer, and unlike ATII epithelial cells and endothelial cells, are motile and able to crawl through the ECM and thus potentially contact other cells and virus. Contact with the alveolar epithelium suggests that in the case where the epithelial barrier is broken and virus enters the lung, fibroblasts may potentially be one of the first cells the virus then comes into contact with and thus these cells may have an vital role in releasing proinflammatory and chemoattractant mediators in response to the virus. Alternative cell types in the other stromal cell population could be pericytes and SMCs, of which only the latter, although isolated from trachea, were shown to be permissive to RSV infection and express IL-11, a cytokine in the IL-6 family (Elias et al. 1997, Moore et al. 2006). Our study was not able to distinguish pericytes or SMCs in the other stromal cell population, and this would be ideal to fully characterise the specific cellular subsets within this mixed population and determine their specific contributions.

The relative abundance of different stromal cell populations in the lung and whether this effects which subsets are major cellular sources of a mediator was not addressed in this study. However, this is unlikely to dispute the conclusions made of the three stromal cell types investigated in this project, but rather provide support. In humans, endothelial cells make up approximately 30% of total lung cells, and the cells in the interstitial space (containing other stromal cells) approximately 37% (Crapo et al. 1982). Both other stromal cells and endothelial cells are enriched for CXCL10 during RSV infection, with the former expressing significantly higher levels than the latter, implying it is a major cellular source. However, the other stromal cells contain a mixed population of cells (like the interstitial space) and each population may not express CXCL10. Based on the results showing primary fibroblasts can express CXCL10 in response to RSV, and $CD90^+$ fibroblasts making approximately 7% of the other stromal cell population, this suggest that a much smaller proportion of the other stromal cells (and thus interstitial space) is a source of CXCL10 making them cell-for-cell a more important source than endothelial cells than originally

thought. The same can also be speculated for CXCL1 expression, which is detected from both other stromal cells and ATII epithelial cells during RSV infection, with significantly higher expression in the former. ATII epithelial cells comprise approximately 15% of total lung cells (Castranova et al. 1988), and drawing on the same reasoning as described above, would again suggest that fibroblasts may be a much more dominant cellular source than initially considered.

One of the most exciting and novel findings from our study was the identification of CCL2 expression in other stromal cells during the early stages of RSV infection *in vivo*. Previous work from our group has demonstrated the crucial role of AM-derived type I IFNs in recruiting inflammatory monocytes via CCL2 for effective clearance of RSV. However, the source of CCL2 was not elucidated (Goritzka, Makris, et al. 2015). In this work we found that CCL2 expression is highly induced in the other stromal cells, and IFNAR1 BM chimeras demonstrated that this expression is partly dependent on IFNAR signalling (Aim 3). These data suggest that type I IFNs from AMs induces a robust CCL2 response from the other stromal cells that is needed for recruitment of effective antiviral inflammatory cells. This unexpected crosstalk of AMs and cells such as fibroblasts during infection, demonstrates that stromal cells can interact with immune cells and provide critical mediators required for a robust host immune response. This has been suggested in other infection models such as in the mouse model of HSV-1 infection in the cornea, where radioresistant stromal cells were shown to be the source of CCL2 required for the recruitment of inflammatory monocytes needed to clear the virus (Conrady et al. 2013). This provides further proof that stromal cells can actively contribute to restricting viral spread and potentially direct immune responses.

As one of the first cells to come into contact with the virus, lung epithelial cells have always conventionally been regarded as one of the most important initiators of the immune response due to detection of virus in cells lining the airway, and *in vitro* data demonstrating moderate type I IFN production from these cells that is regarded as a vital mechanism for initiation of effective anti-

viral responses. This study reveals that ATII epithelial cells are not a major source of type I IFNs *in vivo,* as previously proposed from work using ATII epithelial cell lines. Instead, this role has been attributed to AMs which were shown in this study to express significantly higher levels of type I IFNs than ATII epithelial cells and other stromal cell subsets and is further supported by dedicated AM studies (Goritzka, Makris, et al. 2015). It is still possible for other types of epithelial cells in the lung to express type I IFNs, such as ATI, bronchial and tracheal epithelial cells. However, the lack of robust type I IFN production from ATII epithelial cells *in vivo* could be due to the antagonistic effects of the RSV NS proteins on the IFN signalling pathway (Swedan et al. 2009, Boyapalle et al. 2012), as RSV lacking the NS proteins induce higher levels of type I IFNs in epithelial cells than wildtype virus (Spann et al. 2004). This will most likely also happen in other epithelial cells as they are unlikely to induce abortive replication of RSV that occurs in AMs which might be what allows them to express type I IFNs robustly (Ravi et al. 2013). Thus in light of our findings, it would now be important to consider that to enhance antiviral activity via IFNs during RSV infection, AMs would be the prime target for robust expression. However, it may also be worth considering ways in which to increase type I IFN production from stromal cells, such as drugs that can interfere with NS protein expression or function, as this may help to limit virus infection seen in these cells.

ATII epithelial cells were shown to be a major source of GM-CSF: an activator of DCs and AMs, as well as potent growth factor for AMs and alveolar epithelial cells. In this study, combined intraperitoneal and intranasal administration of GM-CSF antibody into mice led to increased disease severity and viral load during RSV infection, suggesting that GM-CSF has a critical role in limiting disease and viral burden (Aim 4). This is supported by studies using GM-CSF expressing RSV (Bukreyev et al. 2001) and GM-CSF knockout and overexpressing mice in different infection models (Huang et al. 2010, 2011, Steinwede et al. 2011, Unkel et al. 2012). Whilst we were not able to determine the mechanism of protection conferred by GM-CSF in this study, increased protein in the airways of αGM-CSF treated mice suggested that mice had more permeable lungs and possible increased alveolar epithelial damage. Increased alveolar injury and lung

permeability is seen in GM-CSF deficient mice and the converse in mice overexpressing GM-CSF in ATII epithelial cells during IAV infection and hyperoxic lung injury (Paine et al. 2003, Unkel et al. 2012). This demonstrates that GM-CSF is critical for repair and restoration of epithelial cells and maintaining of a tight epithelial barrier. If this is indeed the case in our study, this implies that ATII-epithelial derived GM-CSF could be a vital stromal cell mediator required for limiting lung injury during RSV infection. Histology of lung sections from αGM-CSF treated mice could be used to confirm this.

An alternative mechanism for the protection provided by GM-CSF is provided by studies that demonstrate the ability of GM-CSF to stimulate and activate AMs for efficient phagocytosis, and enhance DCs function for more efficient antigen presentation to T cells and their subsequent migration to the lung to clear virus in both RSV and IAV infection (Bukreyev et al. 2001, Unkel et al. 2012). Functional studies on AMs, DCs and T cells were not performed in our study. However, if they were shown to be as described in previous studies, this would demonstrate that ATII epithelial cells are critical not only for lung repair during injury and inflammation, but also for the efficient activation and induction of both the innate and adaptive response to RSV infection. Thus, it would be wise to consider ways in which to protect and boost the activity of ATII epithelial cells during RSV infection or to administer GM-CSF therapeutically, to prevent more severe disease.

The findings from this study begin to fill in the missing gaps on the cellular sources of soluble mediators detected during RSV infection in *vivo* and demonstrate for the first time the striking contribution of stromal cells to the inflammatory environment during infection. Based on these discoveries, we put forward the following hypothetical crosstalk between stromal cells and immune cells for effective clearance of RSV and restoration of lung barrier integrity (Fig. 6.1). RSV enters the lung and comes into contact with the epithelial barrier. ATII epithelial cells in response to detection and/or infection of the virus induce expression of GM-CSF, IL-33 and amphiregulin. AMs also resident in the lung come into contact with the virus and start to initiate the type I IFN response as well as a proinflammatory response. GM-CSF expressed by ATII epithelial

enhances activation of AMs and antigen presentation by DCs and allows migration to the lymph nodes and activation of T cells. Expression of type I IFNs from AMs induces an antiviral state in surrounding cells and stimulates stromal cells such as fibroblasts to express chemokines such as CCL2 and CXCL10. Production of CCL2 leads to the recruitment of inflammatory monocytes to the site of infection and effective antiviral response that helps in the clearing of the virus. GM-CSF also induces the repair and restoration of dead and damaged alveolar epithelial cells to maintain lung barrier integrity and prevent further spread of the virus.

RSV is a major health burden, affecting millions of people every year. Despite its prevalence, little is known about the host response to disease. Understanding which cells are involved during infection, and their contribution to the immune response is critical to understand what provides protection from more severe disease. In particular, the role of stromal cells which make up the lung, would be important to understand as they could constitute a potentially major resident cellular source of mediators for effective viral clearance and tissue repair. The data from this study have begun to identify some key stromal cell types during RSV infection, as well as important mediators expressed from these cells. These data not only provide further clues on how the host responds to infection, but also identifies and highlights new targets, which could be modulated for potential therapeutic benefits.

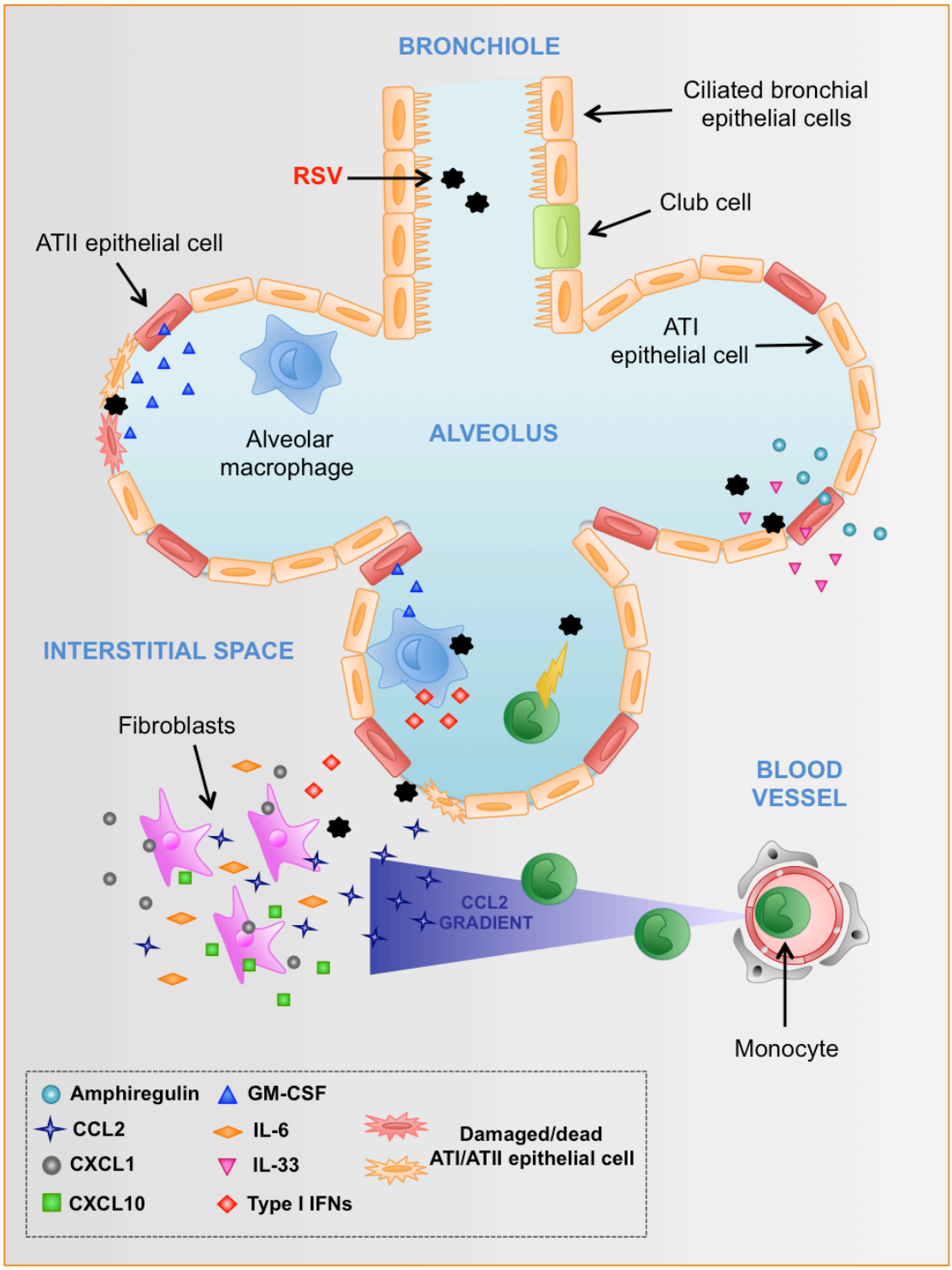


Figure 6.1: Early responses and crosstalk in the lower airway during RSV infection *in vivo*. RSV infection of the lower airway induces the expression of GM-CSF, amphiregulin and IL-33 from ATII epithelial cells and type I IFNs from AMs. GM-CSF can enhance activation of AMs and repair and restore dead and damaged alveolar epithelial cells. Type I IFNs from AMs induce an antiviral state and stimulate stromal cells such as fibroblasts to express chemokines CCL2 and CXCL10. CCL2 induces the recruitment of inflammatory monocytes from the blood to the site of infection via a CCL2 gradient. These monocytes restrict viral replication and spread.

7 Future directions

Complete characterisation and gene expression analysis of other stromal cells

Other stromal cells are a mixed population of non-endothelial non-epithelial stromal cells. Whilst we were able to identify a subpopulation of $CD90^+$ fibroblasts within this group of cells, the identity of the $CD90^-$ cells is not clear and needs to be characterised further. Potential markers include the proteoglycan NG2 for pericytes and α-SMA for smooth muscle cells. The relative contribution of the different identified subpopulations to chemokine and cytokine production also needs to be ascertained to determine whether a particular population has a more dominant role in the recruitment of inflammatory cells and/or induction of a proinflammatory state. Also, additional measurement of these inflammatory mediators at protein level would confirm translation of mRNA into functional protein. As an alternative to flow cytometry and sorting analysis of these cells, lung sections could also be analysed via immunohistochemistry, which would allow us to see exactly where these cells are located in the lung.

Fibroblast-specific knockout for CCL2

The data from this study revealed a potential major cellular source of CCL2, which previous work demonstrated was critical for infiltration of inflammatory monocytes to clear virus. Although a fibroblast-specific marker that is not present in other types of stromal cells has yet to be identified, a mouse in which CCL2 expression is deficient in fibroblasts would enable us to determine if recruitment of monocytes is totally dependent on CCL2 expression from fibroblasts during RSV infection.

Role of stromal cells during the adaptive immune response

This study concentrated on the roles of stromal cells during the innate immune response to RSV and thus it would be interesting to study if these cells also have an important role during the later stages of infection, especially in the T cells and

B cell responses. Mediators expressed past 96hrs and all the way to resolution of infection could be examined, and the effect of neutralisation of these mediators on T and B cell recruitment and function could be determined.

Contribution of ATI, bronchiolar, tracheal and "non-classical" ATII epithelial cells

The role of other types of epithelial cells in the immune response to RSV infection *in vivo* could be investigated and compared to the ATII epithelial subset investigated so far in this study. However, all three require dedicated processing enzymes and methods meaning that each different population of cells would have to be obtained from different mice. Nonetheless, a comparison of all possible epithelial cells in the lung would allow us to determine the main target for RSV infection and whether epithelial cells in the upper and lower airways differ in their ability to control virus spread and mediate an immune response. Again, immunohistochemistry could be utilised as an alternative, and would allow visual analysis of the spread of virus in these cells to determine how infection develops on the lung.

PRRs used by stromal cells during RSV infection *in vivo*

Whilst we were able to show that expression of certain mediators from stromal cells is dependent on IFNAR signalling, the mechanism in which these cells detect virus and subsequently signal to induce the expression of mediators was not examined. Previous work from this group has shown mice deficient in the PRR adaptor molecules MAVS, MyD88 and TRIF have a highly attenuated production of mediators during infection (Goritzka, Makris, et al. 2015, Goritzka, Pereira, et al. 2015). These knockout mice could be used to determine which PRRs are required on stromal cells for expression of mediators from these cells, or whether these cells do not actually require sensing of virus via PRRs and instead get signals from other infected cells such as type I IFNs from AMs for expression of mediators.

Mechanism of GM-CSF protection

How GM-CSF antibodies caused the increased disease severity and viral load in GM-CSF antibody treated mice was not determined and would be important to confirm. Firstly, the initial experiments would have to be repeated and the neutralisation of GM-CSF confirmed. AM, DC and T cells responses could then be characterised to reveal the effect on both the innate and adaptive immune response. The effect on lung barrier function could be determined using markers for apoptosis and using histology to determine lung injury. In addition, converse experiments could be performed in which recombinant GM-CSF is introduced into the lung of mice to see if this reduces viral load and disease severity.

Neutralisation of additional stromal cell-derived mediators

The contribution of the other mediators highly expressed by stromal cells during RSV infection *in vivo* could be determined by neutralising these in the lung similarly to the work shown here using GM-CSF.

Analysis in neonatal/elderly mice

As RSV infection and disease is more severe in the young and elderly, stromal cells could also be analysed in neonatal and elderly mice to see if there are any changes in the expression of mediators from stromal cells that may explain why these groups are more at risk to develop severe disease during RSV infection.

Human stromal cells

Lower airway studies in humans are difficult due to sampling restrictions; nonetheless, it would of course be very interesting to analyse stromal cells during RSV infection in humans. Bronchial brushings and biopsies are regularly taken during experimental infection studies, and these samples, albeit small and limited, could potentially be analysed by flow cytometry for soluble mediator expression for stromal cells in the upper airway. Again, immunohistochemistry could also be used for lung biopsies.

Comparison to other respiratory viruses

It would be interesting to compare the role of stromal cells during different types of respiratory virus infections such as IAV and RV to observe whether different viruses affect stromal cells in different ways and whether this has an impact on the outcome of the infection.

8 Bibliography

Akamatsu, T., Arai, Y., Kosugi, I., Kawasaki, H., Meguro, S., Sakao, M., Shibata, K., Suda, T., Chida, K., and Iwashita, T., 2013. Direct isolation of myofibroblasts and fibroblasts from bleomycin-injured lungs reveals their functional similarities and differences. *Fibrogenesis & tissue repair*, 6 (1), 1-17.

Akdis, M., Burgler, S., Crameri, R., Eiwegger, T., Fujita, H., Gomez, E., Klunker, S., Meyer, N., O'Mahony, L., Palomares, O., Rhyner, C., Ouaked, N., Quaked, N., Schaffartzik, A., Van De Veen, W., Zeller, S., Zimmermann, M., and Akdis, C. A., 2011. Interleukins, from 1 to 37, and interferon-γ: receptors, functions, and roles in diseases. *The Journal of allergy and clinical immunology*, 127 (3), 701–721.

Albrecht, M., Arnhold, M., Lingner, S., Mahapatra, S., Bruder, D., Hansen, G., and Dittrich, A.-M., 2012. IL-4 attenuates pulmonary epithelial cell-mediated suppression of T cell priming. *PloS one*, 7 (9), 1-10.

Alcendor, D. J., Charest, A. M., Zhu, W. Q., Vigil, H. E., and Knobel, S. M., 2012. Infection and upregulation of proinflammatory cytokines in human brain vascular pericytes by human cytomegalovirus. *Journal of neuroinflammation*, 9 (95), 1-16.

Alwan, W. H., Record, F. M., and Openshaw, P. J., 1992. CD4+ T cells clear virus but augment disease in mice infected with respiratory syncytial virus. Comparison with the effects of CD8+ T cells. *Clinical and experimental immunology*, 88 (3), 527–536.

Aoki, Y., Qiu, D., Uyei, A., and Kao, P. N., 1997. Human airway epithelial cells express interleukin-2 in vitro. *The American journal of physiology*, 272 (2 Pt 1), L276–86.

Armulik, A., Abramsson, A., and Betsholtz, C., 2005. Endothelial/pericyte interactions. *Circulation research*, 97 (6), 512–523.

Armulik, A., Genové, G., and Betsholtz, C., 2011. Pericytes: developmental, physiological, and pathological perspectives, problems, and promises. *Developmental cell*, 21 (2), 193–215.

Arnold, R. and König, W., 2005. Respiratory syncytial virus infection of human lung endothelial cells enhances selectively intercellular adhesion molecule-1 expression. *Journal of immunology*, 174 (11), 7359–7367.

Au, W. C., Moore, P. A., Lowther, W., Juang, Y. T., and Pitha, P. M., 1995. Identification of a member of the interferon regulatory factor family that binds to the interferon-stimulated response element and activates expression of interferon-induced genes. *Proceedings of the National Academy of Sciences*, 92 (25), 11657–11661.

Aung, S., Rutigliano, J. A., and Graham, B. S., 2001. Alternative mechanisms of respiratory syncytial virus clearance in perforin knockout mice lead to enhanced disease. *Journal of virology*, 75 (20), 9918–9924.

Autengruber, A., Gereke, M., Hansen, G., Hennig, C., and Bruder, D., 2012. Impact of enzymatic tissue disintegration on the level of surface molecule expression and immune cell function. *European journal of microbiology & immunology*, 2 (2), 112–120.

Awomoyi, A. A., Rallabhandi, P., Pollin, T. I., Lorenz, E., Sztein, M. B., Boukhvalova, M. S., Hemming, V. G., Blanco, J. C. G., and Vogel, S. N., 2007. Association of

TLR4 polymorphisms with symptomatic respiratory syncytial virus infection in high-risk infants and young children. *Journal of immunology*, 179 (5), 3171–3177.

Baglole, C. J., Reddy, S. Y., Pollock, S. J., Feldon, S. E., Sime, P. J., Smith, T. J., and Phipps, R. P., 2005. Isolation and phenotypic characterization of lung fibroblasts. *Methods in molecular medicine*, 117, 115–127.

Bantikassegn, A., Song, X., and Politi, K., 2015. Isolation of epithelial, endothelial, and immune cells from lungs of transgenic mice with oncogene-induced lung adenocarcinomas. *American journal of respiratory cell and molecular biology*, 52 (4), 409–417.

Barratt, S., Medford, A. R., and Millar, A. B., 2014. Vascular endothelial growth factor in acute lung injury and acute respiratory distress syndrome. *Respiration; international review of thoracic diseases*, 87 (4), 329–342.

Bazan, J. F., Bacon, K. B., Hardiman, G., Wang, W., Soo, K., Rossi, D., Greaves, D. R., Zlotnik, A., and Schall, T. J., 1997. A new class of membrane-bound chemokine with a CX3C motif. *Nature*, 385 (6617), 640–644.

Beatty, G. L. and Paterson, Y., 2001. Regulation of tumor growth by IFN-gamma in cancer immunotherapy. *Immunologic research*, 24 (2), 201–210.

Beaty, S. R., Rose, C. E., and Sun-sang, J. S., 2007. Diverse and potent chemokine production by lung CD11bhigh dendritic cells in homeostasis and in allergic lung inflammation. *The Journal of Immunology*, 178 (3) 1882-1895

Beck, J. M., Preston, A. M., Wilcoxen, S. E., Morris, S. B., Sturrock, A., and Paine, R., 2009. Critical roles of inflammation and apoptosis in improved survival in a model of hyperoxia-induced acute lung injury in Pneumocystis murina-infected mice. *Infection and immunity*, 77 (3), 1053–1060.

Becker, S., Quay, J., and Soukup, J., 1991. Cytokine (tumor necrosis factor, IL-6, and IL-8) production by respiratory syncytial virus-infected human alveolar macrophages. *Journal of immunology*, 147 (12), 4307–4312.

Becker, Y., 2006. Respiratory syncytial virus (RSV) evades the human adaptive immune system by skewing the Th1/Th2 cytokine balance toward increased levels of Th2 cytokines and IgE, markers of allergy--a review. *Virus genes*, 33 (2), 235–252.

Bedke, N., Haitchi, H. M., Xatzipsalti, M., Holgate, S. T., and Davies, D. E., 2009. Contribution of bronchial fibroblasts to the antiviral response in asthma. *Journal of immunology*, 182 (6), 3660–3667.

Benoit, A., Huang, Y., Proctor, J., Rowden, G., and Anderson, R., 2006. Effects of alveolar macrophage depletion on liposomal vaccine protection against respiratory syncytial virus (RSV). *Clinical and experimental immunology*, 145 (1), 147–154.

Berclaz, P.-Y., Shibata, Y., Whitsett, J. A., and Trapnell, B. C., 2002. GM-CSF, via PU.1, regulates alveolar macrophage Fcgamma R-mediated phagocytosis and the IL-18/IFN-gamma -mediated molecular connection between innate and adaptive immunity in the lung. *Blood*, 100 (12), 4193–4200.

Bergeron, C., Tulic, M. K., and Hamid, Q., 2010. Airway remodelling in asthma: from benchside to clinical practice. *Canadian respiratory journal*, 17 (4), e85–93.

Bergers, G. and Song, S., 2005. The role of pericytes in blood-vessel formation and maintenance. *Neuro-oncology*, 7 (4), 452–464.

Beyer, M., Bartz, H., Hörner, K., Doths, S., Koerner-Rettberg, C., and Schwarze, J.,

2004. Sustained increases in numbers of pulmonary dendritic cells after respiratory syncytial virus infection. *The Journal of allergy and clinical immunology*, 113 (1), 127–133.

Bhoj, V. G., Sun, Q., Bhoj, E. J., Somers, C., Chen, X., Torres, J.-P., Mejias, A., Gomez, A. M., Jafri, H., Ramilo, O., and Chen, Z. J., 2008. MAVS and MyD88 are essential for innate immunity but not cytotoxic T lymphocyte response against respiratory syncytial virus. *Proceedings of the National Academy of Sciences*, 105 (37), 14046–14051.

Blanken, M. O., Rovers, M. M., Molenaar, J. M., Winkler-Seinstra, P. L., Meijer, A., Kimpen, J. L. L., Bont, L., Dutch RSV Neonatal Network, 2013. Respiratory syncytial virus and recurrent wheeze in healthy preterm infants. *The New England journal of medicine*, 368 (19), 1791–1799.

Blum, J. S., Wearsch, P. A., and Cresswell, P., 2013. Pathways of antigen processing. *Annual review of immunology*, 2013 (31), 443-473.

Boehme, K. W. and Compton, T., 2004. Innate sensing of viruses by toll-like receptors. *Journal of virology*, 78 (15), 7867–7873.

Borchers, A. T., Chang, C., Gershwin, M. E., and Gershwin, L. J., 2013. Respiratory syncytial virus--a comprehensive review. *Clinical reviews in allergy & immunology*, 45 (3), 331–379.

Boyapalle, S., Wong, T., Garay, J., Teng, M., San Juan-Vergara, H., Mohapatra, S., and Mohapatra, S., 2012. Respiratory syncytial virus NS1 protein colocalizes with mitochondrial antiviral signaling protein MAVS following infection. *PloS one*, 7 (2), 1-9.

Boyman, O. and Sprent, J., 2012. The role of interleukin-2 during homeostasis and activation of the immune system. *Nature reviews. Immunology*, 12 (3), 180–190.

Brenner, D., Blaser, H., and Mak, T. W., 2015. Regulation of tumour necrosis factor signalling: live or let die. *Nature reviews. Immunology*, 15 (6), 362–374.

Bukreyev, A., Belyakov, I. M., Berzofsky, J. A., Murphy, B. R., and Collins, P. L., 2001. Granulocyte-macrophage colony-stimulating factor expressed by recombinant respiratory syncytial virus attenuates viral replication and increases the level of pulmonary antigen-presenting cells. *Journal of virology*, 75 (24), 12128–12140.

Bukreyev, A., Whitehead, S. S., Prussin, C., Murphy, B. R., and Collins, P. L., 2000. Effect of coexpression of interleukin-2 by recombinant respiratory syncytial virus on virus replication, immunogenicity, and production of other cytokines. *Journal of virology*, 74 (15), 7151–7157.

Burgess, A. W., Camakaris, J., and Metcalf, D., 1977. Purification and properties of colony-stimulating factor from mouse lung-conditioned medium. *The Journal of biological chemistry*, 252 (6), 1998–2003.

Cakarova, L., Marsh, L. M., Wilhelm, J., Mayer, K., Grimminger, F., Seeger, W., Lohmeyer, J., and Herold, S., 2009. Macrophage tumor necrosis factor-alpha induces epithelial expression of granulocyte-macrophage colony-stimulating factor: impact on alveolar epithelial repair. *Am J Respir Crit Care Med*, 180 (6), 521–532.

Campbell-Harding, G., Sawkins, H., Bedke, N., Holgate, S. T., Davies, D. E., and Andrews, A.-L., 2013. The innate antiviral response upregulates IL-13 receptor α2 in bronchial fibroblasts. *The Journal of allergy and clinical immunology*, 131 (3), 849–855.

Cannon, M. J., Openshaw, P. J., and Askonas, B. A., 1988. Cytotoxic T cells clear virus but augment lung pathology in mice infected with respiratory syncytial virus. *The Journal of experimental medicine*, 168 (3), 1163–1168.

Carta, S., Lavieri, R., and Rubartelli, A., 2013. Different Members of the IL-1 Family Come Out in Different Ways: DAMPs vs. Cytokines? *Frontiers in immunology*, 4 (123), 1-9.

Castranova, V., Rabovsky, J., Tucker, J. H., and Miles, P. R., 1988. The alveolar type II epithelial cell: a multifunctional pneumocyte. *Toxicology and applied pharmacology*, 93 (3), 472–483.

Cervantes-Barragán, L., Kalinke, U., Züst, R., König, M., Reizis, B., López-Macías, C., Thiel, V., and Ludewig, B., 2009. Type I IFN-mediated protection of macrophages and dendritic cells secures control of murine coronavirus infection. *Journal of immunology*, 182 (2), 1099–1106.

Chan, M. C. W., Cheung, C. Y., Chui, W. H., Tsao, S. W., Nicholls, J. M., Chan, Y. O., Chan, R. W. Y., Long, H. T., Poon, L. L. M., Guan, Y., and Peiris, J. S. M., 2005. Proinflammatory cytokine responses induced by influenza A (H5N1) viruses in primary human alveolar and bronchial epithelial cells. *Respiratory research*, 6 (135), 1-13.

Chen, C.-J., Ou, Y.-C., Li, J.-R., Chang, C.-Y., Pan, H.-C., Lai, C.-Y., Liao, S.-L., Raung, S.-L., and Chang, C.-J., 2014. Infection of pericytes in vitro by Japanese encephalitis virus disrupts the integrity of the endothelial barrier. *Journal of virology*, 88 (2), 1150–1161.

Cheng, X., Park, H., Zhou, H., and Jin, H., 2005. Overexpression of the M2-2 protein of respiratory syncytial virus inhibits viral replication. *Journal of virology*, 79 (22), 13943–13952.

Cherrie, A. H., Anderson, K., Wertz, G. W., and Openshaw, P. J., 1992. Human cytotoxic T cells stimulated by antigen on dendritic cells recognize the N, SH, F, M, 22K, and 1b proteins of respiratory syncytial virus. *Journal of virology*, 66 (4), 2102–2110.

Chiaraviglio, L., Brown, D. A., and Kirby, J. E., 2008. Infection of cultured human endothelial cells by Legionella pneumophila. *PloS one*, 3 (4), 1-5.

Chipps, B. E., Sullivan, W. F., and Portnoy, J. M., 1993. Alpha-2A-interferon for treatment of bronchiolitis caused by respiratory syncytial virus. *The Pediatric infectious disease journal*, 12 (8), 653–658.

Chiu, C. and Openshaw, P. J., 2015. Antiviral B cell and T cell immunity in the lungs. *Nature immunology*, 16 (1), 18–26.

Christensen, P. J., Bailie, M. B., Goodman, R. E., O'Brien, A. D., Toews, G. B., and Paine, R., 2000. Role of diminished epithelial GM-CSF in the pathogenesis of bleomycin-induced pulmonary fibrosis. *American journal of physiology. Lung cellular and molecular physiology*, 279 (3), 487–95.

Chun, Y. H., Park, J. Y., Lee, H., Kim, H. S., Won, S., Joe, H. J., Chung, W. J., Yoon, J.-S., Kim, H. H., Kim, J. T., and Lee, J. S., 2013. Rhinovirus-Infected Epithelial Cells Produce More IL-8 and RANTES Compared With Other Respiratory Viruses. *Allergy, asthma & immunology research*, 5 (4), 216–223.

Chuquimia, O. D., Petursdottir, D. H., Periolo, N., and Fernández, C., 2013. Alveolar epithelial cells are critical in protection of the respiratory tract by secretion of factors able to modulate the activity of pulmonary macrophages and directly control bacterial growth. *Infection and immunity*, 81 (1), 381–389.

Collins, P. L. and Melero, J. A., 2011. Progress in understanding and controlling

respiratory syncytial virus: still crazy after all these years. *Virus research*, 162 (1-2), 80–99.

Conrady, C. D., Zheng, M., Mandal, N. A., van Rooijen, N., and Carr, D. J. J., 2013. IFN-α-driven CCL2 production recruits inflammatory monocytes to infection site in mice. *Mucosal immunology*, 6 (1), 45–55.

Corti, M., Brody, A. R., and Harrison, J. H., 1996. Isolation and primary culture of murine alveolar type II cells. *American journal of respiratory cell and molecular biology*, 14 (4), 309–315.

Crapo, J. D., Barry, B. E., Gehr, P., Bachofen, M., and Weibel, E. R., 1982. Cell number and cell characteristics of the normal human lung. *The American review of respiratory disease*, 126 (2), 332–337.

Crotta, S., Davidson, S., Mahlakoiv, T., Desmet, C. J., Buckwalter, M. R., Albert, M. L., Staeheli, P., and Wack, A., 2013. Type I and type III interferons drive redundant amplification loops to induce a transcriptional signature in influenza-infected airway epithelia. *PLoS pathogens*, 9 (11), 1-12.

Crystal, R. G., Randell, S. H., Engelhardt, J. F., Voynow, J., and Sunday, M. E., 2008. Airway epithelial cells: current concepts and challenges. *Proceedings of the American Thoracic Society*, 5 (7), 772–777.

Das, S., Palmer, O. P., Leight, W. D., Surowitz, J. B., Pickles, R. J., Randell, S. H., and Buchman, C. A., 2005. Cytokine amplification by respiratory syncytial virus infection in human nasal epithelial cells. *The Laryngoscope*, 115 (5), 764–768.

De Silva, D., Dagher, H., Ghildyal, R., Lindsay, M., Li, X., Freezer, N. J., Wilson, J. W., and Bardin, P. G., 2006. Vascular endothelial growth factor induction by rhinovirus infection. *Journal of medical virology*, 78 (5), 666–672.

de Weerd, N. A., Vivian, J. P., Nguyen, T. K., Mangan, N. E., Gould, J. A., Braniff, S.-J., Zaker-Tabrizi, L., Fung, K. Y., Forster, S. C., Beddoe, T., Reid, H. H., Rossjohn, J., and Hertzog, P. J., 2013. Structural basis of a unique interferon-β signaling axis mediated via the receptor IFNAR1. *Nature immunology*, 14 (9), 901–907.

De Weerd, W., Twilhaar, W. N., and Kimpen, J. L., 1998. T cell subset analysis in peripheral blood of children with RSV bronchiolitis. *Scandinavian journal of infectious diseases*, 30 (1), 77–80.

Deepe, G. S., Gibbons, R., and Woodward, E., 1999. Neutralization of endogenous granulocyte-macrophage colony-stimulating factor subverts the protective immune response to Histoplasma capsulatum. *Journal of immunology*, 163 (9), 4985–4993.

Demoor, T., Petersen, B. C., Morris, S., Mukherjee, S., Ptaschinski, C., De Almeida Nagata, D. E., Kawai, T., Ito, T., Akira, S., Kunkel, S. L., Schaller, M. A., and Lukacs, N. W., 2012. IPS-1 signaling has a nonredundant role in mediating antiviral responses and the clearance of respiratory syncytial virus. *Journal of immunology*, 189 (12), 5942–5953.

Deng, R., Lu, M., Korteweg, C., Gao, Z., McNutt, M. A., Ye, J., Zhang, T., and Gu, J., 2008. Distinctly different expression of cytokines and chemokines in the lungs of two H5N1 avian influenza patients. *The Journal of pathology*, 216 (3), 328–336.

Descalzi, D., Folli, C., Scordamaglia, F., Riccio, A. M., Gamalero, C., and Canonica, G. W., 2007. Importance of fibroblasts-myofibroblasts in asthma-induced airway remodeling. *Recent patents on inflammation & allergy drug discovery*, 1 (3), 237–241.

Diamond, R. A. and DeMaggio, S., 2012. *In Living Color*: *Protocols in Flow*

Cytometry and Cell Sorting. Springer Science & Business Media.
Doherty, T. and Broide, D., 2007. Cytokines and growth factors in airway remodeling in asthma. *Current opinion in immunology*, 19 (6), 676–680.
Dosanjh, A., Rednam, S., and Martin, M., 2003. Respiratory syncytial virus augments production of fibroblast growth factor basic in vitro: implications for a possible mechanism of prolonged wheezing after infection. *Pediatric allergy and immunology*, 14 (6), 437–440.
Dranoff, G., Crawford, A. D., Sadelain, M., Ream, B., Rashid, A., Bronson, R. T., Dickersin, G. R., Bachurski, C. J., Mark, E. L., and Whitsett, J. A., 1994. Involvement of granulocyte-macrophage colony-stimulating factor in pulmonary homeostasis. *Science,* 264 (5159), 713–716.
Duerr, C. U., McCarthy, C. D. A., Mindt, B. C., Rubio, M., Meli, A. P., Pothlichet, J., Eva, M. M., Gauchat, J.-F., Qureshi, S. T., Mazer, B. D., Mossman, K. L., Malo, D., Gamero, A. M., Vidal, S. M., King, I. L., Sarfati, M., and Fritz, J. H., 2016. Type I interferon restricts type 2 immunopathology through the regulation of group 2 innate lymphoid cells. *Nature immunology*, 17 (1), 65–75.
Durant, L. R., Makris, S., Voorburg, C. M., Loebbermann, J., Johansson, C., and Openshaw, P. J. M., 2013. Regulatory T cells prevent Th2 immune responses and pulmonary eosinophilia during respiratory syncytial virus infection in mice. *Journal of virology*, 87 (20), 10946–10954.
Durbin, R. K., Kotenko, S. V., and Durbin, J. E., 2013. Interferon induction and function at the mucosal surface. *Immunological reviews*, 255 (1), 25–39.
Einarsson, O., Geba, G. P., Zhu, Z., Landry, M., and Elias, J. A., 1996. Interleukin-11: stimulation in vivo and in vitro by respiratory viruses and induction of airways hyperresponsiveness. *The Journal of clinical investigation*, 97 (4), 915–924.
Elias, J. A., Wu, Y., Zheng, T., and Panettieri, R., 1997. Cytokine- and virus-stimulated airway smooth muscle cells produce IL-11 and other IL-6-type cytokines. *The American journal of physiology*, 273 (3 Pt 1), 648–55.
Elias, J. A., Zheng, T., Einarsson, O., Landry, M., Trow, T., Rebert, N., and Panuska, J., 1994. Epithelial interleukin-11. Regulation by cytokines, respiratory syncytial virus, and retinoic acid. *The Journal of biological chemistry*, 269 (35), 22261–22268.
Ennaciri, J., Ahmad, R., and Menezes, J., 2007. Interaction of monocytic cells with respiratory syncytial virus results in activation of NF-kappaB and PKC-alpha/beta leading to up-regulation of IL-15 gene expression. *Journal of leukocyte biology*, 81 (3), 625–631.
Everard, M. L., Swarbrick, A., Wrightham, M., McIntyre, J., Dunkley, C., James, P. D., Sewell, H. F., and Milner, A. D., 1994. Analysis of cells obtained by bronchial lavage of infants with respiratory syncytial virus infection. *Archives of disease in childhood*, 71 (5), 428–432.
Falsey, A. R., Hennessey, P. A., Formica, M. A., Cox, C., and Walsh, E. E., 2005. Respiratory syncytial virus infection in elderly and high-risk adults. *The New England journal of medicine*, 352 (17), 1749–1759.
Fehrenbach, H., 2001. Alveolar epithelial type II cell: defender of the alveolus revisited. *Respiratory research*, 2 (1), 33–46.
Feltes, T. F., Cabalka, A. K., Meissner, H. C., Piazza, F. M., Carlin, D. A., Top, F. H., Connor, E. M., Sondheimer, H. M., Cardiac Synagis Study Group, 2003. Palivizumab prophylaxis reduces hospitalization due to respiratory syncytial

virus in young children with hemodynamically significant congenital heart disease. *The Journal of pediatrics*, 143 (4), 532–540.

Fields, B. N., Knipe, D. M., and Howley, P. M., 2013. *Fields Virology*. Lippincott Williams & Wilkins.

Fleetwood, A. J., Lawrence, T., Hamilton, J. A., and Cook, A. D., 2007. Granulocyte-macrophage colony-stimulating factor (CSF) and macrophage CSF-dependent macrophage phenotypes display differences in cytokine profiles and transcription factor activities: implications for CSF blockade in inflammation. *Journal of immunology*, 178 (8), 5245–5252.

Franke, G., Freihorst, J., Steinmüller, C., Verhagen, W., Hockertz, S., and Lohmann-Matthes, M. L., 1994. Interaction of alveolar macrophages and respiratory syncytial virus. *Journal of immunological methods*, 174 (1-2), 173–184.

Franke-Ullmann, G., Pförtner, C., Walter, P., Steinmüller, C., Lohmann-Matthes, M. L., Kobzik, L., and Freihorst, J., 1995. Alteration of pulmonary macrophage function by respiratory syncytial virus infection in vitro. *Journal of immunology*, 154 (1), 268–280.

Gan, S.-W., Tan, E., Lin, X., Yu, D., Wang, J., Tan, G. M.-Y., Vararattanavech, A., Yeo, C. Y., Soon, C. H., Soong, T. W., Pervushin, K., and Torres, J., 2012. The small hydrophobic protein of the human respiratory syncytial virus forms pentameric ion channels. *The Journal of biological chemistry*, 287 (29), 24671–24689.

Garofalo, R. P., Patti, J., Hintz, K. A., Hill, V., Ogra, P. L., and Welliver, R. C., 2001. Macrophage inflammatory protein-1alpha (not T helper type 2 cytokines) is associated with severe forms of respiratory syncytial virus bronchiolitis. *The Journal of infectious diseases*, 184 (4), 393–399.

Gerhardt, T. and Ley, K., 2015. Monocyte trafficking across the vessel wall. *Cardiovascular research*, 107 (3), 321–330.

Ghildyal, R., Dagher, H., Donninger, H., De Silva, D., Li, X., Freezer, N. J., Wilson, J. W., and Bardin, P. G., 2005. Rhinovirus infects primary human airway fibroblasts and induces a neutrophil chemokine and a permeability factor. *Journal of medical virology*, 75 (4), 608–615.

Gibbs, J. D., Ornoff, D. M., Igo, H. A., Zeng, J. Y., and Imani, F., 2009. Cell cycle arrest by transforming growth factor beta1 enhances replication of respiratory syncytial virus in lung epithelial cells. *Journal of virology*, 83 (23), 12424–12431.

Gill, M. A., Palucka, A. K., Barton, T., Ghaffar, F., Jafri, H., Banchereau, J., and Ramilo, O., 2005. Mobilization of plasmacytoid and myeloid dendritic cells to mucosal sites in children with respiratory syncytial virus and other viral respiratory infections. *The Journal of infectious diseases*, 191 (7), 1105–1115.

Ginhoux, F. and Jung, S., 2014. Monocytes and macrophages: developmental pathways and tissue homeostasis. *Nature reviews. Immunology*, 14 (6), 392–404.

Glezen, W. P., Taber, L. H., Frank, A. L., and Kasel, J. A., 1986. Risk of primary infection and reinfection with respiratory syncytial virus. *American journal of diseases of children (1960)*, 140 (6), 543–546.

Gomez-Cambronero, J., Horn, J., Paul, C. C., and Baumann, M. A., 2003. Granulocyte-macrophage colony-stimulating factor is a chemoattractant cytokine for human neutrophils: involvement of the ribosomal p70 S6 kinase signaling pathway. *Journal of immunology,* 171 (12), 6846–6855.

Gonzalez, R. F. and Dobbs, L. G., 2013. Isolation and culture of alveolar epithelial Type I and Type II cells from rat lungs. *Methods in molecular biology*, 945, 145–159.

Goritzka, M., Durant, L. R., Pereira, C., Salek-Ardakani, S., Openshaw, P. J. M., and Johansson, C., 2014. Alpha/beta interferon receptor signaling amplifies early proinflammatory cytokine production in the lung during respiratory syncytial virus infection. *Journal of virology*, 88 (11), 6128–6136.

Goritzka, M., Makris, S., Kausar, F., Durant, L. R., Pereira, C., Kumagai, Y., Culley, F. J., Mack, M., Akira, S., and Johansson, C., 2015. Alveolar macrophage-derived type I interferons orchestrate innate immunity to RSV through recruitment of antiviral monocytes. *The Journal of experimental medicine*, 212 (5), 699–714.

Goritzka, M., Pereira, C., Makris, S., Durant, L. R., and Johansson, C., 2015. T cell responses are elicited against Respiratory Syncytial Virus in the absence of signalling through TLRs, RLRs and IL-1R/IL-18R. *Scientific reports*, 5, 18533.

Goubau, D., Deddouche, S., and Sousa, C. E., 2013. Cytosolic sensing of viruses. *Immunity*, 38 (5) 855-869

Goulder, P. J., Lechner, F., Klenerman, P., McIntosh, K., and Walker, B. D., 2000. Characterization of a novel respiratory syncytial virus-specific human cytotoxic T-lymphocyte epitope. *Journal of virology*, 74 (16), 7694–7697.

Graham, B. S. and Anderson, L. J., 2013. Challenges and opportunities for respiratory syncytial virus vaccines. *Current topics in microbiology and immunology*, 372, 391–404.

Graham, B. S., Bunton, L. A., Wright, P. F., and Karzon, D. T., 1991. Role of T lymphocyte subsets in the pathogenesis of primary infection and rechallenge with respiratory syncytial virus in mice. *The Journal of clinical investigation*, 88 (3), 1026–1033.

Graham, B. S., Henderson, G. S., Tang, Y. W., Lu, X., Neuzil, K. M., and Colley, D. G., 1993. Priming immunization determines T helper cytokine mRNA expression patterns in lungs of mice challenged with respiratory syncytial virus. *Journal of immunology*, 151 (4), 2032–2040.

Grandvaux, N., Guan, X., Yoboua, F., Zucchini, N., Fink, K., Doyon, P., Martin, L., Servant, M. J., and Chartier, S., 2014. Sustained activation of interferon regulatory factor 3 during infection by paramyxoviruses requires MDA5. *Journal of innate immunity*, 6 (5), 650–662.

Griffith, J. W., Sokol, C. L., and Luster, A. D., 2014. Chemokines and chemokine receptors: positioning cells for host defense and immunity. *Annual review of immunology*, 32, 659–702.

Guerrero-Plata, A., Baron, S., Poast, J. S., Adegboyega, P. A., Casola, A., and Garofalo, R. P., 2005. Activity and regulation of alpha interferon in respiratory syncytial virus and human metapneumovirus experimental infections. *Journal of virology*, 79 (16), 10190–10199.

Guilliams, M., De Kleer, I., Henri, S., Post, S., Vanhoutte, L., De Prijck, S., Deswarte, K., Malissen, B., Hammad, H., and Lambrecht, B. N., 2013. Alveolar macrophages develop from fetal monocytes that differentiate into long-lived cells in the first week of life via GM-CSF. *The Journal of experimental medicine*, 210 (10), 1977–1992.

Guo-Parke, H., Canning, P., Douglas, I., Villenave, R., Heaney, L. G., Coyle, P. V., Lyons, J. D., Shields, M. D., and Power, U. F., 2013. Relative respiratory

syncytial virus cytopathogenesis in upper and lower respiratory tract epithelium. *Am J Respir Crit Care Med*, 188 (7), 842–851.

Gürtler, C. and Bowie, A. G., 2013. Innate immune detection of microbial nucleic acids. *Trends in microbiology*, 21 (8), 413–420.

Habibi, M. S. and Openshaw, P. J. M., 2012. Benefit and harm from immunity to respiratory syncytial virus: implications for treatment. *Current opinion in infectious diseases*, 25 (6), 687–694.

Habibi, M. S., Jozwik, A., Makris, S., Dunning, J., Paras, A., DeVincenzo, J. P., de Haan, C. A. M., Wrammert, J., Openshaw, P. J. M., Chiu, C., Mechanisms of Severe Acute Influenza Consortium Investigators, 2015. Impaired Antibody-mediated Protection and Defective IgA B-Cell Memory in Experimental Infection of Adults with Respiratory Syncytial Virus. *Am J Respir Crit Care Med*, 191 (9), 1040–1049.

Haeberle, H. A., Kuziel, W. A., Dieterich, H. J., Casola, A., Gatalica, Z., and Garofalo, R. P., 2001. Inducible expression of inflammatory chemokines in respiratory syncytial virus-infected mice: role of MIP-1alpha in lung pathology. *Journal of virology*, 75 (2), 878–890.

Haeberle, H. A., Takizawa, R., Casola, A., Brasier, A. R., Dieterich, H.-J., Van Rooijen, N., Gatalica, Z., and Garofalo, R. P., 2002. Respiratory syncytial virus-induced activation of nuclear factor-kappaB in the lung involves alveolar macrophages and toll-like receptor 4-dependent pathways. *The Journal of infectious diseases*, 186 (9), 1199–1206.

Haeryfar, S. and Hoskin, D. W., 2004. Thy-1: more than a mouse pan-T cell marker. *The Journal of Immunology*, 173 (6) 3581-3588

Hall, C. B., Long, C. E., and Schnabel, K. C., 2001. Respiratory syncytial virus infections in previously healthy working adults. *Clinical infectious diseases :* 33 (6), 792–796.

Hammad, H. and Lambrecht, B. N., 2008. Dendritic cells and epithelial cells: linking innate and adaptive immunity in asthma. *Nature reviews. Immunology*, 8 (3), 193–204.

Harker, J. A., Godlee, A., Wahlsten, J. L., Lee, D. C. P., Thorne, L. G., Sawant, D., Tregoning, J. S., Caspi, R. R., Bukreyev, A., Collins, P. L., and Openshaw, P. J. M., 2010. Interleukin 18 coexpression during respiratory syncytial virus infection results in enhanced disease mediated by natural killer cells. *Journal of virology*, 84 (8), 4073–4082.

Hassan, M. A., Eldin, A. M. E., and Ahmed, M. M., 2008. T - helper2 /T - helper1 imbalance in respiratory syncytial virus bronchiolitis in relation to disease severity and outcome. *The Egyptian journal of immunology / Egyptian Association of Immunologists*, 15 (2), 153–160.

Helft, J., Manicassamy, B., and Guermonprez, P., 2012. Cross-presenting CD103+ dendritic cells are protected from influenza virus infection. *The Journal of clinical investigation*, 122 (11) 4037-47

Henderson, F. W., Clyde, W. A., Collier, A. M., Denny, F. W., Senior, R. J., Sheaffer, C. I., Conley, W. G., and Christian, R. M., 1979. The etiologic and epidemiologic spectrum of bronchiolitis in pediatric practice. *The Journal of pediatrics*, 95 (2), 183–190.

Holgate, S. T., Holloway, J., Wilson, S., Bucchieri, F., Puddicombe, S., and Davies, D. E., 2004. Epithelial-mesenchymal communication in the pathogenesis of chronic asthma. *Proceedings of the American Thoracic Society*, 1 (2), 93–98.

Hornsleth, A., Klug, B., Nir, M., Johansen, J., Hansen, K. S., Christensen, L. S., and Larsen, L. B., 1998. Severity of respiratory syncytial virus disease related to type and genotype of virus and to cytokine values in nasopharyngeal secretions. *The Pediatric infectious disease journal*, 17 (12), 1114–1121.

Hoving, J. C., Wilson, G. J., and Brown, G. D., 2014. Signalling C-type lectin receptors, microbial recognition and immunity. *Cellular Microbiology*, 16 (2), 185–194.

Hu, Y., Webb, E., Singh, J., Morgan, B. A., Gainor, J. A., Gordon, T. D., and Siahaan, T. J., 2002. Rapid determination of substrate specificity of Clostridium histolyticum beta-collagenase using an immobilized peptide library. *The Journal of biological chemistry*, 277 (10), 8366–8371.

Huang, F.-F., Barnes, P. F., Feng, Y., Donis, R., Chroneos, Z. C., Idell, S., Allen, T., Perez, D. R., Whitsett, J. A., Dunussi-Joannopoulos, K., and Shams, H., 2011. GM-CSF in the lung protects against lethal influenza infection. *Am J Respir Crit Care Med*, 184 (2), 259–268.

Huang, H., Li, H., Zhou, P., and Ju, D., 2010. Protective effects of recombinant human granulocyte macrophage colony stimulating factor on H1N1 influenza virus-induced pneumonia in mice. *Cytokine*, 51 (2), 151–157.

Huber, L. C., Distler, O., Tarner, I., Gay, R. E., Gay, S., and Pap, T., 2006. Synovial fibroblasts: key players in rheumatoid arthritis. *Rheumatology*, 45 (6), 669–675.

Hussell, T. and Bell, T. J., 2014. Alveolar macrophages: plasticity in a tissue-specific context. *Nature reviews. Immunology*, 14 (2), 81–93.

Hussell, T. and Openshaw, P. J., 1998. Intracellular IFN-gamma expression in natural killer cells precedes lung CD8+ T cell recruitment during respiratory syncytial virus infection. *The Journal of general virology*, 79 (Pt 11), 2593–2601.

IMpact-RSV, 1998. Palivizumab, a humanized respiratory syncytial virus monoclonal antibody, reduces hospitalization from respiratory syncytial virus infection in high-risk infants. The IMpact-RSV Study Group. *Pediatrics*, 102 (3 Pt 1), 531–537.

Ioannidis, I., McNally, B., Willette, M., Peeples, M. E., Chaussabel, D., Durbin, J. E., Ramilo, O., Mejias, A., and Flano, E., 2012. Plasticity and virus specificity of the airway epithelial cell immune response during respiratory virus infection. *Journal of virology*, 86 (10), 5422–5436.

Ioannidis, I., Ye, F., McNally, B., Willette, M., and Flano, E., 2013. Toll-like receptor expression and induction of type I and type III interferons in primary airway epithelial cells. *Journal of virology*, 87 (6), 3261–3270.

Ishioka, T., Kimura, H., Kita, H., Obuchi, M., Hoshino, H., Noda, M., Nishina, A., Kozawa, K., and Kato, M., 2011. Effects of respiratory syncytial virus infection and major basic protein derived from eosinophils in pulmonary alveolar epithelial cells (A549). *Cell biology international*, 35 (5), 467–474.

Jacobs, S. R. and Damania, B., 2012. NLRs, inflammasomes, and viral infection. *Journal of leukocyte biology*, 92 (3), 469–477.

Jaks, E., Gavutis, M., Uzé, G., Martal, J., and Piehler, J., 2007. Differential receptor subunit affinities of type I interferons govern differential signal activation. *Journal of molecular biology*, 366 (2), 525–539.

Janssen, R., Bont, L., Siezen, C. L. E., Hodemaekers, H. M., Ermers, M. J., Doornbos, G., van 't Slot, R., Wijmenga, C., Goeman, J. J., Kimpen, J. L. L., van

Houwelingen, H. C., Kimman, T. G., and Hoebee, B., 2007. Genetic susceptibility to respiratory syncytial virus bronchiolitis is predominantly associated with innate immune genes. *The Journal of infectious diseases*, 196 (6), 826–834.

Jewell, N. A., Cline, T., Mertz, S. E., Smirnov, S. V., Flano, E., Schindler, C., Grieves, J. L., Durbin, R. K., Kotenko, S. V., and Durbin, J. E., 2010. Lambda interferon is the predominant interferon induced by influenza A virus infection in vivo. *Journal of virology*, 84 (21), 11515–11522.

Jewell, N. A., Vaghefi, N., Mertz, S. E., Akter, P., Peebles, R. S., Bakaletz, L. O., Durbin, R. K., Flano, E., and Durbin, J. E., 2007. Differential Type I Interferon Induction by Respiratory Syncytial Virus and Influenza A Virus In Vivo. *Journal of virology*, 81 (18), 9790–9800.

Johnson, J. E., Gonzales, R. A., Olson, S. J., Wright, P. F., and Graham, B. S., 2007. The histopathology of fatal untreated human respiratory syncytial virus infection. *Modern pathology*, 20 (1), 108–119.

Josefowicz, S. Z., Lu, L.-F., and Rudensky, A. Y., 2012. Regulatory T cells: mechanisms of differentiation and function. *Annual review of immunology*, 30, 531–564.

Jost, S. and Altfeld, M., 2013. Control of human viral infections by natural killer cells. *Annual review of immunology*, 31, 163–194.

Jozwik, A., Habibi, M. S., Paras, A., Zhu, J., Guvenel, A., Dhariwal, J., Almond, M., Wong, E. H. C., Sykes, A., Maybeno, M., Del Rosario, J., Trujillo-Torralbo, M.-B., Mallia, P., Sidney, J., Peters, B., Kon, O. M., Sette, A., Johnston, S. L., Openshaw, P. J., and Chiu, C., 2015. RSV-specific airway resident memory CD8+ T cells and differential disease severity after experimental human infection. *Nature communications*, 6, 1-15.

Kaiko, G. E., Loh, Z., Spann, K., Lynch, J. P., Lalwani, A., Zheng, Z., Davidson, S., Uematsu, S., Akira, S., Hayball, J., Diener, K. R., Baines, K. J., Simpson, J. L., Foster, P. S., and Phipps, S., 2013. Toll-like receptor 7 gene deficiency and early-life Pneumovirus infection interact to predispose toward the development of asthma-like pathology in mice. *The Journal of allergy and clinical immunology*, 131 (5), 1331–1339.

Kaiko, G. E., Phipps, S., Angkasekwinai, P., Dong, C., and Foster, P. S., 2010. NK cell deficiency predisposes to viral-induced Th2-type allergic inflammation via epithelial-derived IL-25. *Journal of immunology*, 185 (8), 4681–4690.

Kalluri, R. and Zeisberg, M., 2006. Fibroblasts in cancer. *Nature reviews. Cancer*, 6 (5), 392–401.

Kara, E. E., Comerford, I., Fenix, K. A., Bastow, C. R., Gregor, C. E., McKenzie, D. R., and McColl, S. R., 2014. Tailored immune responses: novel effector helper T cell subsets in protective immunity. *PLoS pathogens*, 10 (2), 1-15.

Kaul, T. N., Welliver, R. C., Wong, D. T., Udwadia, R. A., Riddlesberger, K., and Ogra, P. L., 1981. Secretory antibody response to respiratory syncytial virus infection. *American journal of diseases of children (1960)*, 135 (11), 1013–1016.

Kawai, T. and Akira, S., 2011. Toll-like receptors and their crosstalk with other innate receptors in infection and immunity. *Immunity*, 34 (5), 637–650.

Kim, H. W., Arrobio, J. O., Brandt, C. D., Wright, P., Hodes, D., Chanock, R. M., and Parrott, R. H., 1973. Safety and antigenicity of temperature sensitive (TS) mutant respiratory syncytial virus (RSV) in infants and children. *Pediatrics*,

52 (1), 56–63.
Kim, H. W., Canchola, J. G., Brandt, C. D., Pyles, G., Chanock, R. M., Jensen, K., and Parrott, R. H., 1969. Respiratory syncytial virus disease in infants despite prior administration of antigenic inactivated vaccine. *American journal of epidemiology*, 89 (4), 422–434.
Kim, K. S., Jung, H., Shin, I. K., Choi, B.-R., and Kim, D. H., 2015. Induction of interleukin-1 beta (IL-1β) is a critical component of lung inflammation during influenza A (H1N1) virus infection. *Journal of medical virology*, 87 (7), 1104–1112.
Kim, N. and Vu, T. H., 2006. Parabronchial smooth muscle cells and alveolar myofibroblasts in lung development. *Birth defects research*, 78 (1), 80–89.
Kitamura, H., Cambier, S., Somanath, S., Barker, T., Minagawa, S., Markovics, J., Goodsell, A., Publicover, J., Reichardt, L., Jablons, D., Wolters, P., Hill, A., Marks, J. D., Lou, J., Pittet, J.-F., Gauldie, J., Baron, J. L., and Nishimura, S. L., 2011. Mouse and human lung fibroblasts regulate dendritic cell trafficking, airway inflammation, and fibrosis through integrin αvβ8-mediated activation of TGF-β. *The Journal of clinical investigation*, 121 (7), 2863–2875.
Kolaczkowska, E. and Kubes, P., 2013. Neutrophil recruitment and function in health and inflammation. *Nature reviews. Immunology*, 13 (3), 159–175.
Kolli, D., Gupta, M. R., Sbrana, E., Velayutham, T. S., Chao, H., Casola, A., and Garofalo, R. P., 2014. Alveolar macrophages contribute to the pathogenesis of human metapneumovirus infection while protecting against respiratory syncytial virus infection. *American journal of respiratory cell and molecular biology*, 51 (4), 502–515.
Kouzaki, H., Iijima, K., Kobayashi, T., O'Grady, S. M., and Kita, H., 2011. The danger signal, extracellular ATP, is a sensor for an airborne allergen and triggers IL-33 release and innate Th2-type responses. *Journal of immunology*, 186 (7), 4375–4387.
Kurt-Jones, E. A., Popova, L., Kwinn, L., Haynes, L. M., Jones, L. P., Tripp, R. A., Walsh, E. E., Freeman, M. W., Golenbock, D. T., Anderson, L. J., and Finberg, R. W., 2000. Pattern recognition receptors TLR4 and CD14 mediate response to respiratory syncytial virus. *Nature immunology*, 1 (5), 398–401.
Lam, H. C., Choi, A. M. K., and Ryter, S. W., 2011. Isolation of mouse respiratory epithelial cells and exposure to experimental cigarette smoke at air liquid interface. *Journal of visualized experiments : JoVE*, (48).
Lambert, D. M., 1988. Role of oligosaccharides in the structure and function of respiratory syncytial virus glycoproteins. *Virology*, 164 (2), 458–466.
Lancelin, W. and Guerrero-Plata, A., 2011. Isolation of mouse lung dendritic cells. *Journal of visualized experiments : JoVE*, (57).
Lay, M. K., Gonzalez, P. A., Leon, M. A., Cespedes, P. F., Bueno, S. M., Riedel, C. A., and Kalergis, A. M., 2013. Advances in understanding respiratory syncytial virus infection in airway epithelial cells and consequential effects on the immune response. *Microbes and infection / Institut Pasteur*, 15 (3), 230–242.
Le Goffic, R., Arshad, M. I., Rauch, M., L'Helgoualc'h, A., Delmas, B., Piquet-Pellorce, C., and Samson, M., 2011. Infection with influenza virus induces IL-33 in murine lungs. *American journal of respiratory cell and molecular biology*, 45 (6), 1125–1132.
Lee, C. G., Yoon, H. J., Zhu, Z., Link, H., Wang, Z., Gwaltney, J. M., Landry, M., and Elias, J. A., 2000. Respiratory syncytial virus stimulation of vascular

endothelial cell growth Factor/Vascular permeability factor. *American journal of respiratory cell and molecular biology*, 23 (5), 662–669.

Lee, F. E.-H., Walsh, E. E., Falsey, A. R., Lumb, M. E., Okam, N. V., Liu, N., Divekar, A. A., Hall, C. B., and Mosmann, T. R., 2007. Human infant respiratory syncytial virus (RSV)-specific type 1 and 2 cytokine responses ex vivo during primary RSV infection. *The Journal of infectious diseases*, 195 (12), 1779–1788.

Lee, W. S., Jain, M. K., Arkonac, B. M., Zhang, D., Shaw, S. Y., Kashiki, S., Maemura, K., Lee, S. L., Hollenberg, N. K., Lee, M. E., and Haber, E., 1998. Thy-1, a novel marker for angiogenesis upregulated by inflammatory cytokines. *Circulation research*, 82 (8), 845–851.

Legg, J. P., Hussain, I. R., Warner, J. A., Johnston, S. L., and Warner, J. O., 2003. Type 1 and type 2 cytokine imbalance in acute respiratory syncytial virus bronchiolitis. *Am J Respir Crit Care Med*, 168 (6), 633–639.

Lenzo, J. C., Turner, A. L., Cook, A. D., Vlahos, R., Anderson, G. P., Reynolds, E. C., and Hamilton, J. A., 2012. Control of macrophage lineage populations by CSF-1 receptor and GM-CSF in homeostasis and inflammation. *Immunology and cell biology*, 90 (4), 429–440.

LeVine, A. M., Reed, J. A., Kurak, K. E., Cianciolo, E., and Whitsett, J. A., 1999. GM-CSF-deficient mice are susceptible to pulmonary group B streptococcal infection. *The Journal of clinical investigation*, 103 (4), 563–569.

Levitz, R., Wattier, R., Phillips, P., Solomon, A., Lawler, J., Lazar, I., Weibel, C., and Kahn, J. S., 2012. Induction of IL-6 and CCL5 (RANTES) in human respiratory epithelial (A549) cells by clinical isolates of respiratory syncytial virus is strain specific. *Virology journal*, 9 (190), 1-9.

Li, F., Zhu, H., Sun, R., Wei, H., and Tian, Z., 2012. Natural killer cells are involved in acute lung immune injury caused by respiratory syncytial virus infection. *Journal of virology*, 86 (4), 2251–2258.

Liesman, R. M., Buchholz, U. J., Luongo, C. L., Yang, L., Proia, A. D., DeVincenzo, J. P., Collins, P. L., and Pickles, R. J., 2014. RSV-encoded NS2 promotes epithelial cell shedding and distal airway obstruction. *The Journal of clinical investigation*, 124 (5), 2219–2233.

Lindell, D. M., Lane, T. E., and Lukacs, N. W., 2008. CXCL10/CXCR3-mediated responses promote immunity to respiratory syncytial virus infection by augmenting dendritic cell and CD8(+) T cell efficacy. *European journal of immunology*, 38 (8), 2168–2179.

Ling, Z., Tran, K.-C., and Teng, M. N., 2009. Human respiratory syncytial virus nonstructural protein NS2 antagonizes the activation of beta interferon transcription by interacting with RIG-I. *Journal of virology*, 83 (8), 3734–3742.

Liu, P., Jamaluddin, M., Li, K., Garofalo, R. P., Casola, A., and Brasier, A. R., 2007. Retinoic acid-inducible gene I mediates early antiviral response and Toll-like receptor 3 expression in respiratory syncytial virus-infected airway epithelial cells. *Journal of virology*, 81 (3), 1401–1411.

Loebbermann, J., Durant, L., Thornton, H., Johansson, C., and Openshaw, P. J., 2013. Defective immunoregulation in RSV vaccine-augmented viral lung disease restored by selective chemoattraction of regulatory T cells. *Proceedings of the National Academy of Sciences*, 110 (8), 2987–2992.

Loebbermann, J., Schnoeller, C., Thornton, H., Durant, L., Sweeney, N. P., Schuijs, M., O'Garra, A., Johansson, C., and Openshaw, P. J., 2012. IL-10 regulates viral

lung immunopathology during acute respiratory syncytial virus infection in mice. *PloS one*, 7 (2), 1-8.

Loebbermann, J., Thornton, H., Durant, L., Sparwasser, T., Webster, K. E., Sprent, J., Culley, F. J., Johansson, C., and Openshaw, P. J., 2012. Regulatory T cells expressing granzyme B play a critical role in controlling lung inflammation during acute viral infection. *Mucosal immunology*, 5 (2), 161–172.

Luckheeram, R. V., Zhou, R., Verma, A. D., and Xia, B., 2012. $CD4^+$T cells: differentiation and functions. *Clinical & developmental immunology*, 2012, 1-12.

Lukacs, N. W., Smit, J. J., Mukherjee, S., Morris, S. B., Nunez, G., and Lindell, D. M., 2010. Respiratory virus-induced TLR7 activation controls IL-17-associated increased mucus via IL-23 regulation. *Journal of immunology*, 185 (4), 2231–2239.

Mackall, C. L., Fry, T. J., and Gress, R. E., 2011. Harnessing the biology of IL-7 for therapeutic application. *Nature reviews. Immunology*, 11 (5), 330–342.

Matute-Bello, G., Liles, W. C., Radella, F., Steinberg, K. P., Ruzinski, J. T., Hudson, L. D., and Martin, T. R., 2000. Modulation of neutrophil apoptosis by granulocyte colony-stimulating factor and granulocyte/macrophage colony-stimulating factor during the course of acute respiratory distress syndrome. *Critical care medicine*, 28 (1), 1–7.

McAnulty, R. J., 2007. Fibroblasts and myofibroblasts: their source, function and role in disease. *The international journal of biochemistry & cell biology*, 39 (4), 666–671.

McAnulty, R. J., Campa, J. S., Cambrey, A. D., and Laurent, G. J., 1991. The effect of transforming growth factor beta on rates of procollagen synthesis and degradation in vitro. *Biochimica et biophysica acta*, 1091 (2), 231–235.

McCann, K. L. and Imani, F., 2007. Transforming growth factor beta enhances respiratory syncytial virus replication and tumor necrosis factor alpha induction in human epithelial cells. *Journal of virology*, 81 (6), 2880–2886.

McIntosh, K., Masters, H. B., Orr, I., Chao, R. K., and Barkin, R. M., 1978. The immunologic response to infection with respiratory syncytial virus in infants. *The Journal of infectious diseases*, 138 (1), 24–32.

McKinney-Freeman, S. L., Naveiras, O., Yates, F., Loewer, S., Philitas, M., Curran, M., Park, P. J., and Daley, G. Q., 2009. Surface antigen phenotypes of hematopoietic stem cells from embryos and murine embryonic stem cells. *Blood*, 114 (2), 268–278.

McLellan, J. S., Yang, Y., Graham, B. S., and Kwong, P. D., 2011. Structure of respiratory syncytial virus fusion glycoprotein in the postfusion conformation reveals preservation of neutralizing epitopes. *Journal of virology*, 85 (15), 7788–7796.

McNamara, P. S., Flanagan, B. F., Baldwin, L. M., Newland, P., Hart, C. A., and Smyth, R. L., 2004. Interleukin 9 production in the lungs of infants with severe respiratory syncytial virus bronchiolitis. *Lancet*, 363 (9414), 1031–1037.

McNamara, P. S., Flanagan, B. F., Hart, C. A., and Smyth, R. L., 2005. Production of chemokines in the lungs of infants with severe respiratory syncytial virus bronchiolitis. *The Journal of infectious diseases*, 191 (8), 1225–1232.

Mehta, P. K., Karls, R. K., White, E. H., Ades, E. W., and Quinn, F. D., 2006. Entry and intracellular replication of Mycobacterium tuberculosis in cultured

human microvascular endothelial cells. *Microbial pathogenesis*, 41 (2-3), 119–124.

Mellman, I., 2013. Dendritic cells: master regulators of the immune response. *Cancer immunology research*, 1 (3), 145–149.

Merad, M., Sathe, P., Helft, J., Miller, J., and Mortha, A., 2013. The dendritic cell lineage: ontogeny and function of dendritic cells and their subsets in the steady state and the inflamed setting. *Annual review of immunology*, 31, 563–604.

Messier, E. M., Mason, R. J., and Kosmider, B., 2012. Efficient and rapid isolation and purification of mouse alveolar type II epithelial cells. *Experimental lung research*, 38 (7), 363–373.

Meyerholz, D. K., Gallup, J. M., Lazic, T., de Macedo, M. M. A., Lehmkuhl, H. D., and Ackermann, M. R., 2007. Pretreatment with recombinant human vascular endothelial growth factor reduces virus replication and inflammation in a perinatal lamb model of respiratory syncytial virus infection. *Viral immunology*, 20 (1), 188–196.

Middleton, J., Patterson, A. M., Gardner, L., Schmutz, C., and Ashton, B. A., 2002. Leukocyte extravasation: chemokine transport and presentation by the endothelium. *Blood*, 100 (12), 3853–3860.

Midulla, F., Villani, A., Panuska, J. R., Dab, I., Kolls, J. K., Merolla, R., and Ronchetti, R., 1993. Respiratory syncytial virus lung infection in infants: immunoregulatory role of infected alveolar macrophages. *The Journal of infectious diseases*, 168 (6), 1515–1519.

Miller, A. L., Bowlin, T. L., and Lukacs, N. W., 2004. Respiratory syncytial virus-induced chemokine production: linking viral replication to chemokine production in vitro and in vivo. *The Journal of infectious diseases*, 189 (8), 1419–1430.

Miyairi, I. and DeVincenzo, J. P., 2008. Human genetic factors and respiratory syncytial virus disease severity. *Clinical Microbiology Reviews*, 21 (4), 686–703.

Miyamoto, M., Prause, O., Sjöstrand, M., Laan, M., Lötvall, J., and Lindén, A., 2003. Endogenous IL-17 as a mediator of neutrophil recruitment caused by endotoxin exposure in mouse airways. *Journal of immunology*, 170 (9), 4665–4672.

Mobbs, K. J., Smyth, R. L., O'Hea, U., Ashby, D., Ritson, P., and Hart, C. A., 2002. Cytokines in severe respiratory syncytial virus bronchiolitis. *Pediatric pulmonology*, 33 (6), 449–452.

Moltedo, B., Li, W., Yount, J. S., and Moran, T. M., 2011. Unique type I interferon responses determine the functional fate of migratory lung dendritic cells during influenza virus infection. *PLoS pathogens*, 7 (11), 1-15.

Monick, M. M., Cameron, K., Staber, J., Powers, L. S., Yarovinsky, T. O., Koland, J. G., and Hunninghake, G. W., 2005. Activation of the epidermal growth factor receptor by respiratory syncytial virus results in increased inflammation and delayed apoptosis. *The Journal of biological chemistry*, 280 (3), 2147–2158.

Monticelli, L. A., Sonnenberg, G. F., Abt, M. C., Alenghat, T., Ziegler, C. G. K., Doering, T. A., Angelosanto, J. M., Laidlaw, B. J., Yang, C. Y., Sathaliyawala, T., Kubota, M., Turner, D., Diamond, J. M., Goldrath, A. W., Farber, D. L., Collman, R. G., Wherry, E. J., and Artis, D., 2011. Innate lymphoid cells promote lung-tissue homeostasis after infection with influenza virus. *Nature immunology*,

12 (11), 1045–1054.
Moore, P. E., Cunningham, G., Calder, M. M., DeMatteo, A. D., Peeples, M. E., Summar, M. L., and Peebles, R. S., 2006. Respiratory syncytial virus infection reduces beta2-adrenergic responses in human airway smooth muscle. *American journal of respiratory cell and molecular biology*, 35 (5), 559–564.
Mordstein, M., Neugebauer, E., Ditt, V., Jessen, B., Rieger, T., Falcone, V., Sorgeloos, F., Ehl, S., Mayer, D., Kochs, G., Schwemmle, M., Günther, S., Drosten, C., Michiels, T., and Staeheli, P., 2010. Lambda Interferon Renders Epithelial Cells of the Respiratory and Gastrointestinal Tracts Resistant to Viral Infections. *Journal of virology*, 84 (11), 5670–5677.
Morrissey, P. J., Bressler, L., Park, L. S., Alpert, A., and Gillis, S., 1987. Granulocyte-macrophage colony-stimulating factor augments the primary antibody response by enhancing the function of antigen-presenting cells. *Journal of immunology,* 139 (4), 1113–1119.
Mufson, M. A., Belshe, R. B., Orvell, C., and Norrby, E., 1987. Subgroup characteristics of respiratory syncytial virus strains recovered from children with two consecutive infections. *Journal of clinical microbiology*, 25 (8), 1535–1539.
Muller, U., Steinhoff, U., Reis, L. F., Hemmi, S., Pavlovic, J., Zinkernagel, R. M., and Aguet, M., 1994. Functional role of type I and type II interferons in antiviral defense. *Science*, 264 (5167), 1918–1921.
Murai, H., Terada, A., Mizuno, M., Asai, M., Hirabayashi, Y., Shimizu, S., Morishita, T., Kakita, H., Hussein, M. H., Ito, T., Kato, I., Asai, K., and Togari, H., 2007. IL-10 and RANTES are elevated in nasopharyngeal secretions of children with respiratory syncytial virus infection. *Allergology international*, 56 (2), 157–163.
Murawski, M. R., Bowen, G. N., Cerny, A. M., Anderson, L. J., Haynes, L. M., Tripp, R. A., Kurt-Jones, E. A., and Finberg, R. W., 2009. Respiratory syncytial virus activates innate immunity through Toll-like receptor 2. *Journal of virology*, 83 (3), 1492–1500.
Murayama, T., Kikuchi, M., Miita, T., Yamada, R., Matsubara, K., Sadanari, H., and Mukaida, N., 2014. Human cytomegalovirus replication supported by virus-induced activation of CCL2-CCR2 interactions. *Biochemical and biophysical research communications*, 453 (3), 321–325.
Naessens, T., Schepens, B., Smet, M., Pollard, C., Van Hoecke, L., De Beuckelaer, A., Willart, M., Lambrecht, B., De Koker, S., Saelens, X., and Grooten, J., 2015. GM-CSF treatment prevents respiratory syncytial virus-induced pulmonary exacerbation responses in postallergic mice by stimulating alveolar macrophage maturation. *The Journal of allergy and clinical immunology*, 137 (3) 700-709
Nair, H., Nokes, D. J., Gessner, B. D., Dherani, M., Madhi, S. A., Singleton, R. J., O'Brien, K. L., Roca, A., Wright, P. F., Bruce, N., Chandran, A., Theodoratou, E., Sutanto, A., Sedyaningsih, E. R., Ngama, M., Munywoki, P. K., Kartasasmita, C., Simões, E. A. F., Rudan, I., Weber, M. W., and Campbell, H., 2010. Global burden of acute lower respiratory infections due to respiratory syncytial virus in young children: a systematic review and meta-analysis. *Lancet*, 375 (9725), 1545–1555.
Nakajima, N., Van Tin, N., Sato, Y., Thach, H. N., Katano, H., Diep, P. H., Kumasaka, T., Thuy, N. T., Hasegawa, H., San, L. T., Kawachi, S., Liem, N. T., Suzuki, K., and

Sata, T., 2013. Pathological study of archival lung tissues from five fatal cases of avian H5N1 influenza in Vietnam. *Modern pathology : an official journal of the United States and Canadian Academy of Pathology, Inc*, 26 (3), 357–369.

Neill, D. R., Wong, S. H., Bellosi, A., Flynn, R. J., Daly, M., Langford, T. K. A., Bucks, C., Kane, C. M., Fallon, P. G., Pannell, R., Jolin, H. E., and McKenzie, A. N. J., 2010. Nuocytes represent a new innate effector leukocyte that mediates type-2 immunity. *Nature*, 464 (7293), 1367–1370.

Noah, T. L. and Becker, S., 1993. Respiratory syncytial virus-induced cytokine production by a human bronchial epithelial cell line. *The American journal of physiology*, 265 (5 Pt 1), 472–478.

Noah, T. L., Henderson, F. W., Wortman, I. A., Devlin, R. B., Handy, J., Koren, H. S., and Becker, S., 1995. Nasal cytokine production in viral acute upper respiratory infection of childhood. *The Journal of infectious diseases*, 171 (3), 584–592.

Okabayashi, T., Yokota, S.-I., Yoto, Y., Tsutsumi, H., and Fujii, N., 2009. Fosfomycin suppresses chemokine induction in airway epithelial cells infected with respiratory syncytial virus. *Clinical and vaccine immunology : CVI*, 16 (6), 859–865.

Oliveira-Nascimento, L., Massari, P., and Wetzler, L. M., 2012. The Role of TLR2 in Infection and Immunity. *Frontiers in immunology*, 3, 79–79.

Oliver, B. G. G., Johnston, S. L., Baraket, M., Burgess, J. K., King, N. J. C., Roth, M., Lim, S., and Black, J. L., 2006. Increased proinflammatory responses from asthmatic human airway smooth muscle cells in response to rhinovirus infection. *Respiratory research*, 7 (71), 1-11.

Olivier, A. K., Gallup, J. M., van Geelen, A., and Ackermann, M. R., 2011. Exogenous administration of vascular endothelial growth factor prior to human respiratory syncytial virus a2 infection reduces pulmonary pathology in neonatal lambs and alters epithelial innate immune responses. *Experimental lung research*, 37 (3), 131–143.

Owens, G. K., Kumar, M. S., and Wamhoff, B. R., 2004. Molecular regulation of vascular smooth muscle cell differentiation in development and disease. *Physiological reviews*, 84 (3), 767–801.

Österreicher, C. H., Penz-Österreicher, M., Grivennikov, S. I., Guma, M., Koltsova, E. K., Datz, C., Sasik, R., Hardiman, G., Karin, M., and Brenner, D. A., 2011. Fibroblast-specific protein 1 identifies an inflammatory subpopulation of macrophages in the liver. *Proceedings of the National Academy of Sciences*, 108 (1), 308–313.

Paine, R., Morris, S. B., Jin, H., Wilcoxen, S. E., Phare, S. M., Moore, B. B., Coffey, M. J., and Toews, G. B., 2001. Impaired functional activity of alveolar macrophages from GM-CSF-deficient mice. *American journal of physiology. Lung cellular and molecular physiology*, 281 (5), 1210–1218.

Paine, R., Wilcoxen, S. E., Morris, S. B., Sartori, C., Baleeiro, C. E. O., Matthay, M. A., and Christensen, P. J., 2003. Transgenic overexpression of granulocyte macrophage-colony stimulating factor in the lung prevents hyperoxic lung injury. *The American Journal of Pathology*, 163 (6), 2397–2406.

Pandey, S., Kawai, T., and Akira, S., 2015. Microbial sensing by Toll-like receptors and intracellular nucleic acid sensors. *Cold Spring Harbor perspectives in biology*, 7 (1), 1-18.

Panuska, J. R., Merolla, R., Rebert, N. A., Hoffmann, S. P., Tsivitse, P., Cirino, N. M.,

Silverman, R. H., and Rankin, J. A., 1995. Respiratory syncytial virus induces interleukin-10 by human alveolar macrophages. Suppression of early cytokine production and implications for incomplete immunity. *The Journal of clinical investigation*, 96 (5), 2445–2453.

Pap, T., Müller-Ladner, U., Gay, R. E., and Gay, S., 2000. Fibroblast biology. Role of synovial fibroblasts in the pathogenesis of rheumatoid arthritis. *Arthritis research*, 2 (5), 361–367.

Park, C. O. and Kupper, T. S., 2015. The emerging role of resident memory T cells in protective immunity and inflammatory disease. *Nature medicine*, 21 (7), 688–697.

Parsonage, G., Filer, A. D., Haworth, O., Nash, G. B., Rainger, G. E., Salmon, M., and Buckley, C. D., 2005. A stromal address code defined by fibroblasts. *Trends in immunology*, 26 (3), 150–156.

Perros, F., Lambrecht, B. N., and Hammad, H., 2011. TLR4 signalling in pulmonary stromal cells is critical for inflammation and immunity in the airways. *Respiratory research*, 12 (125), 1-8.

Perry, A. K., Chen, G., Zheng, D., Tang, H., and Cheng, G., 2005. The host type I interferon response to viral and bacterial infections. *Cell research*, 15 (6), 407–422.

Phipps, R. P., Penney, D. P., Keng, P., Quill, H., Paxhia, A., Derdak, S., and Felch, M. E., 1989. Characterization of two major populations of lung fibroblasts: distinguishing morphology and discordant display of Thy 1 and class II MHC. *American journal of respiratory cell and molecular biology*, 1 (1), 65–74.

Phipps, R. P., Penney, D. P., Keng, P., Silvera, M., Harkins, S., and Derdak, S., 1990. Immune functions of subpopulations of lung fibroblasts. *Immunologic research*, 9 (4), 275–286.

Pinto, A. K., Ramos, H. J., Wu, X., Aggarwal, S., Shrestha, B., Gorman, M., Kim, K. Y., Suthar, M. S., Atkinson, J. P., Gale, M., and Diamond, M. S., 2014. Deficient IFN signaling by myeloid cells leads to MAVS-dependent virus-induced sepsis. *PLoS pathogens*, 10 (4), 1-20.

Plantinga, M., Guilliams, M., and Vanheerswynghels, M., 2013. Conventional and monocyte-derived CD11b+ dendritic cells initiate and maintain T helper 2 cell-mediated immunity to house dust mite allergen. *Immunity*, 38 (2) 322-35

Podgrabinska, S., Braun, P., Velasco, P., Kloos, B., Pepper, M. S., and Skobe, M., 2002. Molecular characterization of lymphatic endothelial cells. *Proceedings of the National Academy of Sciences of the United States of America*, 99 (25), 16069–16074.

Pribul, P. K., Harker, J., Wang, B., Wang, H., Tregoning, J. S., Schwarze, J., and Openshaw, P. J. M., 2008. Alveolar macrophages are a major determinant of early responses to viral lung infection but do not influence subsequent disease development. *Journal of virology*, 82 (9), 4441–4448.

Qi, F., Wang, D., Liu, J., Zeng, S., Xu, L., Hu, H., and Liu, B., 2015. Respiratory macrophages and dendritic cells mediate respiratory syncytial virus-induced IL-33 production in TLR3- or TLR7-dependent manner. *International immunopharmacology*, 29 (2), 408–415.

Ramaswamy, M., Shi, L., Varga, S. M., Barik, S., Behlke, M. A., and Look, D. C., 2006. Respiratory syncytial virus nonstructural protein 2 specifically inhibits type I interferon signal transduction. *Virology*, 344 (2), 328–339.

Ravi, L. I., Li, L., Wong, P. S., Sutejo, R., Tan, B. H., and Sugrue, R. J., 2013.

Lovastatin treatment mitigates the pro-inflammatory cytokine response in respiratory syncytial virus infected macrophage cells. *Antiviral research*, 98 (2), 332–343.

Reed, J. L., Brewah, Y. A., Delaney, T., Welliver, T., Burwell, T., Benjamin, E., Kuta, E., Kozhich, A., McKinney, L., Suzich, J., Kiener, P. A., Avendano, L., Velozo, L., Humbles, A., Welliver, R. C., and Coyle, A. J., 2008. Macrophage impairment underlies airway occlusion in primary respiratory syncytial virus bronchiolitis. *The Journal of infectious diseases*, 198 (12), 1783–1793.

Rensen, S. S. M., Doevendans, P. A. F. M., and van Eys, G. J. J. M., 2007. Regulation and characteristics of vascular smooth muscle cell phenotypic diversity. *Netherlands heart journal*, 15 (3), 100–108.

Richards, C. D., 2013. The enigmatic cytokine oncostatin m and roles in disease. *ISRN inflammation*, 2013, 1-23.

Rödel, J., Woytas, M., Groh, A., Schmidt, K. H., Hartmann, M., Lehmann, M., and Straube, E., 2000. Production of basic fibroblast growth factor and interleukin 6 by human smooth muscle cells following infection with Chlamydia pneumoniae. *Infection and immunity*, 68 (6), 3635–3641.

Ruan, Y., Okamoto, Y., Matsuzaki, Z., Endo, S., Matsuoka, T., Kohno, T., Chazono, H., Eiko, I., Tsubota, K., and Saito, I., 2001. Suppressive effect of locally produced interleukin-10 on respiratory syncytial virus infection. *Immunology*, 104 (3), 355–360.

Rudd, B. D., Burstein, E., Duckett, C. S., Li, X., and Lukacs, N. W., 2005. Differential role for TLR3 in respiratory syncytial virus-induced chemokine expression. *Journal of virology*, 79 (6), 3350–3357.

Rutigliano, J. A. and Graham, B. S., 2004. Prolonged production of TNF-alpha exacerbates illness during respiratory syncytial virus infection. *Journal of immunology*, 173 (5), 3408–3417.

Sabbah, A., Hung Chang, Te, Harnack, R., Frohlich, V., Tominaga, K., Dube, P. H., Xiang, Y., and Bose, S., 2009. Activation of innate immune antiviral responses by Nod2. *Nature immunology*, 10 (10), 1073–1080.

Saravia, J., You, D., Shrestha, B., Jaligama, S., Siefker, D., Lee, G. I., Harding, J. N., Jones, T. L., Rovnaghi, C., Bagga, B., DeVincenzo, J. P., and Cormier, S. A., 2015. Respiratory Syncytial Virus Disease Is Mediated by Age-Variable IL-33. *PLoS pathogens*, 11 (10), 1-17.

Satelli, A. and Li, S., 2011. Vimentin in cancer and its potential as a molecular target for cancer therapy. *Cellular and molecular life sciences: CMLS*, 68 (18), 3033–3046.

Schijf, M. A., Lukens, M. V., Kruijsen, D., van Uden, N. O. P., Garssen, J., Coenjaerts, F. E. J., Van't Land, B., and van Bleek, G. M., 2013. Respiratory syncytial virus induced type I IFN production by pDC is regulated by RSV-infected airway epithelial cells, RSV-exposed monocytes and virus specific antibodies. *PloS one*, 8 (11), 1-18.

Schwarze, J., 2008. Lung dendritic cells in respiratory syncytial virus bronchiolitis. *The Pediatric infectious disease journal*, 27 (10 Suppl), S89–91.

Segovia, J., Sabbah, A., Mgbemena, V., Tsai, S.-Y., Chang, T.-H., Berton, M. T., Morris, I. R., Allen, I. C., Ting, J. P.-Y., and Bose, S., 2012. TLR2/MyD88/NF-κB pathway, reactive oxygen species, potassium efflux activates NLRP3/ASC inflammasome during respiratory syncytial virus infection. *PloS one*, 7 (1), 1-15.

Seki, E., Yoshizumi, M., Tanaka, R., Ryo, A., Ishioka, T., Tsukagoshi, H., Kozawa, K., Okayama, Y., Okabe-Kado, J., Goya, T., and Kimura, H., 2013. Cytokine profiles, signalling pathways and effects of fluticasone propionate in respiratory syncytial virus-infected human foetal lung fibroblasts. *Cell biology international*, 37 (4), 326–339.

Sever-Chroneos, Z., Murthy, A., Davis, J., Florence, J. M., Kurdowska, A., Krupa, A., Tichelaar, J. W., White, M. R., Hartshorn, K. L., Kobzik, L., Whitsett, J. A., and Chroneos, Z. C., 2011. GM-CSF modulates pulmonary resistance to influenza A infection. *Antiviral research*, 92 (2), 319–328.

Seymour, J. F., Lieschke, G. J., Grail, D., Quilici, C., Hodgson, G., and Dunn, A. R., 1997. Mice lacking both granulocyte colony-stimulating factor (CSF) and granulocyte-macrophage CSF have impaired reproductive capacity, perturbed neonatal granulopoiesis, lung disease, amyloidosis, and reduced long-term survival. *Blood*, 90 (8), 3037–3049.

Sheeran, P., Jafri, H., Carubelli, C., Saavedra, J., Johnson, C., Krisher, K., Sánchez, P. J., and Ramilo, O., 1999. Elevated cytokine concentrations in the nasopharyngeal and tracheal secretions of children with respiratory syncytial virus disease. *The Pediatric infectious disease journal*, 18 (2), 115–122.

Shi, C. and Pamer, E. G., 2011. Monocyte recruitment during infection and inflammation. *Nature reviews. Immunology*, 11 (11), 762–774.

Shibata, Y., Berclaz, P. Y., Chroneos, Z. C., Yoshida, M., Whitsett, J. A., and Trapnell, B. C., 2001. GM-CSF regulates alveolar macrophage differentiation and innate immunity in the lung through PU.1. *Immunity*, 15 (4), 557–567.

Silzle, T., Randolph, G. J., Kreutz, M., and Kunz-Schughart, L. A., 2004. The fibroblast: sentinel cell and local immune modulator in tumor tissue. *International journal of cancer*, 108 (2), 173–180.

Sinzger, C., Grefte, A., Plachter, B., Gouw, A. S., The, T. H., and Jahn, G., 1995. Fibroblasts, epithelial cells, endothelial cells and smooth muscle cells are major targets of human cytomegalovirus infection in lung and gastrointestinal tissues. *The Journal of general virology*, 76 (Pt 4), 741–750.

Skalli, O., Pelte, M. F., Peclet, M. C., Gabbiani, G., Gugliotta, P., Bussolati, G., Ravazzola, M., and Orci, L., 1989. Alpha-smooth muscle actin, a differentiation marker of smooth muscle cells, is present in microfilamentous bundles of pericytes. *Journal of Histochemistry & Cytochemistry*, 37 (3), 315–321.

Smit, J. J., Lindell, D. M., Boon, L., Kool, M., Lambrecht, B. N., and Lukacs, N. W., 2008. The balance between plasmacytoid DC versus conventional DC determines pulmonary immunity to virus infections. *PloS one*, 3 (3), 1720-1728.

Smit, J. J., Rudd, B. D., and Lukacs, N. W., 2006. Plasmacytoid dendritic cells inhibit pulmonary immunopathology and promote clearance of respiratory syncytial virus. *The Journal of experimental medicine*, 203 (5), 1153–1159.

Smith, P. K., Wang, S. Z., Dowling, K. D., and Forsyth, K. D., 2001. Leucocyte populations in respiratory syncytial virus-induced bronchiolitis. *Journal of paediatrics and child health*, 37 (2), 146–151.

Smith, R. S., Smith, T. J., Blieden, T. M., and Phipps, R. P., 1997. Fibroblasts as sentinel cells. Synthesis of chemokines and regulation of inflammation. *The American Journal of Pathology*, 151 (2), 317–322.

Solis, M., Goubau, D., Romieu-Mourez, R., Genin, P., Civas, A., and Hiscott, J., 2006. Distinct functions of IRF-3 and IRF-7 in IFN-alpha gene regulation and control of anti-tumor activity in primary macrophages. *Biochemical Pharmacology*, 72 (11), 1469–1476.

Soukup, J. M. and Becker, S., 2003. Role of monocytes and eosinophils in human respiratory syncytial virus infection in vitro. *Clinical immunology*, 107 (3), 178–185.

Spann, K. M., Tran, K.-C., Chi, B., Rabin, R. L., and Collins, P. L., 2004. Suppression of the induction of alpha, beta, and lambda interferons by the NS1 and NS2 proteins of human respiratory syncytial virus in human epithelial cells and macrophages [corrected]. *Journal of virology*, 78 (8), 4363–4369.

Srikiatkhachorn, A. and Braciale, T. J., 1997. Virus-specific CD8+ T lymphocytes downregulate T helper cell type 2 cytokine secretion and pulmonary eosinophilia during experimental murine respiratory syncytial virus infection. *The Journal of experimental medicine*, 186 (3), 421–432.

Stadnyk, A. W., Gillan, T. L., and Anderson, R., 1997. Respiratory syncytial virus triggers synthesis of IL-6 in BALB/c mouse alveolar macrophages in the absence of virus replication. *Cellular immunology*, 176 (2), 122–126.

Steinwede, K., Tempelhof, O., Bolte, K., Maus, R., Bohling, J., Ueberberg, B., Länger, F., Christman, J. W., Paton, J. C., Ask, K., Maharaj, S., Kolb, M., Gauldie, J., Welte, T., and Maus, U. A., 2011. Local delivery of GM-CSF protects mice from lethal pneumococcal pneumonia. *Journal of immunology*, 187 (10), 5346–5356.

Stenn, K. S., Link, R., Moellmann, G., Madri, J., and Kuklinska, E., 1989. Dispase, a neutral protease from Bacillus polymyxa, is a powerful fibronectinase and type IV collagenase. *The Journal of investigative dermatology*, 93 (2), 287–290.

Suki, B., Ito, S., Stamenovic, D., Lutchen, K. R., and Ingenito, E. P., 2005. Biomechanics of the lung parenchyma: critical roles of collagen and mechanical forces. *Journal of applied physiology*, 98 (5), 1892–1899.

Sullender, W. M., Mufson, M. A., Prince, G. A., Anderson, L. J., and Wertz, G. W., 1998. Antigenic and genetic diversity among the attachment proteins of group A respiratory syncytial viruses that have caused repeat infections in children. *The Journal of infectious diseases*, 178 (4), 925–932.

Sun, J., Cardani, A., Sharma, A. K., Laubach, V. E., Jack, R. S., Müller, W., and Braciale, T. J., 2011. Autocrine regulation of pulmonary inflammation by effector T-cell derived IL-10 during infection with respiratory syncytial virus. *PLoS pathogens*, 7 (8), 1-11.

Sun, Y., Han, M., Kim, C., Calvert, J. G., and Yoo, D., 2012. Interplay between interferon-mediated innate immunity and porcine reproductive and respiratory syndrome virus. *Viruses*, 4 (4), 424–446.

Swedan, S., Musiyenko, A., and Barik, S., 2009. Respiratory syncytial virus nonstructural proteins decrease levels of multiple members of the cellular interferon pathways. *Journal of virology*, 83 (19), 9682–9693.

Tabarani, C. M., Bonville, C. A., Suryadevara, M., Branigan, P., Wang, D., Huang, D., Rosenberg, H. F., and Domachowske, J. B., 2013. Novel Inflammatory Markers, Clinical Risk Factors, and Virus Type Associated with Severe Respiratory Syncytial Virus Infection. *The Pediatric infectious disease journal*, 32 (12) 437-42

Takaoka, A. and Yanai, H., 2006. Interferon signalling network in innate defence.

Cellular Microbiology, 8 (6), 907–922.

Takeuchi, R., Tsutsumi, H., Osaki, M., Sone, S., Imai, S., and Chiba, S., 1998. Respiratory syncytial virus infection of neonatal monocytes stimulates synthesis of interferon regulatory factor 1 and interleukin-1beta (IL-1beta)-converting enzyme and secretion of IL-1beta. *Journal of virology*, 72 (1), 837–840.

Tayyari, F., Marchant, D., Moraes, T. J., Duan, W., Mastrangelo, P., and Hegele, R. G., 2011. Identification of nucleolin as a cellular receptor for human respiratory syncytial virus. *Nature medicine*, 17 (9), 1132–1135.

Teijaro, J. R., Walsh, K. B., Cahalan, S., Fremgen, D. M., Roberts, E., Scott, F., Martinborough, E., Peach, R., Oldstone, M. B. A., and Rosen, H., 2011. Endothelial cells are central orchestrators of cytokine amplification during influenza virus infection. *Cell*, 146 (6), 980–991.

Tomasek, J. J., Gabbiani, G., Hinz, B., Chaponnier, C., and Brown, R. A., 2002. Myofibroblasts and mechano-regulation of connective tissue remodelling. *Nature reviews. Molecular cell biology*, 3 (5), 349–363.

Tomlinson, M. J., Tomlinson, S., Yang, X. B., and Kirkham, J., 2013. Cell separation: Terminology and practical considerations. *Journal of tissue engineering*, 4, 1-14.

Topham, N. J. and Hewitt, E. W., 2009. Natural killer cell cytotoxicity: how do they pull the trigger? *Immunology*, 128 (1), 7–15.

Trapnell, B. C. and Whitsett, J. A., 2002. Gm-CSF regulates pulmonary surfactant homeostasis and alveolar macrophage-mediated innate host defense. *Annual review of physiology*, 64, 775–802.

Tregoning, J. S., Pribul, P. K., Pennycook, A. M. J., Hussell, T., Wang, B., Lukacs, N., Schwarze, J., Culley, F. J., and Openshaw, P. J. M., 2010. The chemokine MIP1alpha/CCL3 determines pathology in primary RSV infection by regulating the balance of T cell populations in the murine lung. *PloS one*, 5 (2), 9381-9387.

Trinchieri, G., 2010. Type I interferon: friend or foe? *The Journal of experimental medicine*, 207 (10) 2053-63

Tripp, R. A., Oshansky, C., and Alvarez, R., 2005. Cytokines and respiratory syncytial virus infection. *Proceedings of the American Thoracic Society*, 2 (2), 147–149.

Tristram, D. A., Hicks, W., and Hard, R., 1998. Respiratory syncytial virus and human bronchial epithelium. *Archives of otolaryngology--head & neck surgery*, 124 (7), 777–783.

Unkel, B., Hoegner, K., Clausen, B. E., Lewe-Schlosser, P., Bodner, J., Gattenloehner, S., Janßen, H., Seeger, W., Lohmeyer, J., and Herold, S., 2012. Alveolar epithelial cells orchestrate DC function in murine viral pneumonia. *The Journal of clinical investigation*, 122 (10), 3652–3664.

Van Raemdonck, K., Van den Steen, P. E., Liekens, S., Van Damme, J., and Struyf, S., 2015. CXCR3 ligands in disease and therapy. *Cytokine & growth factor reviews*, 26 (3), 311–327.

Varanat, M., Maggi, R. G., Linder, K. E., and Breitschwerdt, E. B., 2013. Infection of human brain vascular pericytes (HBVPs) by Bartonella henselae. *Medical microbiology and immunology*, 202 (2), 143–151.

Vareille, M., Kieninger, E., Edwards, M. R., and Regamey, N., 2011. The Airway Epithelium: Soldier in the Fight against Respiratory Viruses. *Clinical*

Microbiology Reviews, 24 (1), 210–229.

Villenave, R., Thavagnanam, S., Sarlang, S., Parker, J., Douglas, I., Skibinski, G., Heaney, L. G., McKaigue, J. P., Coyle, P. V., Shields, M. D., and Power, U. F., 2012. In vitro modeling of respiratory syncytial virus infection of pediatric bronchial epithelium, the primary target of infection in vivo. *Proceedings of the National Academy of Sciences*, 109 (13), 5040–5045.

Vlahos, R., Bozinovski, S., Chan, S. P. J., Ivanov, S., Lindén, A., Hamilton, J. A., and Anderson, G. P., 2010. Neutralizing granulocyte/macrophage colony-stimulating factor inhibits cigarette smoke-induced lung inflammation. *Am J Respir Crit Care Med*, 182 (1), 34–40.

Walsh, E. E. and Falsey, A. R., 2012. Respiratory syncytial virus infection in adult populations. *Infectious disorders drug targets*, 12 (2), 98–102.

Wang, H., Peters, N., and Schwarze, J., 2006. Plasmacytoid dendritic cells limit viral replication, pulmonary inflammation, and airway hyperresponsiveness in respiratory syncytial virus infection. *Journal of immunology*, 177 (9), 6263–6270.

Wang, S. Z., Xu, H., Wraith, A., Bowden, J. J., Alpers, J. H., and Forsyth, K. D., 1998. Neutrophils induce damage to respiratory epithelial cells infected with respiratory syncytial virus. *The European respiratory journal*, 12 (3), 612–618.

Wang, X.-Y., Keefe, K. M., Jensen-Taubman, S. M., Yang, D., Yan, K., and Linnoila, R. I., 2012. Novel method for isolation of murine clara cell secretory protein-expressing cells with traces of stemness. *PloS one*, 7 (8), 43008-43017.

Weinheimer, V. K., Becher, A., Tonnies, M., Holland, G., Knepper, J., Bauer, T. T., Schneider, P., Neudecker, J., Ruckert, J. C., Szymanski, K., Temmesfeld-Wollbrueck, B., Gruber, A. D., Bannert, N., Suttorp, N., Hippenstiel, S., Wolff, T., and Hocke, A. C., 2012. Influenza A viruses target type II pneumocytes in the human lung. *The Journal of infectious diseases*, 206 (11), 1685–1694.

Weiss, K. A., Christiaansen, A. F., Fulton, R. B., Meyerholz, D. K., and Varga, S. M., 2011. Multiple CD4+ T cell subsets produce immunomodulatory IL-10 during respiratory syncytial virus infection. *Journal of immunology*, 187 (6), 3145–3154.

Welliver, R. C. S., 2008. The immune response to respiratory syncytial virus infection: friend or foe? *Clinical reviews in allergy & immunology*, 34 (2), 163–173.

Welliver, R. C., Kaul, T. N., Putnam, T. I., Sun, M., Riddlesberger, K., and Ogra, P. L., 1980. The antibody response to primary and secondary infection with respiratory syncytial virus: kinetics of class-specific responses. *The Journal of pediatrics*, 96 (5), 808–813.

Welliver, T. P., Garofalo, R. P., Hosakote, Y., Hintz, K. H., Avendano, L., Sanchez, K., Velozo, L., Jafri, H., Chavez-Bueno, S., Ogra, P. L., McKinney, L., Reed, J. L., and Welliver, R. C. S., 2007. Severe human lower respiratory tract illness caused by respiratory syncytial virus and influenza virus is characterized by the absence of pulmonary cytotoxic lymphocyte responses. *The Journal of infectious diseases*, 195 (8), 1126–1136.

Westergren-Thorsson, G., Larsen, K., Nihlberg, K., Andersson-Sjöland, A., Hallgren, O., Marko-Varga, G., and Bjermer, L., 2010. Pathological airway remodelling in inflammation. *The clinical respiratory journal*, 4 (Suppl 1), 1–8.

Wolf, J., Weinberger, B., and Grubeck-Loebenstein, B., 2012. The immunoregulatory effects of CMV-infection in human fibroblasts and the impact on cellular senescence. *Immunity & ageing : I & A*, 9 (1), 1-6.

Wright, C., Oliver, K. C., Fenwick, F. I., Smith, N. M., and Toms, G. L., 1997. A monoclonal antibody pool for routine immunohistochemical detection of human respiratory syncytial virus antigens in formalin-fixed, paraffin-embedded tissue. *The Journal of pathology*, 182 (2), 238–244.

Yamashita, N., Tashimo, H., Ishida, H., Kaneko, F., Nakano, J., Kato, H., Hirai, K., Horiuchi, T., and Ohta, K., 2002. Attenuation of airway hyperresponsiveness in a murine asthma model by neutralization of granulocyte-macrophage colony-stimulating factor (GM-CSF). *Cellular immunology*, 219 (2), 92–97.

Yoon, J.-S., Kim, H. H., Lee, Y., and Lee, J. S., 2007. Cytokine induction by respiratory syncytial virus and adenovirus in bronchial epithelial cells. *Pediatric pulmonology*, 42 (3), 277–282.

Yoshizumi, M., Kimura, H., Okayama, Y., Nishina, A., Noda, M., Tsukagoshi, H., Kozawa, K., and Kurabayashi, M., 2010. Relationships between Cytokine Profiles and Signaling Pathways (IκB Kinase and p38 MAPK) in Parainfluenza Virus-Infected Lung Fibroblasts. *Frontiers in microbiology*, 1 (124), 1-7

You, Y. and Brody, S. L., 2013. Culture and differentiation of mouse tracheal epithelial cells. *Methods in molecular biology (Clifton, N.J.)*, 945, 123–143.

Zaiss, D. M. W., Gause, W. C., Osborne, L. C., and Artis, D., 2015. Emerging functions of amphiregulin in orchestrating immunity, inflammation, and tissue repair. *Immunity*, 42 (2), 216–226.

Zeng, H., Belser, J. A., Goldsmith, C. S., Gustin, K. M., Veguilla, V., Katz, J. M., and Tumpey, T. M., 2015. A(H7N9) virus results in early induction of proinflammatory cytokine responses in both human lung epithelial and endothelial cells and shows increased human adaptation compared with avian H5N1 virus. *Journal of virology*, 89 (8), 4655–4667.

Zeng, R., Li, C., Li, N., Wei, L., and Cui, Y., 2011. The role of cytokines and chemokines in severe respiratory syncytial virus infection and subsequent asthma. *Cytokine*, 53 (1), 1–7.

Zeng, S., Wu, J., Liu, J., Qi, F., and Liu, B., 2015. IL-33 Receptor (ST2) Signalling is Important for Regulation of Th2-Mediated Airway Inflammation in a Murine Model of Acute Respiratory Syncytial Virus Infection. *Scandinavian journal of immunology*, 81 (6), 494–501.

Zhang, L., Peeples, M. E., Boucher, R. C., Collins, P. L., and Pickles, R. J., 2002. Respiratory syncytial virus infection of human airway epithelial cells is polarized, specific to ciliated cells, and without obvious cytopathology. *Journal of virology*, 76 (11), 5654–5666.